BIOMASS PYROLYSIS AND CATALYTIC UPGRADING OF PYROLYSIS VAPORS FOR THE PRODUCTION OF FUELS AND CHEMICALS

MASOUD ASADIERAGHI

THESIS SUBMITTED IN FULFILLMENT
OF THE REQUIREMENTS FOR THE DEGREE OF
DOCTOR OF PHILOSOPHY

FACULTY OF ENGINEERING
UNIVERSITY OF MALAYA
KUALA LUMPUR

2016

UNIVERSITI MALAYA

ORIGINAL LITERARY WORK DECLARATION

Name of Candidate: Masoud Asadieraghi

Registration/Matric No: KHA110070

Name of Degree: DOCTOR OF PHILOSOPHY

Title of Project Paper/Research Report/Dissertation/Thesis ("this Work"):

BIOMASS PYROLYSIS AND CATALYTIC UPGRADING OF PYROLYSIS VAPORS FOR THE PRODUCTION OF FUELS AND CHEMICALS

Field of Study: Chemical Engineering

I do solemnly and sincerely declare that:

(1) I am the sole author/writer of this Work;
(2) This Work is original;
(3) Any use of any work in which copyright exists was done by way of fair dealing and for permitted purposes and any excerpt or extract from, or reference to or reproduction of any copyright work has been disclosed expressly and sufficiently and the title of the Work and its authorship have been acknowledged in this Work;
(4) I do not have any actual knowledge nor ought I reasonably to know that the making of this work constitutes an infringement of any copyright work;
(5) I hereby assign all and every rights in the copyright to this Work to the University of Malaya ("UM"), who henceforth shall be owner of the copyright in this Work and that any reproduction or use in any form or by any means whatsoever is prohibited without the written consent of UM having been first had and obtained;
(6) I am fully aware that if in the course of making this Work I have infringed any copyright whether intentionally or otherwise, I may be subject to legal action or any other action as may be determined by UM.

Candidate's Signature **Date: 22 February 2016**

Subscribed and solemnly declared before,

Witness's Signature **Date: 22 February 2016**

ABSTRACT

The accurate determination of the biomass thermal properties is particularly important while studying biomass pyrolysis processes. The various palm oil biomass samples (palm kernel shell (PKS), empty fruit bunches (EFB) and palm mesocarp fibre (PMF)) thermochemical behavior was investigated during pyrolysis. To eliminate the negative impacts of inorganic constituents during biomass thermochemical processes, leaching method by different diluted acid solutions was chosen. The different palm oil biomass samples were pretreated by various diluted acid solutions (H_2SO_4, $HClO_4$, HF, HNO_3, HCl). Acids with the highest degrees of demineralization were selected to investigate the dematerialization impacts on the biomass thermal characteristics and physiochemical structure. Thermogravimetric analysis coupled with mass spectroscopy (TGA-MS) and Fourier transform infrared spectroscopy (TGA-FTIR) were employed to examine the biomass thermal degradation. TGA and DTG (Derivative thermogravimetry) indicated that the maximum degradation temperatures increased after acid pretreatment due to the minerals catalytic effects.

Pyrolysis bio-oil from biomass comprised varieties of undesirable oxygenates and heavy compounds have to be treated. In-situ upgrading of bio-oil pyrolysis vapor is a promising approach demonstrating numerous benefits. Due to the highly complex nature of bio-oil, understanding the reaction pathways is highly desirable for catalyst and process screening. Therefore, the study of model compounds is the first step in simplifying the problem complexity to develop the fundamental processes and catalysts knowledge required to design bio-oil upgrading strategies. Three most important classes of catalysts including zeolites, mesoporous catalysts and metal based catalysts are mostly utilized for vapor phase bio-oil upgrading.

The in-situ catalytic upgrading of PKS fast pyrolysis vapors was performed over each individual meso-H-ZSM-5, Ga/meso-HZSM-5 and Cu/SiO_2 catalyst or a cascade system of

them in a multi-zone fixed bed reactor. The catalysts were characterized using SEM, XRF, XRD, N_2 adsorption and NH_3-TPD methods. Furthermore, the produced bio-oils were analyzed using GC–MS, FTIR, CHNS/O elemental analyzer and Karl Fischer titration. Among different catalysts, meso-H-ZSM-5 zeolite demonstrated a very good activity in aromatization and deoxygenation during upgrading. The gallium incorporation into the meso-HZSM-5 zeolite increased the bio-oil yield and aromatics selectivity. A cascade system of catalysts comprising meso-HZSM-5, Ga (1.0 wt. %) /meso-HZSM-5 and Cu (5.0 wt. %) /SiO_2 indicated the best performance on aromatics formation (15.05 wt. %) and bio-oil deoxygenation through small oxygenates, lignin derived phenolics and sugar derived compound conversion, respectively.

Furthermore, catalytic upgrading of the PKS biomass pyrolysis vapor and its mixture with methanol were conducted in aforementioned fixed bed multi-zone reactor using HZSM-5 zeolite catalyst. The highly valuable chemicals production was a function of the hydrogen to carbon effective ratio ($H/C_{eff.}$) of the feed. This ratio was regulated by changing the relative amount of biomass and methanol. More aromatics (50.02 wt. %) and less coke deposition on the catalyst (1.3 wt. %) were yielded from the biomass, when methanol was co-fed to the catalytic pyrolysis process ($H/C_{eff.}$ = 1.35). In this contribution, the deposited coke on the catalyst was profoundly investigated. The coke, with high contents of oxo-aromatics and aromatic compounds, was generated by polymerization of biomass lignin derived components.

ABSTRAK

Penentuan yang tepat mengenai sifat haba biomass adalah penting semasa belajar proses pirolisis biomass. Pelbagai sampel sawit biomas minyak (shell isirong sawit (PKS), tandan buah kosong (EFB) dan kelapa mesokarpa serat (PMF)) tingkah laku termokimia disiasat semasa pirolisis. Untuk menghilangkan kesan negatif daripada pengundi bukan organik semasa proses biomass termokimia, kaedah larut lesap oleh penyelesaian asid cair yang berbeza telah dipilih. Sampel biomas minyak sawit yang berbeza telah pra-dirawat oleh pelbagai penyelesaian asid cair (H_2SO_4, $HClO_4$, HF, HNO_3, HCl). Asid dengan darjah tertinggi demineralisasi telah dipilih untuk menyiasat kesan dematerialization kepada ciri-ciri haba biomass dan struktur physiochemical. Analisis Termogravimetri ditambah pula dengan spektroskopi jisim (TGA-MS) dan jelmaan Fourier spektroskopi inframerah (TGA-FTIR) telah digunakan untuk memeriksa degradasi biomass haba. TGA dan DTG (termogravimetri derivatif) menunjukkan bahawa suhu degradasi maksimum meningkat selepas asid prarawatan disebabkan oleh mineral kesan pemangkin.

Pirolisis bio-minyak daripada biomas terdiri jenis oxygenates yang tidak diingini dan sebatian berat yang perlu dirawat. Di-situ menaik taraf wap pirolisis bio-minyak adalah pendekatan yang menjanjikan menunjukkan banyak manfaat. Oleh kerana sifat yang sangat kompleks bio-minyak, memahami laluan tindak balas adalah sangat wajar untuk pemangkin dan pemeriksaan proses. Oleh itu, kajian sebatian model adalah langkah pertama dalam memudahkan kerumitan masalah untuk membangunkan proses asas dan pemangkin pengetahuan yang diperlukan untuk mereka bentuk strategi peningkatan bio-minyak. Tiga kelas yang paling penting pemangkin termasuk zeolit, pemangkin mesoporous dan pemangkin logam berasaskan kebanyakannya digunakan untuk fasa wap peningkatan bio-minyak.

Menaik taraf pemangkin in-situ bagi PKS wap pirolisis pantas telah dilakukan ke atas setiap individu meso-H-ZSM-5 , Ga / reaktor katil meso-HZSM-5 dan Cu / SiO2 pemangkin atau sistem lata daripada mereka dalam pelbagai zon tetap. Pemangkin telah dicirikan menggunakan SEM, XRF, XRD, N_2 dan kaedah penjerapan NH_3-TPD. Tambahan pula, yang dihasilkan bio-minyak dianalisis dengan menggunakan GC-MS, FTIR, CHNS /O analyzer unsur dan Karl Fischer titratan. Antara pemangkin yang berbeza, meso-H-ZSM-5 zeolite menunjukkan satu aktiviti yang sangat baik dalam aromatization dan deoxygenation semasa menaik taraf. Pemerbadanan galium ke dalam meso-HZSM-5 zeolite meningkatkan hasil bio-minyak aromatik dan pemilihan. Sistem lata pemangkin terdiri meso-HZSM-5, Ga (1.0 wt.%) / meso-HZSM-5 dan Cu (5.0 wt.%) / SiO_2 menunjukkan prestasi terbaik pembentukan aromatik (15.05 wt.%) dan bio -oil deoxygenation melalui oxygenates kecil, lignin diperolehi phenolic dan gula yang diperolehi kompaun penukaran, masing-masing.

Tambahan pula, peningkatan pemangkin wap pirolisis PKS biomas dan campuran dengan metanol telah dijalankan di disebutkan di atas katil tetap berbilang zon reaktor menggunakan HZSM-5 zeolite pemangkin. Pengeluaran bahan kimia sangat berharga adalah satu fungsi hidrogen nisbah berkesan karbon ($H / C_{eff.}$) makanan untuk. Nisbah ini telah dikawal dengan menukar jumlah relatif biomas dan metanol. Lebih aromatik (50,02 wt.%) dan kurang kok pemendapan pada pemangkin (1.3 wt.%) telah menghasilkan dari biomass, apabila metanol adalah bersama makan kepada proses pirolisis pemangkin ($H / C_{eff.} = 1.35$). Sumbangan ini, kok yang didepositkan pada pemangkin telah mendalam disiasat. The kok, dengan kandungan tinggi oxo-aromatik dan sebatian aromatik, telah dijana oleh pempolimeran lignin diperolehi komponen biojisim.

To my beloved parents, for their patient, encouragement and full support

To my beloved wife, Farzaneh, for her constant support, understanding & love

ACKNOWLEDGEMENTS

First of all, I would like to express my deepest appreciation to my advisor, Prof. Dr. Wan Mohd Ashri Wan Daud, for his guidance and support. I was very excited and motivated during my doctoral studies owing to his invaluable encouragement and inspiration. I am lucky to meet him as my advisor here at UM.

I am also grateful to my friends, Pouya, Hoda and Saleh, at chemical engineering department. Their friendships and supports always made me to be happy and motivated.

Lastly, I owe a special gratitude to my mother, parents-in-law, sister and her husband and brothers for their support and encouragement throughout my study overseas.

TABLE OF CONTENTS

LIST OF FIGURES

LIST OF TABLES

LIST OF SYMBOLS AND ABBREVIATIONS

A	Ash
β	Heating rate
BA	Bath
BET	Brunauer, Emmette and Teller
BJH	Barrett-Joyner-Halenda
BU	Bubbler
C	Carbon
CH	Chiller
CY	Cyclone
DSC	Differential scanning calorimetry
E_a	Activation energy
E	Exchanger
EFB	Empty fruit bunches
$f(x)$	Model of reaction mechanism
F	Furnace
FI	Flow indicator
FTIR	Fourier transform infrared spectroscopy
GC	Gas chromatograph
H	Hydrogen
HP	Hopper
J	Screw feeder
k	Reaction rate constant

k_0	Rate constant pre-exponential factor
m_0	Initial mass of biomass
m_f	Final mass of biomass
m_t	Biomass sample mass at time t
M	Elecro motor
MFC	Mass flow controller
MS	Mass spectrometer
n	reaction order
N	Nitrogen
NIST	National Institute of Standards and Technology
O	Oxygen
P	Pump
PK01	Catalytic vapor upgrading package
PKS	Palm kernel shell
PMF	Palm mesocarp fibre
R	universal gas constant
R	Multi-zone reactor
S	Sulphur
SEM	Scanning electron microscopy
T	Temperature
TCD	Thermal conductivity detector
TI	Temperature indicator
TIC	Temperature indicator/controller
TPD	Temperature-programmed desorption

V	Vessel
VA	Valve
WHSV	Weight hourly space velocity
x	Conversion degree
XRD	X-ray diffraction
XRF	X-Ray Flouresence

CHAPTER 1: INTRODUCTION

1.1 General

Sustainable developments of societies in recent decades lead them to the high consumption of natural fossil fuel resources. Biomass is considered as the only available sustainable energy source of organic carbon which can appropriately substitute petroleum to yield carbon based materials, chemicals and fuels (Serrano-Ruiz & Dumesic, 2011).

Pyrolysis process can be utilized to convert lignocellulosic biomass to liquid fuel (Asadieraghi & Wan Daud, 2014; Y.-B. Huang, Yang, Dai, Guo, & Fu, 2012). Fast pyrolysis process, which is distinguished by a high heating rate of particles at a short time (Venderbosch & Prins, 2010), has recently attracted the broad attentions and can be considered as one of the most capable technologies which are exploited for the conversion of renewable biomass resources to bio-oil (Ingram et al., 2008; Mohan, Pittman, & Steele, 2006). The bio-oil derived from depolymerization of cellulose, hemicelluloses and lignin, three main building block of lignocellulosic biomass, is a complex mixture of different oxygenated compounds. A typical bio-oil with broad molecular weight range from 18 to 5000 gr /mol or even more can contain more than 400 different compounds which most of them are oxygenated. Most of bio-oil deficiencies comprising its low heating value, corrosiveness and instability under long storage time and transportation conditions caused by these oxygenated compounds(Chiaramonti, Oasmaa, & Solantausta, 2007; Czernik & Bridgwater, 2004; D. C. Elliott et al., 1991; Hicks, 2011a; Q. Lu, Li, & Zhu, 2009).

Different approaches were employed targeting bio-oil's quality enhancement consisting: reduced pressure distillation (J.-L. Zheng & Wei, 2011), pyrolysis under reactive atmosphere (Pütün, Ateş, & Pütün, 2008; Thangalazhy-Gopakumar, Adhikari, Gupta, Tu, & Taylor, 2011; Z. Zhang, Wang, Tripathi, & Jr, 2011) , high pressure thermal treatment (Mercader,

Groeneveld, Kersten, Venderbosch, & Hogendoorn, 2010), hydro-treatment at high pressure (Y. Wang, He, Liu, Wu, & Fang, 2012), pyrolytic lignin removal (A. G. Gayubo, Valle, Aguayo, Olazar, & Bilbao, 2010) , pyrolysis vapor upgrading at low pressure (Stephanidis et al., 2011), and conversion of bio-oil's acidic compounds to esters and ketons over acidic (Junming, Jianchun, Yunjuan, & Yanju, 2008) and basic (Deng, Fu, & Guo, 2009) catalysts, respectively.

Bio-oil upgrading through conventional hydro-treating (HDT) at high pressure could accomplish oxygen removal by high hydrogen consumption, but it will fail to minimize carbon loss. Non-condensable undesirable C_2 - C_3 gases instead liquid C_6 - C_{14} hydrocarbons (appropriate for fuel applications) will be resulted from the small molecules during HDT process (Resasco, 2011b) .

Bio-oils and the model compounds upgrading investigations showed a considerable decrease in product yield as a result of catalyst deactivation and severe tar and char formation during catalytic upgrading (J. D. Adjaye & Bakhshi, 1995a, 1995b). Park et al. (Hyun Ju Park et al., 2007) carried out investigation on the catalytic upgrading of biomass pyrolysis vapor over HY and HZSM-5 zeolite catalysts in a fixed bed reactor. Their investigation outcomes, which were compared with the data from Vitolo et al. (Vitolo, Bresci, Seggiani, & Gallo, 2001), showed that employing biomass as feedstock instead of bio-oil increased upgraded bio-oil yield by 10 wt.%.

The catalytic upgrading of the biomass fast pyrolysis vapor is considered as one of the most promising process to produce upgraded bio-oil. Deoxygenation of the produced bio-oil can be achieved in the presence of selected catalysts to enhance bio-oil properties. Investigations are being conducted towards the design of selective catalysts to achieve production of high added value chemicals (e.g. phenol) or minimizing of the formation of undesirable bio-oil components such as acids and carbonyls (Asadieraghi & Wan Daud, 2015).

The in-situ catalytic upgrading of pyrolysis vapors, over HZSM-5 and HY zeolites in a fixed bed reactor, carried out by Park et al. (H. J. Park et al., 2007). They compared their experimental results with the data from the study of Vitolo et al. (Vitolo et al., 2001). In the case of in-situ catalytic upgrading of biomass pyrolytic vapors, approximately 10 wt% more bio-oil was yielded compared with the use of bio-oil as a feedstock.

Unlike biomass catalytic pyrolysis, which catalyst and feedstock mostly are mixed together, in-situ vapor upgrading is performed while biomass and catalyst are separated during pyrolysis/upgrading process (Pütün et al., 2008). Pyrolysis vapor upgrading is carried out before vapor being condensate, at atmospheric pressure, when vapors are passed through catalyst(s) bed(s). Figure 1.1 indicates this type of pyrolysis/upgrading process. Depending on the catalysts' characteristics, different products can be selectively produced while enhanced deoxygenation can yield bio-oil with improved physical and chemical properties. Research is being directed towards the design of selective catalysts for either increasing the production of specific high added value chemicals (e.g. phenols) or minimizing the formation of undesirable bio-oil components (e.g. acids, carbonyls).

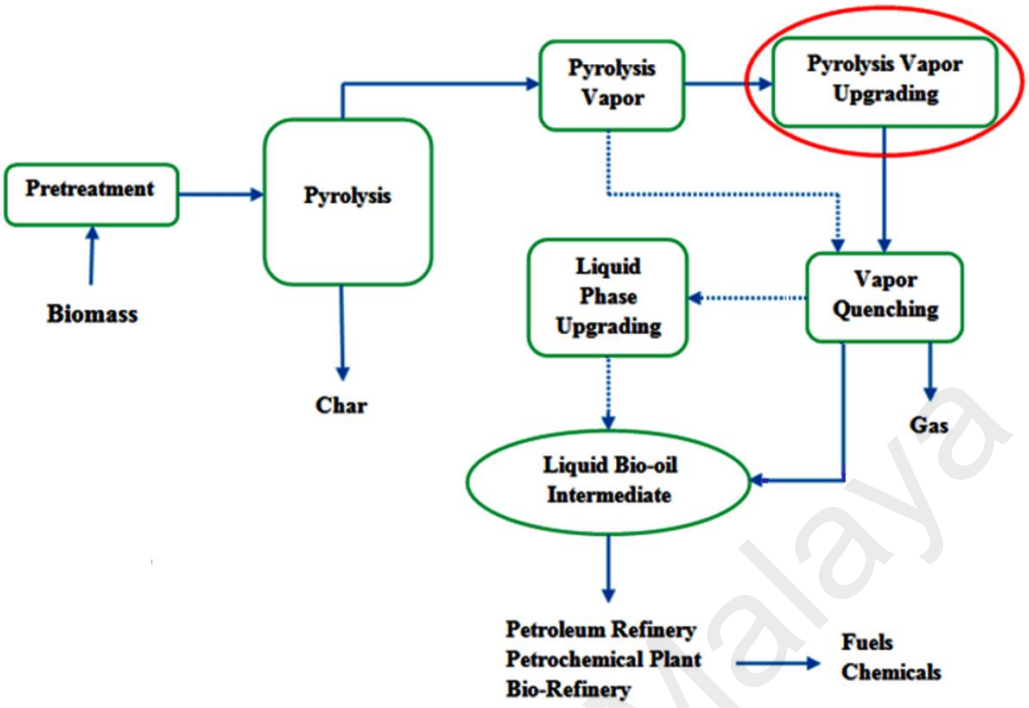

Figure 1.1: Schematic of pyrolyis and upgrading process (Highlighting pyrolysis vapor upgrading).

Three main important oxygenated compounds families available in bio-oil can be characterized as: (1) aldehyde, ketones and acids (like acetone, acetic acid, acetol , etc.); (2) sugar derived compounds (like levoglucson and furfural); and (3) lignin-derived phenolics (Resasco, 2011b). Different available components in the bio-oil are illustrated in Figure 1.2 (GW, S, & A, 2006).

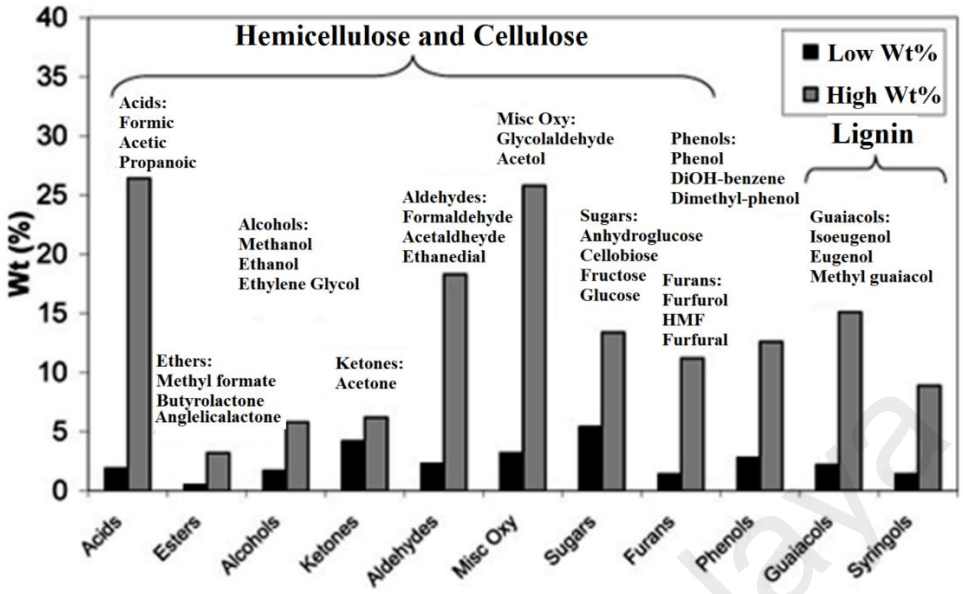

Figure 1.2: Bio-oils (derived from lignocellulosic biomass) chemical composition (GW et al., 2006).

Deoxygenation of these components suggests a great challenge. Accordingly, it is important to investigate the role of different catalysts play in the conversion of oxygenated compounds to fuel-like hydrocarbons. In this regard, development of highly durable and selective catalysts will be crucial and can be considered as key to the success for bio-oil upgrading processes at atmospheric condition and in the absence of hydrogen feeding (Hicks, 2011a). Two important targets in the biomass to bio-fuel conversion researches can be; increase the bio-fuel potential to replace petroleum and its cost competitiveness improvement. These two goals could be attained by minimizing hydrogen consumption and carbon loss. Within this context, model compound studies have been invaluable to identify catalysts and reaction conditions that are favorable for the desired reactions. Model compound studies have also been crucial to understanding catalyst behavior. The knowledge gained from the model compound studies can be applied to convert mixtures and actual pyrolysis oil vapors to gasoline range components (Asadieraghi, Wan Daud, & Abbas, 2014).

1.2 Characterization of biomass thermal degradation and effects of demineralization

Thermal gravimetric analysis (TGA) and derivative thermogravimetry (DTG) have been utilized by different researchers to investigate the biomass pyrolytic behavior and kinetics (Çepelioğullar & Pütün, 2013; D. Chen, Zheng, & Zhu, 2013; Fernandes, Marangoni, Souza, & Sellin, 2013; Magdziarz & Wilk, 2013; Wilson, Yang, Blasiak, John, & Mhilu, 2011) . TGA coupled with mass spectrometry (MS) and infrared spectroscopy (FTIR) provides the conditions for real-time (online) quantitative and qualitative evolved gas analysis, respectively. The utilization of MS and FTIR techniques along with thermal analysis can facilitate a deeper insight of the kinetic scheme and consequently to understanding the actual reaction mechanism (Edreis et al., 2013; White, Catallo, & Legendre, 2011). Several investigations on the biomass thermal analysis have been carried out using integrated TGA-MS (Y. F. Huang, Kuan, Chiueh, & Lo, 2011a; Otero, Sanchez, & Gomez, 2011; Sanchez-Silva, Lopez-Gonzalez, Villasenor, Sanchez, & Valverde, 2012).

Differential scanning calorimetry or DSC is a thermoanalytical technique to investigate the caloric requirement of the biomass pyrolysis. By analyzing DSC curve, the calorimetric characteristic under different conditions can be investigated. Thus, corresponding caloric requirements can be quantified, and the relationship of the caloric requirements with the temperature can be studied. DSC proved to be an effective technique for obtaining reliable values of the heat of reaction (He, Yi, & Bai, 2006).

The effects of inorganic metals on thermal degradation of the lignocellulosic biomass have been intensively studied by researchers (Basta, Fierro, Saied, & Celzard, 2011; Das, Ganesh, & Wangikar, 2004; I. Y. Eom et al., 2012; X. Liu & Bi, 2011; H. Yang et al., 2006). They mostly concluded that, the presence of alkaline and alkaline earth metallic species (K, Na, Mg, and Ca) can influence the quality and quantity of the pyrolysis and gasification products. Commonly, inorganic species are maintained on the char surface instead of being volatized

during pyrolysis process. Therefore, they can catalyze the biomass conversion and char formation reaction (Eom et al., 2011; Fahmi et al., 2007). The high inorganic constituents in the bio-oil ,originated from the biomass having high quantity of minerals, can catalyze polymerization reaction during the bio-oil storage and led to its viscosity increase (Carrier, Neomagus, Görgens, & Knoetze, 2012), whereas their removal from the biomass before pyrolysis can increase the bio-oil yield and stability (Fahmi, Bridgwater, Donnison, Yates, & Jones, 2008).

Biomass demineralization with acid solutions had been indicated to be a suitable method to remove inorganic constituents from the biomass, and to improve its fuel properties. So, various leaching experiments using diverse conventional acid solutions including hydrochloric acid, sulphuric acid, hydrofluoric acid, perchloric acid, nitric acid et al. were conducted (Álvarez, Santamaría, Blanco, & Granda, 2005; Eom et al., 2011; Jiang et al., 2013; X. Liu & Bi, 2011; Ruan et al., 2010).

Biomass pretreatment using acid solution before pyrolysis can eliminate the needs for additional fractionation step. This advantage can facilitate a considerable simplification of the process and large scale bio-oil production, as well as extensive reduction of energy consumption and cost of pyrolysis (Ruan et al., 2010). Furthermore, minerals elimination from the used acid solution (recovery) and its recycling to the pretreatment stage can enhance process economy and make it environment-friendly.

TGA/DTG investigations carried out by Müller-Hagedorn et al.(2003) showed the doped biomass with inorganic spices (Na, K and Ca) shifted DTG curves to lower temperature compared with washed and untreated biomass. Further, it was proved that the doped biomass with potassium decreased activation energy compared to that of washed one (Nowakowski, Jones, Brydson, & Ross, 2007). As mentioned, several researches available in the literatures have focused on the effects of inorganics on the biomass behavior, but only a few

investigations on the leaching process effects on the biomass physiochemical structure (Jiang et al., 2013; X. Liu & Bi, 2011) have been reported.

1.3 In-situ biomass pyrolysis vapor upgrading in a multi-zone reactor

Various oxygenated compounds in the pyrolysis liquid can be divided into three main families of components (Resasco, 2011a): (a) small aldehydes, ketones and acids (like acetol, acetone, acetic acid and etc.); (b) sugar derived compounds such as furfural and levoglucosan; and (c) lignin derived phenolics. The main challenge is not only elimination of oxygen from these components, but also preservation of carbon in the product, with least hydrogen consumption.

Among the various biomass conversion processes, fast pyrolysis coupled with catalytic pyrolysis vapor upgrading before its condensation has been one of the technologically and economically promising thermochemical processes for advanced biofuel production (T. N. Pham, Shi, & Resasco, 2014). This process, which has been studied extensively in recent years (Asadieraghi & Wan Daud, 2015; Asadieraghi et al., 2014; S. D. Stefanidis, Kalogiannis, Iliopoulou, Lappas, & Pilavachi, 2011b), has the advantage of inhibiting some of the gum formation and polymerization reactions that generally occur in bio-oil and therefore, greatly reduce its instability (T. N. Pham et al., 2014).

During biomass pyrolysis and catalytic upgrading, the pyrolysis vapors need to pass through certain stabilizing catalytic processes. In this situation, pyrolysis vapor components undergo several reactions comprising condensation, cracking, dehydration, aromatization, decarboxylation and decarbonylation. Through these reactions, oxygen can be eliminated in the form of CO_2, CO and water. The catalysts could be chosen according to the process necessities. As an initial step, to achieve this objective, fundamental knowledge on reaction pathway is necessary. This can be attained through model compound studies. The model

compound approach investigations could be employed to produce gasoline range molecules through conversion of small oxygenates (with minimum carbon loss), conversion of lignin-derived phenolics and conversion of sugar-derived compounds using appropriate catalysts. Catalytic upgrading of the small oxygenated molecules of the biomass pyrolysis vapors can employ appropriate catalysts that either deoxygenate the oxygenated components or utilize the relatively high reactivity of oxygen functionalities (carbonyl, hydroxyl, ketonic and carboxylic groups) to facilitate C-C bond formation reactions, such as aldol condensation of ketones and aldehydes or ketonization of carboxylic acids (Gaertner, Serrano-Ruiz, Braden, & Dumesic, 2009; Gangadharan, Shen, Sooknoi, Resasco, & Mallinson, 2010; Hoang, Zhu, Sooknoi, Resasco, & Mallinson, 2010). It means, instead of the oxygen functionalities removal too early, a cascade system of catalysts may facilitate the conditions to take the advantages of their reactivity before trying the deoxygenation. Model compounds investigations showed that zeolites (HZSM-5) and metal oxide catalysts (such as $CeZrO_2$) were effective in catalyzing C-C bond formation reactions, but zeolites indicated a higher selectivity to aromatics (Gangadharan et al., 2010; Hoang, Zhu, Lobban, Resasco, & Mallinson, 2010; Yamada, Segawa, Sato, Kojima, & Sato, 2011b). For instance, HZSM-5 could selectively convert propanal to C_7-C_9 aromatics through a reaction path that involved successive aldol condensation, followed by cyclization (Hoang, Zhu, Lobban, et al., 2010; Resasco, 2011a).

In a subsequent stage, selective cleavage of aromatics carbon–oxygen bonds in lignin structure is a crucial goal to unlocking the potential of lignocellulosic biomass to be used for biofuels production. Lignin is very difficult to upgrade due to its complex structure and recalcitrant nature. Moreover, lignin comprises many phenolic moieties, which can deactivate zeolite catalysts (Zakzeski, Bruijnincx, Jongerius, & Weckhuysen, 2010). Guaiacol and anisol were selected as model compound of lignin-derived phenolics for the

investigations (González-Borja & Resasco, 2011; Prasomsri, To, Crossley, Alvarez, & Resasco, 2011; Zhu, Lobban, Mallinson, & Resasco, 2011; Zhu, Mallinson, & Resasco, 2010) .

Hydrodeoxygenation of phenol and methyl-substituted phenols in lignin components is a more demanding reaction for bio-oil upgrading. Researchers have disputed if hydrodeoxygenation of phenolic constituents must proceed through phenyl ring hydrogenation followed by water elimination or it can also proceed via direct C-O bond hydrogenolysis without breaking aromatic structure. The latter, seems unfavorable energetically attributed to the C-O bond stabilization. By contrast, some researchers have supported the role of this route based on the observed low concentration of partially saturated or saturated rings in the product. Thus, bifunctional zeolite supported metal catalysts (like Ga/HZSM-5) are basically effective since hydrogenation and dehydrogenation take place on the metal function (Ga), while dehydration can happen on the acid sites (Kwak, Sachtler, & Haag, 1994; H. J. Park et al., 2010a; Zhu et al., 2011). In contrast to low temperature bio-oil upgrading, that produces saturated rings with high hydrogen consumption, at high temperature, dehydrogenation of the ring is favored and it will conduct to aromatics formation (Zhao, He, Lemonidou, Li, & Lercher, 2011).

Among various oxygenated compounds mostly found in bio-oil, furfural could be chosen as a model for sugar derived compounds. Due to the high reactivity of these compounds, they are needed to be catalytically deoxygenated to improve bio-oil storage stability, water solubility, and boiling point range (Sitthisa & Resasco, 2011). Furfural potentially is produced both during the cellulose pyrolysis and dehydration of sugars.

Group Ib metals like Cu could catalyze furfural conversion to furfuryl alcohol, but decarbonylation was only performed at high temperature with high metal loading (H.-Y. Zheng et al., 2006). The furfural hydrodeoxygenation over three different metal catalysts, Ni,

Cu and Pd supported on SiO_2 was investigated by Sitthisa et al. (Sitthisa & Resasco, 2011). The reactions over silica supported Ni, Cu and Pd catalysts indicated different products distribution in terms of molecular interactions with the metal surface. Furfuryl alcohol was produced over Cu catalyst through hydrogenation of carbonyl group. This was due to preferred adsorption on Cu, η^1(O) – aldehyde.

As the outcome of the authors' survey (Asadieraghi et al., 2014) on model compounds to select catalysts and process for in-situ biomass pyrolysis vapor upgrading, the various catalysts' classes were suggested for conversion of small oxygenates, lignin derived phenolics and sugar-derived components through condensation, deoxygenation and alkylation reactions. The selected zeolite catalysts are prone to accomplish varieties of upgrading reactions including condensation, deoxygenation and alkylation. Deoxygenation can be done by different types of catalysts, comprising zeolites, zeolite supported metals and oxide supported metals. According to our investigations, HZSM-5 selected for aldol condensation of small oxygenates to use the high reactivity of oxygen functionality to yield larger molecules before their oxygen elimination. Further, Ga/HZSM-5 and Cu/SiO_2 were selected for lignin phenolics and sugar-derived components upgrading, respectively. The selected catalysts are active, selective and productive to yield fuel-like components. Based on this aforementioned survey, in-situ atmospheric pyrolysis vapor upgrading with minimum carbon loss and hydrogen consumption can be performed efficiently using a cascade system of selected catalysts in an integrated pyrolysis/ upgrading process.

1.4 Methanol co-feeding during catalytic upgrading of biomass pyrolysis vapor

Over the last twenty years, there have been dozens of investigations focused on the biomass and its derived feedstock catalytic conversion with acidic zeolite catalysts, such as Mordenite,Y, Beta and HZSM-5. They were studied as candidate catalysts for the biomass pyrolysis. Among them, HZSM-5 was the most important zeolite investigated and was found to considerably change the composition of the bio-oils by both increasing the aromatic species and producing gasoline like components and simultaneously reducing the amounts of oxygenated compounds through deoxygenation reactions (W. Liu et al., 2010; H. Zhang, Cheng, Vispute, Xiao, & Huber, 2011a). Formation of large amount of coke and consequently rapid zeolite catalyst deactivation is the main problem for the biomass thermal conversion with zeolites.

A parameter named the hydrogen to carbon effective ratio (H/C_{eff}) has been defined by Chen et al.(1986). This parameter, which is shown in Eq. (1-1), can be utilized to compare the relative amount of hydrogen available in various feeds and to describe if a feed can be economically converted into hydrocarbons using zeolite catalysts according to the amount of hydrogen, carbon and oxygen in the feed. In Eq. (1), H, O and C are the moles of hydrogen, oxygen and carbon in the feed, respectively.

$$H/C_{eff} = \frac{H - 2O}{C} \qquad (1-1)$$

Chen et al.(1986) showed that feedstocks with hydrogen to carbon effective ratio (H/C_{eff}) less than 1 were difficult to upgrade over a HZSM-5 catalyst due to its quick deactivation. The H/C_{eff} ratio of petroleum based feedstocks varies from 1 to 2, whereas that of the biomass feeds are only from 0 to 0.3. Therefore, the biomass contained hydrogen deficient molecules, and approaches for the biomass and its derived feedstocks transformation must consider their H/C_{eff} ratio.

Chang and Silvestri (1977) stated that hydrogen deficient oxygenated compounds could be successfully converted on HZSM-5 zeolite catalyst if co-fed with an adequate amount of hydrogen rich chemicals such as methanol. In the other research, Melligan et al.(Melligan, Hayes, Kwapinski, & Leahy, 2012, 2013) showed major improvement in the biomass pyrolysis vapor by using hydrogen as carrier gas over Ni-HZSM-5 and Ni-MCM-41 catalysts. Ni loading to the catalysts caused acid sites enhancement and consequently increased decarboxylation, dehydration, and cracking reactions. Therefore, the yield of the aromatic hydrocarbons was increased. Recently Zhang et al. (2011a) showed that the thermal conversion of the biomass derived feedstocks to petrochemicals over zeolite catalysts was a function of the H/C_{eff} ratio of the feedstock. This suggested that the petrochemicals yield would be enhanced, while it was co-fed with a feedstock owing a high H/C_{eff} ratio.

Methanol has shown to produce high yield of hydrocarbons, when processed over zeolite catalysts (Asadieraghi & Wan Daud, 2014; Ni et al., 2011). In addition, it is usually recommended as an appropriate co-processing component due to its high H/C_{eff} ratio of 2. Therefore, methanol can be co-fed with biomass to enhance the overall hydrogen to carbon effective ratio of the feed. Figure 1.3 indicates the overall reaction chemistry of the biomass derived feedstocks cofed with methanol over the HZSM-5 catalyst.

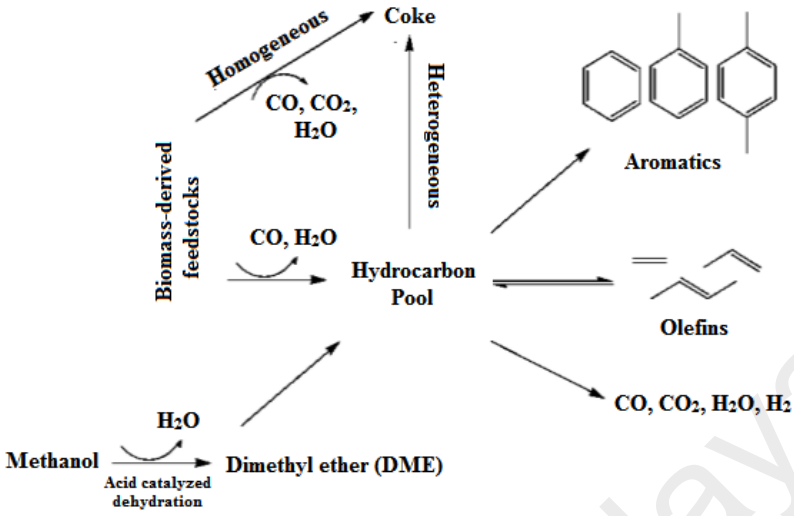

Figure 1.3: Overall reaction chemistry for biomass/methanol co-feeding over HZSM-5 zeolite catalyst during pyrolysis/upgrading (Carlson, Cheng, Jae, & Huber, 2011a; H. Zhang, Carlson, Xiao, & Huber, 2012; H. Zhang, Y.-T. Cheng, et al., 2011a)

The biomass-derived feedstocks first undergo decarbonylation, decarboxylation and dehydration reactions to produce CO_2, H_2O, CO as well as intermediate oxygenated compounds and homogeneous coke on the catalyst's surface. In the second stage, these intermediate oxygenated compounds diffuse into the zeolite catalyst pores and produce olefins and aromatics as well as heterogeneous coke through a series of oligomerization, dehydration, decarbonylation and decarboxylation reactions. The formation rate of the aromatic compounds is quite slow compared to the pyrolysis reaction. The coke generation, from polymerization of the pyrolysis vapors' oxygenated molecules, is the considerable competing reaction with the aromatic's formation. The aromatic production reactions continue through a hydrogen pool or a common intermediate within the framework of zeolite. Methanol co-feeding with the biomass probably alters the hydrocarbon pool and enhances the aromatics formation rate (Carlson et al., 2011a; H. Zhang et al., 2012; H. Zhang, Y.-T. Cheng, et al., 2011a).

1.5 Thesis objectives

The main targets of this thesis are to investigate the palm oil biomasses (PKS, EFB and PMF) thermal behavior during pyrolysis and catalytic improvement of the pyrolysis vapors to yield higher quality bio-oil. More precisely, the objectives of the present study are:

- To study the pyrolysis characteristics, evolved permanent gases products distribution and pyrolysis kinetics.
- To examine the palm biomasses pre-treatment using the most efficient diluted acid solutions in order to eliminate the negative impacts of inorganic constituents during biomass thermochemical processes and to investigate the impacts of these acids on the physiochemical structure and thermal behavior of the biomasses.
- To design catalysts and multi-stage catalytic process for palm kernel shell (PKS) fast pyrolysis vapor upgrading to produce bio-oil with lower content of the oxygenated compounds.
- To investigate the in-situ catalytic pyrolysis vapor upgrading of palm kernel shell (PKS) and its mixture with methanol to study the effects of methanol co-feeding on the improvement of valuable hydrocarbons yield.

1.6 Thesis organization

The present thesis includes seven chapters dealing with different aspects related to the topic of research.

- CHAPTER 1: This chapter briefly introduces the palm oil biomasses thermochemical characteristics and the effects of biomasses pretreatment on their thermal behavior during pyrolysis. Further, a short introduction is addressed on the various methods for

catalytic biomass pyrolysis vapors upgrading. The main objectives of the investigation are also explained.

- CHAPTER 2: This chapter presents a review on the recent researches and trends in the bio-oil catalytic vapor cracking/upgrading followed by deoxygenation focusing on catalysts properties and reaction conditions to selectively direct reactions toward production of fuel-like components and valuable chemicals. Within this context, a review of model compound studies have been employed to identify catalysts and reaction conditions that are favorable for the desired reactions. The knowledge gained from the model compound studies can be applied to convert mixtures and actual pyrolysis oil vapors to gasoline range components.

- CHAPTER 3: The present chapter describes all the experiments procedures for the bio-oil production, catalysts preparation and modification and characterization of biomass, bio-oil and catalyst samples. Details on the raw material, equipment and other related procedures are explained as well.

- CHAPTER 4: This chapter deals with the experimental data and results. In this chapter the results are presented in four parts. Part 1 investigates and characterizes the thermal behavior of the palm oil biomasses (PKS, EFB and PMF) during pyrolysis. Thermogravimetric analysis coupled with mass spectroscopy (TGA-MS), FTIR (TGA-FTIR) and differential scanning calorimetry (DSC) were employed to study the pyrolysis characteristics and pyrolysis kinetics. A fixed bed reactor was employed to study the biomass samples pyrolysis. Part 2 studies the most efficient acid solutions to leach out the minerals from the biomass samples and investigates the impacts of these diluted acids on the physiochemical structure and thermal behavior of the palm oil

biomasses. In this regard, the different palm oil biomass samples (PKS, EFB and PMF) were pretreated by various diluted acid solutions to remove inorganic species through leaching process. Consequently, the treated samples with the highest degree of ash removal were profoundly analyzed to measure the demineralization efficiency and the effects of deashing process on the thermal degradation and the physiochemical structure of the biomasses. In part 3, based on the results of the model compound approach researches, catalysts and process for palm kernel shell (PKS) fast pyrolysis vapor upgrading are selected to produce bio-oil with lower content of the oxygenated compounds. The model compound approach is employed to select the reaction conditions and catalysts that are active and selective for several classes of pyrolysis vapor upgrading reactions. A multi-zone fixed bed reactor is utilized to carry out biomass pyrolysis and its vapors upgrading using three distinct beds of catalysts in series (meso-HZSM-5, Ga/ meso-HZSM-5 and Cu/SiO_2). Part 4 investigates the in-situ catalytic pyrolysis vapor upgrading of palm kernel shell (PKS) and its mixture with methanol in a fixed bed multi-zone reactor to study the effects of methanol co-feeding on the improvement of valuable hydrocarbons yield. Further, special attentions is drawn to reduce catalyst deactivation. This study therefore provides critical insights, as to how the aromatics' yield can be enhanced by co-feeding of PKS with methanol that have a high hydrogen to carbon effective ratio.

- CHAPTER 5: The conclusions based on the results and discussion chapter are presented part by part in this chapter. In addition, the recommendations and suggestions for future works are explained.

All the outcome of this thesis, which published through six papers in tier one journals, are novel and for the first time published.

CHAPTER 2: LITERATURE REVIEW

2.1 Part 1: Heterogeneous catalysts for advanced bio-fuel production through catalytic biomass pyrolysis vapor upgrading: A review

2.1.1 Catalytic biomass pyrolysis vapor upgrading

The produced bio-oil from fast pyrolysis contains various oxygenated compounds that provide shortcomings to be used as transportation fuel. Although, it can be utilized directly for the purpose of heat and electricity generation. The high oxygen content of bio-oils has the negative effect on the energy density (16-19 MJ/kg versus 46 MJ/kg for conventional gasoline), and it is caused poor stability as well as low volatility of the liquid bio-oil (Douglas C. Elliott, 2007; Serrano-Ruiz & Dumesic, 2011). Further, the bio-oils high viscosity and corrosiveness discourage their consumption in internal combustion engines.

One of the known solutions to stabilize the bio-oil and decrease its oxygen contents is to blend it with the hydro-treating process feed, even though bio-oil transportation and storage before its blending makes significant problems (Bridgwater et al., 2008; Douglas C. Elliott, 2007). Hydro-treatment, which is the bio-oil treatment at high hydrogen pressure (30-140 bar) and moderate temperature, is likely the most common route to the bio-oil compounds deoxygenation (HDO) (Furimsky, 2000; T.-S. Kim, Oh, Kim, Choi, & Choi, 2014; Yamada et al., 2011b). In this method, bio-oil is completely deoxygenated and oxygen is removed in the form of water.

HDO is typically carried out in the presence of NiMo and CoMo catalysts (Furimsky, 2000). It is worthwhile to mention that Pt and Ru metals exhibit higher hydrogenation activity, although they show lower tolerance of sulfur impurities (Wildschut et al., 2010; Wildschut, Mahfud, Venderbosch, & Heeres, 2009).

The high hydrogen consumption in the bio-oil HDO process is the main drawback of this technology. Further, high pressure process which leads to high operational cost could be considered as the other disadvantage. One of the main challenges of HDO process is to hydrogenate the aliphatic compounds, whilst avoiding reduction of aromatics. This type of hydrogenation process control is difficult to achieve at high hydrogen pressure required for HDO.

Pyrolysis vapor upgrading can alternatively be carried out before vapor being condensate at atmospheric pressure and 350-500 °C, when vapors are passed through catalyst (s). The pyrolysis vapors need to pass certain stabilizing and oxygen removal processes without external hydrogen supply. At these conditions, vapors components undergo a series of reactions comprising, cracking, aromatization and dehydration. Through these reactions, oxygen is removed in the form of water, CO_2 and CO. Consequently, bio-oil is converted into a mixture of aromatic and aliphatic hydrocarbons, although a large fraction of organic carbon reacts to create solid carbonaceous deposits over catalyst named coke (John D. Adjaye, Katikaneni, & Bakhshi, 1996; Czernik & Bridgwater, 2004; Ana G. Gayubo, Aguayo, Atutxa, Aguado, & Bilbao, 2004; Mohan, Charles U. Pittman, & Steele, 2006 ; Sharma & Bakhshi, 1993) .

Zeolites are the most known catalysts used for the bio-oil pyrolysis vapor upgrading. Generally, coke formation over zeolite catalysts is one of the main problems for upgrading process. Investigation showed about 30% (maximum) of carbon in the feed can deposit as coke on the zeolite. It is due to low effective hydrogen available in the bio-oil. There are various oxygenated compounds in the bio-oil and therefore highly oxidized feed need to be converted to hydrocarbons. During this conversion, the excess carbon subsequently deposits as coke on the catalyst(s) (Taarning et al., 2011).

Chen's effective ratio ($H/C_{eff.}$), which is defined as (H-2O)/C (H, O and C are hydrogen, oxygen and carbon moles, respectively), indicates the feedstock effective hydrogen. Generally, a low H/C_{eff} ratio of feed is conducted to more coke formation than those having higher ratios (N. Y. Chen, Jr., & Koenig, 1986; Taarning et al., 2011).

Considering pyrolysis vapor upgrading approach, due to the similar operating pressure at which pyrolysis and upgrading are carried out, these two processes can be integrated. It is contrary to high pressure HDO process which cannot be easily integrated simultaneously with low pressure pyrolysis. Despite all the advantages associated with this type of upgrading process, there are some drawbacks. The yields of hydrocarbons are somehow modest. Another disadvantage of this technology is irreversible deactivation of catalysts, attributed to the partial de-alumination of zeolite structures in the presence of water (usually found in bio-oils). Researches still undergo toward development of acidic catalysts with better resistance against water (Rinaldi & Schüth, 2009).

By employing high reactive oxygenated compounds (carbonyl, hydroxyl, carboxyl, and ketonic groups) in bio-oils, reactions of C-C bonds formations such as aromatization, aldol condensation and ketonization can be carried out. It means oxygen functionalities potentials can be used to yield high carbon content deoxygenated fuel components instead of their elimination too early (Resasco, 2011b). Through ketonization, two carboxylic acids are condensed into a larger ketone with the release of stoichiometric amounts of water and CO_2. Usually inorganic oxide like Al_2O_3, TiO_2, ZrO_2 and CeO_2, operating at atmospheric pressure and moderate temperature (300- 425 °C), are used as catalyst for these types of reactions(Dooley, Bhat, Plaisance, & Roy, 2007; Gaertner et al., 2009; Gaertner, Serrano-Ruiz, Braden, & Dumesic, 2010; Gärtner, Serrano-Ruiz, Braden, & Dumesic, 2009; Hendren & Dooley, 2003).

It is worthwhile to note that ketonization through carboxylic acids consumption can lead to oxygen removal in the form of carbon dioxide and water. Acids almost make about 30 wt. % (maximum) of bio-oils and their conversion can improve bio-oils properties and mitigate their corrosiveness and chemical instability (Serrano-Ruiz & Dumesic, 2011). As a result, ketonization uses the oxygen functionality of acid groups to produce molecules with high heating value and consequently hydrogen consumption is reduced. Furthermore, through ketonization typical bio-oil components like esters can be condensed. Unlike zeolite catalysts, which their activity is sensitive to water presence, this type of upgrading process can be performed under moderate amounts of water (Gärtner et al., 2009; Gliński, Szymański, & Łomot, 2005; Klimkiewicz, Fabisz, Morawski, Grabowska, & Syper, 2001).

Upon selective catalytic upgrading and deoxygenation of pyrolysis vapor, depending on the catalyst type, biomass composition and process conditions, different products with improved chemical and physical properties can be yielded. Nowadays, various researches are being conducted toward the design and selection of appropriate solid catalysts for production of high added value chemicals (e.g. phenolic compounds) or molecules with enhanced properties to be used as bio-fuel component. Recent catalytic pyrolysis of the lignocellulosic biomass for the phenolic compounds production has employed different catalysts, comprising alkaline catalysts, K_3PO_4 and activated carbon (J. Kim, 2015).

Table 1.1 illustrates what can be anticipated for the characteristics and the compositions between raw pyrolysis oil, hydro-deoxygenated oil (HDO), zeolite cracking oil, and benchmarked crude oil (Mortensen, Grunwaldt, Jensen, Knudsen, & Jensen, 2011).

Table 2.1: Comparison of characteristics of bio-oil, catalytically upgraded bio-oil, and benchmarked crude oil (Mortensen et al., 2011).

	Pyrolysis oil	**HDO**	**Zeolite cracking**	**Crude oil**
Upgraded bio-oil				
Y_{Oil} [wt%]	100	21-65	12-28	-
$Y_{Water\ phase}$ [wt%]	-	13-49	24-28	-
Y_{Gas} [wt%]	-	3-15	6-13	-
Y_{Carbon} [wt%]	-	4-26	26-39	-
Oil characteristics				
Water[wt%]	15-30	1.5	-	0.1
pH	2.8-3.8	5.8	-	-
ρ [kgL^{-1}]	1.05-1.25	1.2	-	0.86
$\mu_{50°C}$ [cP]	40-100	1-5	-	180
HHV[MJ kg^{-1}]	16-19	42-45	21-36	44
C [wt%]	55-65	85-89	61-79	83-86
O [wt%]	28-40	< 5	13-24	< 1
H [wt%]	5-7	10-14	2-8	11-14
S [wt%]	< 0.05	< 0.005	-	< 4
N [wt%]	< 0.4	-	-	< 1
Ash [wt%]	< 0.2	-	-	0.1
H/C	0.9-1.5	1.3-2.0	0.3-1.8	1.5-2.0
O/C	0.3-0.5	< 0.1	0.1-0.3	~ 0

Three categories of catalysts including zeolites, mesoporous catalysts and metal based catalysts have recently attracted the considerations of researchers for the biomass pyrolysis vapor upgrading.

2.1.1.1 Microporous zeolite catalysts

Many zeolites have multi-dimensional microporous structure. This micro-porous system permits small molecules of reactants to diffuse in to the zeolite structure, therefore provide molecules access to internal acid sites. The microporous nature provides another essential feature to the zeolites, called shape-selectivity. The micro-pore channels size-restraints can somehow control the formation of unwanted products (Taarning et al., 2011).

The pores are frequently required to produce sufficiently high surface areas necessary for catalyst high activity. According to the IUPAC definition, porous materials are classified in three main groups; microporous (pore size < 2 nm), mesoporous (2–50 nm), and macroporous

(>50 nm) materials (Rinaldi & Schüth, 2009). Wide varieties of reactions could be catalyzed by zeolites attributed to their shape selectivity. The different zeolites pore size varying from 5 A° to 12 A° affects molecules mass transfer (Jae et al., 2011).

Various types of shape selectivity can be identified depending upon if pore size restricts the reacting molecules entrance, or the product molecules departure, or the creation of certain transition conditions. Selectivity of the reactants achieved while among all the reactant molecules only whom which are small enough can diffuse through the catalyst pores. When parts of the products inside the pores are too large to diffuse out, product selectivity occurs. They are either transformed to smaller molecules or in the worst case block the pores and deactivate the catalyst. Restricted transition state selectivity takes place when particular reactions are avoided because the relevant transition state would need bigger space than available in the cavities. Different pore systems may employ to control the molecular traffic. Reactant molecules may favorably diffuse in the catalyst through one pore, while products leave through the other. So, counter diffusion is minimized (Csicsery, 1986).

One of the most important applications of zeolite catalysts is in fluid catalytic cracking (FCC) process. It provides about 45 % of the global gasoline pool through the large hydrocarbon cracking into the gasoline range molecules (G. Ertl, Schüth, & Weitkamp, 2008). Zeolites are appropriate catalysts for the biomass pyrolysis vapor/ bio-oil upgrading due to containing Lewis and Brønsted acid sites. Reaction selectivity toward desired product can be controlled using acid site's strength and density distribution. Among all zeolites applications, catalytic conversion of oxygenates to hydrocarbons particularly has drawn the attentions. Most known is the methanol conversion to gasoline (MTG) over HZSM-5 catalyst (Asadieraghi et al., 2014).

Biomass in the past decade has been considered as an important renewable resource of transportation fuels and its catalytic conversion over zeolites has been widely employed.

Through several researches, a broad range of zeolites including HZSM-5, Y zeolite and Beta zeolite have been investigated using bio-oils or biomass as feedstock. These studies indicated that the zeolite addition into the pyrolysis reactor could significantly increase the formation of aromatics. CO_2, CO, water, tar and coke were also formed during this process (To & Resasco, 2014). The majority of these investigations resulted that HZSM-5 catalyst gave the highest aromatics yield (Mante & Agblevor, 2011). In Huber et al. (G.W. Huber, Cheng, T. Carlson, & J. Jae, 2009) patented investigations, glucose pyrolysis in the presence of HZSM-5 catalyst, maximum aromatics was yielded at catalyst Si/Al ratio of 60 and 600° C. Agblevor (A.Agblevor, 2009, 2010) patented fractional pyrolytic process, wherein the biomass materials were selectively converted into desired products in the presence of HZSM-5 catalyst, eliminating potential secondary and post-pyrolysis processing steps. He showed that the biomass lignin fraction could be converted to phenolic components with low char production when pryolysis and catalytic processes were carried out simultaneously. Due to the considerable demethoxylation and demethylation, the molecular mass distribution of the fractional catalytic process product was about half of the conventional pyrolysis without catalyst.

Zeolite catalysts could be modified by incorporation of metals. Incorporation of Co or Ni transition metals (1-10 wt.%) into HZSM-5 catalyst indicated significant effect on the performance of the parent HZSM-5 catalyst. Compared to the Co_3O_4, NiO modified catalysts showed more reactivity towards increasing the gaseous products and decreasing the organic phase. All the metal-modified catalysts showed remarkable reactivity towards production of phenols and aromatics, although exhibited limited reactivity toward water production. These are attributed to different hydrocarbon conversion reactions, comprising dehydrogenation, cracking, and aromatization / cyclization reactions, which are catalyzed by Brønsted acid sites of the zeolite. In addition, water production enhancement was due to increased

decarboxylation/dehydration of the oxygenated compounds on the zeolite acid sites (Iliopoulou et al., 2012; Lappas, Bezergianni, & Vasalos, 2009). Catalytic conversion of particle board biomass over microporous zeolite catalyst exhibited that impregnation of 1 wt.% Ga on HZSM-5 through incipient-wetness technique enhanced catalyst selectivity toward aromatic production. It is attributed to the dehydrocyclization of bio-oil intermediate products. Ga incorporation to the zeolite caused reduction of acid sites numbers. Although the selectivity towards aromatics was improved, but it caused lower degree of bio-oil deoxygenation (lower water yield) (Choi et al., 2013).

2.1.1.1.1 Summary of the fast pyrolysis vapor upgrading studies on microporous zeolites

Table 2.2 summarizes the most recent researches performed on fast pyrolysis vapor upgrading over zeolite catalysts. In this regard, some of the key aspects are as follows:

- HZSM-5 zeolite catalysts showed very good performance. It yielded bio-oil with low oxygen contents, less acidic, less viscous and stable with high energy content(French & Czernik, 2010; Mante & Agblevor, 2011; Mihalcik, Mullen, & Boateng, 2011; S. D. Stefanidis, Kalogiannis, Iliopoulou, Lappas, & Pilavachi, 2011a; Stephanidis et al., 2011).
- HZSM-5 zeolite catalysts led to water increase in the bio-oil via dehydration reactions, and enhancement of organics, aromatic hydrocarbons and gaseous products caused by decarbonylation, dealkylation, decarboxylation, cracking, and aromatization reactions. Coke formation over catalysts was also increased during catalytic upgrading (Mante & Agblevor, 2011; Mihalcik, Mullen, et al., 2011; S. D. Stefanidis et al., 2011a; Stephanidis et al., 2011).
- Pore size and Si/Al ratio played important role on HZSM-5 catalyst performance, product distribution and selectivity. Metal substituted HZMS-5 enhanced bio-oil

Table 2.2: Summary of most recent researches of vapor phase bio-oil upgrading over microporous zeolite catalysts.

Biomass/feed	Catalyst	Reactor(s)Type	Operating Conditions	Carrier Gas	Analysis Method(s)	Comments- Highlighted Points	Ref.
Wood	HZSM-5	Fluidized Bed	T=450-475 °C P= atm.	Nitrogen	GC FTIR	1- Low coke formation and prolong catalyst activity. 2- The bio-syncrude oils were low in oxygen, less viscous, less acidic, stable, and high in energy density.	(Mante & Agblevor , 2011)
White oak wood	Ca-Y zeolite (β zeolite)	Fluidized Bed	T= 500°C P= atm.	Nitrogen	GC-MS	1-Catalysts successfully reduced oxygenates, producing aromatics and increasing bio-oil C/O ratio(5.9/1). 2- Bio-oil yield decreased due to carbon deposition on catalysts. 3- The Ca-Y zeolite deactivated less quickly possibly due to the presence of Ca^{2+} ions in place of Brønsted acid sites.	(Mullen, Boateng, Mihalcik, & Goldberg , 2011)
Wood pine	H- β-zeolite	Fluidized Bed	T=450 °C P= atm.	Nitrogen	GC-MS	1- In comparison to non catalytic pyrolysis, bio oil water contents increased (from 5.4 wt% to about 13 wt%)due to formation of polyaromatic hydrocarbons, gas yield fairly remained constant, char formation increased, bio-oil yield decreased.	(Aho et al., 2007)
Aspen wood	X,Y Zeolite, ZSM-5 and its modified with (Co, Fe, Ni, Ce, Ga, Cu, Na)	Fixed Bed	T=400-600 °C P= atm.	He - Ar	MBMS	1-ZSM-5 showed best performance while larger pore zeolites showed less deoxygenation activity. 2-Highest bio-oil (16 wt%) yielded from nickel-substituted ZSM-5 zeolite 3- - ZSM-5 catalyst in a fixed bed pyrolyzer and at 500°C showed good deoxygenation.	(French & Czernik, 2010)
Beech wood	HZSM-5	Fixed Bed	T= 500 °C P= atm.	Nitrogen	GC-MS	1- HZSM-5 zeolite, led to increase of water in the bio-oil via dehydration reactions and decrease of organics, increase of gases and coke due to decarbonylation, decarboxylation, dealkylation, cracking and aromatization reactions. 2- H-ZSM-5 reduced the organics oxygen content (from 41.68% to 30.45 %) by decreasing the concentration of acids, ketones and phenols in the bio-oil.	(S. D. Stefanidis et al., 2011a; Stephanidis et al., 2011)
Pine	Zelites (beta, Y, ferrierite) NH4-Beta-25, NH4-Y-12 NH4-Fer-20	Dual-fluidized bed reactor	Reactor1 T= 490 °C P= atm. Reactor2 T= 450 °C P= atm.	Nitrogen	GC-MS TEN3 Gas Analyzer	1- First FBR used as pyrolyzer while second one as upgrading reactor. 2-Water and CO formation were increased over all zeolites while CO_2 formation increased in some extent. 3- Beta zeolite was the most active in the de-oxygenation reactions followed by Y and ferrierite zeolites.	(Aho et al., 2010)
Woody biomass, energy crops, agricultural residues	Zeolites H-Mordenite H-ZSM-5, H-Y, H-Beta, H-Ferrierite	Pyroprob	T= 550 °C P= atm.	He	GC-MS	1- The H-ZSM-5 catalyst was the most effective catalyst at producing aromatic hydrocarbons from the oxygen-rich vapors 2- The structure and Si/Al ratio of the catalysts played a major role in their abilities to effectively deoxygenate the pyrolysis vapors and produce aromatic hydrocarbons.	(Mihalcik , Mullen, et al., 2011)

‘Table 2.2, continued’

Biomass/feed	Catalyst	Reactor(s)Type	Operating Conditions	Carrier Gas	Analysis Method(s)	Comments- Highlighted Points	Ref.
maple wood glucose, furan	ZSM-5	Fixed Bed	T= 600 °C P= atm.	He	GC-MS	1- Different ZSM-5 catalysts properties(silica-to-alumina ratio, mesoporosity and removal of external surface acid site) on the yield and aromatic hydrocarbons distribution. 2- Glucose catalytic fast pyrolysis yeided max. aromatics(~42%) and min. coke formation(~32%) at Si/Al=30 .	(Foster, Jae, Cheng, Huber, & Lobo, 2012)
Oak	β-zeolite Y-zeolite (CaY)	Fast pyrolysis@ Fluidized Bed Upgrading@ Fixed Bed	T= 500 °C @ Fluidized Bed T=425°C @ Fixed Bed P= atm.	Nitrogen	GC-MS	1-Both catalysts efficiently deoxygenated a significant fraction of the pyrolytic vapor stream to produce aromatic hydrocarbons, but CaY offered a superior ability to produce aromatics, compared to β-zeolite. 2- The higher-moisture vapors cracking on the upstream of the pyrolysis system resulted in slower coke formation and more naphthalenes.	(Mihalcik, Boateng, Mullen, & Goldberg, 2011)

yield and properties(French & Czernik, 2010; Mihalcik, Mullen, et al., 2011; S. D. Stefanidis et al., 2011a; Stephanidis et al., 2011; Vichaphund, Aht-ong, Sricharoenchaikul, & Atong, 2014).

- β-zeolite, Y-zeolite and ferrierite zeolite showed very good performance in the bio-oil deoxygenation and aromatic compounds production. β-zeolite showed high activity in the de-oxygenation reactions followed by Y and ferrierite zeolites. Ca-Y-zeolite deactivated less quickly and offered a superior ability to produce aromatics, compared to β-zeolite (A.Agblevor, 2009; Mante & Agblevor, 2011; Mihalcik, Boateng, et al., 2011).

2.1.1.1.2 Reaction pathway for biomass pyrolysis vapor upgrading over HZSM-5 catalyst

In general, during pyrolysis and upgrading processes, lignocellulosic biomass pyrolysis vapor passes through a series of pyrolysis reactions followed by catalytic conversion of oxygenated compounds available in pyrolysis vapors(Bridgwater et al., 2008; K. Wang, Kim, & Brown, 2014). Recently Wang et al. (K. Wang et al., 2014) revealed deoxygenation pathway over HZSM-5 catalyst for cellulose, hemicellulose, and lignin (three most important building blocks of lignocellulosic biomasses). According to their investigation, the proposed reactions networks for the biomass catalytic pyrolysis vapor upgrading is shown in Figure 2.1. It was assumed that there is negligible interaction effects among three biomass components during both thermal pyrolysis and catalytic conversion of pyrolysis vapors.

The biomass oxygenated organic compounds over zeolite catalysts at 350 °C to 500 °C passed through decarboxylation, cracking, alkylation, polymerization, condensation and aromatization reactions. When acidic zeolite catalysts like HZSM-5 was employed, dehydration was the dominant mechanism. Under this condition, the yielded products was a mixture of low molecular weight olefins and aromatic hydrocarbons(Talmadge et al., 2014).

During biomass pyrolysis and catalytic upgrading, the major product from cellulose pyrolysis was levoglucsoan, which could produce smaller furanic compounds through decarbonylation, decarboxylation or dehydration reactions (Shen, Xiao, Gu, & Luo, 2011). These furans then could diffuse into the acidic zeolite pores to produce olefins and aromatics through oligomerization and decarbonylation reactions. On the other hand, double hydrated xylose, the predominant product from hemicellulose pyrolysis could diffuse together with other low molecular weight molecules like acetic acid, furaldehyde, acetol and formic acid into zeolite pores without any further reaction. Lignin pyrolysis initially yielded monomeric phenolic components, which showed very low reactivity over HZSM-5 catalyst. Phenols acid-dehydration conducted to the formation of large amounts of cokes, whereas phenols cracking generated aromatics. Alkyl- phenols cracking to produce olefins might be another intermediate to yield aromatic compounds. Their investigation also showed that the aromatics yield of three main building block of lignocellulosic biomasses increased in the following order: lignin << hemicellulose < cellulose. Moderately higher temperature indicated lower coke generation and higher aromatics yield for three components of biomasses. It was attributed to the higher desorption of the coke precursors and generation of lower molecular weight oxygenated components during pyrolysis and upgrading. Lignin, among the three biomass components, had the most complicated structure and phenolic molecules produced from its thermal degradation were prone to the coke and char formations, which could decrease the carbon efficiency for the biomass pyrolysis and catalytic upgrading. Therefore, product distribution of the biomass pyrolysis and catalytic upgrading was highly depending on the biomass composition.

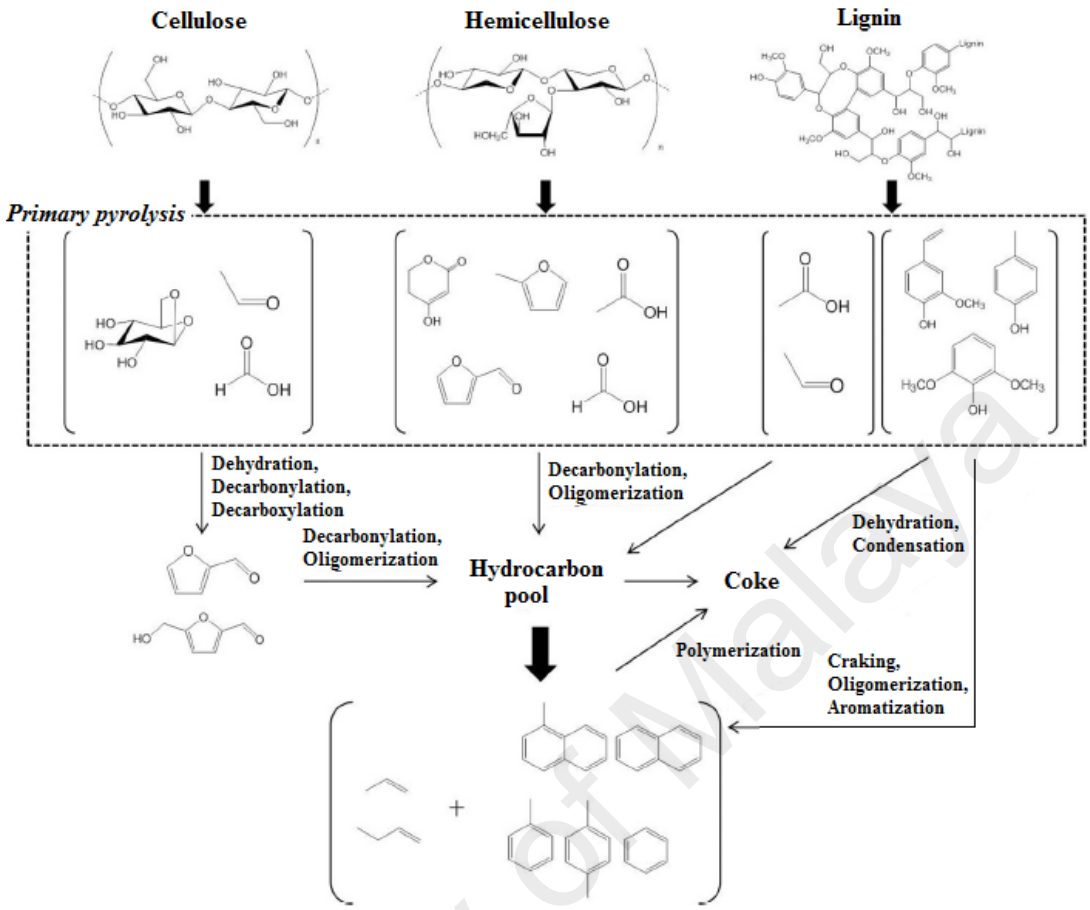

Figure 2.1: Reaction pathways for pyrolysis and catalytic pyrolysis vapor upgrading of lignocellulosic biomass over HZSM-5 catalyst. Adapted from Wang et al. (K. Wang et al., 2014)

2.1.1.2 Mesoporous Catalysts

To eliminate the possibility of secondary reactions, which enhance the coke formation and consequently catalyst deactivation caused by a slow mass transport to and away from the catalytic center, suitable catalyst should have all advantages of microporous zeolite while provide additional diffusion pathways for larger molecules as shown in Figure 2.2 (Moller & Bein, 2013).

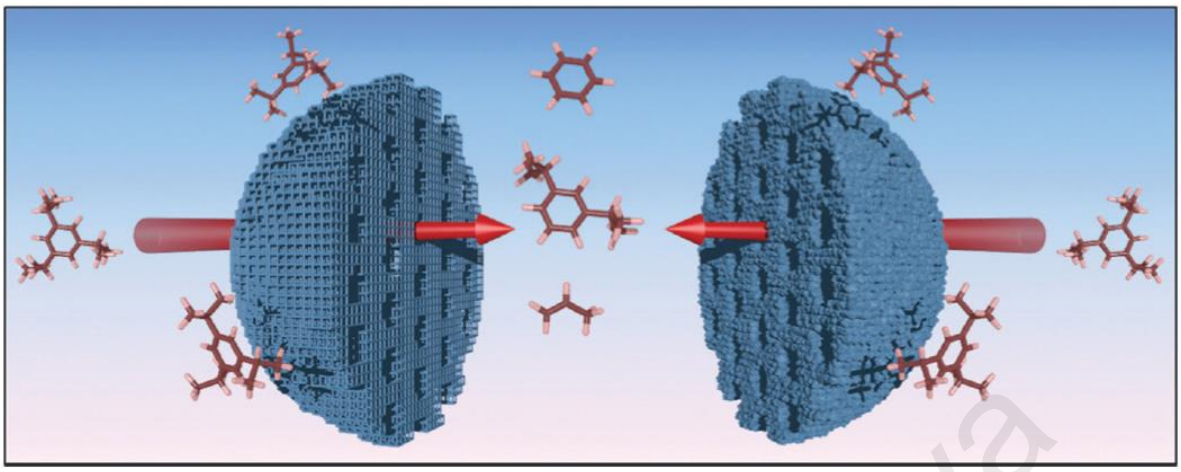

Figure 2.2: Schematic illustration of a secondary pore system to enable diffusion of large molecules within microporous zeolites. These mesopores can be created as intercrystalline pores in nanozeolite aggregates (right) or may be formed as intracrystalline voids within zeolite single crystals (left). Adapted from Moller et al. (Moller & Bein, 2013)

Since the pyrolysis vapor comprised various components with different sizes and molecular weight, porosity can play an important role toward production of desired products. Macroporous and mesoporous materials can be selected as the first choice for catalytic process in the presence of large molecules (Önal, Uzun, & Pütün, 2011). However, while size selectivity is desired, pores need to have a defined structure and be narrow enough to provide reagents; products and/or transition state selectivity. Macroporous materials, due to the high exposure of active site to substrates, restrict the reaction pathway toward selective reaction. To overcome this type of drawback, recently mesoporous materials with highly ordered structures have attracted the attentions (Dutta, 2012).

Biomass catalytic pyrolysis by the use of different acid catalysts has been employed to improve the bio-oil quality through deoxygenation reactions. Catalysts deactivation through coke formation is one of the main problems during deoxygenation. Coking is mostly caused by the phenolic compounds condensation. Further, the bio-oil components having large molecular volume cannot diffuse to the active sites placed inside the zeolite pores. Therefore,

deoxygenation process of the bio-oil components is obstructed. To enhance the molecular transport and to prevent the pore blockage by coke generation, mesoporosity formation into the zeolite catalysts seems to be promising approach. Mesopores presence in the zeolite crystalline framework would be equivalent to external surface enhancement. It makes a large number of pore openings accessible to the large molecules. Shortened diffusion path length and enlarged external surface area would ease the coke precursors mass transfer from the micropores to the external surface of zeolite catalyst and consequently prevent its quick deactivation(Hua, Zhou, & Shi, 2011). Therefore, catalytic performance of catalyst is enhanced (Na, Choi, & Ryoo, 2013; S. Stefanidis et al., 2013).

Isomerization and aromatization of 1-hexene over micro-/mesoporous HZSM-5 catalyst (alkali-treated) indicated similar phenomena. The mechanism for catalytic stability improvement of alkali- treated HZSM-5 catalyst is illustrated in Figure 2.3. As can be seen, due to the mesopores and micropores interconnection, the diffusion path in the micropores is considerably shortened. So, the isomerization and aromatization products or even precursors of coke (here naphthalene as the representative), which are created in the micropores, can diffuse out of the pores before deposition. It leads to the coke deposition in the mesopores of HZSM-5 catalyst and prevents micopores blockage. Consequently, the improvement of the stability of the catalyst in isomerization and aromatization can be attained attributed to the reduced diffusion path and coke formation in the mesopore structure (Hua et al., 2011; Li et al., 2008).

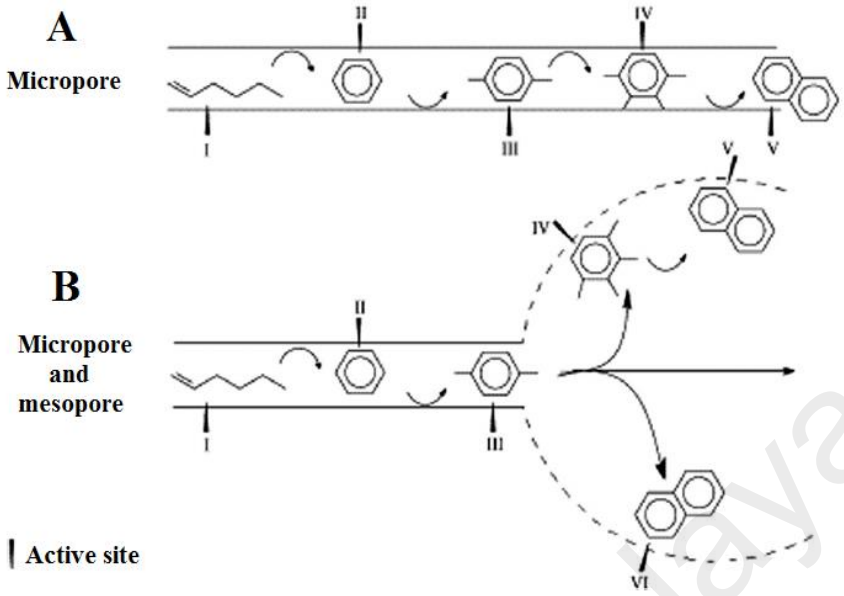

Figure 2.3: Mechanism for catalytic stability enhancement of the alkali-treated HZSM-5 zeolite with micro-mesopore porosity. Adapted from Li et al.(Li et al., 2008)

2.1.1.2.1 Mesoporosity creation in the zeolites during synthesis

During the last decade various investigations performed to synthesize zeolites with additional mesoporosity (Agostini et al., 2009; Silaghi, Chizallet, & Raybaud, 2014) (Hua et al., 2011; Schmidt et al., 2013). Generally, different synthesize strategies can be used to generate mesoporosity in the zeolites structure as following(Moller & Bein, 2013; Silaghi et al., 2014) : (a) dual templating method, in which the secondary template is used along with the common zeolites directing agent for mesostructuring the crystals of zeolites, (b) use a single but multifunctional templating route, having structure directing agents for the meso- and microscale in the same component, (c) adjustment of the synthesis reaction conditions, in which the secondary templates are unnecessary.

The dual templating method (a) uses the same basis that was already proven to be a very successful route in the synthesis of the microporous zeolites. In this method, a sacrificial scaffold is used to create mesoporosity during crystallization and can be eliminated from the

zeolite framework without loss of its final structural characteristics. Based on the physiochemical nature of the secondary templates, they can be divided to hard and soft templates. Soft templates also can be categorized to amphiphilic surfactants derivatives, macromolecular polymers and silylating agents. Applying multifunctional templates (b) produce micro- and mesopore structure in the zeolites at the same time through a single templating molecule. The third method (c) simplify the zeolite synthetic requirements and save additional cost of the production by directing the process toward synthesis of nanozeolite aggregates and mesoporous network.

2.1.1.2.2 Mesoporosity creation in the premade zeolite through leaching

Apart from the zeolites synthesis methods for mesoporosity creation (explained in section 2.2.1), it is also possible to generate mesoporosity in the zeolites through a secondary reaction(Silaghi et al., 2014). This is generally performed after the micropore zeolite synthesis and calcination, when it is free from micropore templates. Different desilication or dealumination leaching methods may be employed to generate amorphous regions in the zeolite framework. Extraction of these amorphous debris can create mesoporosity in the zeolites. Generally, leaching is a destructive process, in which part of the micron-sized zeolite structure is sacrificed for the generation of larger external surfaces in the form of mesopores (Moller & Bein, 2013; Silaghi et al., 2014).

2.1.1.2.2.1 Mesoporosity generation through desilication

Post-synthetic desilication of pre-synthesis zeolite catalyst can be used to induce intracrystalline mesopores. Local dissolution of zeolite frameworks in a basic solution (like NaOH) is a known strategy for mesoporosity creation (Ogura et al., 2001). Figure 2.4 depicts

schematically the effect of Al content on the desilication treatment of MFI zeolites in alkali solution(Groen, Jansen, Moulijn, & Pérez-Ramírez, 2004).

The desilication process is more effective for zeolites with high silica (Si/Al > 20) than high Al because SiO- removal, which is bonded directly to Al, is very difficult (Na et al., 2013). The zeolites desilication can be easily carried out at low concentration of alkali metal hydroxide. Mesoporosity generation highly depends on the Al distribution and concentration within zeolite crystals. Al-rich textures almost remain unchanged, while silica-rich textures are easily leached out to produce large mesopores. Investigations showed that the Si/Al molar ratios in the range of 25-50 were most favorable for the uniform mesoporosity development and keeping the HZSM-5 crystal morphology (Groen et al., 2004). HZSM-5 with Si/Al molar ratio less than 20 was very difficult to desilicate. Under mild basic conditions its framework was insoluble, while strong basic condition totally destroyed its zeolite framework. Alternatively, zeolites with high Si/Al molar ratio (> 50) exhibited unselective and excessive dissolution generating too large pores (Na et al., 2013). Highly uniform mesopores could be generated within the zeolite frameworks by the addition of cetyltrimethylammonium bromide (CTAB) surfactant to the desilication medium (Chal, Gerardin, Bulut, & van Donk, 2011). This surfactant could contribute to the local desilication process, making micelles joint with base in the partly desilicated zeolite. The modified zeolite catalyst through this process showed that the acidic properties of the resultant zeolite changed slightly during desilication process.

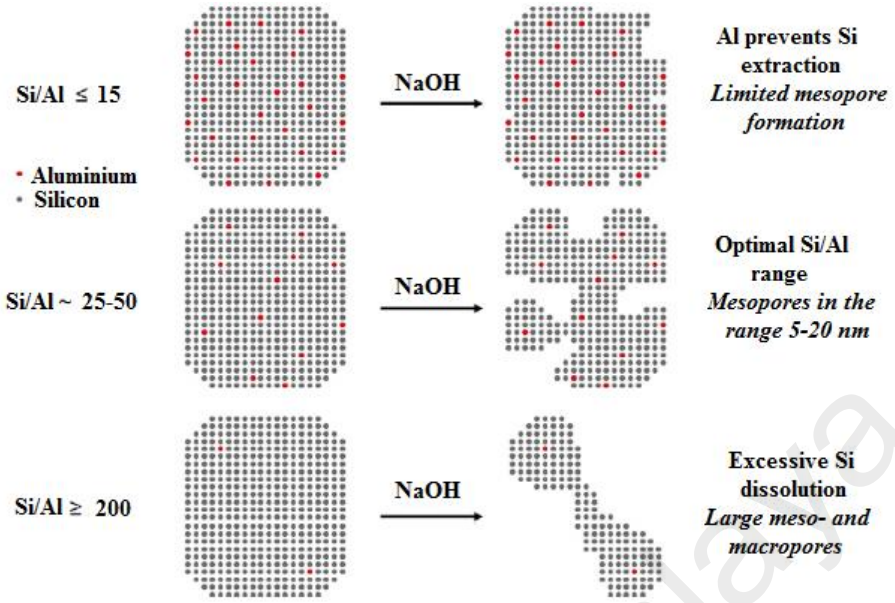

Figure 2.4: Schematic illustration of the effect of Al content on the desilication treatment of MFI zeolites in alkali solution. Adapted from Groen et al.(Groen et al., 2004)

2.1.1.2.2.2 Mesoporosity generation through dealumination

During the decades selective dealumination has been utilized because it was understood that production of zeolite with higher ratio of Si/Al could create stable zeolites with higher strength acid sites. Generally, during calcination some parts of alumina species are removed from the zeolite structure, when it is less stable. Hydrolysis of the Si–O–Al bonds creates defect sites, therefore extra-framework alumina species can be eliminated. Using extra steam, which is commonly used for zeolite Y dealumination, increases the hydrolysis severity. Then, ultra-stable Y zeolite with higher Si/Al ratio (USY), which is used as cracking catalyst in FCC (fluidized catalytic cracking) process, can be produced (Agostini et al., 2009). Amorphous alumina residues extraction is then performed by diluted nitric acid or oxalic acid. Hence, cavities and pores with broad sizes between 2-50 nm are generated (Hua et al., 2011; Moller & Bein, 2013).

Apart from Y zeolite, dealumination can be applied to ferrierite, mordenite and beta zeolites mostly by direct leaching with more concentrated acids. Depends on the nature of zeolites, different acids such as oxalic, acetic, tartaric, nitric, hydrochloric and sulfuric were utilized with various concentration (even 6.0 M HCl). For example, in a comparative investigation of three different structures, dealumination of beta zeolite was easier than mordenite, whereas HZSM-5 was almost unaffected under similar situations. Furthermore, beta zeolite dealumination conducted to higher loss of crystallinity, whereas mordenite indicated considerable mesopore volume(González, Cesteros, & Salagre, 2011).

Principally, aluminum extraction from the zeolite structure inevitably conducted to a change in Si/Al ratio, and consequently the acidity, while mesopores are created at the same time. In this conditions, understanding the effects of mesoporosity on changes of zeolite catalytic activity seems to be difficult. This type of complication may be one the main reason which mesopore generation through leaching process has been recently carried out by desilication process instead (Agostini et al., 2009; Moller & Bein, 2013).

2.1.1.2.3 Summary of the fast pyrolysis vapor upgrading studies on mesoporous catalysts

Varieties of mesoporous catalysts consisting MCM-41, Al-MCM-41, metal- Al-MCM-41, MCM-48, Al-MCM-48, meso-MFI, Pd/SBA-15, MSU-S and SBA-15 were investigated for bio-oil/biomass pyrolysis vapor upgrading (Adam et al., 2005; Antonakou, Lappas, Nilsen, Bouzga, & Stöcker, 2006; Fogassy, Thegarid, Schuurman, & Mirodatos, 2011; Lee Hw Fau - Jeon et al., 2011; Q. Lu, Tang, Zhang, & Zhu, 2010; H. J. Park et al., 2010b; H. J. Park et al., 2012a; Triantafyllidis et al., 2007). Among different mesoporous materials, MCM-41 and meso-MFI based catalysts were extensively used for bio-oil upgrading. These mesoporous catalysts, alternatively, could resolve microporous zeolites drawbacks where it was difficult for large molecules to diffuse the catalyst pores.

The recent catalytic biomass to bio-fuel conversion investigations, conducted under different conditions over mesoporous catalysts, are summarized in Table 2.3. In this regard, the following key features could be concluded:

- Compare to nano Al-MCM-48, meso-MFI showed higher catalytic activity and higher yield of aromatic, phenolic and gaseous components thanks to its strong acidic sites and high porosity, which accelerated cracking reactions. High acidity caused decreasing of organic fraction. Incorporation of Ga to meso-MFI led to less cracking, increasing of aromatic components and coke formation diminishing (Lee Hw Fau - Jeon et al., 2011; H. J. Park et al., 2010b).
- Mesoporous Al-MCM-48 and Al-MCM-41 catalysts showed high selectivity toward phenolic compounds, while meso-MFI (which possesses strong acid sites) indicated high selectivity toward aromatic components production. Pt incorporation to meso-MFI catalyst promoted dehydrogenation and cracking then conducted to enhanced aromatization and deoxygenation. Enlargement of MCM-41 pore size and loading of transition metals to it reduced acetic acid and water yield among the pyrolysis products (Adam et al., 2005; H. J. Park et al., 2012a).
- Al-MCM-41 catalyst led to decarbonylation, decarboxylation, dealkylation, cracking and aromatization reactions. Higher coke formation, compared to zeolite catalysts, could be strong evidence of mentioned reactions. Higher Al content or in the other

Table 2.3: Summary of most recent researches of vapor phase bio-oil upgrading over mesoporous catalysts.

Biomass/feed	Catalyst	Reactor(s)Type	Operating Conditions	Carrier Gas	Analysis Method(s)	Comments- Highlighted Points	Ref.
Laminaria japonica	Nano Al-MCM-48 meso-MFI zeolites (Si/Al=20)	Pyroprob	T=500 °C P= atm.	He	GC-MS	1-Meso-MFI showed higher catalytic decomposition ability than nano Al-MCM-48. 2-Meso-MFI produced high yields of aromatics, phenolics, and gases due to its strong acidic sites which accelerate d cracking of pyrolyzed bio-oil molecules.	(Lee Hw Fau - Jeon et al., 2011)
Poplar wood	Pd/SBA-15 (Pd : 0.79 wt % - 3.01 wt %)	Pyroprob	T=600 °C P= atm.	He	GC-MS	1- Lignin cracked to phenols without side chains of carbonyl and unsaturated C-C. 2- The anhydrosugars were almost completely eliminated, and the furans were decarbonylated to form light compounds. 3- Linear aldehydes were significantly decreased, while the acids were slightly decreased. Linear ketones without the hydroxyl group, methanol, and hydrocarbons were all increased.	(Q. Lu, Tang, et al., 2010)
Radiata pine sawdust	Mesoporous MFI 5 wt.% Ga/Meso-MFI	Fixed Bed	T=500 °C P= atm.	Nitrogen	GC-TCD GC–FID	1-Meso MFI exhibited the highest activity due to synergic effect of a high porosity and strong acidic property, mainly in the deoxygenation. 2- High acidity induced decreasing of organic fraction. This drawback solved by incorporation of gallium in to the catalyst. It then led to less cracking, increase of organic fraction (aromatics) and low coke formation.	(H. J. Park et al., 2010b)
Beech wood	MSU-S(aluminosilicate mesostructures)	Fixed Bed	T=500 °C P= atm.	Nitrogen	Not Available	1-Compared to non-catalytic pyrolysis, MSU-S led to low organic phase and high coke and char. MSU-S was selective toward PAHs and heavy fractions, while they produced almost no acids, alcohols and carbonyls, and very few phenols.	(Triantafyllidis et al., 2007)
Miscanthus	Al-MCM-41, Al-MCM-48, Meso-MFI, Pt/ Meso-MFI	Fixed Bed	T=450 °C P= atm.	Nitrogen	GC GC-MS	1- Mesoporous Al-MCM-41 and Al-MCM-48 catalysts indicated high selectivity toward the production of phenolics while meso-MFI, which possesses strong acid sites, showed high selectivity to aromatics. 2- Loading of Pt on meso-MFI zeolite, which has both mesopores and high acidity, promoted cracking and dehydrogenation and resulted enhanced deoxygenation and aromatization.	(H. J. Park et al., 2012a)
Sprucewood	Al-MCM-41 Mesoporous catalysts	Pyroprob	T=450 °C P= atm.	He	GC-MS	1- The lack of levoglucosan was the most important catalytic effect on the products. 2- MCM-41pore size enlargement and transition metal incorporation reduced the yield of acetic acid and water among pyrolysis products.	(Adam et al., 2005)
Beech wood	Al-MCM-41 Mesoporous catalysts	Fixed Bed	T=500 °C P= atm.	Nitrogen	GC-MS	1- Higher amount of coke formation observed in comparison to zeolites. It likely was due to decarbonylation, decarboxylation, dealkylation, cracking and aromatization reactions.	(Aho et al., 2010)

‘Table 2.3, continued’

Biomass/feed	Catalyst	Reactor(s)Type	Operating Conditions	Carrier Gas	Analysis Method(s)	Comments- Highlighted Points	Ref.
Beech wood	Al-MCM-41 Metal-Al-MCM-41	Fixed Bed	T=500 °C P= atm.	Nitrogen	GC-MS	1- Higher Al content (low Si/Al ratio) and the consequent higher surface acidity of the catalyst resulted in an increase in the yields of the high value aromatic compounds. 2- By metals incorporation into the mesoporous catalysts, the levels of phenols remained high, while the levels of both hydrocarbons and PAHs were low. 3-Fe–Al-MCM-41 and Cu–Al-MCM-41 together with the parent material with the lower Si/Al ratio were the optimum for the production of phenols.	(Antonakou et al., 2006)

world lower Si/Al ratio caused an increase in the yield of the aromatic components. Incorporation of metals (like Fe and Cu) to Al-MCM-41 enhanced the phenols yield and decreased the level of both hydrocarbons and poly-aromatic hydrocarbons (PAHs) (Aho et al., 2010; Antonakou et al., 2006).

2.1.1.3 Metal Based Catalysts

As explained within the context, there are several methods for the bio-oil upgrading comprising catalytic upgrading, steam reforming and hydrogenation. Among all these, the latter is the most widely used commercial process for the bio-oil upgrading and conducting hydro-deoxygenation reactions. Through these reactions, some components like aldehydes can be converted into stable chemicals like alcohols and hydrocarbons with high heating value and low oxygen contents (Fogassy et al., 2011; Rioche, Kulkarni, Meunier, Breen, & Burch, 2005; H. Zhang, R. Xiao, et al., 2011).

Mostly noble metal catalysts (e.g., Pt, Ru and Pd) at high temperature and pressure are employed to carry out hydro-deoxygenation reactions. These types of reactions often suffer from catalyst deactivation and clogging of the reactor at high temperatures. To overcome these problem, an approach for the bio-oil deoxygenation into high yield commodity products was employed. In this approach, hydro-processing of the bio-oil performed over supported metal catalysts (Ru/C and Pt/C) followed by conversion over zeolite catalyst (HZSM-5). Using this strategy, drawbacks associated with the conventional hydrogenation processes were overcome by operating the process at moderate temperature (≤ 250 °C), at which no reactor plugging or catalyst coking was observed. Alternatively, the bio-oil upgrading at atmospheric pressure is the other promising strategy to overcome the aforementioned problems (Tang, Yu, Mo, Lou, & Zheng, 2008; Vispute, Zhang, Sanna, Xiao, & Huber, 2010; W. Yu et al., 2011b).

Some metal based catalysts like Fe, Zn, Al, and Mg can participate in organic reactions as strong reductants. For instance, Zn and Fe are commonly used for reducing nitro compounds to amines. Further, Zn is a key metal catalyst in the conversion of carbonyl groups (e.g. aldehyde and ketones) into methylene groups. These reactions are usually carried out with a high selectivity and yield at ambient temperature and pressure in acidic conditions (W.-J. Liu, Zhang, Qv, Jiang, & Yu, 2012).

Bio-oil is a mixture of many oxygenated compounds like aldehydes, ketones and acids, which conduct bio-oil toward instability and corrosiveness. Therefore, the use of mentioned metal based catalysts can effectively enhance the bio-oil quality. Contrary to conventional hydrogenation process, low pressure pyrolysis vapor upgrading process over mentioned catalysts can be conducted without the presence of other catalysts and additional hydrogen gas (W.-J. Liu et al., 2012).

Catalytic cascade approach for the biomass pyrolysis vapor upgrading has recently attracted the attentions of researchers. The idea is to maximize carbon efficiency during bio-oil quality enhancement. In this regard, instead of oxygen functionalities (carbonyl, carboxylic, ketonic, and hydroxyl groups) elimination too early, their high reactivity is utilized to conduct C-C bond formation reactions, including aldol condensation and ketonization. Metal oxide catalysts are mostly efficient in catalyzing carboxylic acids ketonization, but reducible oxides like ceria can even catalyze the small aldehyde ketonization (Resasco, 2011b). Figure 2.5 depicts the proposed reaction mechanism of small aldehyde (propanal) conversion over $Ce_{0.5}Zr_{0.5}O_2$ catalyst. The contribution of two major reactions comprising ketonization and aldol condensation could be observed in the network, involving several condensation steps. Furthermore, there were also different side reactions that could take place in parallel. It is well understood that aldol condensation can happen on both basic and acid sites. In the mixed

oxide catalysts, the oxygen anions can behave as either Brønsted or Lewis base sites, while the exposed cations are Lewis acid sites (Asadieraghi et al., 2014; Gangadharan et al., 2010).

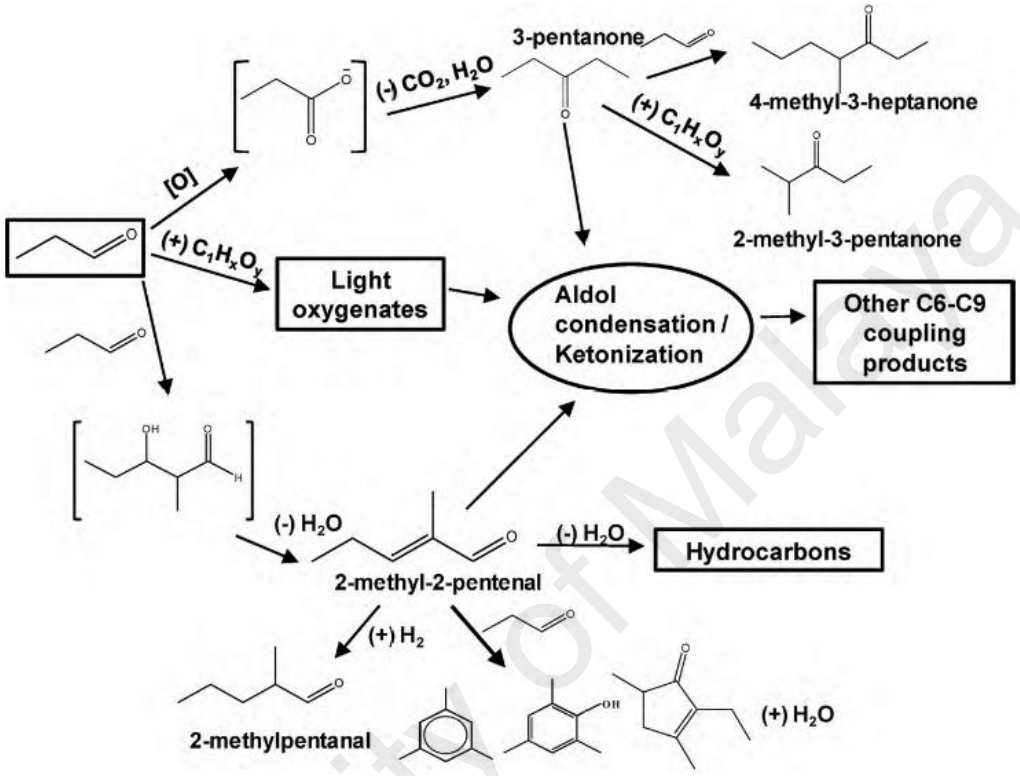

Figure 2.5: Proposed reaction mechanism for propanal conversion over $Ce_{0.5}Z_{0.5}O_2$ - Adapted from Gangadharan et al. (Gangadharan et al., 2010)

Zeolites are also effective catalysts for C-C bond formation, but the selectivity is toward aromatics formation. For instance, propanal can be selectively converted to C_7-C_9 aromatics through aldol condensation over HZSM-5 catalyst (Resasco, 2011b).

Pacific Northwest National Laboratory (PNNL) in USA has recently focused on the pyrolysis vapor upgrading with the objectives of maximizing carbon efficiency and minimizing hydrogen consumption. They employed a new concept based on chemical looping and utilizing metal oxide catalysts to selectively eliminate oxygen from the pyrolysis

vapors without hydrogen feeding ("NABC, Catalytic Fast Pyrolysis: Pyrolysis Vapors Upgrading," 2011). The concept is shown in Figure 2.6.

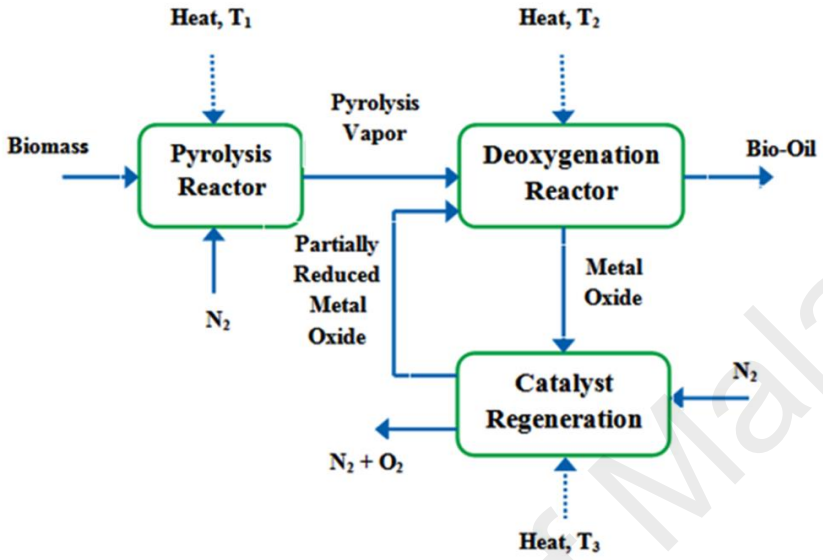

Figure 2.6: Schematic of the chemical looping deoxygenation (Over metal oxide catalysts) concept ($T_3 > T_1 > T_2$) ("NABC, Catalytic Fast Pyrolysis: Pyrolysis Vapors Upgrading," 2011).

The pyrolysis vapors react with the partially reduced metal oxide (MeOx-1) while they pass over the deoxygenation catalyst. The metal oxide is oxidized (MeOx) while the pyrolysis vapors are reduced (deoxygenated). To reduce the catalyst (MeOx-1) having the ability to be recycled back to the reactor, the metal oxide is heated under N_2 stream at a higher temperature. Model compound experiments and theoretical calculations identified some promising metal oxide catalysts for such type of vapor phase deoxygenation ("NABC, Catalytic Fast Pyrolysis: Pyrolysis Vapors Upgrading," 2011). A similar investigation was patented by Lissianski et al. (Lissianski & R.G. Rizeq, 2012) where pyrolyzing the biomass was performed in the presence of a transition metal, using microwave energy.

In an earlier study, Sanna and Andrersen (2012) suggested new catalysts for the biomass (wheat spent grains) conversion into deoxygenated bio-oil in a fluidized bed reactor. They used two Mg-rich activated olivine (ACOL) and activated serpentine (ACSE), and alumina (ALU) as catalyst. A considerable reduction of oxygen content in the bio-oil was observed in following order: ACOL>ACSE>ALU. Particularly, compared to ACOL which was able to remove about 40 wt.% of the original oxygen from the bio-oil, ACSE and ALU decreased it to less than 20-30 wt.%. The oxygenated compounds of the bio-oil interacted in the catalyst's active sites with the metallic species and produced C_5-C_6 components through decarboxylation.

The catalytic vapor upgrading, which is an attractive process with lots of advantages, has been widely investigated employing acidic zeolites. Nevertheless, zeolite catalysts suffer from fast coke deposition and PAHs formation during upgrading. Furthermore, MCM-41 based mesoporous catalysts exhibited crucial disadvantages; high production cost and poor hydrothermal stability (H. Park et al., 2011). Due to the advantages associated with metal based catalysts and in order to likely resolve zeolites and mesoporous catalysts problems, several researches recently have been performed on varieties of metal based catalysts, which some of them are summarized in Table 2.4.

Table 2.4: Summary of most recent researches of vapor phase bio-oil upgrading over metal base catalysts.

Biomass/feed	Catalyst	Reactor(s)Type	Operating Conditions	Carrier Gas	Analysis Method(s)	Comments- Highlighted Points	Ref.
Cotton seed	Magnesium oxide	Fixed Bed	T= 400-700 °C P= atm.	Nitrogen	GC-MS	1- Following to the catalytic pyrolysis, almost all of the long chain alkanes and alkenes have been converted to lower molecular weight material of the short chain and alkyl substituted forms. Oxygen content also decreased. 2-Catalyst increasing , decreased liquid yield while increased gas and char yields.	(Pütün, 2010)
Euphorbia rigida	Alumina	Fixed Bed	T= 550 °C P= atm.	Nitrogen - Steam	GC-MS	1- Using steam atmosphere instead of nitrogen during pyrolysis produced less paraffins, enriched ketones, carboxylic acids and triterpenoid compounds, while decreased phenol formation. 2- Yield and composition of the oil were depended on the catalyst ratio and pyrolysis atmosphere.	(Pütün et al., 2008)
Poplar wood	Titanium Oxide Zirconium Oxide	Pyroprob	T= 600 °C P= atm.	He	GC-MS	1- Good thermal stability compared to mesoporous silicates and MCM 2- Incorporation of Pd to catalysts, exhibited very promising effects to convert the lignin-derived oligomers to monomeric phenols. Favored reducing the aldehydes and sugars, while increasing the ketones, acids and cyclopentanones 3- TiO_2 + ZrO_2 catalysts reduced the acids deeply, and moreover increased the hydrocarbons. So, yielded bio-oil had improved fuel properties.	(Q. Lu, Zhang, Tang, Li, & Zhu, 2010)
Corncob	Calcium Oxide	Fixed bed- TGA	T=25-1000°C P= atm. Ramp=90K/min	Nitrogen	FTIR	1-The pyrolysis vapor composition changed markedly in the presence of CaO; the molality of acids, phenols and carbonyl compounds decreased, while the molality of hydrocarbons increased; CaO was very effective in deacidification and the conversion of acids promoted the formation of hydrocarbons.	(D. Wang, Xiao, Zhang, & He, 2010)
White pine	Calcium Oxide	Fluidized Bed	T=520°C P= atm.	Nitrogen	GC-MS	1- CaO/Pine ratio increasing, decreased LG, formic acid, acetic acid, and D-allose, guaiacol while increased phenol, ortho-cresol, para-cresol, and meta-cresol. 2- Furfural, furfuryl alcohol, hydroxymethyl furfural as dehydration product increased with CaO/Pine ratio increasing. It was due to dehydration reactions.	(Lin, Zhang, Zhang, & Zhang, 2010)
Beech wood	MgO, NiO, Alumina, Zirconia/titania, Tetragonal zirconia, Titania, Silica alumina	Fixed Bed	T=500°C P= atm.	Nitrogen	GC-MS	1- The most interesting catalyst was zirconia/titania formulation with the highest surface area (85 m^2/g), which yielded organic liquid products with reduced oxygen and higher aromatics content compared to the non-catalytic runs.	(S. D. Stefanidis et al., 2011a)

‘Table 2.4, continued’

Biomass/feed	Catalyst	Reactor(s)Type	Operating Conditions	Carrier Gas	Analysis Method(s)	Comments- Highlighted Points	Ref.
Pine sawdust	CuO, Fe_2O_3, ZnO, CoO	Pyroprob	T=525°C P= atm.	He	GC-MIP-AED	1-The most interesting catalysts were CuO which exhibited the highest yields(49 %) in semi-volatile compounds. 2-Mixed metal oxide catalysts (Fe_2O_3, and mixed metal oxides containing copper and cobalt) and ZnO reduced the proportion of heavy fraction in the bio-oil (from 22% to 15%) with a limited decrease in its yield.	(Torri et al., 2010)
Palm oil fruit bunch (EFB) Oil palm fronds (OPF)	Boric oxide (B_2O_3)	Fixed Bed	T=400°C P= atm.	Nitrogen	GC-MS NMR	1-Boric oxide had a deoxygenation effect leading to elimination of hydroxyl and methoxy group from the bio-oil compound .This was associated with a significant suppression in the gas yield and a substantial increase in char yield 2- The catalytic mechanism of boric oxide suggests that the addition of boric oxide promotes the removal of hydroxyl groups with the generation of alkyl substituted compounds with reduced oxygen content.	(X. Y. Lim & Andrésen, 2011)
Wood chips of Canadian white pine	Na_2CO_3/ γ- Al_2O_3 (20 wt.%)	Fixed Bed	T=500°C P= atm.	Nitrogen	GC-MS	1-Catalytic vapor upgrading in the presence of Na_2CO_3/ γ- Al_2O_3 resulted in high level of selective deoxygenation (12.3 wt. %) compared to non-catalytic bio-oil (42 wt. %). 2-The bio-oil produced from catalytic trial had comparable properties to those of fuel oil, for instance neutral in terms of acidity/basicity (pH = 6.5) and having high energy density (37 MJ kg^{-1} of bio-oil compared to 40 MJ kg^{-1} of fuel oil).	(Nguyen, Zabeti, Lefferts, Brem, & Seshan, 2013b)
Wheat spent grains (WSG) Brewers spent grain (BSG)	Alumina sand (Al_2O_3 content of 91%)	Fluidized Bed	T=460°C P= atm.	Nitrogen	GC-MS	1-Although the higher energy content retained in the bio-oils produced at 520 °C, but the bio-oils yielded at lower temperature (460 °C) indicated better quality in terms of low oxygen, lower aromatics and nitrogen content. This condition should be favored for the pyrolysis process. 2- The high O/C ratio of the bio-chars at 460 °C evidenced that the produced chars at this temperature might have retained oxygen from the bio-oils.	(Sanna, Li, Linforth, Smart, & Andresen, 2011)

Some of the key features of metal oxide catalysts used for bio-oil vapor phase upgrading can be noted as follows:

- Several metal oxides including MgO, NiO, alumina, zirconia/titania, zirconia and titania were used as catalyst. Deoxygenation occurred up to some extents in compare to non-catalytic pyrolysis, but zirconia/titania showed the most interesting deoxygenation and highest yield of aromatic compounds. Alumina showed that bio-oil yield and composition depended on pyrolysis atmosphere and the catalysis/feed ratio. The bio-oil produced over Na_2CO_3/ γ- Al_2O_3 had comparable properties to those of fuel oil (Imran, Bramer, Seshan, & Brem, 2014; Nguyen et al., 2013b; Payormhorm, Kangvansaichol, Reubroycharoen, Kuchonthara, & Hinchiranan, 2013; Pütün, 2010; Pütün et al., 2008; S. D. Stefanidis et al., 2011a).
- TiO_2 and ZrO_2 investigations indicated that they both had very good heat stability compare to mesoporous catalysts. TiO_2 + ZrO_2 mixed oxides resulted high hydrocarbon yield and significantly decreasing of acid contents (Q. Lu, Zhang, et al., 2010).
- Reaction over CaO yielded bio-oil with low acid, carbonyl and phenols contents while the molality of hydrocarbons increased. CaO/feed ratio increasing enhanced dehydration reactions (Lin et al., 2010; D. Wang et al., 2010).
- CuO exhibited very interesting results to yield semi-volatile compounds and high bio-oil yield. Boric oxide promoted hydroxyl group removal with generation of alkyl groups which consequently reduced oxygen contents (X. Y. Lim & Andrésen, 2011; Torri et al., 2010).

2.1.1.4 Catalyst deactivation

The catalyst deactivation is one of the challenging issues in catalytic biomass pyrolysis vapor upgrading. It is not only caused by coke formation, but also the strong adsorption of the oxygenate components on the surface of catalyst support. Generally two types of cokes are formed over catalyst during biomass catalytic vapor upgrading. One, which has thermal origin, is called thermal coke and the other, which has catalytic origin, is called catalytic coke. Thermal coke, which is often formed over outside of catalyst's particle, is due to phenolic compounds polymerization. Catalytic coke, which is mostly deposited inside the catalyst's channels, is caused by aromatization, oligomerization condensation and cyclization of oxygenate components (Ana G. Gayubo, Valle, Aguayo, Olazar, & Bilbao, 2009; Graça et al., 2009; Graça et al., 2009; Horne & Williams, 1995; Valle, Castaño, Olazar, Bilbao, & Gayubo, 2012). Catalyst characteristics and biomass feedstock properties can influence catalyst deactivation and coke formation.

2.1.1.4.1 Effects of catalyst characteristics

The catalyst deactivation will be more pronounced on the aluminosilicate type of catalysts, which contain acid sites. Carlson et al. (Carlson, Cheng, Jae, & Huber, 2011b) investigated the zeolite catalyst deactivation caused by acid sites lost during biomass (pine wood sawdust) catalytic pyrolysis. They used temperature programmed desorption (TPD) to measure the total number of acid sites. The related TPD curves for the spent and fresh catalyst are illustrated in Figure 2.7. As can be seen, there were two peaks with centers at ~275 °C and ~475 °C. The high temperature peak was related to the more strongly bound ammonia on Brønsted acid sites, while the low temperature peak corresponded to weakly bound ammonia on Lewis acid sites (Carlson et al., 2011b; Jeongnam Kim, Choi, & Ryoo, 2010; Ni et al., 2011; H. J. Park et al., 2010a). From the TPD curves it was concluded that the zeolite

catalyst's acidity loss was attributed to a Lewis acid sites deactivation as the high temperature peak did not change much.

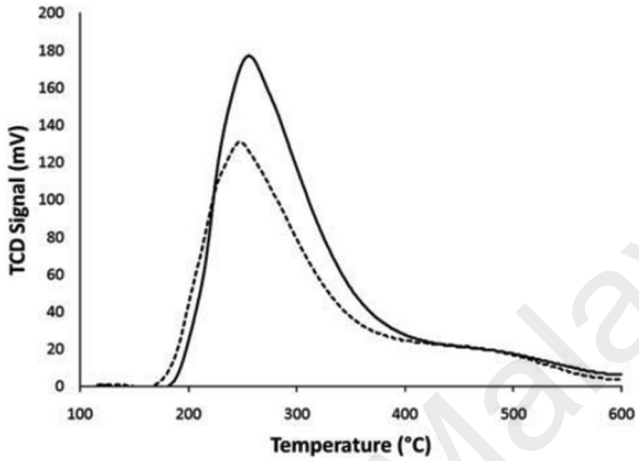

Figure 2.7: Ammonia temperature programmed desorption (TPD) for the fresh (solid line) and spent (dotted line) catalyst (Carlson et al., 2011b).

In zeolites, coke and tar deposits, which block the catalyst pores and cover its acid sites, significantly are influential on the catalyst activity and selectivity reduction (Horne & Williams, 1995). Dealumination of the zeolite catalysts (like HZSM-5) in the presence of steam was reported by several researchers. It can be conducted to catalyst acidity lost and irreversible deactivation (Carlson et al., 2011b).

Physical characteristics of the zeolite catalyst comprising pore shape, pore size and crystallite size can highly affect the coke formation (Ben & Ragauskas, 2012). Catalytic upgrading of pine wood in a fluidized bed reactor using HBeta-25, HY-12, HZSM-5 and HMOR-20 (Mordenite) catalysts showed that coke formation was fairly low for both Mordenite and HZSM-5. Spent Y zeolite (HY-12) exhibited the highest coke content. This was possibly due to the highest initial surface area and large cavities in the structure of Y zeolite, which allowing bigger molecules to diffuse to the inner part of zeolite (Aho et al., 2008).

Catalytic pyrolysis, using different zeolite catalysts having small (ZK-5, SAPO-34), medium (Ferrierite,ZSM-23, MCM-22, SSZ-20, ZSM-11, ZSM-5, IM-5, TNU-9) and large (SSZ-55, Beta zeolite, Y zeolite) pore size, were studied by Jae et al.(Jae et al., 2011). Compared to zeolites with large pore size, small pore size produced less coke. The least coke formation was resulted from medium pore size with moderate internal pore space catalysts.

In addition, coke formation over catalyst can be influenced by zeolite crystallite size. Small crystallites showed much slower deactivation and less coke formation compared to large crystallites. This was due to the shorter diffusion path and quicker removal of products from the catalyst's channels. So, products did not have sufficient time to be converted to coke precursors and coke (Hoang, Zhu, Lobban, et al., 2010).

2.1.1.4.2 Effects of feedstock properties

The availability of oxygenated compounds, such as guaiacol or phenol in bio-oil, contributes to the coke formation. Part of this coke blocks the pores thanks to the bulky oxygenated molecules (which are adsorbed on the outer zeolite crystal surface) diffusional constraints (Ibáñez, Valle, Bilbao, Gayubo, & Castaño, 2012). The different roles of the bio-oil components in the formation of coke have been investigated by Gayubo et al. (Ana G. Gayubo, Aguayo, Atutxa, Valle, & Bilbao, 2005). They identified the phenols and aldehydes as the main precursors of cokes (Ana G. Gayubo, Aguayo, Atutxa, Prieto, & Bilbao, 2004).

Increasing $H/C_{eff.}$ mole ratio in oxygenated bio-oil favored the formation of olefins and aromatics and attenuates coke formation(H. Zhang, Cheng, Vispute, Xiao, & Huber, 2011b). Investigations showed that feedstocks with hydrogen to carbon effective ratio (H/C_{eff}) less than 1.0 were difficult to upgrade over a HZSM-5 catalyst due to quick deactivation (coke formation) of the catalyst (N. Chen et al., 1986). The H/C_{eff} ratio of the petroleum based feedstocks varies from 1 to 2, whereas that of the biomass feeds are only from 0 to 0.3.

Therefore, the biomass contained hydrogen deficient molecules, and approaches for the biomass and its derived feedstocks transformation must consider their H/C_{eff} ratio. Co-feeding of alcohol (like methanol) and biomass is one of the possible ways to enhance H/C_{eff} ratio (Asadieraghi & Wan Daud, 2015). Zhang et al.(H. Zhang et al., 2012) showed that methanol co-feeding with biomass (pine wood) at H/C_{eff} ratio of 1.25 increased the aromatics yield and decreased coke formation over HZSM-5 catalyst.

The quantity and composition of the deposited coke on the HZSM-5 catalyst showed the significance of catalyst acidity for the formation of catalytic and thermal coke fractions. The major fraction of the produced coke was possibly due to the polymerization of the products derived from the biomass components pyrolysis (mostly lignin). Mostly, two fractions of coke were formed on the catalyst. The fraction of coke which was burned at low temperature was formed by condensation- degradation of lignin based oxygenated compounds. This type of coke was deposited on macro- and mesoporous structure of the zeolite catalyst matrix. The other one, which was burned at higher temperature and being deposited on the catalyst's micropores, was formed by condensation reactions activated by the acid sites. Formation of this type of coke was considerable in pure methanol catalytic conversion. Methanol addition to the pyrolysis vapor decreased the coke formation attributed to the attenuation of the phenolic compounds (lignin originated) polymerization and their deposition on the catalyst. According to the literature, pure methanol catalytic conversion on HZSM-5 catalyst formed non- oxygenated aromatics and aliphatic hydrocarbons as major components (Ana G. Gayubo et al., 2009; Valle et al., 2012).

Lignin derived phenolic compounds like anisole and guaiacol and mostly those with multiple oxygen functionalities (-OH, $-OCH_3$, C=O) are the major deactivating components. The presence of alkalis, as well as N- and likely S-containing compounds in the biomass, improve catalyst deactivation (Graça et al., 2012a; Mullen & Boateng, 2010).

2.1.1.4.3 Summary of researches on catalyst deactivation

Due to the importance of catalyst deactivation in the biomass to bio-fuel catalytic conversion, the present study tried to have a survey on the related investigations. Its outcome is summarized in Table 2.5.

Table 2.5: Summary of most recent researches of vapor phase bio-oil upgrading catalyst deactivation.

Biomass/Feed	Catalyst	Reactors Type	Operating Conditions	Carrier Gas	Analysis Method	Comments- Highlighted points	Ref.
Lignin	HZSM-5	Py-GC/MS pyrolyzer	T= 650 °C P= atm.	He	GC-MS	1- The partial deoxygentaion of the lignin aromatic units produced simple phenols, which could be potential sources of catalyst deactivation and coke formation. 2- HZSM-5 used for catalytic pyrolysis of biomass feedstocks might be more quickly deactivated by feedstocks containing a higher proportion of H-lignin which could produce a higher concentration of simple phenols.	(Mullen & Boateng, 2010)
Swedish pine-Wood	HZSM-5	Fixed bed L= 700 mm D= 20 mm	T= 600 °C P= atm.	Nitrogen	GC/MS	1- Beginning from the first regeneration, a gradual decrease of the regenerated catalyst activity was observed up to an irreversible poisoning after the fifth upgrading- regenerating cycle. 2- The active acid sites in the upgrading reactions were presumed to be preferentially Brønsted acid sites that were gradually deactivated by the repeated regeneration treatments. 3- The regeneration of the catalyst was performed by heating the spent catalyst, once it was washed with acetone and dried, in a furnace at 500°C in the presence of air for 12 h.	(Vitolo et al., 2001)
Oak	β-zeolite Y-zeolite (CaY)	Fast Pryolysis @ Fluidized Bed Upgrading@ Fixed Bed	Pyrolysis T = 500 °C P=atm. Upgrading T= 425° P=atm.	Nitrogen	GC-MS	1-Catalysts could be fully reactivated by ex-situ regeneration by heating in an oven at 500 °C in air atmosphere. 2-Cracking of the higher-moisture pyrolysis vapors found on the upstream end of the pyrolysis system resulted in slower coke formation and more naphthalenes. 3-The cracking of the less-moisture-laden, downstream pyrolysis vapors with greater concentrations of medium to large molecules, led to greater C-rich hydrocarbon product. This was richer in monocyclic benzene compounds, but it resulted in faster catalyst deactivation by coking.	(Mihalcik, Boateng, et al., 2011)
Pine (Pinus insignis) sawdust	Ni- HZSM-5 (1 wt% of nickel)	Pyrolysis@ spouted-bed reactor Upgrading@ Fluid bed reactor	Pyrolysis T=450 °C P=atm. Upgrading T=450 °C P=atm.	Nitrogen	GC-MS	1- The co-feeding of methanol with crude bio-oil had a significant effect of reducing coke deposition and catalyst deactivation, which was the main cause of catalyst deactivation it was attributable to two factors: (a) coke formation from methanol was lower than that from oxygenate components in the bio-oil; and (b) the water generation in the dehydration of methanol on the catalyst acid sites contributed to inhibiting coke formation. Nevertheless, a very high content of methanol in the feed also had an unfavorable effect on the conversion of the bio-oil contained in the bio-oil/methanolmixture, A feed of 40 wt% bio-oil/60 wt% methanol was suitable for balancing these two effects.	(Valle, Gayubo, Aguayo, Olazar, & Bilbao, 2010)
white oak wood	Ca_Y zeolite (β zeolite)	Pyroprob-GC/MS	T= 500°C P= atm.	Nitrogen	GC-MS	1- Decreasing of bio-oil yield due to carbon deposition of catalyst surface observed. 2- The Ca-Y zeolite appeared to be deactivated less quickly, possibly as a result of the presence of Ca^{2+} ions in place of Brønsted acid sites, which allowed for more oxygen removal following decarboxylation pathways. This allowed for slower coke formation because slightly more hydrogen was conserved in the pyrolysis products.	(Mullen et al., 2011)

‘Table 2.5, continued’

Biomass/Feed	Catalyst	Reactors Type	Operating Conditions	Carrier Gas	Analysis Method	Comments- Highlighted points	Ref.
Beech wood	H-ZSM-5(Si/Al =25) Al-MCM-41 (Si/Al = 30)	Fixed bed	T= 500 °C P= atm.	Nitrogen	GC-MS	1- Strongly acidic HZSM-5 zeolite, led to increase of water in the bio-oil via dehydration reactions and decrease of organics, increase of gases and coke due to decarbonylation, decarboxylation, dealkylation, cracking and aromatization reactions. 2- Higher amount of coke deposited on the Al-MCM-41 mesoporous catalyst compared to HZSM-5 zeolite.	(Stephanidis et al., 2011)
Beech wood	MSU-S Al-MCM-41	Fixed Bed	T= 500 °C P=atm.	Nitrogen	-	1-The high selectivity towards aromatics, PAHs and coke, as well as the higher production of propylene in the pyrolysis gases with the MSU-S catalysts, compared to Al-MCM-41, suggested that the former possessed stronger acid sites.	(Triantafyllidis et al., 2007)

Some key aspects in this regard are as following:

- Feedstock (biomass and lignin) pyrolysis product deoxygenation over HZSM-5 catalyst indicated that higher content of H-lignin, which could produce higher concentration of phenols, could cause quick catalyst deactivation. An irreversible poisoning was observed after some regeneration cycles due to the Brønsted acid sites deactivation. Strong acidic HZSM-5 zeolite catalyst led to coke formation due to dealkylation, decarboxylation, decarbonylation, aromatization and cracking reactions. The methanol co-feeding indicated a significant effect on coke deposition reduction on Ni-HZSM-5 catalyst during bio-oil upgrading (Mullen & Boateng, 2010; Stephanidis et al., 2011; Valle et al., 2010; Vitolo et al., 2001).
- Cracking of the high moisture pyrolysis vapors resulted slower catalyst deactivation and coke formation on β- and Y- zeolites. Incorporation of Ca to Y-zeolite caused more oxygen removal and slower catalyst deactivation. It is due to conservation of slightly more hydrogen in pyrolysis products (Mihalcik, Boateng, et al., 2011; Mullen et al., 2011).
- MSU-S catalyst high selectivity toward aromatics, PAHs and coke formation (catalyst deactivation) were attributed to its stronger acid sites in comparison to Al-MCM-41 catalyst. Compared to HZSM-5 zeolite, Al-MCM-41 showed higher tendency toward coke formation and catalyst deactivation (Stephanidis et al., 2011; Triantafyllidis et al., 2007).

2.2 Part 2: Model compound approach to design process and select catalysts for in-situ bio-oil upgrading

2.2.1 Lignocellulosic biomass structure and pretreatment

Three main building blocks of biomass are cellulose, hemicellulose, and lignin. Cellulose (a crystalline glucose polymer) and hemicellulose (a complex amorphous polymer) make up to 60-90 wt % of terrestrial biomass. Lignin (a large polyaromatic compound) is the other major component of biomass(George W. Huber, Iborra, & Corma, 2006).

Cellulose polymer chain is constructed by cellobiose monomers linked by β-(1,4)-glycosidic bonds. Hydrogen and van der Waals bonds link long chain cellulose polymers and cause the cellulose to be packed into microfibrils. Hemicelluloses and lignin cover the microfibrils (Béguin & Aubert, 1994).

Hemicellulose has branches with short chains comprising different sugars. This is the main difference between cellulose and hemicelluloses. These monosaccharides include pentoses (xylose, rhamnose, and arabinose), hexoses (glucose, mannose, and galactose), uronic acids (e.g., 4-*o*-methylglucuronic, D-glucuronic, and D-galactouronic acids) (Kuhad, Singh, & Eriksson, 1997).

Lignin, which is present in the primary cell wall, is structured as a complex cross linked phenolic polymers. It provides structural support, impermeability, and resistance against microbial attack (Pérez, Muñoz-Dorado, de la Rubia, & Martínez, 2002). Three phenyl propionic alcohols exist as monomers of lignin: coniferyl alcohol, coumaryl alcohol and sinapyl alcohol. Alkyl-aryl, alkyl-alkyl, and aryl-aryl ether bonds link these phenolic monomers together. Lignin contents vary based on the type of biomass. Some, like herbaceous plants as grasses have lowest content of this complex phenolic compound, whereas softwoods have the highest content (Jørgensen, Kristensen, & Felby, 2007).

Figure 2.8 (Nguyen, Zabeti, Lefferts, Brem, & Seshan, 2013a) depicts the major components of lignocellulosic biomass and the probable pyrolysis products. As can be seen in Figure 2.8, three main families of oxygenated compounds available in bio-oil can be defined as :(1) acids, aldehydes, and ketones (such as acetic acid, acetol, acetone, etc.); (2) furfural, levoglucosan, and other sugar-derived compounds; and (3) lignin-derived phenolics (Resasco, 2011a).

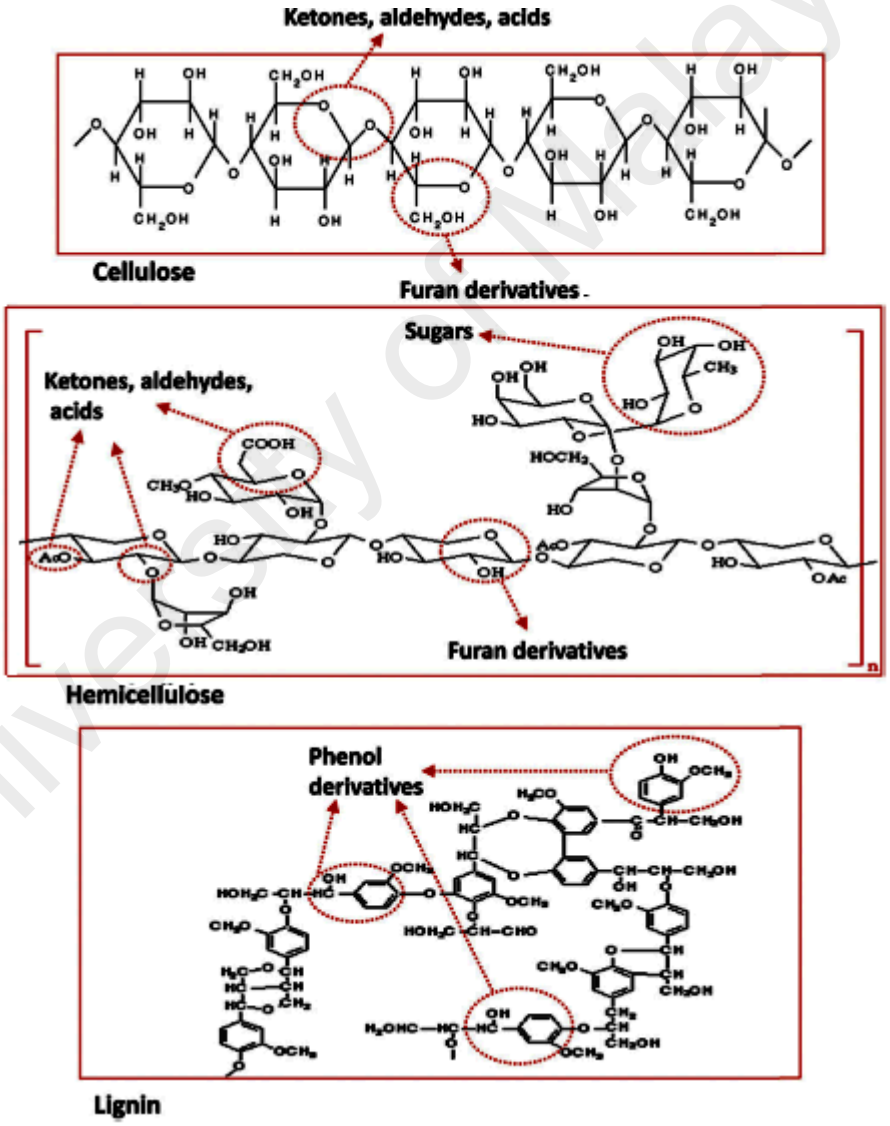

Figure 2.8: The major chemical functionalities of bio-oil released during pyrolysis originated from cellulose, hemicellulose and lignin(Nguyen et al., 2013a).

In the conversion of lignocellulosic biomass to fuel, biomass needs to be passed through certain treatment. Pretreatment is an important tool for biomass-to-biofuels conversion processes. Figure 2.9 shows the schematic of biomass pretreatment (Kumar, Barrett, Delwiche, & Stroeve, 2009).

The beneficial effects of pretreatment of lignocellulosic materials have been recognized for a long time. The goal of pretreatment process is to break down lignin and hemicelluloses, reduce cellulose crystallinity and induce porosity to lingocellulosic materials (Mosier et al., 2005). Different pretreatment methods can be divided into: physical (milling and grinding), physicochemical (steam pretreatment/autohydrolysis, hydrothermolysis, and wet oxidation), chemical (alkali, dilute acid, oxidizing agents, and organic solvents), biological, electrical, or a combination of these (Kumar et al., 2009).

In some cases, combination of chipping, grinding, and/or milling can be applied to reduce cellulose crystallinity of lignocellulosic materials. The size of the materials is usually 10-30 mm after chipping and 0.2-2 mm after milling or grinding (Sun & Cheng, 2002).

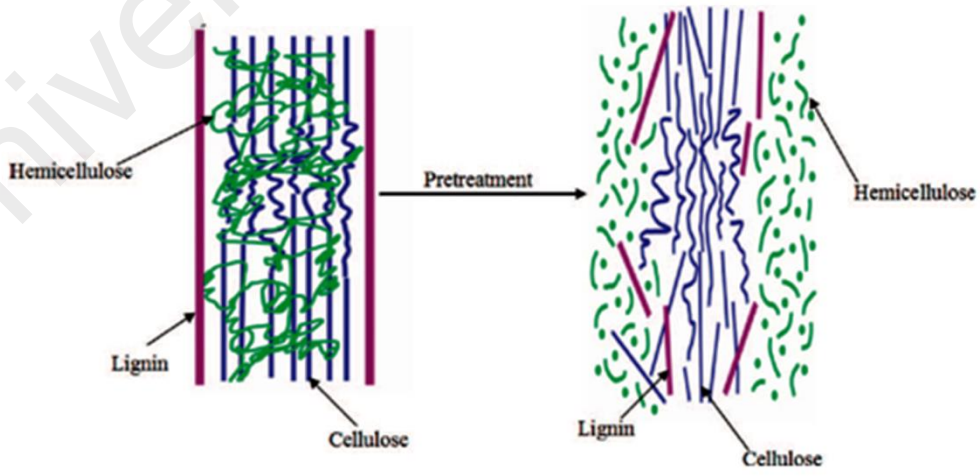

Figure 2.9: Schematic of the role of pretreatment in the conversion of biomass to fuel (Kumar et al., 2009).

2.2.2 Biomass to bio-oil by fast pyrolysis

Fast pyrolysis is a promising process for biomass to bio-fuel conversion. The milled biomass feedstock is heated in the absence of air, forming a gaseous product and char. Four types of currently available commercial pyrolysis reactors are (1) fluidized beds, (2) circulating fluid beds, (3) ablative pyrolyzer, both cyclonic and plate type, and (4) vacuum pyrolyzer (George W. Huber et al., 2006; Scott, Majerski, Piskorz, & Radlein, 1999). Figure 2.10 (Isahak, Hisham, Yarmo, & Yun Hin, 2012) briefly shows the schematic of fast pyrolysis process.

Contrary to circulating fluid bed reactors, bubbling or fluid bed reactors have the merits of good temperature control, short residence time of vapors, efficient heat transfer and being technically feasible. Fluidizing gas flow rate controls the residence time which is higher for char than vapors. Short volatiles residence time is achieved by shallow bed depth and/or high fluidizing gas flow rate (George W. Huber et al., 2006; Scott et al., 1999).

Small particle sizes of less than 2-3 mm are fluidized while the reactor is heated through hot walls, hot tubes, hot fluidization gas injection, and/or hot sand recycling. In contrast to circulating fluidized bed reactors, in this type of reactors, high quality bio-oil is produced due to low concentration of char. Contrary to fluid bed reactors, the char residence time in circulating fluid bed reactors is almost the same as the vapor and gas residence time (George W. Huber et al., 2006; Scott et al., 1999).

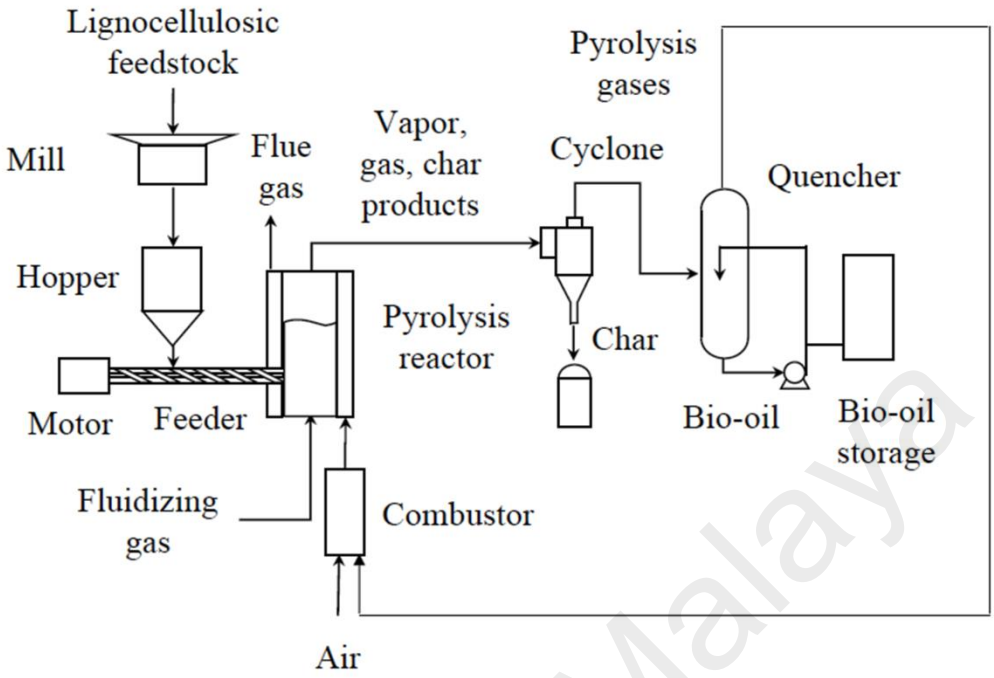

Figure 2.10: Schematic of Fast Pyrolysis System (Isahak et al., 2012).

In ablative pyrolyzer, biomass species are moved at high speed against a hot metal surface. Ablation of formed chars at a particle's surface maintains a high heat transfer rate. This can be achieved by using a metal surface spinning at high speed. Complexity of design, as moving parts which are subjected to the high temperatures of pyrolysis, and high heat loss are the main disadvantages of this pyrolyzer (Scott et al., 1999). In vacuum pyrolysis, feedstock is heated in a vacuum and the substrate residence time at the working temperature is limited as much as possible in order to minimize adverse secondary chemical reactions. This technology suffers from poor mass and heat transfer rates, and needs larger scale equipment (Scott et al., 1999).

Three key building blocks of lignocellulosic materials as cellulose, hemicelluloses and lignin have different thermal behavior depends on heating rate and the presence of contaminants (Sanchez-Silva et al., 2012). Figure 2.11 (Venderbosch & Prins, 2010) shows a typical mass loss rate of the reed decomposition performed through thermo-gravimetric analysis (TGA).

Figure 2.11A shows the total mass loss rate versus the temperature, while Figure 2.11B indicates TGA data in terms of cellulose (almost 30%), hemicellulose (25%), and lignin (20%). The decomposition of first component, which is hemicelluloses, starts at about 220°C and completed around 400°C. Cellulose starts to decompose at approx. 310°C and continued to 420°C. Within this range, the produced vapor consists of non-condensable gas and condensable organic vapor. Lignin appears to be stable up to approx. 160°C. Disruption of lignin structures through pyrolysis slowly continued and supposed to be extended up to approx. 800–900°C. The conversion of lignin compound at temperature around 500°C is probably limited to about 40%. The solid residue, produced from fast pyrolysis, is almost char. It is mainly derived by lignin (40 wt %) and some hemicelluloses (20 wt %) decomposition. From this TGA data, it can be concluded that bio-oil is mainly derived by cellulose decomposition while partially from hemicelluloses (about 80 % conversion to oil and gas) and lignin (roughly 50% conversion to oil and gas). In biomass structure, covalent ester and ether bonds link lignin and hemicelluloses which cannot be easily released upon pyrolysis. In contrast, cellulose and hemicelluloses are linked by much weaker hydrogen bonds. Pyrolysis-derived char has an elemental composition close to lignin, this could be indirect evidence for this hypothesis (Brown & Stevens, 2011).

Depending on the reaction temperature and feed type, the pyrolysis of biomass can be either endothermic or exothermic. Pyrolysis of hemicellulosic materials is endothermic at temperature below about 450°C and exothermic at higher temperatures. Different reactions and mechanisms involved in pyrolysis might be the reason (Haiping Yang, Yan, Chen, Lee, & Zheng, 2007a). Ball et al. (Ball, McIntosh, & Brindley, 2004) pointed out that the charring process was highly exothermal, whereas volatilization was endothermal.

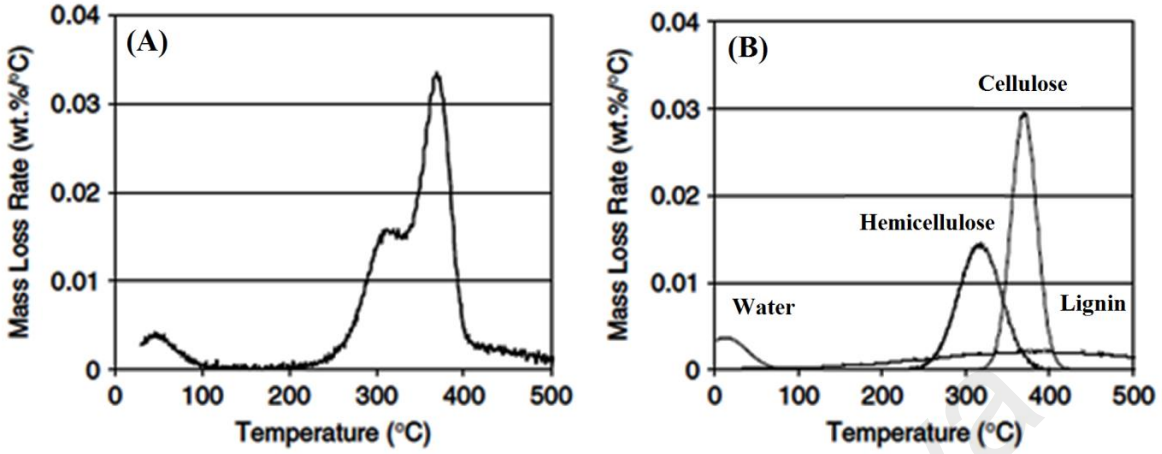

Figure 2.11: Differential thermogravimetric analysis curve for Reed(A) and the differential plot interpreted in terms of hemicelluloses, cellulose and lignin(B) (Venderbosch & Prins, 2010).

The compounds in bio-oil can vary by more than an order of magnitude. Bio-oil contains acids (acetic, propanoic), esters (methyl formate, butyrolactone, angelica lactone), alcohols (methanol, ethylene glycol, ethanol), ketones (acetone), aldehydes (acetaldehyde, formaldehyde, ethanedial), miscellaneous oxygenates (glycolaldehyde, acetol), sugars (1,6-anhydroglucose, acetol), furans (furfurol, HMF, furfural), phenols (phenol, DiOH benzene, methyl phenol, dimethyl phenol), guaiacols (isoeugenol, eugenol, 4-methyl guaiacol), and syringols (2,6-DiOMe phenol, syringaldehyde, propyl syringol). Depolymerization and fragmentation reactions of cellulose, hemicelluloses and lignin yield multi-component mixtures. The guaiacols and syringols are the example of lignin formed components, whereas sugars and furans are the example of cellulose and hemicellulose components, respectively. Decomposition of the miscellaneous oxygenates, sugars, and furans probably yield esters, acids, alcohols, ketones and aldehydes (George W. Huber et al., 2006).

Bio-oil potentially can be used as a fuel, but there are some demerits associated with it as poor volatility, high viscosity, high corrosiveness, instability and cold flow problems (Czernik & Bridgwater, 2004).

Reactive oxygenated compounds in bio-oil such as ethers, aldehydes, ketons, acids and alcohols can react and form higher molecular weight species. These heavy compounds formation, which is accelerated by increasing temperature and under oxygen and UV light exposure, can induce problems such as increased viscosity and phase separation (George W. Huber et al., 2006). High contents of aldehydes and ketones in bio-oil make it hydrophilic and highly hydrated, which result difficult elimination of water (T.-S. Kim et al., 2012; Q. Zhang, Chang, Wang, & Xu, 2007). Carboxylic acids available in bio-oil lead to low pH value of 2-3. High bio-oil acidity makes it very corrosive especially at elevated temperature, which imposes more requirements on storage vessels material of construction and transportation (Q. Zhang et al., 2007).

These problems have limited bio-oil applications as an engine fuel due to its low heating value, presence of oxygenated compounds and high water contents. So, bio-oil must be upgraded or blended to be used in diesel engines (George W. Huber et al., 2006).

2.2.3 Pyrolysis vapour upgrading using model compound approach

Bio-oil produced from the fast pyrolysis contains different types of oxygenated compound that make it unacceptable as transportation fuel component. One of the proposed solutions to stabilize bio-oil and reduce its oxygen content is to blend it with the feed of conventional hydrotreating processes (Douglas C. Elliott, 2007), although the pyrolysis oil transportation and storage before its blending are still seriously complicated.

Another alternative is pyrolysis vapor upgrading before being condensate. The vapors need to pass through certain stabilizing catalytic processes. In this condition, pyrolysis vapor

components undergo several reactions including cracking, aromatization, condensation, dehydration, decarbonylaation and decarboxylation. Through these reactions, oxygen can be removed in the form of CO, CO_2 and water. The catalysts could be selected as per process requirement. To achieve this goal, as an initial step, fundamental knowledge on reaction pathway is required. This can be achieved through model compound investigations. The outcome of these studies can provide direction toward selection of proper process and catalysts (Czernik & Bridgwater, 2004; Mohan et al., 2006).

The results of the model compound approach investigations to produce gasoline range molecules through conversion of small oxygenates (with minimum carbon loss), conversion of lignin-derived phenolics and conversion of sugar-derived compounds have been presented here under. The catalyst deactivation, as one of the important problems associated with catalytic bio-oil upgrading, has been studied as well.

2.2.3.1 Conversion of small oxygenates (with minimum carbon loss)

Small oxygenated compounds available in pyrolysis vapor such as acids, aldehydes, alcohols and ketones can be catalytically deoxygenated through dehydration, decarbonylation and decarboxylation to stable fuel like molecules. Also, by utilizing the appropriate catalysts and relatively high reactivity of the oxygen functionalities (carboxylic, carbonyl, hydroxyl, and ketonic groups) bonds (like C-C) forming reactions, such as ketonization, etherification, aldol condensation and aromatization can be conducted. It means instead of oxygen functionalities elimination too early, utilize them as a potential for production of high carbon deoxygenated fuel components (Resasco, 2011a).

2.2.3.1.1 Deoxygenation of small aldehyde

Pyrolysis vapor/bio-oil stabilization can be achieved through oxygen removal from its oxygenated compounds. Light aldehydes are one of the abundant oxygenated chemical groups available in pyrolysis vapor/bio-oil (Mullen & Boateng, 2008; Mullen, Boateng, Hicks, Goldberg, & Moreau, 2009). Recently, Ausavasukhi et al. (Ausavasukhi, Sooknoi, & Resasco, 2009) investigated the catalytic deoxygenation of benzaldehyde over gallium-modified ZSM-5 zeolite. A continuous flow system was utilized to investigate the effects of reaction condition varations (Table 2.6) such as carrier gas (H_2 or He), reaction temperature, and water co-feeding. Toluene and benzene were the main products of benzaldehyde conversion over Ga/HZSM-5 catalyst. Direct deoxygenation over Brønsted acid sites yielded benzene, while toluene was only produced in the presence of H_2 over GaH_2^+ species (Figure 2.12). These species were only generated under H_2 environment. In the absence of hydrogen, no toluene was yielded. Water co-feeding in the presence of Ga-modified HZSM-5 catalyst increased benzene/toluene ratio.

Table 2.6: Effect of catalyst type on product distribution (Ausavasukhi et al., 2009).

Type of catalyst	Temperature(°C)	Carrier gas	%Conversion	Product distribution(% yield)		
				Benzene	Toluene	Methane
HZSM-5	450	He	56.32	56.32	0.00	0.00
		H_2	54.23	54.23	0.00	0.00
3Ga/HZSM-5	450	He	55.80	55.80	0.00	0.00
		H_2	58.20	19.95	36.40	1.85
3Ga/HZSM-5	500	He	69.07	69.07	0.00	0.00
		H_2	70.22	20.42	43.71	6.09

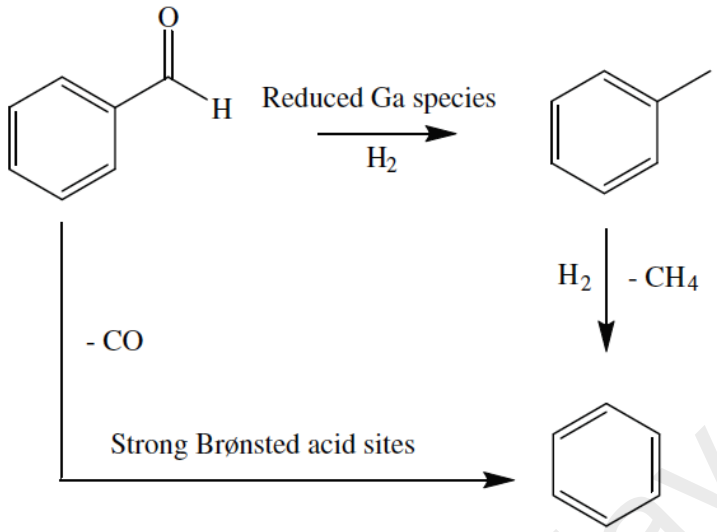

Figure 2.12: Catalytic deoxygenation of benzaldehyde over Ga/HZSM-5(Ausavasukhi et al., 2009).

In the other study done by Peralta et al. (Peralta, Sooknoi, Danuthai, & Resasco, 2009), deoxygenation of benzaldehyde to benzene and toluene over basic CsNaX and NaX zeolite catalysts was examined. The reaction was carried out at atmospheric pressure either in the presence of an inert gas or H_2 (Figure 2.13). Highly basic catalyst with excess Cs content conducted direct decarbonylation of benzaldehyde to benzene. However, condensation of surface products took place in parallel with direct decarbonylation. Toluene and benzene were produced through decomposition of surface condensation products. Dissociation of H_2 from zeolite (with and without Cs) surface cleaned the catalyst by decreasing the residence time of intermediates on surface. So, accumulation of non-decomposable products that caused the catalyst deactivation was decreased. After H_2 dissociation, it participated in decomposition of condensation surface products and consequently primary toluene was formed. NaX and CsNaX catalysts did not show a high initial activity for direct decarbonylation, but they operated to decompose surface condensation products to benzene

and toluene. A faster deactivation of NaX catalyst than CsNaX was observed due to the presence of residual acidity in it.

Comparing aforementioned ZSM-5 and NaX catalysts, incorporation of Ga and Cs, respectively, into the catalysts as well as reaction atmosphere changed the selectivity and yield toward benzene and toluene. High yield and selectivity toward benzene using Ga/HZSM-5 catalyst was observed under helium and water atmosphere whereas, CsNaX exhibited high yield and selectivity toward benzene under hydrogen atmosphere (Ausavasukhi et al., 2009; Peralta et al., 2009).

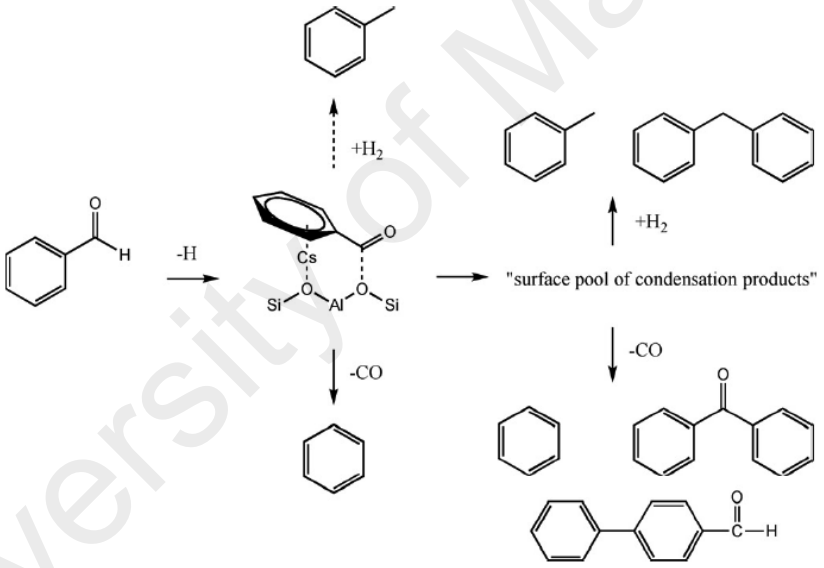

Figure 2.13: Reaction pathway of benzaldehyde conversion to benzene and toluene on basic CsNaX and NaX catalysts (Peralta et al., 2009).

2.2.3.1.2 Condensation/ketonization/aromatization of small aldehyde

Stabilized bio-oil can be achieved by utilizing the molecules oxygen functionalities to facilitate C-C bonds formation via aldol condensation or ketonization (Gaertner et al., 2009; Gangadharan et al., 2010). Gangadharan et al. (Gangadharan et al., 2010) selected propanal to investigate condensation reaction over $Ce_X Zr_{1-X} O_2$ mixed oxides catalyst. This reaction

modeled short aldehydes (found in bio-oil mixtures) conversion to gasoline range molecules. Different operating parameters comprising incorporation of acid and water in the feed were studied. The following important conclusions were drawn by them (Gangadharan et al., 2010): (a) Aldol condensation and ketonization were two pathways for propanal conversion to higher carbon chain oxygenates over ceria–zirconia catalyst. (b) Aldehyde aldol condensation reactions observed to be limited due to the competitive adsorption of acids presented in the feed. Presence of acid reduced the aldehyde adsorption and conversion. (c) Presence of water increased concentration of surface hydroxyl groups. It led to increase the catalyst activity by enhancing the formation of surface carboxylates. So, aldehyde ketonization was promoted, whereas aldol condensation was inhibited. (d) Presence of water improved the catalyst stability. (e) Cracking reaction was promoted to produce light oxygenates and light hydrocarbons in the presence of hydrogen. While the light hydrocarbon did not react further, the light oxygenates may be incorporated again to produce secondary products. (f) Shifting the balance of the acid-base properties of catalyst active sites could change the catalyst selectivity. Zr increasing favored formation of aldol products, while Ce increasing favored ketonization.

The reaction network shown in Figure 2.14 was proposed based on mentioned results. The contribution of two major reactions (aldol condensation and ketonization) can be seen in the network, involving various condensation steps (Gangadharan et al., 2010).

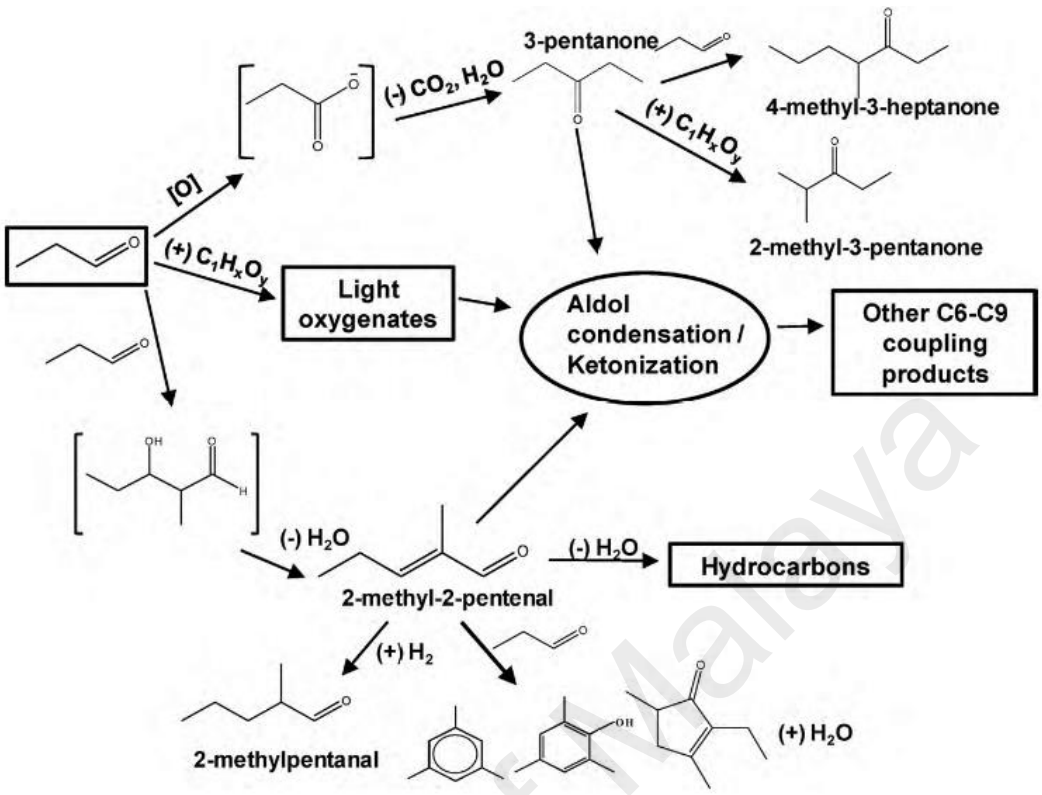

Figure 2.14: Proposed reaction pathway for propanal conversion over $Ce_{0.5}Zr_{0.5}O_2$ (Gangadharan et al., 2010).

The investigations on the conversion of propanal over large (2–5 μm) and small (0.2–0.5 μm) crystallite HZSM-5 catalysts at 400 °C and atmospheric pressure was undertaken by Hoang et al. (Hoang, Zhu, Lobban, et al., 2010). HZSM-5 crystallite size effects on the conversion of propanal to aromatics were investigated at rather mild conditions, 400 °C and atmospheric pressure. Due to the faster removal of products from small crystallite zeolite channels, which reduces production of coke precursors and coke, much slower catalyst deactivation was observed. Simultaneously, shorter diffusion path of small crystallites showed considerably less isomeration of xylene products to para-xylen than large crystallites.

In small crystallites, due to the shorter time for cracking before molecules diffuse out of zeolite, a higher fraction of C_9 aromatics was observed. C_9 aromatics were produced via propanal aldol condensation followed by cyclization. Therefore, the use of smaller crystallite

HZSM-5 was suitable to improve production of fuel- like alkyl aromatics from light oxygenates at mild operating conditions (Hoang, Zhu, Lobban, et al., 2010). On the other hand, in mixed oxide catalysts, increasing amount of zirconia led to a high yield of aromatic compounds due to an enhancement of the acid sites with zirconia increasing. The aromatization reactions were catalyzed by the acid sites (Gangadharan et al., 2010).

2.2.3.1.3 Etherification of alcohols and aldehyde

Ethers as one of the potential fuel components are prepared from oxygenates that could be used either in diesel blends or gasoline. More recently, Pham et al. (T. T. Pham et al., 2010) investigated on selectively production of di-alkyl ethers from etherification of alcohols and aldehydes on supported Pd catalysts. Figure 2.15 indicates the proposed reaction pathway. High rates of ether formation could be achieved while both alkoxide and η^2-adsorbed species were available on the catalyst surface. Moreover, stoichiometric 1:1 ratio of aldehyde and alcohol was found to be the optimum. Larger sintered and annealed metal particles showed higher ether selectivity, but lower conversion. It is due to enhancement of ensembles needed for etherification.

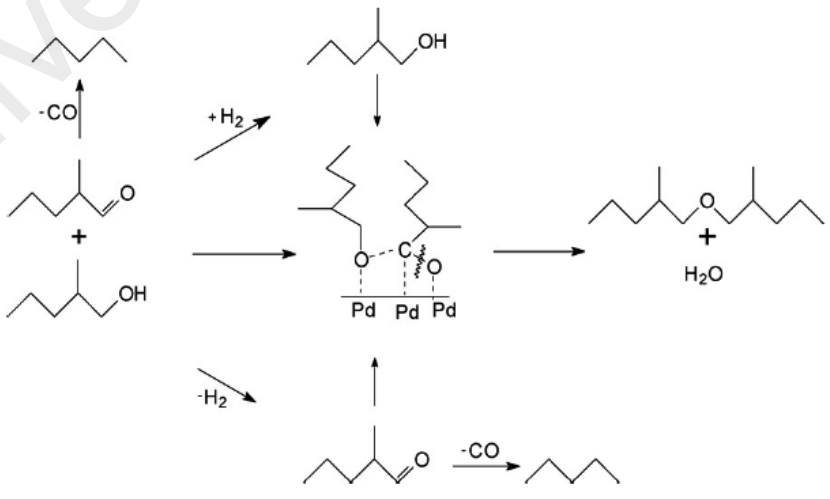

Figure 2.15: Schematic reaction pathway of 2-methylpentanal on Pd catalyst (T. T. Pham et al., 2010).

2.2.3.1.4 Hydrodeoxygenation of small aldehyde

Generally, removal of oxygen from biomass originated molecules is essential to improve the fuel properties. Research octane number (RON), as a primary screening tool, is an important indicator to show if a molecule is potentially suitable to be used as fuel. Studies showed quite high octane numbers for the alcohols produced from 2-methyl-2-pentenal hydrogenation (Do, Crossley, Santikunaporn, & Resasco, 2007). Pham et al. (T. T. Pham, Lobban, Resasco, & Mallinson, 2009) studied hydrodeoxygenation and hydrogenation of 2-methyl-2-pentenal over platinum, palladium, and copper catalysts supported on precipitated silica in the temperature range of 200–400°C. The catalyst's activity followed the order Pt > Pd > Cu. The reaction pathway has been shown in Figure 2.16. The modeled reactions rate constants are tabulated in Table 2. The mentioned aldehyde is a molecule with the reactive functional groups of C=C and C=O which are typical in the oxygenated molecules available in bio-oil produced from pyrolysis. Hydrogenation activity of both C=C and C=O bonds over 0.5 wt.% Pd and Pt catalysts was investigated. Strong hydrogenation of the C=C bond to form 2-methyl-pentanal was observed over 0.5 wt. % Pd and Pt. Cu/SiO_2 (5 wt. %) showed strong C=O initial hydrogenation activity to produce 2-methyl-2-pentenol. It then converted to 2-methyl-pentanol which was in equilibrium with 2-methyl-pentanal at higher conversion. As shown in Table 2.7, the relative hydrogenation rate of C=C versus C=O bond could be estimated by the ratio of k_1/k_2 for all catalysts. Considering Pt and Pd, this ratio was about 6, which indicated these metals were more selective for C=C hydrogenation. Conversely, much lower k_1/k_2 ratio for Cu (0.65) showed this metal was less selective for this type of hydrogenation. C–C cleavage over Pt and Pd catalysts, which led to decarbonylation, became significant at higher temperature or higher ratio of catalyst to feed. C–O hydrogenolysis on Cu yielded 2-methyl-pentane as minor product at 200 °C. It became the major product over

Cu, when temperature was increased to 400 °C. Due to the stability of 2-methyl-pentanol and its fairly good octane number, practically its production may be desirable over Cu catalyst at low temperature. Cu showed to be a desirable catalyst for total oxygen removal without carbon loss at higher temperatures. Despite higher Pt and Pd catalysts activity and their high selectivity for C=C hydrogenation, the loss of carbon through decarbonylation (yielding n-pentane and CO) was a disadvantage when the goal was conversion of small molecules to useful fuel range molecules with low carbon loss.

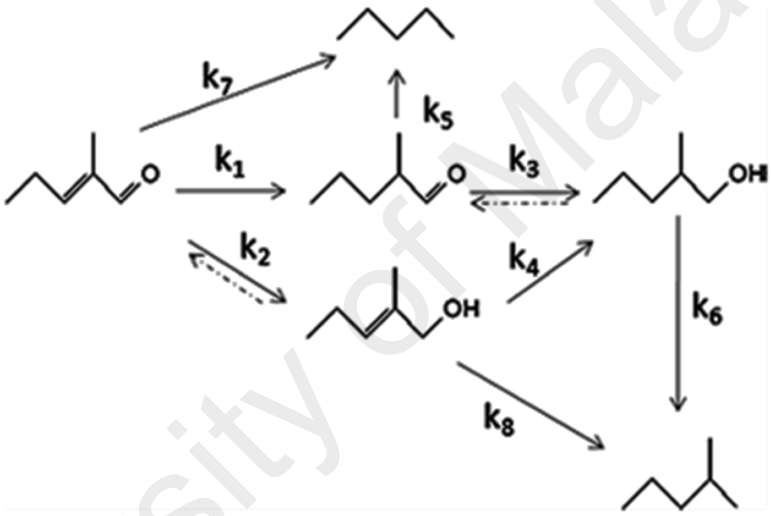

Figure 2.16: Schematic conversion of 2-methyl-2-pentenal on Pt, Pd, and Cu(see Table 2) (T. T. Pham et al., 2009).

Table 2.7: First-order model rate constants (s^{-1}) (See Fig.11) (T. T. Pham et al., 2009).

Metal	Pt	Pd	Cu
Loading (wt %)	0.5%	0.5%	5%
k_1	2.65	0.2	0.01
k_2	0.41	0.04	0.01
k_3	0.29	0.44	0.00
k_4	19.64	1.12	0.09
k_5	0.29	0.02	0
k_6	0	0	0.01
k_7	0.93	0.10	0
k_8	0	0	0.02
k_1/k_2 ratio	6.5	5.67	0.65
k_7/k_1 ratio	0.35	0.47	0

2.2.3.1.5 Ketonization of small carboxylic acid

Small acid compounds such as propanoic acid and acetic acid are the most abundant oxygenated molecules available in bio-oil (I. Y. Eom et al., 2012; Eom et al., 2013). They not only cause corrosion problems, but also significantly reduce bio-oil stability.

In ketonization reaction, coupling of two carboxylic acid molecules produce ketone molecule while H_2O and CO_2 are eliminated. The produced ketones have potential to undergo further aldol condensation reactions (C-C coupling) to produce larger fuel-like hydrocarbons (T. N. Pham et al., 2014).

Recently, Yamada et al. (Yamada, Segawa, Sato, Kojima, & Sato, 2011a) investigated the ketonization of acetic acid over a series of rare earth oxides (REOs) catalysts at 350° C and under atmospheric pressure of nitrogen. Acetic acid conversion and selectivity over calcined (1000 °C) REOs catalysts at mentioned operating conditions has been shown in Table 2.8. The REOs catalysts such as La_2O_3, CeO_2, Pr_6O_{11}, and Nd_2O_3 showed the acetic acid conversion of ~38 to ~80% and the selectivity to acetone over 99.9%. Among fourteen studied REOs, Pr_6O_{11} showed the highest yield of 80% and Nd_2O_3 showed the highest selectivity of 100%. After acetic acid ketonization, several active REO catalysts were converted into an oxyacetate such as MO(AcO), M = La, Pr, and Nd (AcO indicates CH_3COO group). On the other hand, in case of CeO_2, its surface was converted into acetate while the bulk structure of CeO_2 was retained during the ketonization. The specific surface area of CeO_2 and produced oxyacetate was proportional to acetone yield. It was concluded that, acetic acid ketonization over REOs catalysts continued on the surface of the oxyacetate like MO(AcO) via the catalytic cycle between MO(AcO) and $M_2O(AcO)_4$ to produce acetone and CO_2 with the consumption of acetic acid.

Table 2.8: Conversion and selectivity of acetic acid (Yamada et al., 2011a).

Rare earth oxides	Surface area (m^2g^{-1})	Conversion (%)	Selectivity (mol %)			Acetone yield (%)
			Acetone	Acetic anhydride	Others	
La_2O_3	6.8	77.7	99.9	0.0	0.1	77.6
CeO_2	13.2	51.3	99.9	0.0	0.1	51.2
Pr_6O_{11}	4.6	80.1	99.9	0.0	0.1	80.0
Nd_2O_3	3.7	37.9	100	0.0	0.0	37.9

2.2.3.1.6 Conversion of small alcohol to hydrocarbon

Bio-oil, which is a complex mixture of oxygenates, is immiscible with hydrocarbons and relatively unstable. Bio-oil deoxygenation and its transformation into a mixture of hydrocarbons over zeolite catalysts could guarantee compatibility with conventional gasoline (Mentzel & Holm, 2011). Conversion of methanol to hydrocarbon (MTH) over H-ZSM-5 catalyst and the pertained reactions mechanism was studied by Bjorgen et al. (Bjorgen et al., 2007). They suggested two simultaneous mechanistic cycles run during the MTH reaction over H-ZSM-5 as follows: (a) formation of ethane/aromatics from methylbenzenes and then remethylation, and (b) ethylation/cracking cycle producing propene and higher alkenes. This can be observed in Figure 2.17, where cycle I is aromatics (toluene and trimethylbenzene) /ethane cycle and cycle II is alkene-based cycle.

It may be asked whether two cycles (I and II) act independently or they are linked together in some manner. According to the results obtained by Bjorgen et al. (Bjorgen et al., 2007), it was concluded that they could not run completely independent over H-ZSM-5 catalyst.

Considering the mentioned mechanism, Ilias et al. (Ilias & Bhan, 2012) investigated on the selectivity of methanol-to-hydrocarbons conversion on H-ZSM-5 by co-processing olefin or aromatic compounds. They could control the composition of organic hydrocarbons and therefore manipulate the contributions of aromatic methylation and olefin cycles in MTH. Consequently, they could manage the selectivity of aromatics, C_4–C_7 aliphatics and ethene.

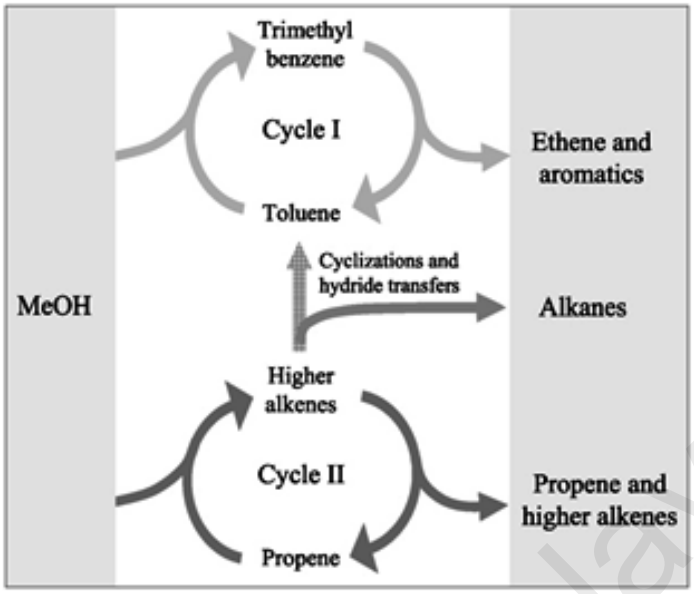

Figure 2.17: Dual cycle concept for the conversion of methanol over H-ZSM-5 (Bjorgen et al., 2007).

2.2.3.2 Conversion of lignin-derived phenolics

Selective cleavage of carbon-oxygen bonds of aromatics in lignin structure is a primary goal to unlocking the potential of lignocellulosic biomass to be used for biofuels production. Lignin is very difficult to upgrade due to its complex structure and recalcitrant nature. Furthermore, lignin comprises many phenolic moieties which can deactivate zeolite catalysts (Zakzeski et al., 2010). Anisol and guaiacol have been selected as model compound of lignin-derived phenolics for the investigations (Hicks, 2011b).

2.2.3.2.1 Anisole and guaiacol alkylation and deoxygenation

Zeolite catalysts have been widely studied for industrial alkylation and transalkylation of aromatic compounds (Perego & Ingallina, 2002). Anisole, a typical component of bio-oil, conversion over HZSM-5 catalyst was studied by Zhu et al. (Zhu et al., 2010). It was selected as a model compound in catalyst and reaction evaluation for bio-oil upgrading. The kinetics studies (pseudo first-order kinetic model) showed anisole (which its methoxy group could

provide interesting chemistry) could participate in both unimolecular and bimolecular reactions. Figure 2.18 shows the reaction pathways. In order to quantify the contribution of each suggested reaction pathway and determine the dominant paths, a simple kinetic model was employed. Table 2.9 indicates the proposed reactions kinetics data. Bimolecular anisole transalkylation was observed to be dominated at low contact time and higher feed concentrations. At higher space time, secondary bimolecular reactions involving cresol, phenol and methylanisole became significant. Moreover, several parallel unimolecular reactions also took place. Shape selectivity was obvious in the distribution of different methylanisole isomers. Contrary, cresol isomers distribution was dominated by electrophilic substitution at low conversions and then by thermodynamic equilibrium. Conversion variation by reaction parameters such as reaction temperatures, space time, presence of hydrogen carrier, or catalyst deactivation gained the same product distribution. Contrary, product distribution drastically changed while water was added to the feed. Moreover, it was observed that the presence of water in the feed improved the zeolite catalyst activity without changing the stability, most likely due to the involvement of methoxy group hydrolysis.

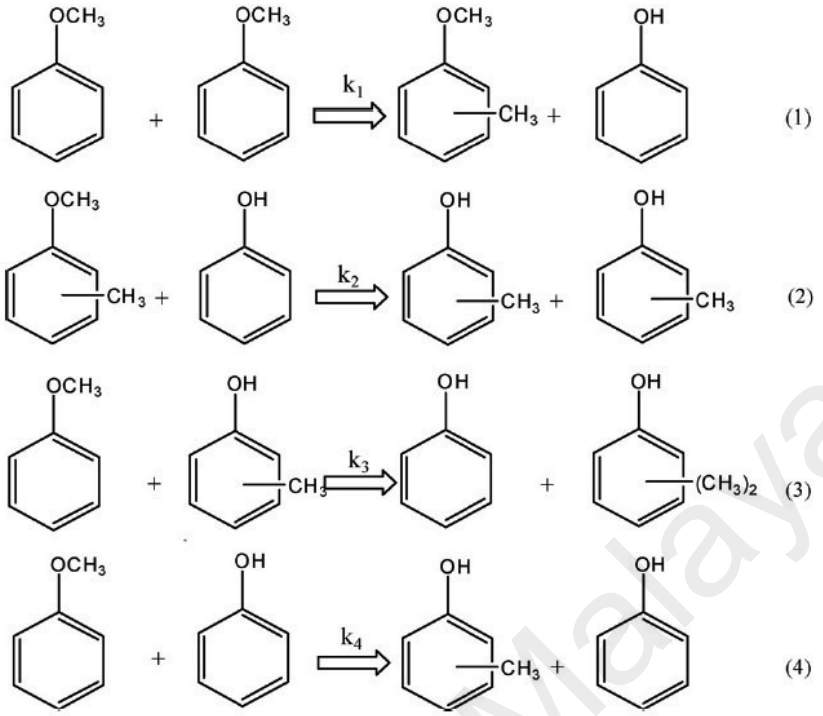

Figure 2.18: Proposed major reaction pathways of anisole conversion over HZSM-5 (see Table 2.9) (Zhu et al., 2010).

Table 2.9: Proposed elementary reactions and fitted reaction rate constant k_i over HZSM-5(Zhu et al., 2010). (An: Anisole, Ph:Phenol, MA: Methylanisole, Cr: Cresol, Xol: xylenol isomers).

Number	Reaction	Fitted k_i	
		($\times 10^{-5}$ L mol^{-1}h^{-1})	(h^{-1})
1	An + An → Ph + MA	0.032	
2	Ph + MA → Cr + Cr	0.25	
3	Cr + An → Ph + Xol	0.20	
4	Ph + An → Cr + Ph	0.16	
5	MA → Cr		0.093
6	Xol → Cr		0.38
7	Cr → Ph		0.37
8	An → Ph		0.093
9	An → Cr		0.35
10	MA → Xol		0
11	Cr + Cr → Ph + Xol	0	

In an earlier study, Zhu et al. (Zhu et al., 2011) investigated the catalytic conversion of anisole over a bifuctional Pt/HBeta catalyst (Figure 2.19) at 400 °C and atmospheric pressure. Comparison of bifunctional and monofunctional catalysts (Pt/SiO_2 and HBeta) indicated that

acidic function (HBeta) catalyzed transalkylation from methoxy to the phenolic ring. Therefore, phenol, xylenols, and cresols were produced as the main products. On the other hand, Pt was observed to only catalyze demethylation, hydrodeoxygenation, and hydrogenation reactions, sequentially. Methyl transfer and hydrodeoxygenation reactions were accelerated by Pt addition to zeolite. These reactions took place with low hydrogen consumption and low carbon loss as methane. Rate of O–CH_3 cleavage was improved in the presence of metal and therefore enhanced the overall rate of methyl transfer reactions (catalyzed by Brønsted acid). Further, the stability of catalyst with moderate coke reduction was achieved due to metal addition to zeolite. Thus, it was concluded that, metal-zeolite properties optimization might be led to an efficient catalyst for the hydrodeoxygenation of phenolics rich bio-oils.

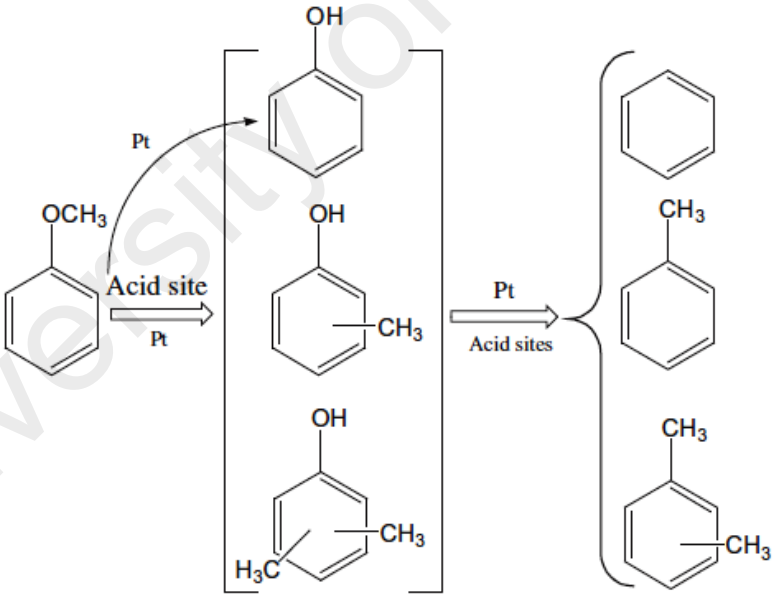

Figure 2.19: Major reaction pathway for anisole conversion over 1% Pt/H-Beta. Reaction conditions: T = 400 °C, P = 1 atm, H_2/Anisole = 50, TOS = 0.5 h (Zhu et al., 2011).

Recently, Prasomsri et al. (Prasomsri et al., 2011) utilized flow and pulse reactors to examine the conversion of pure anisole and its mixtures with propylene, n-decane, benzene, or tetralin, over HY(Table 5) and HZSM-5 zeolites. Most of the studies were done on HY zeolites,

which are known active components in fluid catalytic cracking (FCC) catalysts. During several dominant transalkylation steps, anisole conversion produced phenol, cresols, xylenols and methylanisoles as the main products over HY zeolite. As can be seen in Table 2.10, due to addition of anisole to tetralin (an effective hydrogen donor molecule), considerable effects on distribution of products were observed. Moreover, while pure anisole feeding showed fast catalyst deactivation due the coke deposition, the addition of tetralin to the feed caused lower quantities of carbon deposits and catalyst stability enhancement.

Table 2.10: Product distributions from conversion of anisole and anisole-tetralin mixture (~50% tetralin) over HY zeolite. T = 400 °C, P = 1 atm under He (Prasomsri et al., 2011).

Feed	Anisole		Anisole + Tetralin	
	TOS=0.5 h	TOS=3.0 h	TOS=0.5 h	TOS=3.0 h
Conversion of Anisol	83.6	13.9	100	100
Conversion of Tetralin			98.4	96.6
Weight Percent at reactor outlet				
C_1-C_5	1.2	0.2	8.8	8.2
Anisole	16.4	86.1	0.0	0.0
Phenol	35.2	6.8	28.1	29.2
Methylanisoles	3.3	4.2	0.0	0.0
Cresols	26.4	1.4	12.5	13.1
Xylenols	17.5	1.3	2.8	2.8
Benzene	0.0	0.0	2.1	1.9
Toluene	0.0	0.0	3.5	3.0
Alkylbenzene	0.0	0.0	9.7	8.8
Tetralin	0.0	0.0	0.8	1.7
Naphthalene	0.0	0.0	20.0	19.9
Alkylnaphthalene	0.0	0.0	9.9	9.5
Heavies	0.0	0.0	1.8	1.9
Selectivity of anisole product (wt%)				
Methane	1.4	1.4	2.8	1.1
Phenol	42.1	48.9	63.7	64.0
Methylanisoles	3.9	30.2	0.0	0.0
Cresols	31.6	10.1	27.4	28.7
Xylenols	20.9	9.4	6.1	6.1

In the other investigation, Gonzalez-Borja et al. (González-Borja & Resasco, 2011) carried out hydrodeoxygenation of anisole and guaiacol over monolithic Pt-Sn catalysts. Figure 2.20 depicts deoxydenation and transalkylation/deoxygenation pathways of anisole and guaiacol over Pt-Sn/CNF/Inconel catalyst. Generally, monolithic catalysts have important advantages

thanks to the generation of low pressure drop even at high reactants flow rate. So, they are a very good candidate for biomass pyrolysis vapor upgrading, where pyrolysis reactors operate at atmospheric condition. In this study, mono and bimetallic (Pt-Sn alloy) monoliths catalysts were synthesized and tested for the deoxygenation of guaiacol and anisole. Fully deoxygenation of guaiacol and anisole observed over both Pt-Sn/Inconel and Pt-Sn/CNF/Inconel (Coated inconel monoliths with in-situ-grown carbon nanofibers) catalysts. Phenol and benzene were the most important products obtained from the mentioned feeds over monolithic catalysts. Compared with the monoliths without coating, CNFs coated catalysts increased monoliths surface area more than 10 times, which provided higher metal uptake during active-phase incorporation. Although, Pt-Sn/CNF/Inconel monolith found to be a promising catalyst for the upgrading of pyrolysis bio-oil, but catalyst deactivation needed to be improved.

As explained above, incorporation of Pt and Pt-Sn metals into HBeta and CNF/Inconel monolith catalysts, respectively, could improve catalysts selectivity and stability (González-Borja & Resasco, 2011; Zhu et al., 2011). Although, in case of HY zeolite, these improvements of catalyst could be achieved by addition of a hydrogen donor molecule (like tetralin) to the feed (Prasomsri et al., 2011).

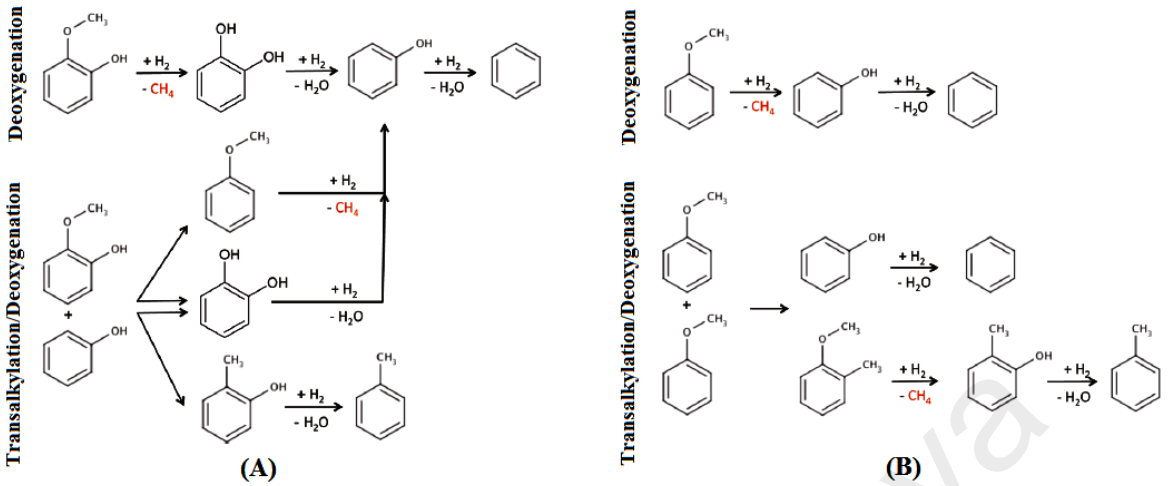

Figure 2.20: Reaction pathways for guaiacol(A) and anisole(B) deoxygenation on the Pt Sn/CNF/Inconel catalyst (González-Borja & Resasco, 2011).

2.2.3.3 Conversion of sugar-derived compounds

Among numerous oxygenated compounds commonly found in bio-oil, furfural was selected as a model for sugar derived compounds. These compounds have high reactivity and needed to be catalytically deoxygenated to improve bio-oil storage stability, boiling point range, and water solubility (Sitthisa & Resasco, 2011). Furfural is produced both during the dehydration of sugars and cellulose pyrolysis.

2.2.3.3.1 Furfural decarbonylation, hydrogenation and hydrodeoxygenation

Conversion of aldehydes, one of undesirable reactive components available in bio-oil, to alcohols has been studied over different metal based catalysts by several researchers (Ausavasukhi et al., 2009; Bejblová, Zámostný, Červený, & Čejka, 2005). Group Ib metals like Cu could catalyze conversion of furfural to furfuryl alcohol, but decarbonylation only observed with high metal loading at high temperature (H.-Y. Zheng et al., 2006). In contrast, metals like Pd from group VIII, indicated much higher activity for furfural decarbonylation (R. D. Srivastava & Guha, 1985). Sitthisa et al. (Sitthisa et al., 2011) carried out the

conversion of furfural under hydrogen and over silica- supported monometallic Pd and bimetallic Pd–Cu catalysts. Figure 2.21 shows two parallel routes in furfural conversion over Pd catalyst. First, its decarbonylation to furan and then hydrogenation to terahydrofuran (THF), and second, furfural hydrogenation to furfuryl alcohol and then hydrogenation to tetrahydro furfuryl alcohol. Studies on furfural deoxygenation reactions over Pd and Pd–Cu catalysts concluded the following: (a) Decarbonylation of furfural as an aldehyde over Pd catalyst was the dominant reaction even at low space time (W/F= catalyst mass/ mass flow rate of reactant). This was due to the decomposition of an acyl intermediate in to CO and hydrocarbons at higher temperatures. In the presence of Pd catalyst, high decarbonylation/hydrogenation ratio was observed. (b) Furfural hydrogenation probably occurred via a stable hydroxyalkyl intermediate. (c) Pd–Cu alloy catalyst was made through incorporation of Cu on to Pd/SiO2 catalyst. Due to different electronic structure of alloy from pure Pd, the formation of the side-on η^2-(C–O) aldehyde species were less stable on Pd–Cu than on pure Pd. So, the formation of the acyl intermediate likely decreased and it led to reduction of decarbonylation rate on Pd-Cu catalysts, whereas the hydrogenation rate was increased.

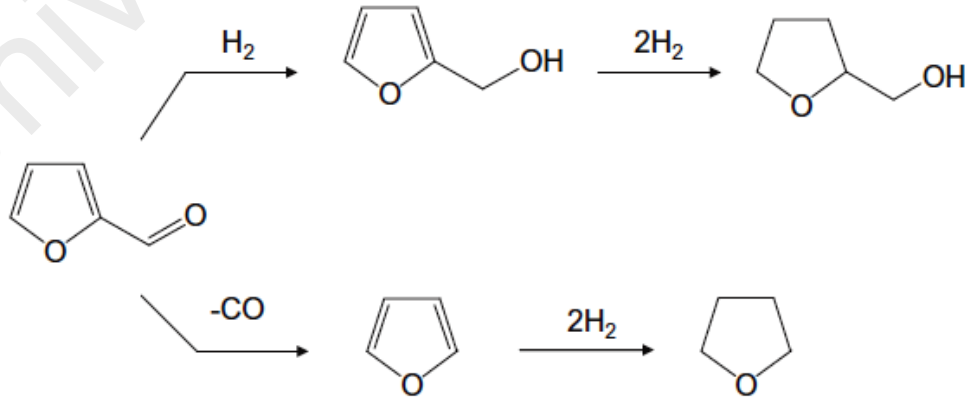

Figure 2.21: Major reactions pathway for furfural conversion over Pd catalyst (Sitthisa et al., 2011).

The hydrodeoxygenation of furfural over three various metal catalysts, Cu, Pd and Ni supported on SiO_2 was carried out by Sitthisa et al. (Sitthisa & Resasco, 2011). The catalysts studies were performed in a continuous-flow reactor under hydrogen atmosphere and temperature range of 210–290 °C. The products distribution was a strong function of used metal catalyst. Figure 2.22 indicates the possible furfural conversion reaction pathways and shows which paths are favored over Pd, Ni and Cu catalysts. The reactions over silica supported Cu, Pd, and Ni catalysts showed different products distribution in terms of molecular interactions with the metal surface as following: (a) Furfuryl alcohol was produced over Cu catalyst via carbonyl group hydrogenation. This was due to preferred adsorption on Cu, η^1 (O) – aldehyde. Since furan ring adsorption was not favored on Cu surface, no products from furanyl ring activation was observed. (b) Due to the formation of acyl surface spices, Pd catalyst yielded decarbonylation products. Since there was a strong interaction between Pd and ring, products yielded from ring hydrogenation were observed. (c) Ni showed a product distribution similar to that of Pd. Due to furan stronger interaction with Ni surface; it further reacted with hydrogen, thus formed ring opening products.

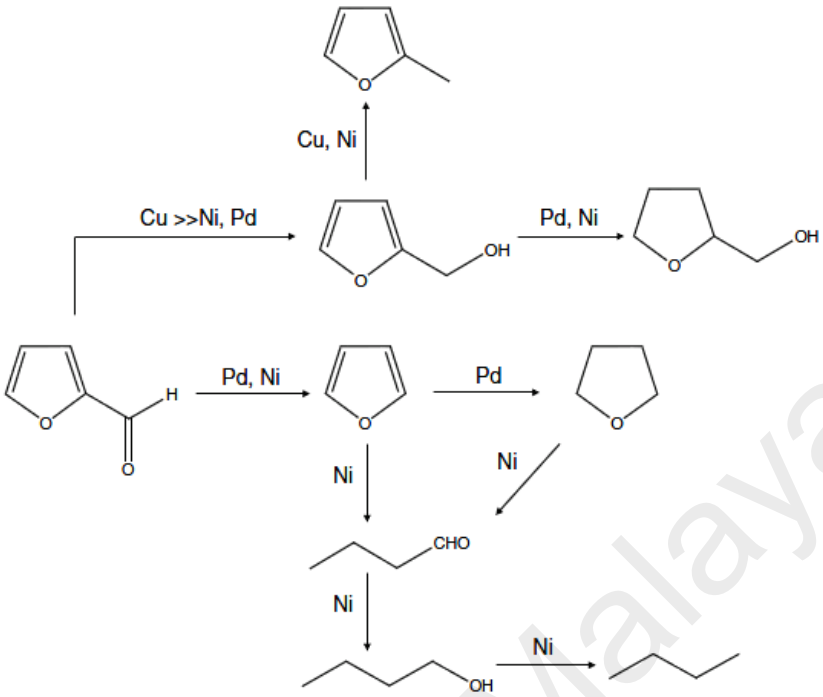

Figure 2.22: Possible reaction pathways for furfural conversion over Cu, Pd and Ni catalysts (Sitthisa & Resasco, 2011).

2.2.3.3.2 Hydrogenation- esterification of furfural

Bio-oil mostly comprises furan and acid compounds with the approx. weight percentage of 26% and 12%, respectively (George W. Huber et al., 2006). The major abundant acid and furan components in bio-oil are acetic acid and furfural, respectively (George W. Huber et al., 2006). They are undesirable components in bio-oil due to their high corrosiveness and reactivity (W. Yu et al., 2011a, 2011b; Q. Zhang et al., 2007). The desired combustible products can be stable oxygenates such as alcohols and esters. So, reaction of acids and aldehydes can lower bio-oil acidity and improve its stability.

Furfural and other furan derivatives are prone to deactivate catalysts significantly; therefore it is quite a serious challenge to convert available furfural in crude bio-oil to a stable compound. So, furfural and acetic acid were selected as model compounds to be studied in this investigation. Yu et al. (W. Yu et al., 2011a) evaluated Al-SBA-15 and $Al_2(SiO_3)_3$

supported palladium bifunctional catalysts for one-step hydrogenation–esterification (OHE) of furfural and acetic acid as a model reaction for bio-oil upgrading. The OHE reaction of furfural and acetic acid is illustrated in Eq.(2-1) (W. Yu et al., 2011a).

The results of their researches were summarized as following: (a) Al-SBA-15 showed better performance as supports of bifunctional catalysts than $Al_2(SiO_3)_3$. OHE of furfural and acetic acid in the presence of Al-SBA-15 catalyst (support) yielded desired products. (b) Esterification of furfuryl alcohol and acetic acid was favored by Al-SBA-15 with medium acidity. So, it could benefit the one-step hydrogenation–esterification of furfural and acetic acid. (c) A synergistic effect between acid and metal sites for the OHE reaction over composite bifunctional catalysts of 5% $Pd/Al_2(SiO_3)_3$ or 5% Pd/Al-SBA-15 was observed compared with the mixed bifunctional catalysts. (d) The OHE reaction of furfural and acetic acid was viable over either composite bifunctional (5% Pd/Al-SBA-15) or mixed bifunctional (5% Pd/C + Al-SBA- 15) catalysts, attributed to the performing of hydrogenation and esterification reactions. OHE reaction on mesoporous materials supported metal as catalysts was a more efficient route for catalytic upgrading of real bio-oil, since there is greater accessibility of large molecules to acid sites in Al-SBA-15 relative to $Al_2(SiO_3)_3$.

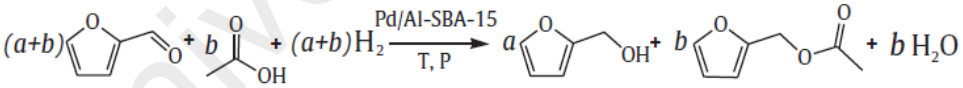

(2-1)

Although in this study one-step hydrogenation-esterification reaction was carried out at high pressure, but it could give an interesting idea for further investigation on performing the similar reactions at atmospheric condition, which would be desirable for in-situ biomass vapor upgrading in an integrated process.

Table 2.11: Summary of model compounds used in bio-oil upgrading researches under different catalysts and reaction conditions.

Feed	Product	Reaction Type	Catalyst	Operating Conditions	Yield (Y) & Selectivity (S) (%)	Ref.
Benzaldehyde	Benzene- Toluene	Deoxygenation-Decarbonylation	Ga/HZSM-5	T = 500°C P= 1 atm	$Y^{(b)}_{Benzene}$= 69.07 $S^{(b)}_{Benzene}$= 100	(Ausavasukhi et al., 2009)
Benzaldehyde	Benzene - Toluene	Deoxygenation Decarbonylation	Basic CsNaX, NaX zeolite	T = 500 °C P= 1 atm.	$Y^{(c)}_{Benzene}$= 70 $S^{(c)}_{Benzene}$= 77.8 $Y^{(c)}_{Toluene}$= 20 $S^{(c)}_{Toluene}$= 22.2	(Peralta et al., 2009)
Propanal	C_6- C_9	Aldol condensation Ketonization	Ce_X Zr_{1-X} O_2 mixed oxides	T = 400°C P= 1 atm.	$Y^{(d)}$ = ~35 $S^{(d)}$ = ~40	(Gangadharan et al., 2010)
Propanal	Aromatics	Aldol condensation Aromatization	Crystallite HZSM-5	T = 400° C P= 1 atm.	$Y^{(e)}$ = ~50 $S^{(e)}$ = ~52	(Hoang, Zhu, Lobban, et al., 2010)
Aldehydes - alcohols	Di-alkyl ethers	Etherification	Supported Pd catalysts	T= 125° C P= 1 atm.	$Y^{(f)}$ = 11.9 $S^{(f)}$ = 50.1	(T. T. Pham et al., 2010)
2-Methyl-2-pentenal	2-Methyl-2-pentane 2-Methyl-2 pentanol	Hydrodeoxygenation and hydrogenation	Platinum, palladium, and copper on silica	T= 200°C P= 1 atm	$Y^{(g)}_{2\text{-Me-2-pentanol}}$= 70 $S^{(g)}_{2\text{-Me-2-pentanol}}$ = 70	(T. T. Pham et al., 2009)
Acetic acid	Acetone	Ketonization	Rare earth oxides (REOs) such as La_2O_3, CeO_2, Pr_6O_{11}, and Nd_2O_3	T = 350°C P= 1 atm.	$Y^{(h)}$ = 99.9-100 $S^{(h)}$ = 37.9(Nd_2O_3)-80(Pr_6O_{11})	(Yamada et al., 2011a)
Methanol	Hydrocarbons, Aromatics	Deoxygenation, Aromatization	HZSM-5	T = 290-390°C $P^{(a)}$ = 1 atm	$Y_{C6+}{}^{(i)}$ = 20.7 $S_{C6+}{}^{(i)}$ = 28.4	(Bjorgen et al., 2007; Ilias & Bhan, 2012)
Anisole	Cresol, Phenol & Methylanisole	Transalkylation	HZSM-5	T = 400°C P= 1 atm.	$Y^{(j)}$= 6(MA), 32(Cr), 33(Ph) $S^{(j)}$= 6.7(MA), 35.5 (Cr), 36.7(Ph)	(Zhu et al., 2010)
Anisole	Benzene Alkylbenzenes	Transalkylation-Hydrodeoxygenation	Pt/HBeta	T = 400°C P= 1 atm	$Y^{(k)}$=S=51.2(Bn), 27.6(Tn), 10.6(Xn)	(Zhu et al., 2011)
Anisole and tetralin	Phenol, cresols, xylenols and methylanisoles	Transalkylation	HY- HZSM-5	T = 400°C P= 1 atm.	$Y^{(l)}$ = 29.2(Ph), 13.1(Cr), 2.8(Xnol) $S^{(l)}$= 64(Ph), 28.7(Cr), 6.1(Xnol)	(Prasomsri et al., 2011)

‘Table 2.11, continued’

Feed	Product	Reaction Type	Catalyst	Operating Conditions	Yield (Y) & Selectivity (S) (%)	Ref.
Anisol- guaiacol	Toluene, benzene, phenols	Deoxygenation-Transalkylation	Pt-Sn/Inconel Pt-Sn/CNF/Inconel	T = 400°C P= 1 atm	(An: $Y^{(m)}$ = 12(Ph), 35(Bn), 3(Tn) $S^{(m)}$= 21.8(Ph), 63.6(Bn), 5.4(Tn)) (Gu: $Y^{(m)}$ = 70(Ph), 10(Bn), 2(Tn) $S^{(m)}$= 71.4(Ph), 10.2(Bn), 2(Tn))	(González-Borja & Resasco, 2011)
Furfural	Furan- C_4	Hydrodeoxygenation	Metal catalysts, Cu, Pd on SiO_2	T = 210-290° C P= 1 atm.	$Y^{(n)}$=$S^{(n)}$=50(Furan), 24(Butane)	(Sitthisa & Resasco, 2011)
Furfural-2-methylpentanal	THF, Furfuryl alcohol, Furan, Ether, C_5, 2-methylpentanol	hydrogenation, decarbonylation, etherification	Pd, Pd–Cu on SiO_2	T =125-250°C P=1 atm	(Furf: $Y^{(o)}$ = 16(Fu), 8(FOL), 2.5(THF) $S^{(o)}$= 58(Fu), 28(FOL), 9(THF)) (MP: $Y^{(o)}$ = 15(Et), 10(MPOL), 4(C_5) $S^{(o)}$= 53(Et), 36(MPOL), 14(C_5))	(Sitthisa et al., 2011)
Furfural and acetic acid	Furfuryl alcohol, Ester(furfuryl acetate)	Hydrogenation–Esterification (OHE)	Al-SBA-15 and Al_2 $(SiO_3)_3$ supported palladium	T= 150°C P= 2 MPa	$Y^{(p)}$=43.2(FOL),12.8 (FA), $S^{(p)}$= 61.8 (FOL), 18.2(FA)	(W. Yu et al., 2011a)

(a) Feed partial pressure in He carrier gas at 20 °C is 13 kPa; (b) W/F = 100 g h/mol, carrier gas = He; (c) W/F = 942 g h/mol, carrier gas = H_2, TOS=400 min, catalyst: CsNaX; (d) W/F= 1 h under H_2; (e) Small crystalline HZSM-5 (Si/Al=45) catalyst, TOS=30 min, W/F=0.2 h under H_2 ; (f) 16 wt.% Pd/SiO_2 catalyst, W/F=1 h under H_2; (g) On 5 wt.% Cu/SiO_2 catalyst at W/F = 1 h, H_2: feed ratio = 12:1; (h) Conversion and selectivity were averaged in the initial 2.5 h, W/F = 0.187 g h cm^{-3};(i) Reaction temperature T= 350°C; (j) MA: Methylanisole, Cr: Cresol, Ph: Phenol, W/F=0.5 h, carrier gas = He; (k) Bn: Benzene, Tn: Toluene, Xn: Xylene, W/F=0.33h on 1%Pt/HBeta catalyst; (l) Ph: Phenol, Cr:Cresols, Xnol:Xylenols, anisole-tetralin mixture (50% tetralin) over HY zeolite catalyst, W/F = 0.42 h, TOS=3h; (m) An:Anisol, Gu:Guaiacol, Ph:Phenol, Bn:Benzene, Tn:Toluene, TOS=45 min, $(W/F)_{An}$=1.3 h, $(W/F)_{Gu}$ =1 h; (n) T=250° C, W/F=9.6 gcat/(mol/h), H_2/Feed ratio = 25, TOS = 15 min; (o) Furf=Furfural, Fu=Furan, FOL= Furfuryl alcohol, Et=Ether, MP=2-methylpentanal, MPOL=2-methyl-pentanol; Y&S (Furf): Pd-Cu/SiO_2(0.5%Cu) catalyst, W/F = 0.1 h, Temp = 230 °C, H_2/Feed = 25, TOS = 15 min ; Y&S (MP): Pd-Cu/SiO_2(2.5%Cu) catalyst, W/F = 3 h, Temp = 125 °C, H_2/Feed = 12, TOS = 15 min; (p) FA: furfuryl acetate , FOL: furfuryl alcohol.

Table 2.11 shows summary of the different model compound approach investigations have been surveyed under different catalyst types and reaction conditions.

2.2.3.4 Catalyst deactivation

The catalyst deactivation is one of the major problems in catalytic bio-oil upgrading. It is proposed that the deactivation is caused by not only coke formation, but also the strong adsorption of the oxygenate compounds on the surface of catalyst supports. It is noted that, this effect is much more prominent on the aluminosilicate-type of catalysts, which contain acid sites (Graça et al., 2009; Graça et al., 2009).

Model compound studies may reasonably propose some efficient catalyst for certain bio-oil component upgrading, but the situation tends to be much more complicated while the entire mixture of pyrolysis oil compounds is fed on a given catalyst. The presences of some impurities like alkalis, as well as S- and N-containing compounds make the task even more difficult. Among all bio oil components, lignin derived phenolics those with multiple oxygen functionalities (-OH, -OCH3, C=O) are the most highly deactivating and make greatest challenges of bio-oil upgrading (Popov et al., 2010)

The presented oxygen contents in bio-oil derived compounds, mostly phenolics, strongly interact with active acid sites of catalysts and deactivate them. Anisole and guaiacol, among those phenolic compounds in bio-oils, have been selected as model compounds to investigate catalysts behavior. They exhibited highly competitive adsorption and rapid catalyst deactivation. A highest heat of adsorption of guaiacol has been reported (González-Borja & Resasco, 2011).

Popov et al.(Popov et al., 2010) investigated the influence of acid-base properties of oxides on the adsorption modes of phenolic type molecules. They observed doubly anchored phenates were created from guaiacol chemisorptions on alumina while phenol and anisole

adsorption on catalyst made monoanchored species. Besides phenolic compounds, which speeded up catalysts deactivation through strong adsorption, the presence of oligomers, char particles, and inorganics typically found in pyrolysis oil greatly accelerated deactivation. It is not still clear whether the presence of heavy oligomers are due to phenolics and other components re-condensation as the vapors condense or they are even present in the original vapor phase. If their presence is not considerable in the original vapor phase, methods such as catalytic pyrolysis and upgrading of vapors might greatly stabilize the most reactive components and improve catalyst life (Popov et al., 2010; Resasco, 2011a).

The conversion of anisole on HY zeolite, which yielded phenol, cresols, xylenols and methylanisoles as main products during several transalkylation steps, was performed by Prasomsri et al. (Prasomsri et al., 2011). Significant catalyst deactivation under reaction conditions was caused by strong adsorption of phenolic compounds on catalyst and coke formation. Contrary to coke formation which was irreversible, phenolic compounds adsorption was reversible and could be minimized by incorporation of molecules such as tetralin with high H-transfer capacity. Anisol conversion and coke formation reduction, effectively improved by tetralin (or other H-donors) co-feeding. Other hydrocarbons with a weaker H-transfer capacity like n-decane, benzene and propylene observed to have respectively lower, negligible and even detrimental effect on catalyst activity.

As indicated in Figure 2.23, in the case of anisole co-feeding with tetralin, a significant increase in anisole conversion from ~20% to ~100% was observed as a function of time on stream (TOS). In this case, the roles of tetralin were: (a) H-transmission and removal of the species that deactivate the catalyst surface (b) Starting the non-dissociative bimolecular transalkylation on the open structure of HY zeolite (Prasomsri et al., 2011).

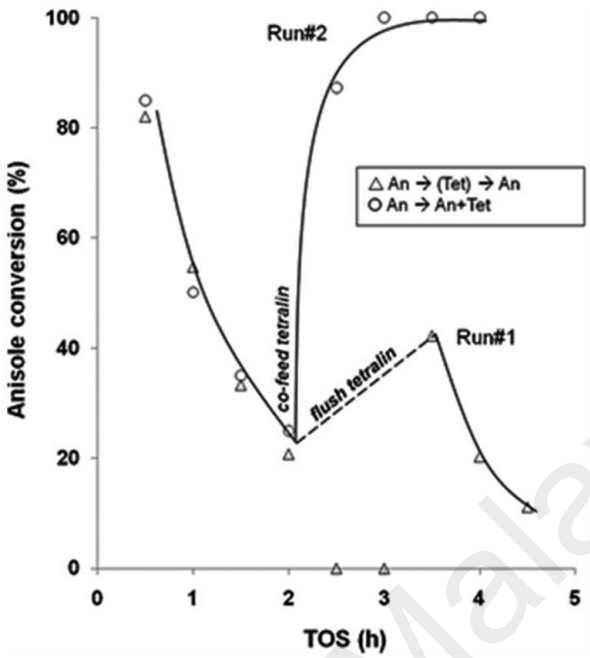

Figure 2.23: Effect of co-fed tetralin on anisole conversion over the HY zeolite. Reaction conditions: W/F = 0.42 h (wrt. anisole for co-feed reaction), co-feed concentration= ~50%, T = 400 ◦C, P = 1 atm He (Prasomsri et al., 2011).

In Borja et al. (González-Borja & Resasco, 2011) researches, catalytic species (Pt, Sn, and bimetallic Pt-Sn) were impregnated on low-surface-area inconel monoliths coated with in-situ-grown carbon nanofibers (CNFs). These monoliths were tested for the deoxygenation of guaiacol and anisole, two lignin derived pyrolysis compounds present in bio-oil. Phenol and benzene were the main products of guaiacol and anisole reactions on monolithic catalysts. CNFs coating, provided high surface area and anchoring sites for Pt and Sn active spices. It consequently improved the yield of desired products. The behavior of platinum and palladium catalysts supported on both carbon nanofiber (CNF)-coated monoliths and alumina washcoated monoliths were studied. It was found: (a) surface area was doubled when CNFs were grown. (b) Water adsorption on the support caused to reduction of catalyst deactivation due to the higher hydrophobicity of carbon compared to alumina.

Graça et al. (Graça et al., 2012b) studied the n-heptane reactions over zeolites catalysts mixtures to understand the influence of phenol on conversion and the products distribution. They also investigated the effect of each zeolite on the pure n-heptane transformation and on the phenol adsorption.

Data found from the zeolites mixtures were compared to the pure HY and HZSM-5 zeolites. Regarding pure zeolites, phenol increased the zeolites mixtures deactivation due to the high carbon accumulation. However, mixing the HY and HZSM-5 zeolites provided a further resistance to phenol poisoning. An initial adsorption of phenol on HY reduced its detrimental effects over HZSM-5 zeolite. The products distributions analysis in the presence of phenol and HY + HZSM-5 zeolites mixtures also indicated an initial preferential adsorption of phenol on the HY zeolite. It led to an increase of the paraffins/ olefins molar ratio and the amount of branched species on the effluent, as observed for the pure HY zeolite.

Investigations on the bio-oil model compounds comprising phenols, aldehydes, acids, alcohols and ketones over HZSM-5 catalyst indicated that deposition of coke is highly depending on operating conditions like space time, reaction medium and temperature. Increase of water content and space time caused mitigation of coke deposition. Further, at lower temperature, less coke contents were observed (Ana G. Gayubo, Aguayo, Atutxa, Aguado, & Bilbao, 2004; Ana G. Gayubo, Aguayo, Atutxa, Aguado, Olazar, et al., 2004). High reaction temperature could cause cracking and condensation reactions promotion, resulting coke contents enhancement (Meng, Xu, & Gao, 2007).

During methanol to hydrocarbon (MTH) process, HZSM-5 showed rapid deactivation due to the deposition of carbonaceous residue (coke) on the catalyst and hindering the reactants to access the active sites (Bibby, Howe, & McLellan, 1992). Investigations done by Srivastava et al. (R. Srivastava, Choi, & Ryoo, 2006) reported that HZSM-5 zeolite having hierarchical MFI pore topology was deactivated at much slower rate compared to conventional MFI

zeolite (HZSM-5). Further, Kim et al. (Jeongnam Kim et al., 2010) showed that the generation of secondary mesoporosity within MFI zeolite could increase the catalyst life time by three times. Their results indicated that in the case of mesoporous zeolite, the coke mainly appeared on mesoporous walls. On the other hand, in the case of microporous zeolites, the coke was mainly deposited inside micropores. They concluded that, facile diffusion of coke precursors attributed to their short diffusion path length could probably improve the catalyst lifetime.

Novel ideas are being explored to minimize the catalyst deactivation complexity while whole real bio-oil mixture is treated. This challenging area will open the doors toward new research opportunities. Following examples (Resasco, 2011a) could be evidences for the carried out attempts in this regard. (a) The combination of hydrolysis with catalytic pyrolysis was studied by Jaer et al. (Jae et al., 2010). This method separated the products into different streams which were enriched in any of the mentioned families. Successive catalytic refining steps to focus on the required specific chemistry, like C-C bond formation and C-O bond cleavage, were done by multistage method. (b) A liquid phase catalytic depolymerization method for lignin was dedicated by Roberts et al. (Roberts et al., 2011), in which phenolic monomers as the only primary products were produced through base-catalyzed hydrolysis, while oligomers were formed in the secondary re-condensation steps. To inhibit oligomerization, boric acid was used to suppress condensation reactions.

2.2.4 Proposed catalysts and process for bio-oil upgrading

The main technical challenge on bio-oil stabilization and development is to design catalytic process and catalysts that fulfill deoxygenation while minimizing hydrogen consumption and maximize carbon efficiency. Model compound approach, as a fundamental key tool, has been

utilized to identify the catalysts behavior and the relevant chemical process for bio-oil improvement.

2.2.4.1 Proposed pyrolysis-upgrading integrated process

High-pressure pyrolysis product treatment cannot be easily integrated with conventional fast pyrolysis atmospheric reactors. The only option is therefore to somehow isolate two process means condense the pyrolysis vapors and then feed the liquid bio-oil to the high pressure units. The great challenge in doing this in large scale is the low chemical and thermal stability of bio-oil. A more desirable option would be to directly feed the vapors coming out of the pyrolysis unit into upgrading reactors (González-Borja & Resasco, 2011).

Based on the comprehensive investigation done on model compound approach researches and following to catalysts selections, an integrated process for biomass pyrolysis and upgrading has been suggested (Figure 2.24). Fluid bed fast pyrolysis of biomass was selected due to the merits associated with this type of process mentioned earlier in the context. As depicted in Figure 2.24, pretreated milled biomass is introduced to the pyrolyzer (R01) through screw feeder. The preheated Nitrogen gas provides the fluidization condition during pyrolysis. The exit vapor from R01 after passing from two CY01 and CY02 cyclones and following to the separation of remaining chars is directed to Catalytic Vapor Upgrading Package (PK01) where bio-oil vapor is upgraded during cascade catalytic process. The updated bio-oil vapor after condensation in E12 is collected in V05. The vapor streams from pyrolyzer, PK01 and E12 off gas can be analyzed by on line Gas Chromatograph (GC). Figure 2.25 shows detail of catalytic vapor upgrading package (PK 01). The said package is equipped with three fixed bed reactors of R02, R03 and R04. For the possibility of temperature adjustment in cascade fixed bed reactors, E001 and E002 have been considered. The design of catalytic vapor upgrading reactors is enough flexible for different reactors'

configurations. It can facilitate the conditions for the different researches on in-situ bio-oil upgrading, which is still immature.

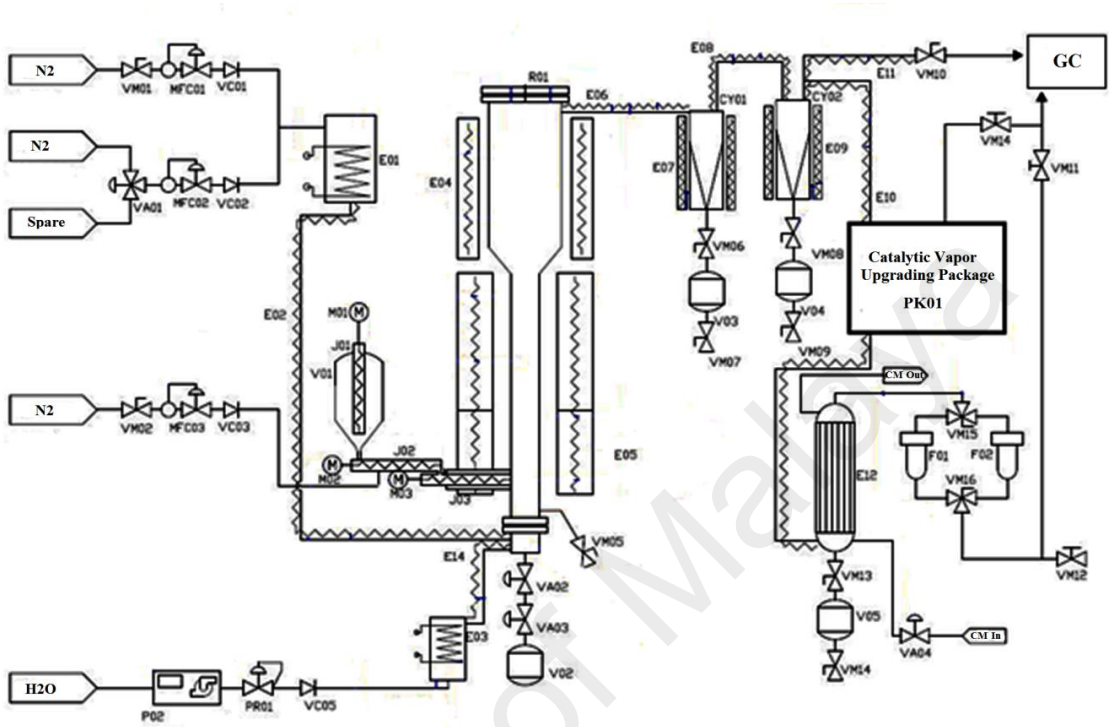

Figure 2.24: Suggested biomass pyrolysis and vapour phase bio-oil upgrading integrated process (See PK01 detail in Figure 2.25)(E: Exchanger, V: Vessel, MFC: Mass Flow Controller, VA-VC-VA: Valve, F: filter, R: Pyrolyzer, CY: Cyclone, J: Screw Feeder, M: Electro motor, P: Pump, GC: Online Gas Chromatograph).

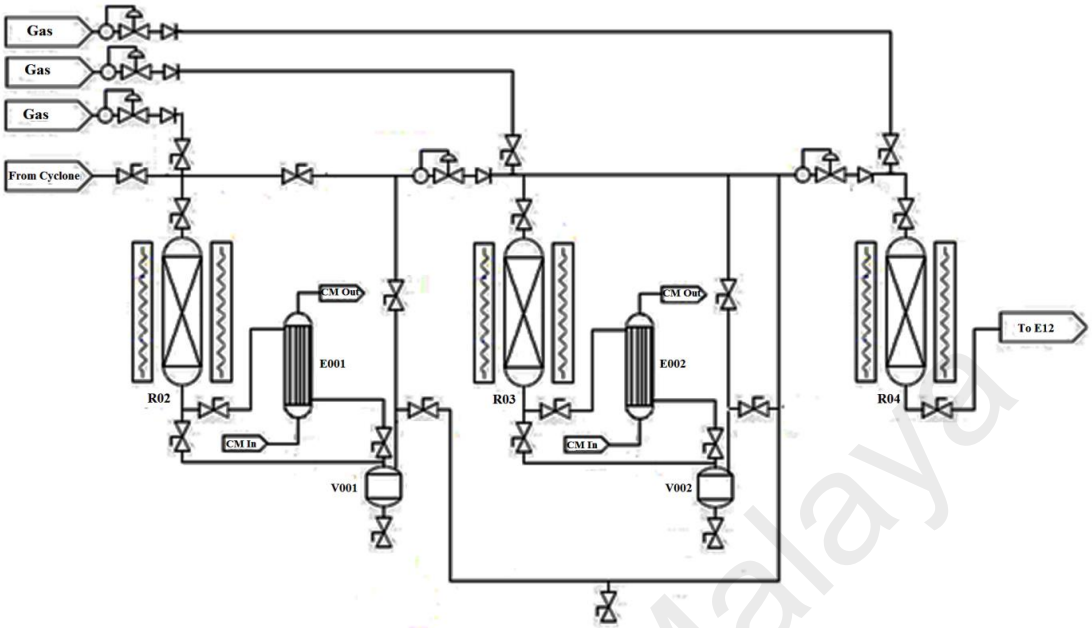

Figure 2.25: Catalytic vapor upgrading package (PK01) detail (see Figure 2.24) (R: Fixed bed reactor, V: Vessel, E: Exchanger).

2.2.4.2 Catalysts selection

As the outcome of done survey, Figure 2.26 at a glance shows simply the different catalysts' classes suggested for each individual reaction type. As indicated in Figure 2.26, zeolite catalysts are prone to accomplish varieties of reactions comprising deoxygenation, condensation and alkylation. Deoxygenation, as one of the crucial reactions to achieve fuel-like molecules, can be performed by different types of catalysts, including zeolites, zeolite supported metals and oxide supported metals. According to the done survey, the selected catalysts are active, selective and productive to yield fuel-like components. Based on this investigation, efficient in-situ atmospheric pyrolysis vapor upgrading with minimum carbon loss and hydrogen consumption can be carried out using a cascade system of proposed catalysts (Figure 2.26) in an integrated pyrolysis/upgrading process.

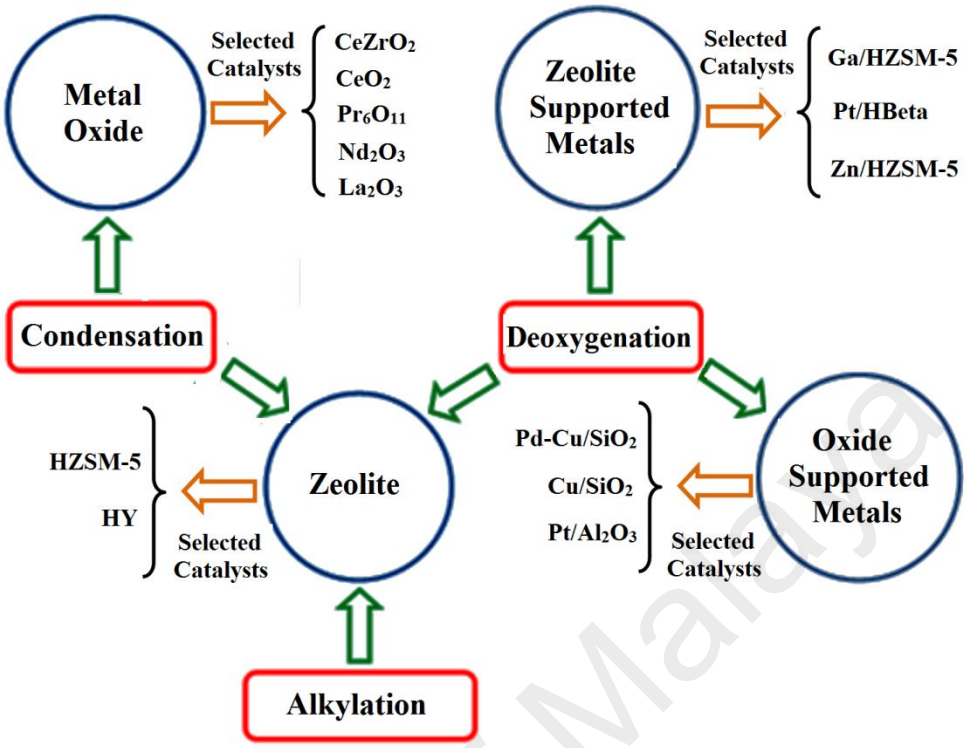

Figure 2.26: Selected catalysts from different catalysts' groups for various chemical upgrading reactions.

CHAPTER 3: MATERIALS AND METHODS

3.1 Biomass Materials

The palm oil biomasses comprising palm kernel shell (PKS), empty fruit bunches (EFB) and palm mesocarp fibre (PMF) were obtained from Szetech Engineering Sdn. Bhd. located in Selangor, Malaysia. The samples were crushed using high-speed rotary cutting mill and sieved to desired particle size (< 300 μm). Then, the samples were dried at 105 °C for 24 h and kept in tightly screw cap plastic bottles.

3.2 Demineralization Pretreatments

Different types of the dried palm oil biomasses (PKS, EFB and PMF) were subjected to diverse diluted acid solutions (H_2SO_4 (96 wt. %), $HClO_4$ (70 wt. %), HF (49 wt. %), HNO_3 (65 wt. %), HCl (37 wt. %)), all supplied by R&M Chemicals, for the purpose of inorganics removal. Acid washing pretreatment process aimed to maximize the ash extraction through leaching process. For this purpose, 20 gram of the biomass samples were treated by 2.0M acid solutions at room temperature for 48 h and then filtered and washed with distilled water. The ratio of the acid solutions to the biomass samples was considered as 15 (g solution/g biomass). The washing process was continued to a constant pH value. The leached biomass samples were dried in oven at 105 °C over 24 h and kept in tightly screw cap bottles.

3.3 Biomasses proximate and ultimate analysis

Proximate analysis was carried out by utilizing thermogravimetric analysis. Volatile matter, fixed carbon and moisture contents were measured according to ASTM D-5142-02a using TGA/Q500 manufactured by TA Instruments. Ash content of the biomasses samples was determined by their ignition in a muffle furnace at 575 °C for 24 h according to ASTM E-

1755-01 standard method. Ash content (wt. %) was calculated by dividing ash weight to initial weight of dried biomass sample at 105 ° C.

Ultimate analysis was carried out to determine the basic elemental composition of the biomass samples. The samples' ultimate analysis was done using a Perkin-Elmer model 2400, Series II CHNS/O analyzer to measure carbon, hydrogen, nitrogen and sulphur contents. Oxygen content was then calculated by difference. Higher heating value (HHV) was calculated from the elemental compositions using Eq.(3-1) from Channiwala & Parikh (2002):

$$HHV\ \left(\frac{MJ}{kg}\right) = 0.3491C\ +\ 1.1783H\ +\ 0.1005S - 0.1034O - 0.0151N - 0.0211A \qquad (3-1)$$

where C,H,N,O,S and A represents carbon, hydrogen, nitrogen, oxygen, sulphur and ash contents of materials, respectively, expressed in dry basis weight percentage.

3.4 TGA-MS, TGA-FTIR experiments

TGA-MS and TGA-FTIR analysis were carried out by simultaneous thermal analyzers (TA Instruments Q500 and NETZSCH STA 449/F3) coupled with MS type (PFEIFFER Vacuum-Thermostar TM) and FTIR type (BRUKER TGA-IR), respectively. Pure Nitrogen (99.999 %) was used as carrier gas in all experiments. In order to prevent unnecessary evolved gas (like tar and etc.) condensation in both assemblies, a skimmer coupling system was employed while the connected capillary tube between TGA and evolved gas analyzers (MS and FTIR) were kept at 200 °C. To minimize the effects of heat and mass transfer limitations during the samples analysis, the samples quantity was selected approximately 5 mg with the particle size less than 300 µm at pure nitrogen flow rate of 150 ml/min. The samples loaded to alumina crucible pan were heated from 35 °C to 850 °C at heating rate of 15°C/min.

Mass spectrometer worked with electron ionization energy of 70 eV and provided mass spectra up to 300 a.m.u, while FTIR online gas analysis was recorded from 4000 to 400 cm^{-1}. MS spectra corresponded to 2, 28, 44 a.m.u. indicated the release of main pyrolysis gases H_2, CO, and CO_2 , respectively (Y. F. Huang, Chiueh, Kuan, & Lo, 2013).

3.5 Biomass pyrolysis reaction kinetics

The solid state biomass pyrolysis kinetics using various mathematical and methodological models have been investigated by several researchers (Y. F. Huang, Kuan, Chiueh, & Lo, 2011b). Eq.(3-2) shows the general rate equation as:

$$\frac{dx}{dt} = k\, f(x) \qquad (3-2)$$

where x is the conversion degree of the biomass feedstock expressed in Eq.(3-3), k is the reaction rate constant and $f(x)$ refers to a selected model of reaction mechanism.

$$x = \frac{m_0 - m_t}{m_0 - m_f} \qquad (3-3)$$

where m_t is corresponded to the sample mass at time t, m_0 and m_f are initial and final mass of biomass, respectively. The reaction rate constant can be obtained from Arrhenius equation as Eq.(3-4).

$$k = k_0 \exp\left(\frac{-E_a}{RT}\right) \qquad (3-4)$$

where k_0 is rate constant pre-exponential factor, E_a , R and T are activation energy (Kj/ mol) , universal gas constant (8.314 J/mol K), and temperature (K), respectively. Furthermore, the reaction model expressed in Eq.(3-2) can be defined as Eq.(3-5).

$$f(x) = (1-x)^n \qquad (3-5)$$

where n is the reaction order. According to the literature (D. Chen et al., 2013; Y. F. Huang et al., 2011a, 2011b), in many applications, the biomass pyrolysis was assumed to be a reaction with first order (n=1).

For a constant pyrolysis heating rate of β, β= dT/dt , rearrangement of Eq.(3-2) and its integration by using the Coats-Redfern method (Coats & Redfern, 1964) conducted to Eq.(3-6).

$$ln\left[-\frac{\ln(1-x)}{T^2}\right] = ln\left[\frac{k_0 R}{\beta E_a}(1-\frac{2RT}{E_a})\right] - \frac{E_a}{RT} \qquad (3-6)$$

In Eq.(3-6), the value of $2RT/E_a$ <<1 (K.-M. Lu, Lee, Chen, & Lin, 2013) therefore, it can be simplified to:

$$ln\left[-\frac{\ln(1-x)}{T^2}\right] = ln\left[\frac{k_0 R}{\beta E_a}\right] - \frac{E_a}{RT} \qquad (3-7)$$

Thus, the plot of $ln[-\ln(1-x)/T^2]$ versus $1/T$ is a linear line with the slope and intercept of $-E_a/R$ and $ln[k_0 R/\beta E_a]$, respectively. Accordingly, the pre-exponential factor (k_0) and activation energy (E_a) can be determined.

3.6 DSC analysis

Differential scanning calorimetry (DSC) was employed to compute the energy required to thermally decompose palm oil biomasses. The DSC (Model DSC1/500, METTLER TOLEDO) with refrigerated cooling system operated under nitrogen atmosphere at a flow rate of 20 ml/min. Approximately 5 mg samples were heated at heating rate of 15 °C/min from 25 °C to 500 °C using aluminum sealed pan with a pinhole in the lid to enable removal of adsorbed water and released gases during analysis. Heat flow (mW), temperature (°C) and time (min) were all recorded during analysis. The equipment was calibrated before use according to manufacturer's specifications.

3.7 Preparation of the catalytic materials

The catalytic materials used for the in-situ biomass pyrolysis vapor upgrading experiments, in a cascade system of the catalysts, were crystalline mesoporous HZSM-5 and Ga/HZSM-5 zeolite and also Cu/SiO_2. Parent NH_4 form ZSM-5 zeolite was provided by Zeolyst International (CBV5524G, SiO_2/Al_2O_3 molar ratio = 50). The as-received parent zeolite catalyst was calcined at 550 °C/12 h/air with heating ramp of 3 °C/min to remove adsorbed water and possible available template. Mesoporous HZSM-5 zeolite was produced by its desilication using NaOH solution (0.2 M) at temperature of 60°C for 30 min under stirring conditions.13 g of zeolite was treated with 400 ml NaOH solution. Afterwards, suspension was cooled down immediately in ice-bath to stop the desilication and then filtered. Subsequently, the sample was washed and filtered until neutral pH to eliminate the excess Na^+ ions and then dried at 90°C overnight. Mesoporous Na^+ form of the zeolite was then protonated by ion-exchange of Na^+ with NH_4^+ in 1.0 M NH_4Cl solution (250 ml/ g catalyst) under stirring at 60°C for 16 h. The NH_4^+ form zeolite was filtered, washed with distilled water and dried at 90° C overnight. The solid catalyst powder was then calcined at 550 °C at the rate of 3°C/min for 12 h in order to remove NH_3 for the creation of mesoporous NH_4-ZSM-5 in H^+ form.

The mesoporous HZSM-5 support was impregnated by incipient wetness technique with a gallium (III) nitrate hydrate (supplied by Aldrich, crystalline 99.9 % purity) solution using a (solution volume)/ (total pore volume) ratio of 3 (Escola et al., 2011). The Ga amount added was 1.0 and 5 wt% based on the mass of the catalyst. Before impregnation, the solid support was outgassed under vacuum (using Micrometrics ASAP 2020). Then, the samples were impregnated and homogenized by shaker for 3 h. After that, the catalysts were dried under static air at ambient temperature for 24 h and then were dried in oven at 100°C overnight.

The dried samples were calcined under static air in a muffle furnace at 550 °C at the rate of 3°C/min for 12 h. Subsequently, the catalysts were activated by hydrogen reduction (0.5 l/min) in the fixed bed multi-zone reactor at 500 °C and held at this temperature for 1.0 h before upgrading trials. The impregnated catalysts were labeled as Ga (1)/HZSM-5 and Ga (5)/HZSM-5.

Cu/SiO_2 catalyst with metal loading was prepared by incipient wetness impregnation with aqueous solution of metal precursor (Copper (III) nitrate trihydrate (99.1 wt. %), supplied by Sigma-Aldrich). Silica powder (Supplied by R&M Chemicals) was employed as support. It was calcined at 500°C and then degassed under vacuum before impregnation. A solution/silica ratio of 1.5 ml/g was used for impregnation. The copper loadings on silicon support was 5 wt. %. After impregnation, the sample homogenized using shaker for 3h and then dried in static air at ambient temperature for 24 h. The samples further dried overnight at 100 °C and calcined at 500 °C for 12h in a muffle furnace. The catalyst was then activated by hydrogen reduction (0.5 l/min) at 500 °C in the fixed bed multi-zone reactor and held at this temperature for 1.0 h before upgrading experiments. The impregnated catalysts was named as Cu (5)/SiO_2.

3.8 X-Ray Flouresence (XRF) analysis

The inorganic contents of the catalyst samples was quantified using X-Ray Flouresence (XRF) instrument (PANalytical Axios ^{mAX}).

3.9 Scanning electron microscopy (SEM) analysis

SEM (model FEI QUANTA 450 FEG, operating at a 5 kV accelerating voltage and low vacuum) was employed to investigate the surface nature of the catalysts and to characterize

their physical structure. Conductive coating was not applied to prepare the samples for SEM analysis. Samples were prepared by their sticking on carbon sheet.

3.10 Surface area and porosity analysis

The surface area and pore size of the catalysts samples were measured by a Micrometrics ASAP 2020 gas adsorption analyzer, using nitrogen (N_2) adsorption/ desorption isotherm at -196 °C. All the samples were degassed in vacuum at 130° C for 24 h before the measurement. Barrett-Joyner-Halenda (BJH) method was utilized to estimate of pore size diameter.

3.11 Temperature-programmed desorption (TPD)

Ammonia temperature-programmed desorption (NH_3-TPD) was employed to determine the acid sites of the zeolites catalysts, using a Micromeritics Chemisorb 2720. Each catalyst sample (approximately 500 mg of finely ground powder) was firstly pretreated through heating in 30 ml/min of pure He (99.995 %) from ambient to 600 °C at a rate of 10 °C /min and was held at this temperature for 2 h. After that, the temperature of the sample was stabilized at 170 °C. Then, the sample was dosed with 30 ml/min of 10% NH_3/He (supplied by Linde) for 30 min. Afterward, the catalyst sample was flushed with 30 ml/min of He for 30 min to eliminate physisorbed (weakly bound) NH_3 and then, the sample's temperature was reduced to 50 °C. When the thermal conductivity detector (TCD) indicated a stable baseline, the temperature was then ramped from 50 °C at a rate of 10 °C /min to 600 °C and was held for 2 h. The ammonia desorption rate was recorded by TCD during this process.

3.12 X-ray diffraction (XRD)

X-ray powder diffraction (XRD) was carried out to verify the crystallinity of the zeolites. The diffraction patterns were monitored on a PANanalytical diffractometer utilizing Cu as anode material with Ka (k = 1.54443 A) radiation to create diffraction patterns from powder crystalline samples at room temperature. The spectra were scanned in the range 2θ = 5–80° at a rate of 2.0 °/min.

3.13 Bio-oil water and oxygen content

The water content of the as-produced bio-oil was measured using a Karl Fischer 737 KF Coulometer from Metrohm. Analysis was performed according to the ASTM E 203 method. Hydranal-coulomat AG and Hydranal-coulomat CG were used as anolyte and catholyte reagent, respectively. After titration completion, the sample's water content was indicated as percentage (%). The accuracy of the analysis was very high (less than 1% of water content). The bio-oil and biomass samples' ultimate analysis were performed using a Perkin-Elmer model 2400, Series II CHNS/O analyzer to measure carbon, hydrogen, nitrogen and sulphur contents. Oxygen content was then calculated by difference.

3.14 FTIR spectroscopy

Fourier transform infrared spectroscopy (FTIR; model: BRUKER TENSOR 27) was used to qualitatively analyze the functional groups of the chemical components available in the raw and upgraded bio-oil. The samples were scanned with a resolution of 4 cm^{-1}over the range from 600 to 4000 cm^{-1}.

3.15 GC-MS analysis

For the qualitative identification and quantitative measurement of the volatile organic compounds and semi-volatile in the bio-oil, GC/MS-QP 2010 SHIMADZU, equipped with flame ionization and mass spectrometry detection (GC-FID-MS) was utilized. A capillary column with a diameter of 0.25 mm and length of 30 m coated with a 0.25 µm film of DB-5 was employed. The GC was equipped with a split injector with a split ratio of 1:50 at 290 °C. Pure helium gas (99.995%) was used as carrier gas at flow rate of 1.26 ml/min. The initial oven temperature was set at 50 °C for 5 min and then increased to 300 °C at a rate of 10 °C min^{-1} and held for 10 min. The NIST (National Institute of Standards and Technology) library was employed to identify the chemical compounds. Mass spectrometer (MS) worked with ion source temperature of 200 °C in the range of 40–1000 m/z and at an interface temperature of 240 °C.

The organic fraction of the bio-oil samples was separated and then diluted with ethyl acetate (99.8 wt.% supplied by R&M Chemicals) solvent to a dilution factor of 5 and then filtered using a 25 µm syringe filter prior to the injection to GC-MS.

Before analyzing the samples, the instrument was calibrated with various mixture of known compounds including different types of aromatics and phenolics. We found a very good agreement between components weight percent and the relevant peak area (%), relatively with less than ~ 5.0 % difference. Therefore, it was possible to consider peak area of each component (%) equivalent to its weight percent in the organic phase of the bio-oil with almost high accuracy.

3.16 Coke analysis

The coke formation on the HZSM-5 catalyst, during the biomass pyrolysis vapor upgrading and its co-feeding with methanol, was analyzed. The quantitative analysis was carried out by

dissolving 1500 mg of the catalyst in 100 ml of 15% hydrofluoric acid (HF (49 wt.%) supplied by R&M Chemicals). Consequently, the extracted coke in HF was dissolved in 80 ml of ethyl acetate. Then, the ethyl acetate fraction was analyzed by GC-MS (QP 2010 SHIMADZU) equipped with DB-5 column. The thermogravimetric-temperature programmed oxidation (TGA-TPO) analysis, using Diamond TGA/DTG (PerkinElmer) instrument, was employed to quantitatively measure the amount of the coke formed on the catalyst. The sample was heated from 30 to 700 °C at a rate of 10 °C/min under the synthetic air flow at 200 ml/min. Then, the samples were kept at final temperature for 20 min.

The amounts of internal and external coke within the different zeolite catalysts were measured by combining the data from gas adsorption measurements and TGA. The total amount of coke (external + internal) was estimated by TGA analysis. It was assumed that the fresh samples micropore volume reduction (from the gas adsorption measurements) was corresponded to the internal coke amount (assuming a coke density of 1.22 g/cm^3). The remaining coke amount (calculated by subtraction) is then assumed to be external (Bleken et al., 2013).

3.17 Catalysts regeneration

The partially deactivated zeolites were regenerated in a muffle furnace at 550 °C with a heating rate of 3°C /min for 12 h in the presence of air. Thereafter, the temperature was gradually lowered to 35 °C. The regeneration removed most of the deposited coke from the zeolite structure. The surface area, crystalline structure and surface morphology of catalysts were investigated for the regenerated zeolites.

3.18 Catalytic and non-catalytic biomass pyrolysis experiments

3.18.1 Catalytic pyrolysis experiment

The PKS biomass pyrolysis/upgrading experiments were performed in a stainless steel (SS-316L) bench scale multi-zone fixed bed tubular reactor (ID 7.5 cm, height 60 cm), heated by a two zones furnace controlled by two PID (Proportional- Integral- Differential) controllers. The biomass amount used in all experiments was 60 g and the quantity of the each catalyst (meso-HZSM-5, Ga/meso-HZSM-5 and Cu/SiO_2) was 6 g. In a typical pyrolysis experiment, calcined catalysts were introduced to the first (meso-HZSM-5), second (Ga/meso-HZSM-5) and third (Cu/SiO_2) catalytic zone of the reactor and they were kept at 500 °C under nitrogen flow (0.5 l/min) for 30 min. The catalysts were then reduced by pure hydrogen (99.999 %) at 500°C for 60 min and then the gas was switched to a mixture of nitrogen and hydrogen each one having 1 l/min flow rate. Thereafter, the solid biomass was introduced from the top of the reactor through a hopper, while it was purge by N_2, to the pyrolysing zone of the reactor (at 500 °C). Different zones of the reactor (pyrolyzer and three catalytic zones) were cylindrical cups with wire mesh (# 400) at the bottom sides. All three catalytic zones had equal volumes to provide the same residence time for pyrolysis vapor in each catalytic zone. The material of construction of internal parts was stainless steel. Four K-type thermocouples were used to indicate the relevant temperature of pyrolyzer and three fixed bed catalytic zones. The thermocouples were calibrated before experiments. The above mentioned catalytic pyrolysis trials could be referred as in-situ upgrading of pyrolysis vapors. Furthermore, all the experimental conditions (i.e., low residence time (~ 3.0 s), fast heating of biomass (~ 120 °C/ min) and fast cooling of products (-5.0 °C)) resemble those of the biomass fast pyrolysis (BFP) type of experiments. The bio-oil liquid products were collected using two condensers cooled down by a chilling media at -5 °C. The pyrolytic vapors, upon their condensation in the condensers, formed the bio-oil. The liquid bio-oils products

collected at the bottom of two condensers were transferred to the pre-weighted glass bottles and the quantities of the bio-oils were measured by direct weighting. The condensed pyrolytic vapors, collected in the bottles, formed multiple phases; a liquid organic phase, an aqueous phase and viscous organic deposits on the bottle's walls. The bio-oils were first fully homogenized inside the bottles using ethyl acetate as the solvent and then collected as two phase solutions (aqueous and organic). The organic phase was then separated, filtered and submitted for analysis. After each trial, to remove the adsorbed volatile components from the catalyst, it was purged under nitrogen flow (2 l/min) for 30 min at 500 °C. One stream of nitrogen (0.5 l/min) gas saturated with ethyl acetate was introduced to the reactor's top at 50 °C through a bubble saturator to wash the internal parts of the reactor and condensers after each experiment. The bubbler temperature was adjusted by a constant temperature bath. The pyrolysis/upgrading setup is shown in Figure 3.1.

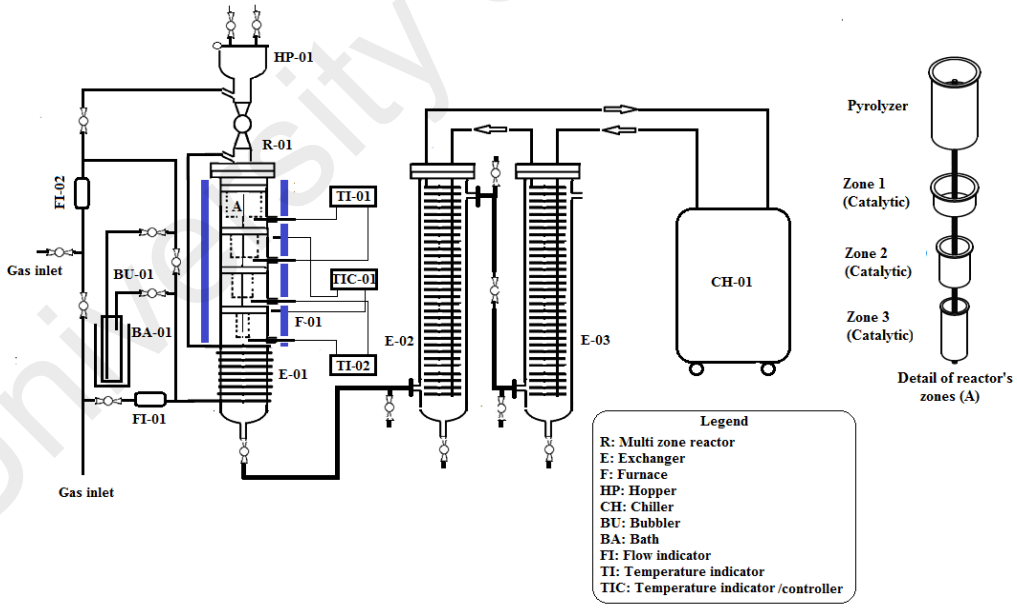

Figure 3.1: Schematic of biomass fast pyrolysis/upgrading multi-zone reactor and its accessories.

3.18.2 Non-catalytic pyrolysis experiment

In a typical pyrolysis experiment, the solid biomass (60 g) was introduced from the top of the reactor, through a hopper while it was purged by N_2, to the top zone of the reactor at 500 °C. Top zone of the reactor (pyrolyzer zone) was a cylindrical cup with wire mesh (# 400) at the bottom side. Nitrogen gas stream was introduced to the reactor's top (2.0 l/min). Further detailed description of the pyrolysis experiment can be found elsewhere (Asadieraghi & Wan Daud, 2015).

3.18.3 Methanol co-feeding in catalytic pyrolysis experiment

The amount of the biomass used in all experiments was 60 g (1 gr/min) and the quantity of the catalyst was 6 g. In a typical pyrolysis experiment, calcined catalyst was charged to the second zone of the reactor and it was kept at 500 °C under nitrogen flow (0.5 l/min) for 60 min. Thereafter, the solid biomass was introduced from the top of the reactor through a hopper, while it was purge by N_2, to the first zone of the reactor (at 500 °C). Two zones of the reactor were cylindrical cups with wire mesh (# 400) at the bottom sides. The parts material of construction was stainless steel. Two streams of nitrogen gas were introduced to the reactor's top, one (0.5 l/min) was saturated with methanol (99.6 wt. % supplied by Merck) at different temperatures (40 °C, 50 °C and 55 °C) through a bubble saturator. The bubbler temperature was adjusted by a constant temperature bath. The feeding rate of methanol at various temperatures was estimated from the saturation vapor pressure of the methanol vapor (using Antoine Equation) and the gas flow rate. The other stream was pure nitrogen with the flow of 2 l/min. The mixture of two streams carrying methanol and biomass pyrolysis vapor was driven through a catalyst's bed.

CHAPTER 4: RESULTS AND DISCUSSION

4.1 Part 1: In-depth investigation on thermochemical characteristics of palm oil biomasses as potential biofuel sources

4.1.1 Chemical structure evaluation of the biomass samples

The chemical structure of the lignocellulosic biomass samples is frequently studied using infrared spectroscopy. In this investigation, FTIR technique was employed to study the biomasses chemical structure. Figure 4.1 depicts the FTIR spectra of the various biomasses. Table 3 shows the assignment of FTIR peaks to the chemical functional groups and biomass components according to the literature.

In the infrared spectra, the first strong broad band at 3700-3000 cm^{-1} was related to O-H stretching vibration of phenolic, alcoholic and carboxylic functional groups. Also, the band between 2800 and 3000 cm^{-1} was attributed to C-H stretching vibration of - CH_2 and -CH_3 functional groups.

The band around 1730 cm^{-1} was the result of C= O (aldehydes, ketones or carboxyl) stretching vibration of free carbonyl groups of hemicellulose component. The next spectrum bands around 1650-1510 cm^{-1} (C=C stretching vibrations of aromatics) were corresponded to lignin.

The spectral region of 1400-600 cm^{-1}, where various vibration modes existed, was very complicated to be analyzed. However, in this region, vibration of some specific units related to lignin could be detected. The spectra of different samples indicated the characteristic vibration of lignin unit at 1240 cm^{-1} (C=O stretching) and 850-750 cm^{-1} (C-H bending) (Fierro, Torne-Fernandez, Celzard, & Montane, 2007; Parshetti, Kent Hoekman, & Balasubramanian, 2013).

The spectra between 1440 and1400 cm^{-1} contained several bands in the O-H bending region, which were most probably cellulose and hemicellulose related transmission.

The spectra between 950 and 1200 cm^{-1} could be due to C-O-functional groups stretching. PKS and PMF exhibited the lowest and highest spectra intensity, respectively, at 1060 cm^{-1}. This might be possibly due to the presence of C-O- functional group.

As can be seen in Figure 4.1, unlike PKS, the virgin EFB and PMF indicated relatively similar chemical structure. It might be attributed to the biomasses nature and composition. Among different biomass samples, PKS showed more bands intensity compared with EFB and PMF at 1240 cm^{-1} (C=O stretching) and 850-750 cm^{-1} (C-H bending). It could be an evidence for higher lignin content of PKS (50.7 wt. %). These information are in agreement with the biomass samples composition. Therefore, FTIR spectrums could verify biomasses nature and composition. Further details on the biomass composition can be found elsewhere (Asadieraghi & Wan Daud, 2014).

Table 4.1: Assignment of peaks to the chemical functional groups and biomass components using FTIR.

Wavenumbers (cm^{-1})	Vibration	Functional group	Biomass Component	Ref.
3700-3000	O-H(Stretch)	Phenolic, alcoholic , carboxylic		(Fierro et al., 2007)
3000-2800	C-H(Stretch)	- CH_2 , -CH_3		(Fierro et al., 2007)
1730	C=O(Stretch)	Carbonyl	Hemicellulose	(Mayer, Apfelbacher, & Hornung, 2012a)
1510-1650	C=C(Stretch)	Aromatic ring	Lignin,Cellulose	(Fierro et al., 2007)
1440-1400	O-H(bend)	Alcoholic , carboxylic	Hemicellulose, Cellulose	(Haiping Yang et al., 2007a)
1235	COOH(Stretch)	Carbixylic, acetic acid ester	Hemicellulose	(Smidt & Schwanninger, 2005)
1246-950	C-O-C, C-O, C-OH (Stretch)	Lignin, Polysaccharides	Cellulose, Lignin, Hemicellulose	(Mayer et al., 2012a)
850-750	C-H(bend)	Aromatic compounds	Lignin	(Parshetti et al., 2013)

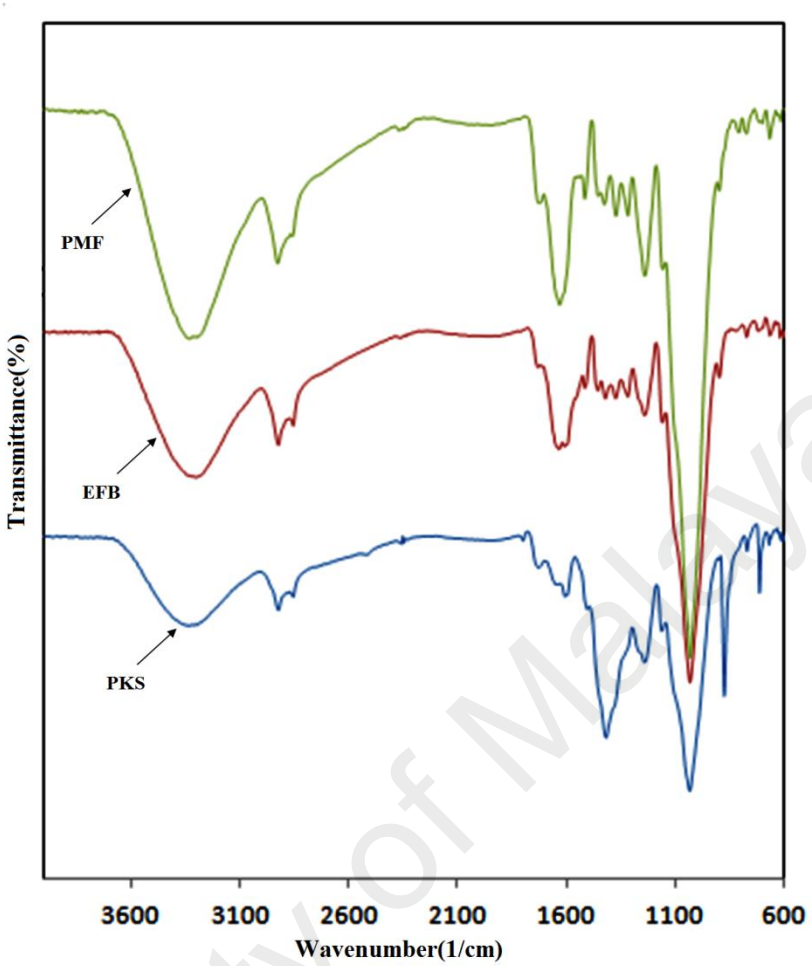

Figure 4.1: FTIR spectra of different biomass samples (PKS, EFB and PMF).

4.1.2 Thermogravimetric analysis (TGA) of the biomasses samples

Fig.4.2 shows the palm oil biomasses samples (PKS, EFB, PMF) TGA (weight loss) and DTG (derivative thermogravimetric) analysis evolution profiles as a function of temperature, at a constant heating rate of 15°C/min. As indicated in Figure 4.2, the palm oil biomasses thermal degradation behavior could be divided into three main stages. In Stage 1, the biomasses moisture content dropped quickly due to a dehydration process at temperature below 150 °C. In Stage 2, the samples went through a slow depolymerization process in the temperature range of 150-225 °C. Subsequently, in Stage 3, the TGA curves dropped sharply

in the temperature range of 225 to ~400 °C attributed to the complex thermal decomposition reaction. In this stage, where TGA curves were relatively flat, residues comprising mainly lignin components were decomposed.

Generally, the pyrolysis process of the lignocellulosic biomass can be divided into four main sections: moisture and very light volatiles components removal (< 120 °C); degradation of hemicellulose (220-315 °C); lignin and cellulose decomposition (315-400 °C) and lignin degradation (> 450 °C) (Sanchez-Silva et al., 2012; Haiping Yang et al., 2007a).

In Fig.4.2, the DTG peaks attributed to cellulose decomposition were observed at 329 °C, 351°C and 364°C for EFB, PMF and PKS, respectively. The DTG shoulders of PMF and PKS curves observed at ~300°C were caused by hemicelluloses devolatilisation (Idris et al., 2010; Vamvuka, Kakaras, Kastanaki, & Grammelis, 2003). The palm oil biomasses lignin decomposition was occurred slowly over a broad range of temperature (137- 667 °C) (Vamvuka et al., 2003). In the section corresponded to lignin degradation (> 450 °C), EFB overlapped PMF, whereas that of PKS occurred with different weight loss rates indicating one peak in DTG curve started at about 650°C.

The first peak in the various DTG curves in Figure 4.2 indicated the moisture content of the biomass samples dropped rapidly at the temperature of ~ 60 °C (Table 4.2). This observation was thanks to the significant moisture evaporation as temperature increased.

The different lignocellulosic materials thermal behavior could be attributed to the various contents of cellulose, hemicellulose and lignin (Asadieraghi & Wan Daud, 2014). The lowest temperature peak in DTG curve could indicate the highest content of hemicellulose in EFB. Furthermore, the differences in residue yield could represent the different lignin contents of the biomasses samples. PKS indicated the highest content of the lignin due to the largest residue. Moreover, maximum weight loss rate could be an indication of volatile matters and cellulose content in the biomass samples (Damartzis, Vamvuka, Sfakiotakis, & Zabaniotou,

2011). The maximum decomposition rate of EFB was higher than that of PMF and PKS, because its cellulose and volatiles contents were greater.

DTG curve corresponded to PKS showed a third isolated peak started at temperature ~650 °C and reached to maximum at ~700 °C. Literature investigations on similar sample indicated that except Idris et al (2010) who reported this third peak, it has not been expressed elsewhere. Further details on the reasons for occurrence of this peak will be explained in the next sections using TGA-MS and TGA-FTIR analysis.

Reactivity of the biomass samples can be estimated from the peak height and position. The peak height is directly proportional to the biomass reactivity, whereas the temperature in which the peak takes place is inversely proportional to the biomass reactivity (Vamvuka et al., 2003). As can be seen in Table 4.2, the highest degradation rate belongs to EFB at lowest peak temperature. So, EFB indicates the highest reactivity among palm oil biomasses samples (Idris et al., 2010).

Table 4.2: Pyrolysis properties of the palm oil biomasses samples by TGA and DTG; N_2 gas flow rate: 150 ml/min; Heating rate: 15 °C/min.

Biomass	Maximum Temperature (°C)				Maximum Deriv. Weight(wt%/°C)				Char Content(*) (wt %)
	First Peak	Shoulder	Second Peak	Third Peak	First Peak	Shoulder	Second Peak	Third Peak	
PKS	61	300	364	700	0.035	0.395	0.535	0.148	29.3
EFB	60	-	329	-	0.078	-	0.9	-	14.5
PMF	61	301	351	-	0.064	0.50	0.70	-	23.4

(*) Char content (wt.%)= Ash (wt. %) + Fixed carbon (wt. %)

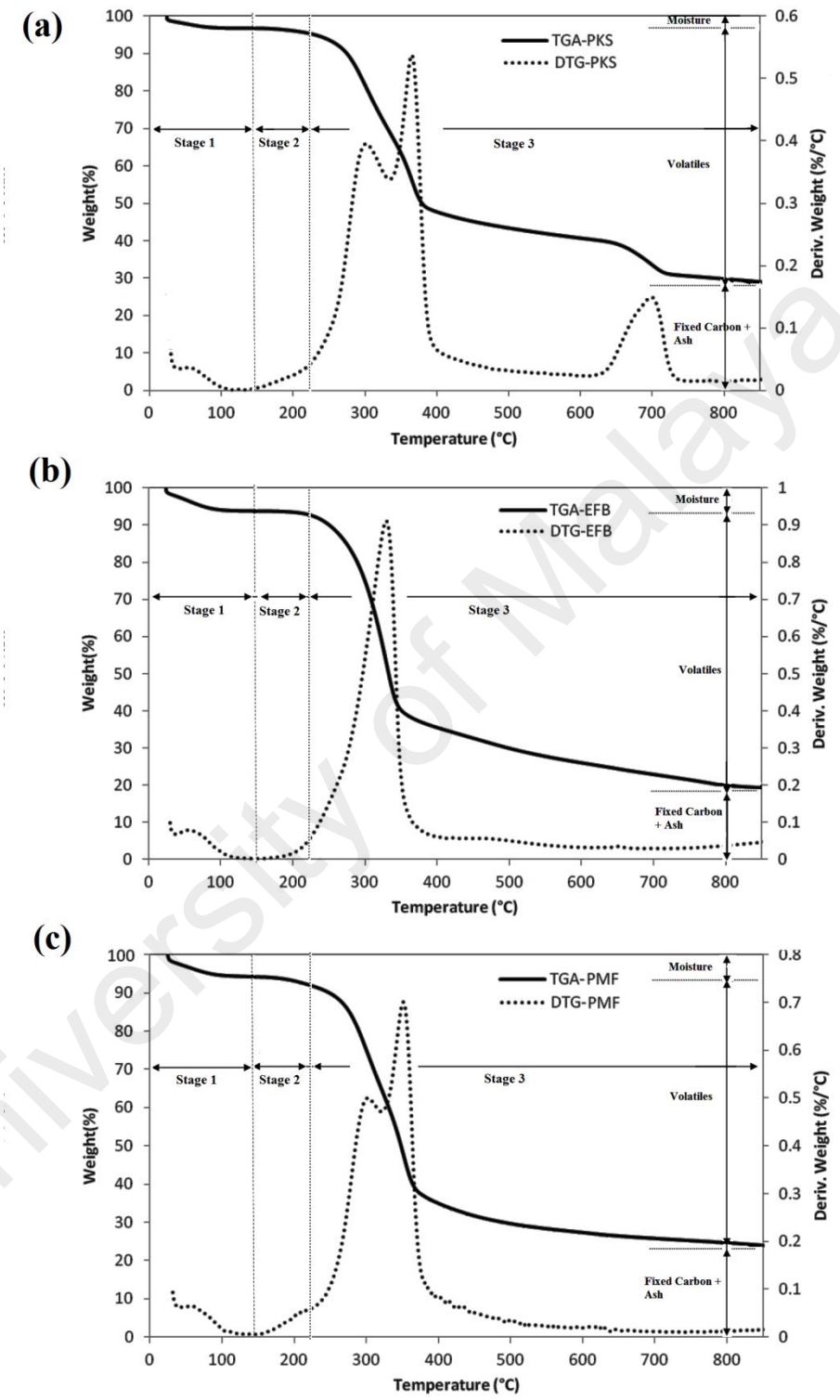

Figure 4.2: Thermogravimetric analysis (TGA) and differential thermogravimetic (DTG) curves of the palm oil biomasses during pyrolysis process. (a) PKS; (b) EFB; (c) PMF; N_2 gas flow rate: 150 ml/min; Heating rate: 15 °C/min.

4.1.3 Thermal decomposition energy

Figure 4.3 indicates the measured heat flow (mW) during the palm oil biomass samples thermal degradation at heating rate of 15 °C/min within the temperature range of 25 °C to 500 °C. The negative values indicate endothermic behavior, whereas positive values show exothermic performance.

The heat flow analysis was performed by dividing the collected data into three stages. Stage 1 showed the endothermic behavior corresponded to the absorption of required energy to remove moisture from the palm oil biomasses at the temperature below 150 °C (Fasina & Littlefield, 2012; Fernandes et al., 2013).

Stage 2 indicated minor changes in the heat flow due to the moisture free biomasses slow depolymerization process and rupture of the chemical links of hemicellulose and cellulose in the temperature range of ~150 to ~225 °C. The major thermal decomposition of the palm oil biomasses samples was carried out in stage 3 at temperature above 225 °C. These exothermic occurrences corresponded to the decomposition of the lignocellulosic fractions (volatile matter) under higher temperature, but with low energy intensity. The thermochemical behaviors of the biomasses depended primarily on their structure and chemical composition.

Energy required for the biomasses moisture evaporation (stage 1) and their thermal decomposition (stage 2 and stage3) were calculated by integrating the heat flow curve using STAR^e software (Version 9.20) provided by DSC manufacturer (METTLER TOLEDO).

The calculated energy values for the three stages are tabulated in Table 4.3. As indicated, the required energy for the biomass samples thermal degradation (Stage 3) was higher than that needed to evaporate the moisture contents from the biomasses (Stage 1). The total thermal decomposition energy to increase the temperature of 1 kg of dry PKS, EFB and PMF from 35 °C to 500 °C at the experimental condition was also shown in Table 4.3. Similar

results were reported by Velden et al. (2010) for different biomasses and He et al.(2006) for wheat straw, cotton stalk, pine and peanut.

The gained information from this investigation will be beneficial when sizing and designing palm oil biomasses thermally decomposition equipment (gasifiers and pyrolyzers).

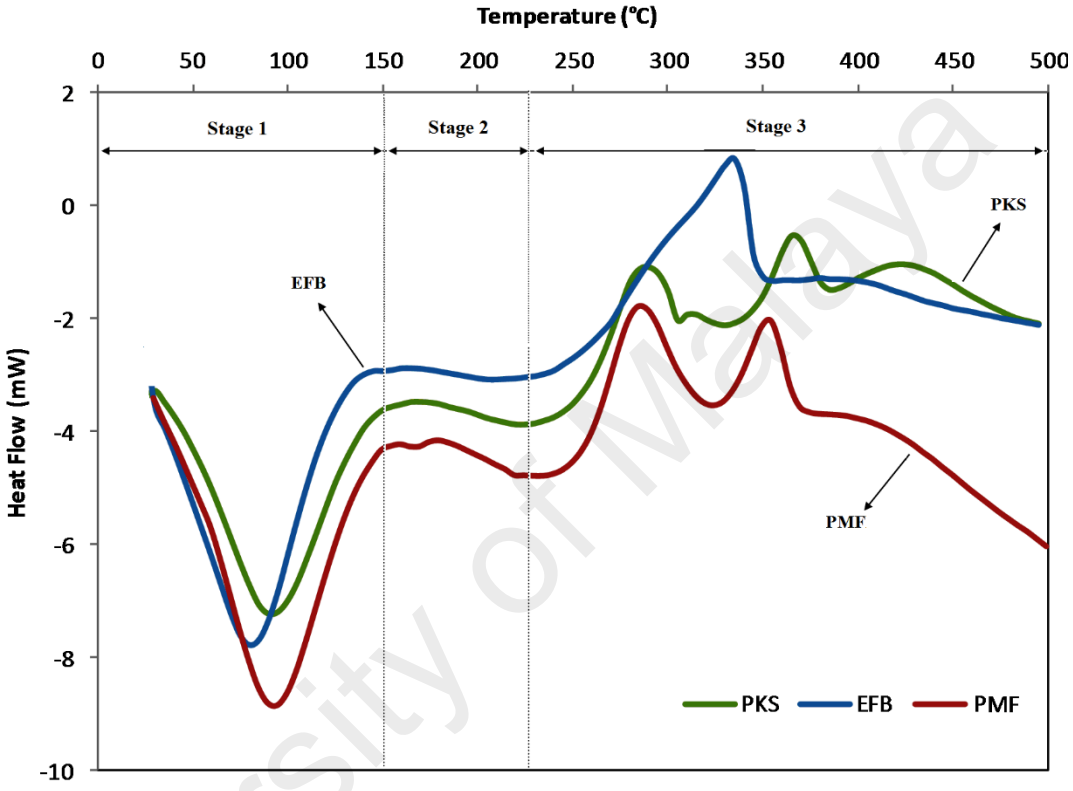

Figure 4.3: Heat flow during thermal decomposition of palm oil biomasses at heating rates of 15 °C/min under N_2 gas flow.

Table 4.3: Energy required to thermally decompose palm oil biomasses.

Biomass	Required Energy (kJ/kg)			Total Required Energy (kJ/kg)
	Stage 1	Stage 2	Stage 3	
PKS	133.08	2.92	181.05	317.05
EFB	182.6	2.44	225.76	410.80
PMF	215.41	3.27	280.61	499.29

4.1.4 Yield of the pyrolysis bio-oils

The yield of the bio-oils, solid products and gas (wt. %) for the PKS, EFB and PMF pyrolysis are shown in Table 4.4. The results of products yield were in agreement with the investigations already performed on the various biomasses pyrolysis (Iliopoulou et al., 2012; H. J. Park et al., 2010a; H. J. Park et al., 2012b).

The relatively high yield of bio-oil may be attributed to the high volatiles fraction of biomass samples, as indicated in Table 4.4 biomasses with high fraction of volatile components favor a high yield of bio-oil (Asadullah et al., 2008). Ash content increasing (PKS=16.3; EFB=7.0; PMF=8.4 wt. %) of the feed reduces the yield of liquid organic fraction. Specifically calcium components in ash (PKS= 71.57; EFB= 15.52; PMF= 20.83 wt. %) reduces the yield of liquid organic in fast pyrolysis (Chiaramonti et al., 2007).

Products yield from the biomass pyrolysis are a complex mixture of the products from the individual pyrolysis of hemicellulose, cellulose, lignin and extractives; each component has its own kinetic characteristics. Furthermore, products of the secondary reaction result from cross-reactions of primary pyrolysis products and the reactions between the original feedstock molecules and pyrolysis products. The yields of bio-oil derived from PKS, EFB and PMF were approximately 49.8 wt. %, 58.2 wt. % and 53.1 wt. %, respectively. As could be observed in Table 4.4, various bio-oils contained high quantity of water. The lowest water content (39.0 wt. %) in bio-oil was produced from EFB pyrolysis, whereas the highest water content (64.7 wt. %) was obtained from PMF. The major amount of water in bio-oils was caused by dehydration reaction during the initial stage of biomass samples pyrolysis (100–300 °C). The volatile organic components undergo dehydration reaction to produce water. According to literature, the similar results on the high amount of water generation could be observed during wheat shell and mesquite sawdust biomasses pyrolysis (Bertero, de la Puente, & Sedran, 2012) .

The composition and yield of the pyrolysis products may vary depending on feedstock pyrolysis conditions and reactor configurations (Chiaramonti et al., 2007). Pinewood pyrolysis in conical spouted bed pyrolyzer produced high yield bio-oil at 500 °C (75 wt. %) (Amutio et al., 2012). In addition, in the other investigation performed on EFB pyrolysis, the maximum bio-oil (52 wt. %) was observed at 450 °C using a fluidized bed reactor (Sulaiman & Abdullah, 2011).

Table 4.4: The yield of bio-oil, gas and char (wt. % on biomass) for the different palm biomasses pyrolysis.

PKS (gr)	EFB (gr)	PMF (gr)	Bio-oil (wt. %)	Gas [(a)] (wt. %)	Char (wt. %)	Water content[(b)] (wt.% in the bio-oil)
60			49.8	16.1	34.1	49.3
	60		58.2	11.8	30.0	39.0
		60	53.1	12.2	34.7	64.7

(a) Calculated by difference (Gas (wt. %) = 100- (Bio-oil (wt. %) + Char (wt. %)))
(b) Measured using Karl Fischer titration.

4.1.5 Bio-oils chemical composition

4.1.5.1 Quantitative analysis using GC-MS

The composition of the bio-oils' organic fraction measured by GC-MS analysis is shown in Table 4.5. As stated in the literature, the different bio-oil's organic compounds have been categorized into 13 groups; aliphatic hydrocarbons, aromatic hydrocarbons, phenols, acids, furans, alcohols, esters, ethers, ketones, aldehydes, sugars, polycyclic, nitrogen containing compounds and polycyclic aromatic hydrocarbons (PAHs). Among these components, undesirables were carbonyls, acids, polycyclic aromatic hydrocarbons (PAHs) and heavier oxygenates. Conversely, aliphatic hydrocarbons, alcohols and aromatics were known as desirables, while furans and phenols were considered as high added value chemicals. Acid components available in the bio-oils created corrosiveness, while aldehydes and ketones conducted to the bio-oils instability during transportation and practically challenging to be

utilized as engine fuels (Iliopoulou et al., 2012; H. J. Park et al., 2010a; S. D. Stefanidis et al., 2011b). Acids, aldehydes, and ketones could be likely derived from cellulose and hemicellulose pyrolysis, whereas sugar derived components (sugars and furan) and PAHs would be mostly yielded from hemicellulose and lignin components, respectively (Asadieraghi et al., 2014).

Table 4.5 shows the bio-oils (organic phase) composition (wt. %) produced by PKS, EFB and PMF biomass samples pyrolysis. The bio-oils acidity caused by carboxylic acid formation like hexanoic acid and 2-Propenoic acid probably formed by cellulose and hemicellulose fractions of the biomass samples decomposition (GW et al., 2006). Phenolic compounds, which produced by the lignin fraction of the biomasses, contributed to the bio-oils acidity but to a much lesser degree (Oasmaa, Elliott, & Korhonen, 2010). Ketones and aldehydes as carbonyl components had tendency toward condensation reactions causing the bio-oils instability through their viscosity enhancement. Furans and hydrocarbons formed from hollocellulose were the desirable components attributed to their high content of energy (GW et al., 2006).

As can be seen in Table 4.5, the produced bio-oils via pyrolysis indicated low content of acids, ketones and alcohols, but were rich in phenolic components. High content of phenolic compounds available in the PKS, EFB and PMF bio-oils could be caused by relatively high lignin content of the biomasses (50.7, 22.1 and 25.7 wt. %, respectively), especially in PKS. Hence, the produced bio-oils through thermal pyrolysis of the biomasses were considered as low quality products.

High quantity of furan based components (i.e. furfural and vinylfuran), derived from cellulose and hemicellulose (hollocellulose) compounds, was observed in EFB (16.41 wt. %) and PMF (13.85 wt. %) bio-oils, where their hollocellulose content was 77.9 and 74.3 wt. %, respectively.

Table 4.5: The bio-oils (organic phase) composition (wt. %) produced by PKS, EFB and PMF biomass samples pyrolysis.

Compound	PKS pyrolysis	EFB pyrolysis	PMF pyrolysis
Hexanoic acid	3.87	5.31	2.89
Furfural	7.15	9.21	8.05
2-Cyclopentene -1-one		1.67	2.01
2-Butenal, 2-methyl-	4.35		
Furfuryl alcohol	1.18		
2-Propanone, 1-(acetyloxy)	2.28		
Butryrolactone		7.18	9.87
2-Propenoic acid	4.21	5.91	4.8
Phenol	61.8	34.8	40.8
Vinylfuran		7.2	5.8
Acetic acid, phenyl ester		1.32	
3-Methyl phenol	2.49		
2- Methyl phenol	3.34	8.7	7.65
2-Metoxy phenol			1.23
2,5 dimethyl phenol		1.15	
1,2-Benzenediol	4.91	6.8	3.83
1,3-Cyclohexadiene, 1-methyl-4-(1-methylethyl)-		1.0	
1,4:3,6-Dianhydro-.alpha.-d-glucopyranose		4.11	2.73
2-Isopropoxyphenol	1.3	1.39	
Methyl benzenediol	2.68	4.02	1.09

4.1.5.2 Qualitative analysis using FTIR

The FTIR spectra of the various palm biomasses pyrolysis bio-oils are shown in Figure 4.4. The spectra related to EFB and PMF were very similar, whereas the PKS bio-oil's spectrum was somehow different. This is attributed to similar biomass compositions of EFB and PMF. The strong absorption bonds between 3700 and 3000 cm^{-1}, which is O-H stretching characteristics, showed the availability of alcohols and phenolic compounds in the bio-oils. The presence of aldehydes, carboxylic acids and ketones (C=O stretching) could be observed around 1730 cm^{-1}. The bands between 1246-950 cm^{-1}, which are relevant to C-O-C, C-O and C-OH stretching, indicated the presence of alcohols and phenolic components.

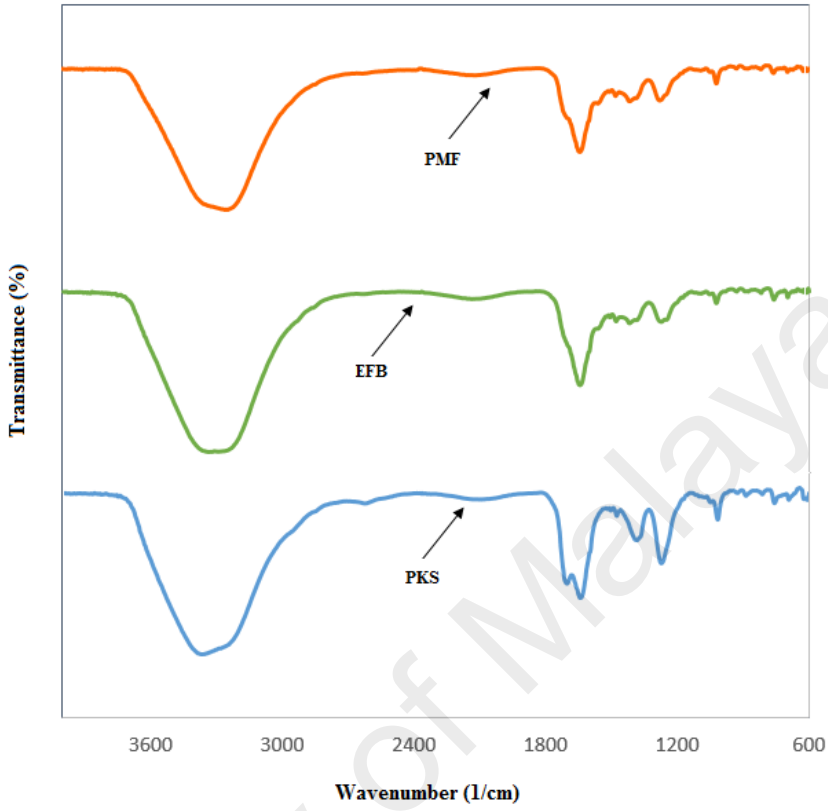

Figure 4.4: Peaks assignment to the chemical functional groups of the bio-oil using FTIR.

4.1.6 Reaction pathway for biomass pyrolysis

Generally, biomass pyrolysis vapors pass through a series of reactions during pyrolysis (Bridgwater et al., 2008; K. Wang et al., 2014). Degradation pathway for hemicellulos, cellulose and lignin, three building blocks of lignocellulosic biomass, was recently suggested by Wang et al. (K. Wang et al., 2014). Figure 4.5 shows the proposed reaction pathway. In their investigation, it was assumed that there is minor interaction between three mentioned biomass components during pyrolysis. The biomass oxygenated compounds passed through cracking, decarboxylation, decarbonylation and dehydration reactions at 350 °C to 500 °C. During pyrolysis, cellulose could yield butyrolactone and furanic components like furfural and vinyl furan (Shen et al., 2011). Pyrolysis of lignin compounds initially produced

monomeric phenolics such as phenol, 2- methyl phenol, 1,2-benzenediol and methyl benzenediol. Lignin, among the three main biomass components, had the complex structure and phenolics yielded from its thermal decomposition were prone to the formation of char and coke. Therefore, the product distribution from biomass pyrolysis was highly depending on the biomass composition.

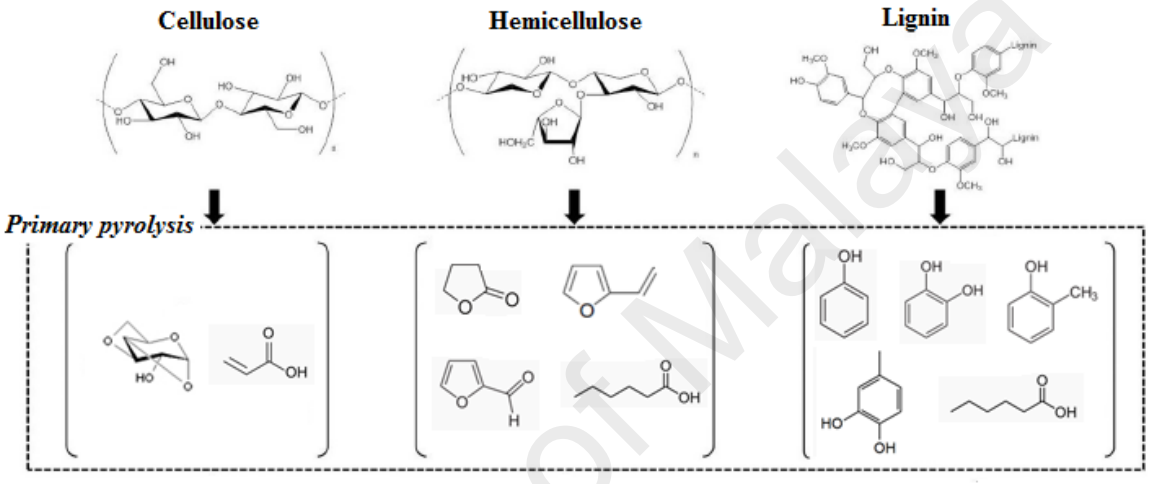

Figure 4.5: Reaction pathways for pyrolysis of lignocellulosic biomass. Adapted from Wang et al. (K. Wang et al., 2014)

4.2 Part 2: Characterization of lignocellulosic biomass thermal degradation and physiochemical structure: Effects of demineralization by diverse acid solutions

4.2.1 Basic characterization of the biomass samples

Figure 4.6 shows the ash content of the virgin and pretreated palm oil biomass samples. The biomasses ultimate/proximate analysis and their inorganic constituents (before and after demineralization) are summarized in Table 4.6 and Table 4.7, respectively. Compared to the virgin samples, a significant ash removal from EFB (7% to 0.43%) and PMF (8.4% to 1.35%) was performed by HF diluted solution, while PKS-HF indicated more resistance to ash elimination. The maximum ash removal from PKS (16.3% to 4.6%) was observed when diluted acid leaching process was carried out by HCl. Different ash removal from the biomasses using same acid solution was possibly due to the inorganic contents (Table 4.7), nature, composition and structure of the various lignocellulosic biomass samples. Biomass virgin samples indicated various lignocellulosic contents (wt. %) (Mohammed et al., 2011): PKS (20.8 % cellulose, 22.7% hemicellolose and 50.7% lignin), EFB (38.3% cellulose, 35.8% hemicellolose and 22.1% lignin), and PMF (34.5% cellulose, 31.8% hemicellolose and 25.7 % lignin). As can be observed, the cellulose and hemicellulose content of EFB was greater than that of PMF and PKS. On the other hand, PKS showed the highest lignin content. EFB and PMF indicated relatively similar lingocellulosic compositions and mineral contents (Table 4.7), whereas PKS showed completely different inorganics and lingocellulosic contents compared with EFB and PMF.

Proximate analysis of the biomass samples (with maximum ash removal) can be seen in Table 4.6. While the ash contents of the samples remarkably decreased, their volatile contents increased after leaching process. This could be led to the improvement of the biomass fuel properties like heat value. Also, ash removal from the biomasses could prevent the severe problems associated with the presence of high inorganic contents such as slagging,

agglomeration, deposition and heated side corrosion in the thermochemical processes (Jiang et al., 2013).

The biomass organic compounds are different oxygenated hydrocarbons which their major constituents are carbon, oxygen and hydrogen. The molecular mass of carbon is much heavier than hydrogen therefore; H/C wt% ratio could reflect the amount of hydrocarbon components (W. S. Lim et al., 2013). Removal of hydrocarbons during leaching process will be conducted to the H/C ratio enhancement. As can be seen in Table 4.6, the H/C wt% elemental ratio in PKS-HCl, EFB-HF and PMF-HF slightly increased. This could specify that the compositional properties of these demineralized biomasses were slightly changed probably due to the removal of a fraction of organic components (Eom et al., 2013; Eom et al., 2011; Jiang et al., 2013; W. S. Lim et al., 2013).

Higher heating value (HHV) of the various biomass samples was calculated from the elemental compositions using Eq. (3-1) and summarized in Table 4.6. As shown in Table 4.6, the ash removal was in direct relation with the biomasses HHV increasing.

The XRF results tabulated in Table 4.7 indicate the major inorganic constituents (Al, Ca, Fe, K, Mg, P and Si) reduction after the biomasses demineralization. The amount of Ca, K, Mg and Si after demineralization showed different degrees of their removal most likely associated with the solubility of the different metal oxides in the various acids. Most of the acid diluted solutions like HCl, H_2SO_4, HNO_3 and $HClO_4$ were very efficient in Ca and Mg reduction, while HF showed considerable results on Si diminution. K_2O and SiO_2 were the main minerals available in EFB and PMF which could be efficiently leached out by HF. CaO, which was the most dominant inorganic species in PKS, efficiently leached out by HCl (from 71.57 to 1.27 wt %), whereas HF was not successful to remove it. It might be likely attributed to the higher H^+ concentration of HCl compared with HF (weak acid owing to strong H-F bond) due to its higher dissolution in water (Habbache, Alane, Djerad, & Tifouti, 2009; Jiang

et al., 2013). It is worthwhile to mention that, various diluted acids had different acid strength increasing in the following order: $HClO_4$> HCl> H_2SO_4> HNO_3>HF.

Acid leaching processes are very effective on removal of inorganic species, but it may impose a negative impact on the biomass physiochemical structure. Therefore, investigations on the physiochemical structure of the samples needs to be taken to the consideration.

In this study, among the demineralized biomass samples pretreated by diverse diluted acid solutions, those which showed the maximum inorganics removal have been selected for elaborated analysis. EFB and PMF demineralized by HF and PKS pretreated by HCl indicated maximum ash removal.

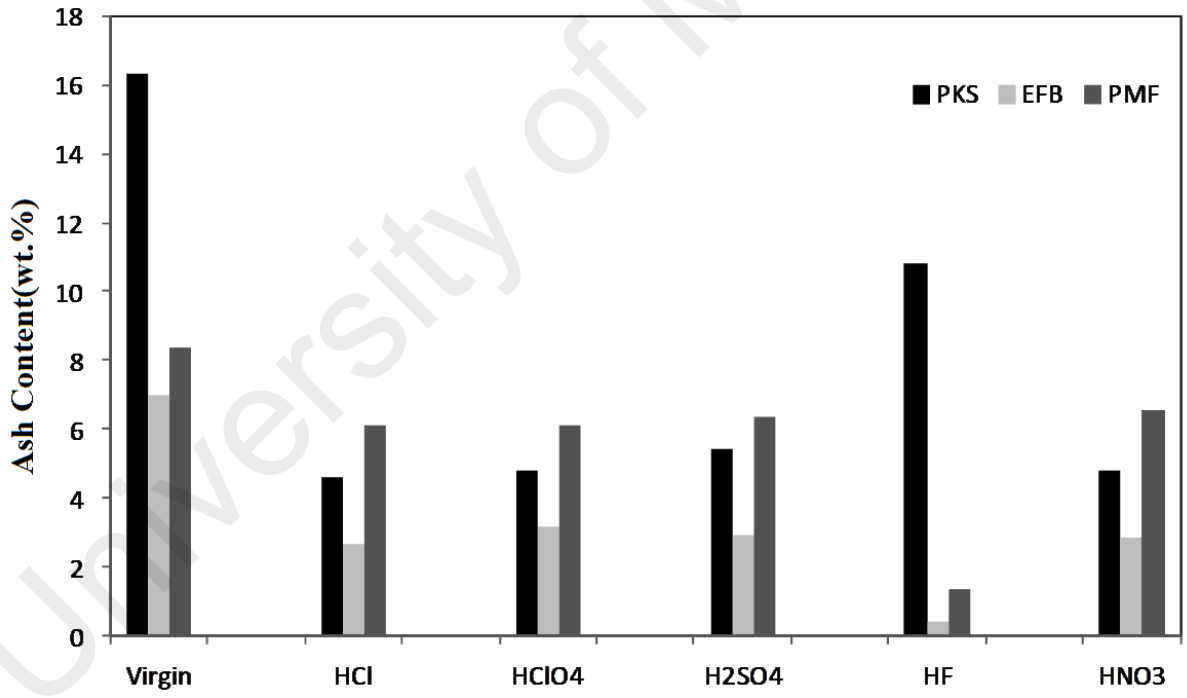

Figure 4.6: Ash content of the different untreated and treated palm oil biomasses.

Table 4.6: Proximate and ultimate analysis of the virgin and demineralized palm oil biomasses (PKS, EFB and PMF).

Proximate analysis (wt. %)

Biomass	Moisture	Volatile Matters	Fixed Carbon	Ash
PKS	2.8	67.9	13.0	16.3
EFB	6.3	79.2	7.5	7.0
PMF	5.8	70.8	15.0	8.4
PKS-HCl	5	72.8	17.6	4.6
EFB-HF	5	82.0	12.57	0.43
PMF-HF	5.3	81.7	11.65	1.35

Ultimate analysis (wt. %)

Acid	Biomass	Carbon	Hydrogen	Nitrogen	Sulphur	Oxygen[(1)]	H/C[(2)]	O/C[(3)]	HHV (MJ/kg)
-	PKS	49.05	5.59	0.76	0.38	44.60	0.114	0.909	16.1
	EFB	44.84	5.81	1.41	0.40	47.94	0.129	1.069	16.2
	PMF	47.76	5.59	2.13	0.49	44.52	0.117	0.932	17.0
HCl	PKS	49.79	5.89	0.77	0.38	43.55	0.118	0.874	18.8
	EFB	46.32	6.55	1.27	0.44	45.86	0.141	0.990	18.5
	PMF	47.68	6.39	2.06	0.47	43.87	0.134	0.920	18.3
$HClO_4$	PKS	50.03	6.14	0.79	0.33	43.04	0.122	0.860	19.2
	EFB	47.34	6.48	1.5	0.42	44.68	0.137	0.943	18.8
	PMF	48.18	6.31	2.1	0.43	43.41	0.131	0.901	18.4
H_2SO_4	PKS	48.48	6.06	0.79	0.35	44.67	0.125	0.921	18.3
	EFB	47.2	6.38	1.36	0.42	45.06	0.135	0.954	18.7
	PMF	48.16	6.35	1.93	0.43	43.56	0.132	0.904	18.4
HF	PKS	47.37	5.84	0.89	0.34	45.9	0.123	0.969	16.3
	EFB	46.9	6.31	1.59	0.36	45.38	0.131	0.967	19.0
	PMF	47.92	5.69	2.29	0.39	44.10	0.119	0.920	18.5
HNO_3	PKS	47.93	6.02	1.07	0.30	44.98	0.125	0.938	18.2
	EFB	45.48	6.12	2.42	0.34	45.98	0.134	1.011	17.7
	PMF	46.68	6.12	3.01	0.37	44.19	0.131	0.946	17.6

(1)By difference; (2) Hydrogen/Carbon ratio ;(3) Oxygen/Carbon ratio

Table 4.7: Biomass samples inorganic contents before and after pretreatment (wt. %) (XRF results).

Biomass Samples	Al_2O_3	CaO	Fe_2O_3	K_2O	MgO	Na_2O	P_2O_5	SiO_2	ZnO
PKS Virgin	2.10	71.57	4.89	1.29	1.77	0.32	0.98	16.46	0.02
EFB Virgin	0.77	15.52	5.78	39.98	3.68	0.23	4.29	19.24	0.32
PMF Virgin	2.71	20.83	9.67	15.55	4.20	0.25	6.76	26.05	0.30
PKS-HCl	9.67	1.27	26.07	1.39	0.39	2.69	0.75	50.11	0.29
EFB-HCl	2.28	0.94	4.83	1.48	0.19	0.32	1.54	66.46	0.52
PMF-HCl	5.26	0.18	7.32	1.41	0.19	0.18	1.76	65.47	0.12
PKS-$HClO_4$	7.77	0.88	29.95	1.43	0.25	0.47	0.94	47.95	0.38
EFB-$HClO_4$	1.97	0.39	6.92	1.03	0.13	0.14	1.46	63.57	0.19
PMF-$HClO_4$	4.90	0.54	9.16	1.45	0.15	0.15	1.47	62.24	0.16
PKS-H_2SO_4	9.03	6.16	29.81	1.27	0.19	0.37	0.91	40.33	0.22
EFB-H_2SO_4	2.00	0.62	3.70	0.91	0.11	-	1.70	66.23	0.15
PMF-H_2SO_4	5.05	0.40	7.42	1.42	0.15	0.13	1.34	66.79	0.07
PKS-HF	1.67	69.10	3.73	0.18	0.79	0.16	0.23	0.81	0.02
EFB-HF	1.08	42.26	8.41	0.58	5.09	-	4.73	3.45	0.51
PMF-HF	4.88	32.42	10.49	4.19	3.37	0.50	3.54	6.45	0.22
PKS-HNO_3	7.08	5.75	31.30	1.13	0.28	0.57	0.67	46.56	0.20
EFB-HNO_3	2.75	1.14	10.08	1.02	0.20	0.20	1.14	68.82	0.20
PMF-HNO_3	4.73	0.77	8.79	1.12	0.15	0.17	1.27	69.80	0.14

4.2.2 Physical characterization of the biomasses

Figure 4.7 shows SEM images of the virgin and pretreated biomass samples with some differences in particle shape. After pretreatment, some morphological changes were observed indicating partial damage in biomasses structure although, their main framework was unchanged. As could be observed in SEM images, there were originally few pores on the surface of untreated biomasses. However, after acid pretreatment, surface porosity of the samples was increased. It was in agreement with the porosity characteristics of the biomasses were shown in Table 4.8. The virgin biomass samples (Figure 4.7a, 4.7c, 4.7e) showed small particles adhered to their surfaces. After leaching of EFB (Figure 4.7d) and PMF (Figure 4.7f) by diluted hydrofluoric acid and pretreatment of PKS by diluted hydrochloric acid (Figure 4.7b), some particles were leached away and the biomass samples structure seemed to be eroded. The removed particles from the biomasses samples by various diluted acid solutions might be minerals and extractives (Haykiri-Acma, Yaman, & Kucukbayrak, 2011; Jiang et al., 2013).

All the leached samples showed some changes in the biomasses stomata and epidermis, which could be an evidence for the effects of acid leaching on the fiber structure of biomass samples by dissolving some contents of hemicellulose and probably cellulose (Jiang et al., 2013; Vassilev, Baxter, Andersen, Vassileva, & Morgan, 2012). On the other hand, partially dissolution of mineral constituents and adhered amorphous hemeicellulose during acid pretreatment resulted higher available surface area and pore volume (C. T. Yu, Chen, Men, & Hwang, 2009).

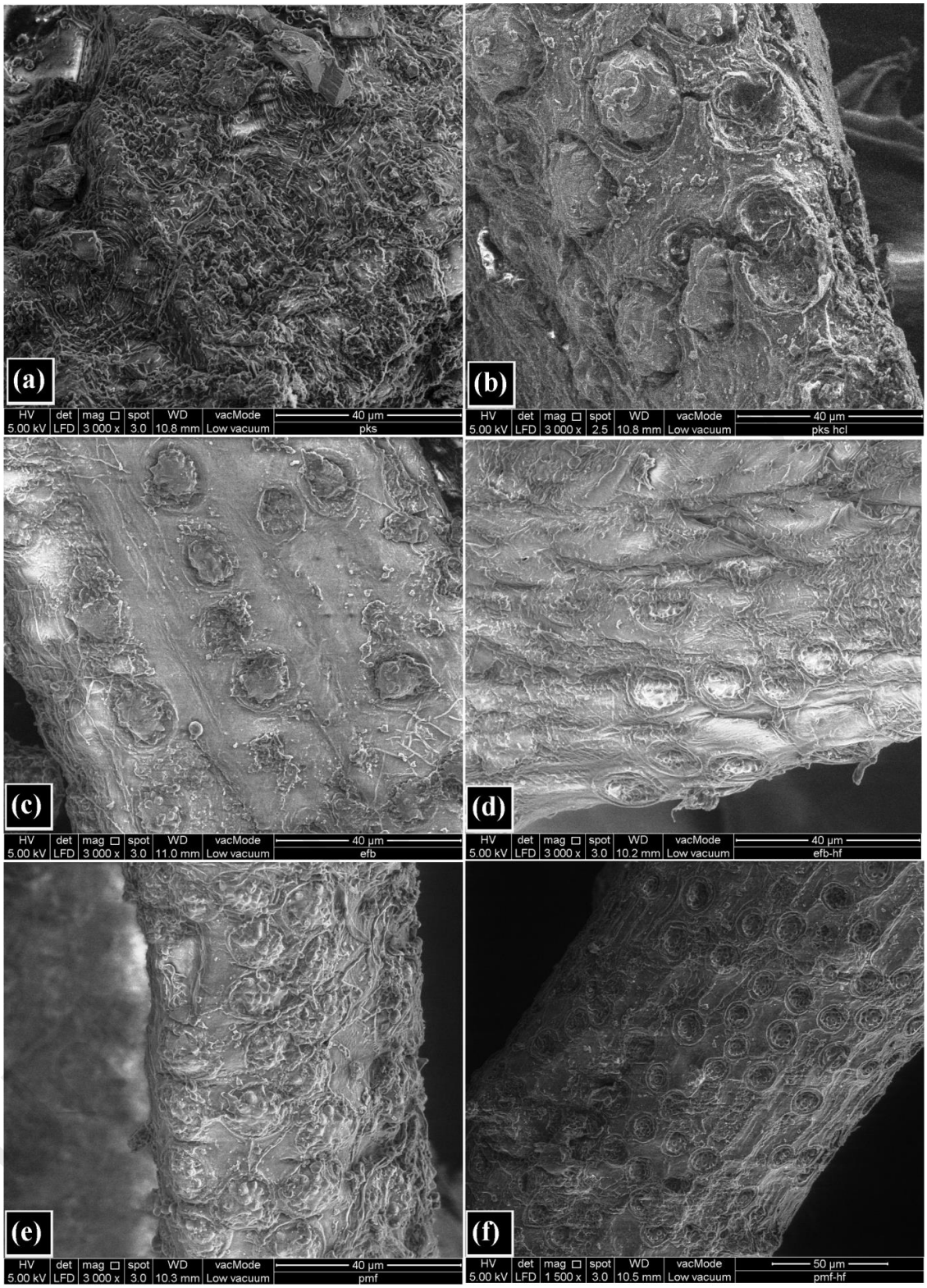

Figure 4.7: SEM images of the virgin (PKS (a), EFB(c) and PMF (e)) and pretreated (PKS-HCl (b), EFB-HF (d) and PMF-HF (f)) palm oil biomass samples.

Table 4.8 shows the adsorption characteristics of raw and pretreated biomass samples. All tests were carried out in duplicate to ensure reproducibility of the results; the mean of these two measurements (with less than 3% difference) was taken to represent each evaluation. EFB and PMF leached by HF solution and PKS pretreated by HCl indicated that their total pore volume and BET surface area were both increased, whereas their average pore diameter was decreased. This could indicate that leaching process of the biomass samples by diluted hydrofluoric acid (EFB-HF and PMF-HF) and hydrochloric acid (PKS-HCl) probably eroded the biomass fiber structure and led to the creation of numbers of pores, thus conducted to BET surface and total pore volume increasing. This was in agreement with SEM results explained before.

Table 4.8: Porosity characteristics of the virgin and pretreated biomass samples.

Biomass sample	BET surface area (cm^2/g)	Total pore volume (cm^3/g)	Average pore diameter (nm)
PKS	0.3106	0.001292	45.1133
EFB	0.1188	0.001936	36.0622
PMF	1.2528	0.008705	40.0061
PKS- HCl	0.6051	0.003769	37.3816
EFB- HF	0.9615	0.004993	33.6010
PMF- HF	1.6051	0.009859	29.6556

4.2.3 Chemical structure evaluation of the biomass samples

The chemical structure of the lignocellulosic biomass samples is frequently studied using infrared spectroscopy. In this investigation, FTIR technique was employed to study the effects of ash removal on the biomasses chemical structure. Figure 4.8 depicts the FTIR spectra of the various virgin and pretreated biomasses. Table 4.1 shows the assignment of FTIR peaks to the chemical functional groups and biomass components according to the literature.

In the infrared spectra, the first strong broad band at 3700-3000 cm^{-1} was related to O-H stretching vibration of phenolic, alcoholic and carboxylic functional groups. Also, the band between 2800 and 3000 cm^{-1} was attributed to C-H stretching vibration of - CH_2 and -CH_3 functional groups. As can be seen in Figure 4.8, both of these bands slightly declined after demineralization, which was in agreement with the studies done by Jiang et al. (Jiang et al., 2013) and Fierro et al.(Fierro et al., 2007).

The band around 1730 cm^{-1} was the result of C= O (aldehydes, ketones or carboxyl) stretching vibration of free carbonyl groups of hemicellulose component. The next spectrum bands around 1650-1510 cm^{-1} (C=C stretching vibrations of aromatics) were corresponded to lignin.

After demineralization, slight changes of the intensity of band around 1730 cm^{-1} ,compared with more intense change of band around 1650 cm^{-1}, could be attributed to the joint vibration(stretching) of carbonate inorganics and lignin. As indicated in Figure 4.8, EFB and PMF showed more significant decrease of the band around 1650 cm^{-1} probably due to the high degree of inorganics (carbonate) removal(Fierro et al., 2007; Jiang et al., 2013).

The spectral region of 1400-600 cm^{-1}, where various vibration modes existed, was very complicated to be analyzed. However, in this region, vibration of some specific units related to lignin could be detected. The spectra of different samples indicated the characteristic vibration of lignin unit at 1240 cm^{-1} (C=O stretching) and 850-750 cm^{-1} (C-H bending) (Fierro et al., 2007; Parshetti et al., 2013). Among different biomass samples, PKS pretreated by HCl showed more considerable changes of these bands intensity compared with EFB-HF and PMF-HF.

The spectra between 1440 and1400 cm^{-1} contained several bands in the O-H bending region, which were most probably cellulose and hemicellulose related transmission. A significant change of bands intensity in this region could be observed for PKS-HCl (Figure 4.8a).

Changing of the spectra(after biomasses pretreatment) at 1730 cm^{-1} and between 950 and 1200 cm^{-1} could be due to C-O-C, C-O and C-OH functional groups stretching, most likely related to hemicelluloses and cellulose components.

As can be seen in Figure 4.8, unlike PKS, the virgin EFB and PMF indicated relatively similar chemical structure. Also, after pretreatment they exhibited rather comparable FTIR spectra. It might be attributed to the leaching acids type and the biomasses nature and composition already explained in section 4.2.1. Pretreatment of EFB and PMF by diluted hydrofluoric acid introduced slight effects on the biomasses chemical structure (Eom et al., 2011; I.-Y. Eom et al., 2012), whereas leached PKS by hydrochloric acid showed more considerable changes in the biomass chemical structure.

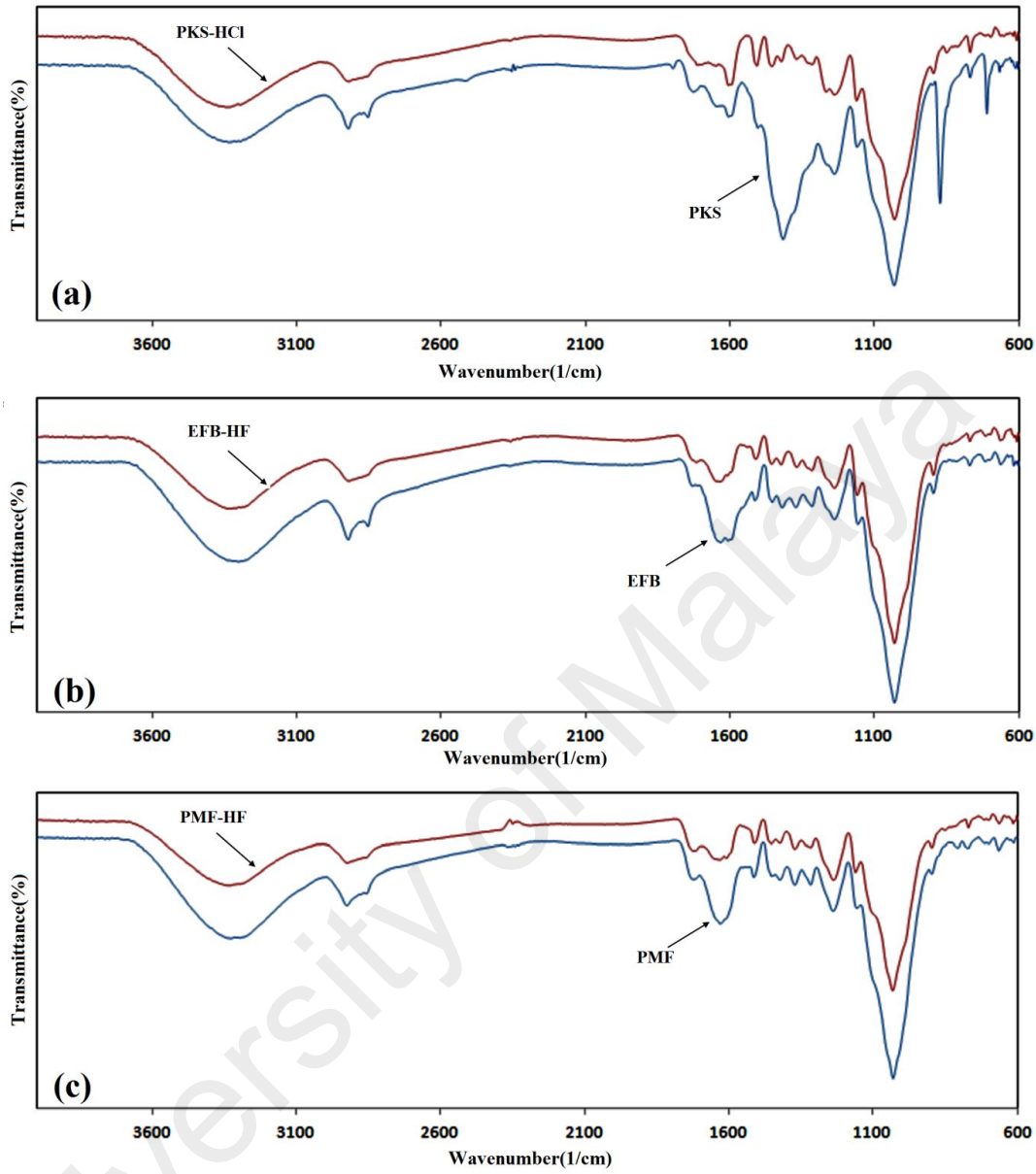

Figure 4.8: FTIR spectra of different virgin and pretreated biomass samples. (a) PKS and PKS-HCl; (b) EFB and EFB-HF; (c) PMF and PMF-HF.

4.2.4 Pyrolysis characteristics

Figure 4.9 shows the TGA (weight loss) and DTG (derivative thermogravimetric) analysis evolution profiles as a function of temperature for the virgin and pretreated palm oil biomass samples at a constant heating rate of 15°C/min. As a whole, the pyrolysis process of the lignocellulosic biomass can be divided into four main sections: moisture and very light volatiles components removal (< 120 °C); degradation of hemicellulose (220-315 °C); lignin

and cellulose decomposition (315-400 °C) and lignin degradation (> 450 °C) (Sanchez-Silva et al., 2012; Haiping Yang et al., 2007a). As indicated in Figure 4.9, various untreated (virgin) palm oil biomass samples showed different thermal behavior. The DTG peaks attributed to cellulose decomposition were observed at 364°C, 329 °C and 351°C for PKS, EFB and PMF, respectively. The DTG shoulders of PKS and PMF curves observed at ~300°C were caused by hemicelluloses devolatilisation (Idris et al., 2010; Vamvuka et al., 2003). The palm oil biomasses lignin decomposition was occurred slowly over a broad range of temperature (137-667 °C) (Vamvuka et al., 2003). In the section corresponded to lignin degradation (> 450 °C), EFB overlapped PMF, whereas that of PKS occurred with different weight loss rates indicating one peak in DTG curve started at about 650°C.

The different thermal behavior of the lignocellulosic materials could be attributed to the various contents of cellulose, hemicellulose and lignin (section 4.2.1) (Y. F. Huang et al., 2011a; Sanchez-Silva et al., 2012). The lowest temperature peak in DTG curve could indicate the highest content of hemicellulose in EFB. Furthermore, the differences in residue yield could represent the different lignin contents of the biomass samples. PKS indicated the highest content of the lignin due to the largest residue. Also, maximum weight loss rate could be an indication of volatile matters and cellulose content in the biomass samples (Damartzis et al., 2011). The maximum decomposition rate of EFB was higher than that of PKS and PMF, because its cellulose and volatiles contents were greater.

DTG curve corresponded to PKS showed a third isolated peak started at temperature ~650 °C and reached to maximum at ~700 °C. Literature investigations on similar sample indicated that except Idris et al. (2010) ,who reported this third peak, it has not been expressed elsewhere. Further details on the reasons for occurrence of this peak would be explained in section 4.2.6 using TGA-MS and TGA-FTIR analysis.

Reactivity of the biomass samples can be estimated from the peak height and position. The peak height is directly proportional to the biomass reactivity, whereas the temperature in which the peak takes place is inversely proportional to the biomass reactivity(Vamvuka et al., 2003). As can be seen in Figure 4.9b, the highest degradation rate belonged to EFB at lowest peak temperature. So, EFB indicated the highest reactivity among palm oil biomass samples (Idris et al., 2010).

As shown in Figure 4.9, regardless of the biomass sample type and pretreatment process, all the biomass samples were pyrolyzed at the temperature range of ~250°C to ~400 °C.

From literature it is known that hemicellulose is degraded at peak temperature of ~300 °C , while cellulose is decomposed at the peak ~ 365 °C (Y. F. Huang et al., 2011a; Müller-Hagedorn et al., 2003; Nowakowski et al., 2007; Sanchez-Silva et al., 2012). As can be observed in Figure 4.9b, demineralized EFB by diluted HF solution showed a shoulder in the relevant peak at around 311 °C in DTG curve. It was caused by hemicellulose decomposition, while the peak at 379 °C was associated with cellulose degradation. However, cellulose and hemicellulose decomposition in the virgin EFB biomass were overlapped due to the presence of inorganics. In this case, the catalytic effects of inorganics moved cellulose pyrolysis to lower temperature and combined together with the pyrolysis of hemicellulose.

DTG curves related to PMF and PMF-HF have been shown in Figure 4.9c. As represented in Figure 4.9c, peak shoulder showed hemicellulose decomposition, while the main peak indicated cellulose degradation. Deminiralization shifted hemicellulose and cellulose degradation to a higher temperature (351°C and 371°C, respectively). The same could be observed for PKS and PKS-HCl (Figure 4.9a). Unlike EFB and PMF, PKS showed third peak at ~ 700 °C. This peak was disappeared whilst PKS demineralized by HCl solution. It was possibly due to the catalytic effects of minerals at high temperature (~650 °C ~750 °C). An elaborated study on this phenomenon would be expressed in section 4.2.6.

As explained in subsection 4.2.1, K_2O and SiO_2 (the main minerals available in EFB and PMF) could be efficiently leached out by HF, whereas CaO (which was the most dominant inorganic species in PKS) could be highly extracted by HCl. Since their elimination changed the biomass thermal behavior, they probably had significant effects on the catalytic behavior of inorganics available in the various biomasses.

Pretreatment has a significant influence on the biomasses thermal behavior in terms of both gas product distributions and pyrolysis temperature. Considering DTG curves in Figure 4.9, pretreatment using the diluted acid solutions transferred the biomass samples pyrolysis to a higher temperature by 5-50 °C. Pyrolysis properties of the virgin and pretreated palm oil biomass samples using TGA and DTG are summarized in Table 4.9. As reported in Table 4.9, in comparison with the virgin samples, the maximum decomposition rate of HF pretreated biomass samples around 365 °C (cellulose components degradation) was almost unchanged, whereas HCl pretreated samples showed considerable increase in degradation rate from 0.535 %/°C to 0.737 %/°C. These changes in cellulose components decomposition rate was associated with cellulose crystallinity and structure. Therefore, it could be concluded that the biomass pretreatment by HCl relatively disrupted cellulose crystalline, whereas HF had not significant effect on cellulose structure. These results are similar to those reported by Eom et al. (2011). The lignocellulosic biomass pretreatment with HF solution could be interesting from two main aspects; (a) its efficient demineralization effects on the reduction of biomass samples (here EFB and PMF) ash content to negligible amount (Eom et al., 2011; I.-Y. Eom et al., 2012) and (b) unlike most of the acids pretreatments which considerably changed the biomass chemical structure (degradation) during pretreatment, HF did not indicate significant effects on the biomass chemical degradation during the demineralization. Therefore, more precise effects of demineralization on the biomass samples thermal behavior could be investigated (Eom et al., 2011).

Moreover, as can be seen in Table 4.9, the char yield decreased after deashing pretreatment. This indirectly could be an evidence for the effect of the biomass demineralization on the production of more volatile components during pyrolysis.

The first peak in the various DTG curves in Figure 4.9 indicated the moisture content of the biomass samples dropped rapidly at the temperature of ~ 60 °C (Table 4.9). This observation was thanks to the significant moisture evaporation as temperature increased.

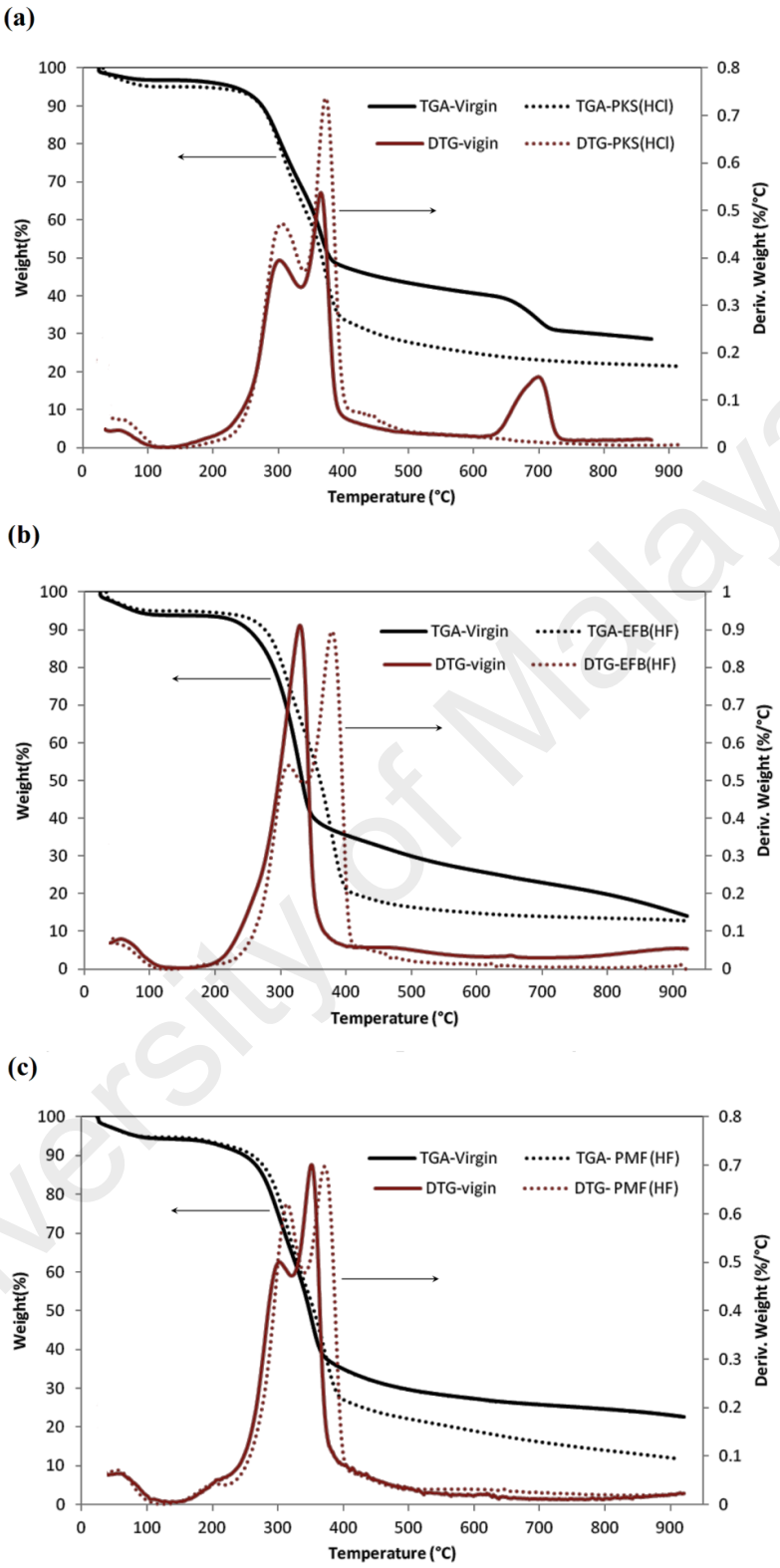

Figure 4.9: Thermogravimetric analysis (TGA) and differential thermogravimetic (DTG) curves of the virgin and demineralized palm oil biomass samples during pyrolysis process. (a) PKS and PKS-HCl; (b) EFB and EFB-HF; (c) PMF and PMF-HF; N2 gas flow rate: 150 ml/min; Heating rate: 15 °C/min.

Table 4.9: Pyrolysis properties of the virgin and demineralized palm oil biomass samples using TGA and DTG; N_2 gas flow rate: 150 ml/min; Heating rate: 15 °C/min.

Biomass	Maximum Temperature (°C)				Maximum Deriv. Weight(wt%/°C)				Char Content (wt %)
	First Peak	Shoulder	Second Peak	Third Peak	First Peak	Shoulder	Second Peak	Third Peak	
PKS	61	300	364	700	0.035	0.395	0.535	0.148	29.3
PKS-HCl	62	305	373	-	0.059	0.47	0.737	-	22.2
EFB	60	-	329	-	0.078	-	0.90	-	14.5
EFB-HF	61	311	379	-	0.061	0.54	0.895	-	13.0
PMF	61	301	351	-	0.064	0.50	0.70	-	22.2
PMF-HF	60	314	371	-	0.070	0.62	0.70	-	13.0

4.2.5 Kinetics analysis results

Referring to Eq. (3-7) and applying the TGA (mass change by temperature) results, $ln[-\ln(1-x)/T^2]$ versus $1/T$ was plotted for the virgin and pretreated biomass samples. Among TGA data, those which provided the best linear regression were selected. Therefore, from the calculated slope and intercept ($-E_a/R$ and $ln[k_0R/\beta E_a]$, respectively), the kinetics parameters (pre-exponential factor (k_0) and activation energy(E_a)) were determined. The results of kinetics parameters at corresponded temperature are shown in Table 4.10. Calculated regression results having coefficient of determination (R^2) from 0.9930 to 0.9990 and standard error from 7.83×10^{-7} to 6.19×10^{-6} indicated that the assumption of the biomass pyrolysis reaction undergoing a first order reaction should be proper. High R^2 coefficient and low standard error values could prevent the data noise (experimental errors disturbance) and provide more reliable kinetic parameters at related temperature ranges.

As can be seen in Table 4.10, activation energy varied after biomasses demineralization. Compared with the virgin biomasses (26.11- 60.30 kJ/mol), the acid pretreated samples showed higher activation energy varied in the range of 28.64-68.10 kJ/mol associated with minerals removal. The catalytic effects of various inorganic constituents available in the biomasses altered their thermal behavior. It is worthwhile to know that, the biomass inorganic composition has also significant effect on its catalytic performance (I.-Y. Eom et al., 2012).

At pyrolysis temperatures of 280-320 °C, the moderate reactivity of PKS, EFB, PMF and their pretreated samples could be an indication of multi-components composite reactions. It means, part of the three main biomass building blocks comprising cellulose, hemicellulose and lignin were decomposed at this temperature range. The pre-exponential factor (k_0) for the virgin biomass samples at the temperature range of 280-320 °C were 1.15×10^2 - 6.00×10^2 1/s ,while pretreated samples showed 1.63×10^2 - 2.31×10^3 1/s. The pyrolysis kinetics data calculated by the present investigation were in agreement with the similar kinetics studies earlier reported assuming first-order lignocellulosic biomass pyrolysis reaction (Y. F. Huang et al., 2011a; Vamvuka et al., 2003; H. Yang et al., 2006). Various virgin biomass samples indicated different pyrolysis kinetics parameters (activation energy and pre-exponential factor). These parameters were highly influenced by the composition and type of biomass feedstock (Sanchez-Silva et al., 2012). The calculated biomasses activation energy and pre-exponential factors did not differ much from the kinetic parameters of bamboo leaves and sugarcane peel biomasses investigated in the literature assuming first order reaction kinetics.

The activation energy and pre-exponential factors shown in Table 4.10 indicated an increasing tendency with the temperature rising. The kinetics parameters exhibited a kinetic compensation effect, which could be sort of interdependence between them. There were positive correlation between the activation energy and pre-exponential factor. The latest might be due to the fact that the pre-exponential factor was greatly related with the temperature dependent collision frequency explained in collision theory. Some components of the biomass like hemicelluloses could be pyrolyzed at lower temperature. Lower activation energy at lower temperature was possibly attributed to the decomposition of the mentioned biomass components.

As explained, in this kinetics studies, some part of TGA data which could provide the best linear regression results were selected. Therefore, pre-exponential factor (k_0) and activation energy(E_a) were calculated from straight line intercept and slope, respectively. Since the thermal behavior of the lignocellulosic biomass may vary during the pyrolysis due to their complex composition, therefore too many poor regression data may be resulted. So, in this investigation, TGA data over narrow ranges of temperature could provide a good linear regression.

Table 4.10: The pyrolysis kinetics parameters of the biomass samples.

Biomass	Temperature range(°C)	K_0(1/s)	E_a(kJ/mol)	R^2	Standard error
PKS	250-270	8.7×10^{-1}	34.10	0.9944	3.72×10^{-6}
	280-320	2.50×10^{2}	57.28	0.9960	3.54×10^{-6}
PKS-HCl	260-280	1.07×10^{1}	44.37	0.9931	1.97×10^{-6}
	280-320	1.24×10^{3}	64.52	0.9974	1.79×10^{-6}
EFB	250-270	$1.0\ 0\times 10^{0}$	33.81	0.9986	7.83×10^{-7}
	280-320	6.00×10^{2}	60.30	0.9957	2.32×10^{-6}
EFB-HF	260-280	1.05×10^{0}	35.64	0.9960	1.89×10^{-6}
	280-320	2.31×10^{3}	68.10	0.9990	1.11×10^{-6}
PMF	250-270	1.60×10^{-1}	26.11	0.9970	2.06×10^{-6}
	275-360	1.15×10^{2}	52.66	0.9976	3.46×10^{-6}
PMF-HF	260-280	2.23×10^{-1}	28.64	0.9932	1.85×10^{-6}
	275-360	1.63×10^{2}	55.78	0.9930	6.19×10^{-6}
Bamboo leaves (Y. F. Huang et al., 2011a)	195-220	2.10×10^{-1}	31.41	0.9980	
	245-280	5.85×10^{2}	62.74	0.9996	
Sugarcane peel (Y. F. Huang et al., 2011a)	180-205	2.76×10^{1}	50.03	0.9990	
	250-290	2.42×10^{2}	59.27	0.9998	

4.2.6 Evolved gas analysis

4.2.6.1 TGA-MS analysis of gas products

TGA-MS technique can identify and analyze simultaneously the evolved gas during the biomass pyrolysis in real time. The primary pyrolysis products are mainly condensable gases and solid char. The condensable gases might be further decomposed through gas phase homogenous and gas-solid heterogeneous reactions into non condensable gases, liquid and

char(Dong, Zhang, Lu, & Yang, 2012). To study the effects of the biomass samples demineralization on the gaseous products evolution during pyrolysis, the present investigation focused on the production of non-condensable permanent gases like CO_2, CO and H_2 having the atomic mass units (a.m.u) 44, 28 and 2, respectively (Y. F. Huang et al., 2013) across the temperature range of 35-850 °C. Figure 4.10 shows the mass spectroscopy (MS) spectra for the virgin and pretreated biomass samples. As indicated in Figure 4.10, most of the aforementioned gases were produced at the temperature range of 250-750 °C probably attributed to the biomasses oxygenated functional groups cleavage, inorganic species decomposition and some secondary reactions like steam reforming (Eq.(4-1)), water-gas shift reaction (Eq.(4-2)) and char gasification with water (Eq.(4-3) and Eq.(4-4)) (Sanchez-Silva et al., 2012; Widyawati, Church, Florin, & Harris, 2011). As can be seen in Figure 4.10, the production of CO_2, CO and H_2 gases were in strong correlation with the biomass reactivity. Inorganic constituents, which probably catalyzed the pyrolysis reactions, increased the biomass reactivity. The acid pretreated palm oil biomass samples showed lower gas evolution compared with the virgin samples. CO_2 and CO evolutions during pyrolysis might be attributed to the cleavage of oxygen containing functional groups via decarboxylation and decarbonylation reactions, respectively. Decreasing in CO_2 and CO release after biomasses demineralization could demonstrate the catalytic role of inorganic species.

At high temperature (above 600 °C), the coincident occurrence of CO_2, CO and H_2 peaks for the virgin PKS could be an evidence for char decomposition through water-gas shift reaction. High content of CaO (71.6 wt% according to XRF results) in the virgin PKS could catalyze this type of reaction. Also, some fraction of CO_2, CO generation at this temperature might be due to inorganic carbonates degradation. Disappearance of these peaks after PKS acid pretreatment (minerals elimination) could be a reasonable evidence for the catalytic effects of inorganics.

$CH_4 + H_2O \leftrightarrow CO + 3H_2$ (Steam reforming) (4-1)

$CO + H_2O \leftrightarrow CO_2 + H_2$ (Water-gas shift) (4-2)

$C + H_2O \leftrightarrow CO + H_2$ (Char gasification) (4-3)

$C + 2H_2O \leftrightarrow CO_2 + 2H_2$ (Char gasification) (4-4)

H_2 formation from the virgin palm oil biomass samples at temperature above 600 °C (where CO and CO_2 evolution were not observed) could be probably caused by hydrocarbons (aromatics and aliphatics) thermal cracking and dehydrogenation(Eq.(4-5)) (Faix, Jakab, Till, & Székely, 1988). These reactions most likely were catalyzed by the mineral constituents presented in the biomass samples. As indicated in Figure 4.10c, after the biomasses demineralization, a significant decrease in H_2 evolution was observed.

$C_nH_m \leftrightarrow C_{n-x}H_{m-y} + H_2 + C + CH_4$ (thermal cracking) (4-5)

The studies on the effects of inorganics on the biomasses thermal behavior indicated that their presence increased permanent gas yield during pyrolysis and lowered the pyrolysis temperature.

The investigations on the thermogravimetric analysis and evolved gas data presented some information about the biomass samples reactions. In the temperature range ~250 °C < T < ~400 °C, where pyrolysis reactions (most part of cellulose and hemicellulose degradation) was occurred, the significant amount of gases were released. Demineralization shifted the maximum pyrolysis (Figure 4.9) and gas evolution (Figure 4.10) to a higher temperature. For the biomass samples, in the temperature range ~400 °C < T < ~600 °C, CO_2 generation was observed, whereas CO was not detected. It probably could indicate the existence a pathway of secondary reactions which diminished the CO evolution (Eq. (4-6)).

$CO + 0.5O_2 \leftrightarrow CO_2$ (4-6)

where O_2 could be originated from the condensable gases further degradation and inorganic carbonates decomposition.

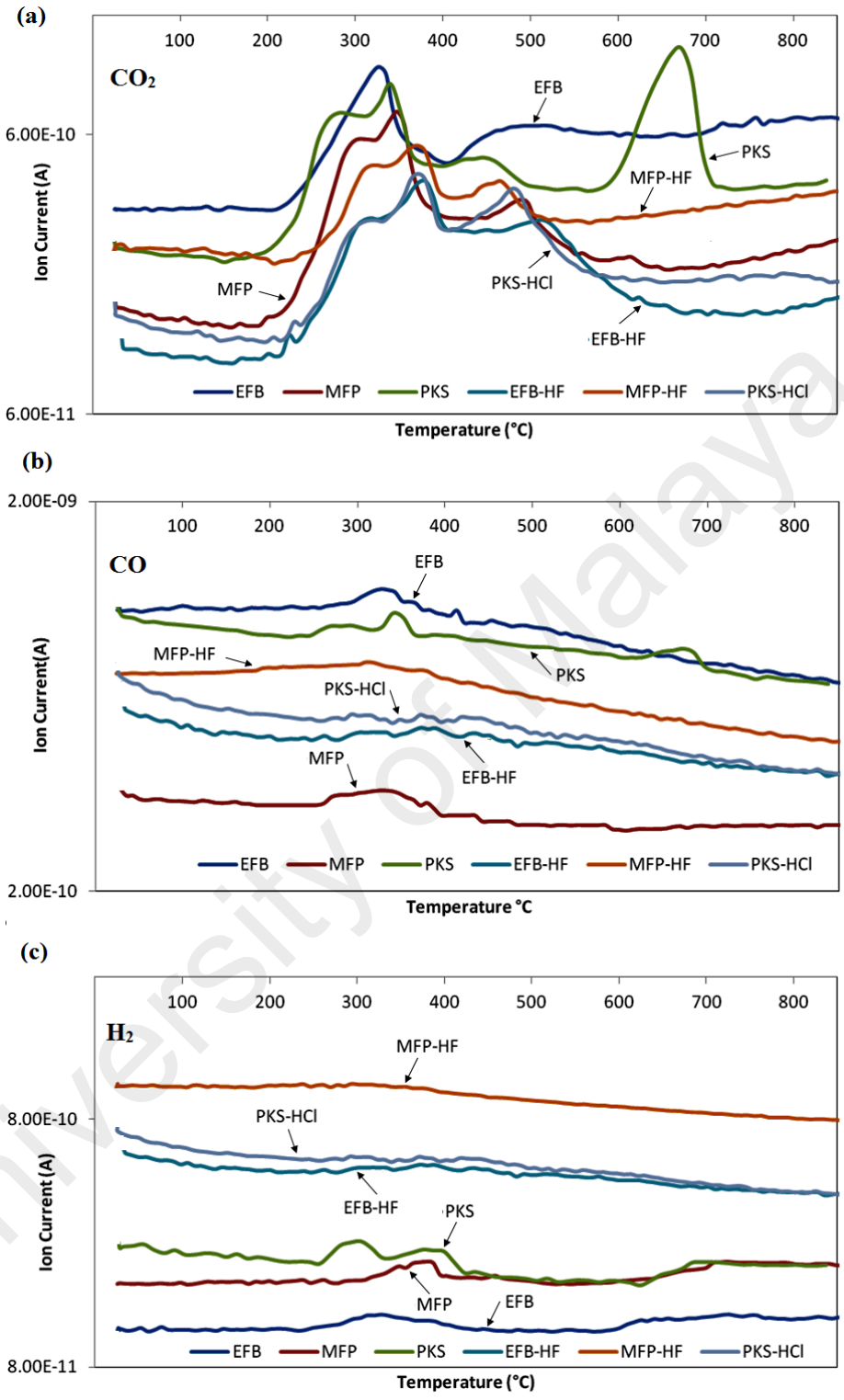

Figure 4.10: Mass spectra (MS) related to the gas products from pyrolysis of the different virgin and pretreated palm oil biomass samples: (a) CO_2, (b) CO and (c) H_2 detection.

4.2.6.2 TGA-FTIR analysis of gas products

The produced pyrolysis vapors from the biomass samples were analyzed by using the FTIR spectroscopy to study the effects of the biomass demineralization on the permanent gases production. Going deeper to the issue and to verify the TGA-MS results earlier explained, TGA-FTIR was employed to analyze the CO_2 and CO gases evolution in the temperature range 35 to 850 °C. The released gases were measured online using TGA coupled with FTIR. The formation of CO_2 at 2402-2240cm^{-1} could be attributed to the cracking and reforming of the organics functional groups like carbonyl (C=O) and carboxyl (-C (=O) O-). Also, it may be caused by inorganic carbonates decomposition (Edreis et al., 2013; P. Fu et al., 2011; Yan, Jiang, Han, & Liu, 2013). Further, the characteristic peaks of CO, which could be attributed to C=O and -C (=O) O- functional groups breakage, were observed at the bands 2240-2000 cm^{-1}(Edreis et al., 2013; Peng Fu et al., 2010). As explained before, CO_2 and CO formation may be also attributed to the secondary degradation of char and volatile components (Edreis et al., 2013; P. Fu et al., 2011).

Figure 4.11 depicts the FTIR spectrums of CO_2 and CO release during the biomasses (virgin and demineralized) pyrolysis. The major CO_2 evolution for the virgin palm oil biomass samples was detected in the temperature range ~250 to ~350 °C , while demineralized samples showed its major detection shifted to higher temperature range (~290 to ~370 °C). This phenomenon could confirm the catalytic role of inorganic constituents, which is in direct relation with the biomasses reactivity, during thermal analysis. It is in agreement with the TGA-MS results explained before.

As indicated in Figure 4.11a and Figure 4.11b, PKS showed a peak at temperature about ~700 °C for CO_2 release. This peak was disappeared after PKS demineralization by HCl. This phenomenon could be an evidence of catalytic effect of inorganics on CO_2 formation at temperature ~ 700 °C.

Considering CO evolution, as shown in Figure 4.11c and Figure 4.11d, most of the released gases from the virgin biomasses were detected in temperature range ~300 °C to ~360 °C ,while the demineralized biomass samples showed very low intensity absorption peak at 350-400 °C. Virgin PKS illustrated a CO peak at about 700 °C, whereas this peak was not observed after demineralization by HCl. This could also confirm the catalytic behavior of minerals available in the biomasses at about ~700 °C. On the other hand, CO_2 and CO peaks for the virgin PKS at high temperature (>600 °C) could be also attributed to the char and inorganic carbonates degradation reactions.

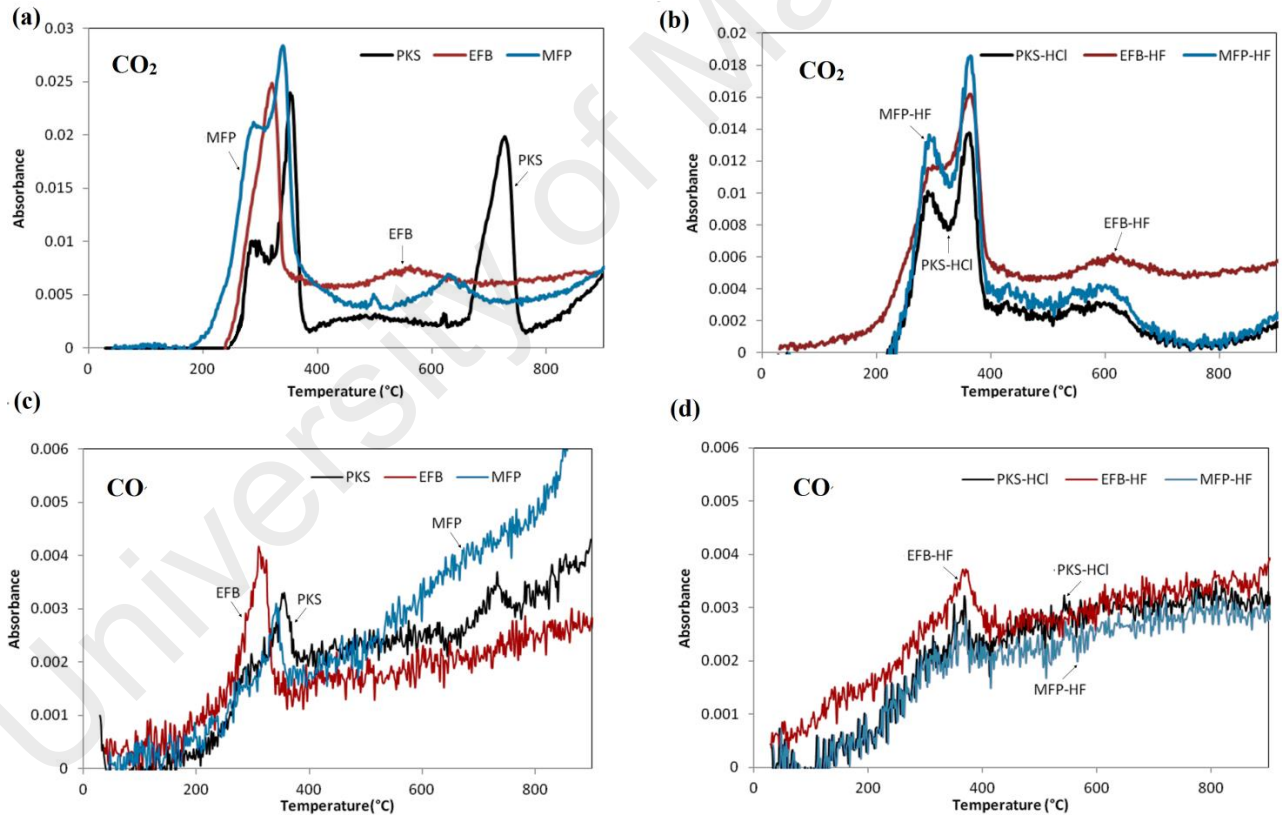

Figure 4.11: FTIR spectra of the permanent released gas during the palm oil biomass samples pyrolysis: (a) CO_2 detection from the virgin biomasses. (b) CO_2 detection from the pretreated biomasses. (c) CO detection from the virgin biomasses. (d) CO detection from the pretreated biomasses.

4.3 Part3: In-situ catalytic upgrading of biomass pyrolysis vapor: Using a cascade system of various catalysts in a multi-zone fixed bed reactor

4.3.1 Physicochemical characteristics of the catalysts

The main physiochemical characteristics of the catalysts (meso-HZSM-5, Ga/meso-HZSM-5 and Cu/SiO_2) used in the catalytic upgrading of PKS pyrolysis vapor are shown in Table 2.

Table 4.11: Chemical and textural properties of the catalysts.

Sample	SiO_2/Al_2O_3 mole ratio[a]	Ga or Cu (wt%)[a]	Crystal length (nm)[b]	Crystal width (nm)[b]	S_{BET} (m^2g^{-1})[c]	S_{meso} (m^2g^{-1})[d]	S_{BET}/S_{meso} (m^2g^{-1})	V_{total} (cm^3g^{-1})[e]	V_{micro} (cm^3g^{-1})[f]	V_{meso} (cm^3g^{-1})[g]	D (nm)[h]
HZSM-5	56.7		326.3	239	325	110	2.95	0.205	0.104	0.101	12.76
Meso- HZSM-5	40.35		302.6	221	321	120	2.70	0.250	0.098	0.152	12.39
Ga(1)/meso-HZSM-5	40.83	0.95	329.9	233	317	152	2.11	0.215	0.083	0.132	11.74
Ga(5)/meso-HZSM-5	40.56	4.55	319.9	197	300	140	2.14	0.206	0.079	0.127	11.88
SiO_2					157	119	1.32	0.532	0.108	0.424	17.10
Cu(5)/SiO_2		5.20			145	133	1.09	0.518	0.097	0.421	19.29

[a] Determined by XRF.
[b] Estimated from SEM images.
[c] Surface areas were obtained by the BET method using adsorption data in p/p_0 ranging from 0.05 to 0.25.
[d] Measured by t-plot method.
[e] Total pore volumes were estimated from the adsorbed amount at $p/p_0 = 0.995$.
[f] Measured by t-plot method.
[g] $V_{meso} = V_{ads,p/p0=0.99} - V_{micro}$.
[h] Average pore width was derived from the adsorption branches of the isotherms by the BJH method.

Parent HZSM-5 was selected as a well-known shape selective crystalline zeolite catalyst having a two dimensional channel like pore system with vertically intersection channels of ~0.55 nm in diameter, which can control the formation of unwanted products (Stephanidis et al., 2011). The surface area of the parent HZSM-5 zeolite utilized in the present investigation was 325 m^2/g with meso/microporous structure. To eliminate the microporous HZSM-5 zeolite mass transfer limitations and to decrease the possibility of secondary reactions of reagents (coke formation), suitable catalyst should have all advantages of microporous zeolite while provide additional diffusion pathways for larger molecules. Therefore, mesoporosity formation into the zeolite catalysts seems to be promising approach. Mesopores presence in the parent zeolite crystalline framework (meso-HZSM-5) would be

equivalent to external surface enhancement. It makes a large number of pore openings accessible to the large molecules. Shortened diffusion path length and enlarged external surface area would ease the coke precursors mass transfer from the micropores to the external surface of zeolite catalyst and consequently prevent its quick deactivation (Hua et al., 2011). Therefore, catalytic performance of catalyst is enhanced (Asadieraghi, Ashri Wan Daud, & Abbas, 2015; Na et al., 2013; S. Stefanidis et al., 2013).

Gallium may be present in various forms over meso-HZSM-5 catalyst. It can be existed as gallium oxide either as small particles occluded in the zeolite micropores or in aggregated form on the external zeolite surface. Furthermore, it can be stabilized in cationic form as either reduced Ga^+ and GaH^+_2 species or oxidic GaO^+ (Kazansky, Subbotina, van Santen, & Hensen, 2004).

Surface area and porosity analysis of Cu/SiO_2 using N_2 adsorption/desorption indicated porosity in the range of micro-, macro- and mesopores. The data from BJH method showed that there were three kinds of pore size distribution mainly attributed to meso- and macropores. The SiO_2 support illustrated a high BET surface area (157 m^2/g), while a decrease surface area for Cu/SiO_2 catalyst (145 m^2/g) was observed attributed to the Cu deposition. The BET surface area and the pore volume of Cu/SiO_2 were slightly reduced in comparison with the SiO_2 support.

The H^+ form of ZSM-5 zeolite catalyst possessed mostly Brønsted acid sites of high acidic strength. However, during the catalyst's calcination at about 550 °C, for transformation of its NH_4^+-exchanged form into the H^+ -form, few acid sites were generated attributed to positively charged tri-coordinated Si atoms as well as extra-framework octahedrally coordinated aluminum oxyhydroxy species (Iliopoulou et al., 2012).

The acidic properties of HZSM-5 zeolite based catalysts was studied by NH_3-TPD technique and the relevant profiles are shown in Figure 4.12. As indicated in this Figure, two major

desorption peaks could be conducted to the assumption that at least two types of acid sites presented (Carlson et al., 2011a; Jeongnam Kim et al., 2010; Ni et al., 2011). The HZSM-5 parent catalyst indicated two major peaks (related to the acid sites) at ~175 °C and ~341°C were attributed to the NH_3 desorption from the weak acid sites and strong Brønsted acid sites, respectively.

The meso-HZSM-5(desilicated) zeolite exhibited a distribution of acid sites analogous to that of parent HZSM-5. Compared to the parent HZSM-5, the low temperature peak of desilicated meso-HZSM-5 catalyst shifted to a higher temperature, whereas high temperature peak moved slightly to a lower temperature. This was attributed to an increase in the Lewis acid species caused by alumina increasing in the catalyst framework. Further, after desilication, the total Brønsted acid sites concentration (0.08 mmol g^{-1}) decreased due to the catalyst framework desilication. The parent zeolite catalyst represented more Brønsted acid sites (0.19 mmol g^{-1}) (stronger acidic hydroxyl group) compared to desilicated meso-HZSM-5 catalyst. Desilicated zeolites showed slightly weaker acid strength than the parent zeolite catalysts with the same aluminum fraction, but it would provide suitable pore structure that could allow a rapid molecular diffusion and, subsequently, improve the reaction kinetics (Possato et al., 2013).

Subsequent to Ga-incorporation on meso-HZSM-5 zeolite, the strong acid sites amount decreased in proportion to the amount of incorporated gallium to the catalyst. Then, the low temperature desorption peak at ~226 °C was shifted to ~168 °C. These shifts were attributed to the creation of gallium induced acidic sites as new active sites for aromatization (C.-S. Chang & Lee, 1995). It is believed that most gallium species are deposited outside of the meso-HZSM-5 zeolites. However, after catalyst reduction and activation by hydrogen, their migration into the zeolite pores, could result in the gallium species exchange with the protons of the Brønsted acid sites. This could cause the decrease in the number of strong acid sites

with increasing Ga loading to the catalyst (H. J. Park et al., 2010a). When the Si/Al ratio of HZSM-5 was decreased from 56.7 to 40.35 in meso-HZSM-5 (catalyst desilication for the mesoporosity creation), the number of Brønsted acid sites increased (Heo et al., 2011).

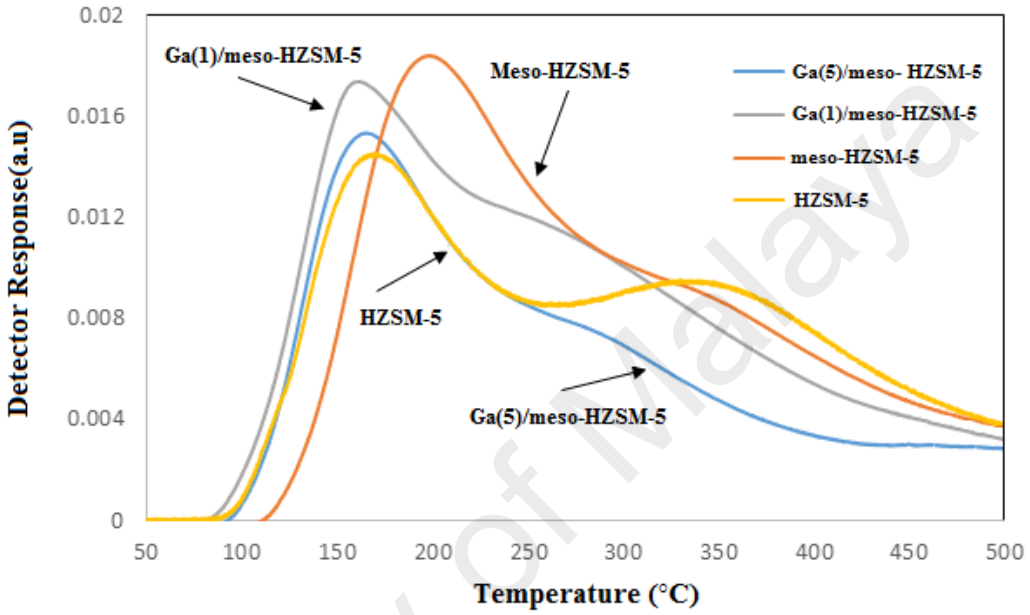

Figure 4.12: NH_3-TPD patterns of the parent and modified HZSM-5 zeolite catalysts.

X-ray diffraction (XRD) patterns of Cu/SiO_2 and the parent and modified HZSM-5 catalysts are shown in Fig.4. The XRD pattern of the calcined Cu/SiO_2 showed a broad peak at 21.7°, which could be corresponding to the amorphous silica. The peaks at 35.5° and 38.9° attributed to CuO were observed for the calcined catalyst (B. Zhang, Zhu, Ding, Zheng, & Li, 2012).

As illustrated in Figure 4.13, the XRD patterns of the parent and modified H-ZSM-5 zeolites are coincident with the conventional MFI zeolite structure (Shetti, Kim, Srivastava, Choi, & Ryoo, 2008). As shown, compared to virgin catalyst, the crystalline structure of the HZSM-5 samples was not changed after modification. Gallium species were not detected on the Ga-incorporated meso-HZSM-5 zeolites. Further, there was practically no decrease in the zeolite

catalysts crystallinity, even when the Ga incorporation was increased to 5 wt. %. This could suggest that Ga species were well dispersed in the meso-HZSM-5 zeolites (H. J. Park et al., 2010a).

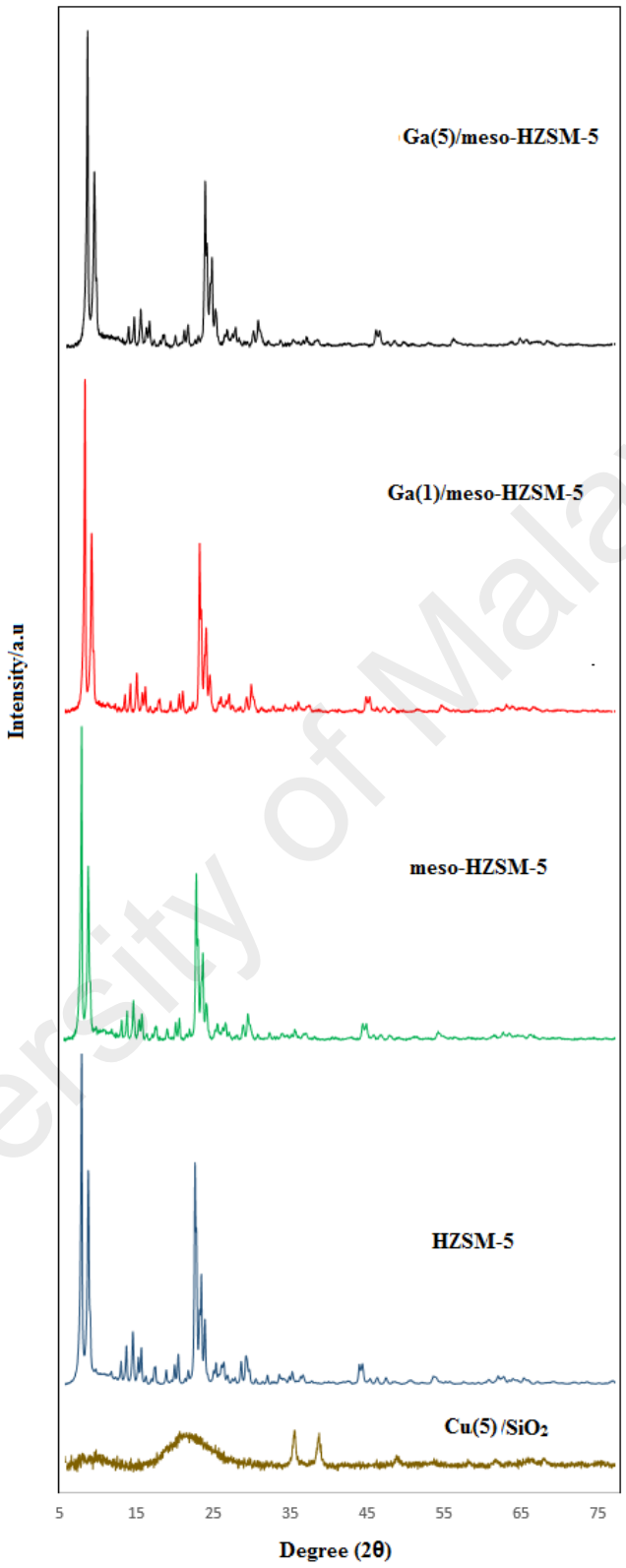

Figure 4.13: X-ray diffraction patterns of Cu/SiO_2 and the parent and modified HZSM-5 catalysts.

Figure 4.14 represents SEM photographs of the parent (a), meso- (b) Ga impregnated (c,d) HZSM-5 zeolite catalysts. As can be seen in Figure 4.14, the parent HZSM-5 zeolite was formed by uniform nano-range (100-400 nm) crystals. The SEM photographs of the modified HZSM-5 catalysts were very similar to that of the fresh one, whereas the meso- and Ga incorporated catalysts (modified HZSM-5) showed smaller crystals (see Table 4.11) compared with the parent zeolite sample. The Ga particles could not be observed at 100000 magnification since they were available in small amount.

The SEM images in Figure 4.14 (e,f) show the surface morphology of 5 wt.% Cu/SiO_2 catalyst in two different scales; 10000 and 5000 magnification. Pictures (e) and (f) revealed that the Cu (5)/SiO_2 catalyst was cottony, which was considered to be the amorphous state. This is in agreement with the Cu (5)/SiO_2 sample XRD results. The dots with relatively high brightness were possibly assigned to Cu particles, whereas the rest of the area with much weaker brightness indicated the SiO_2 support surface (Shi et al., 2012).

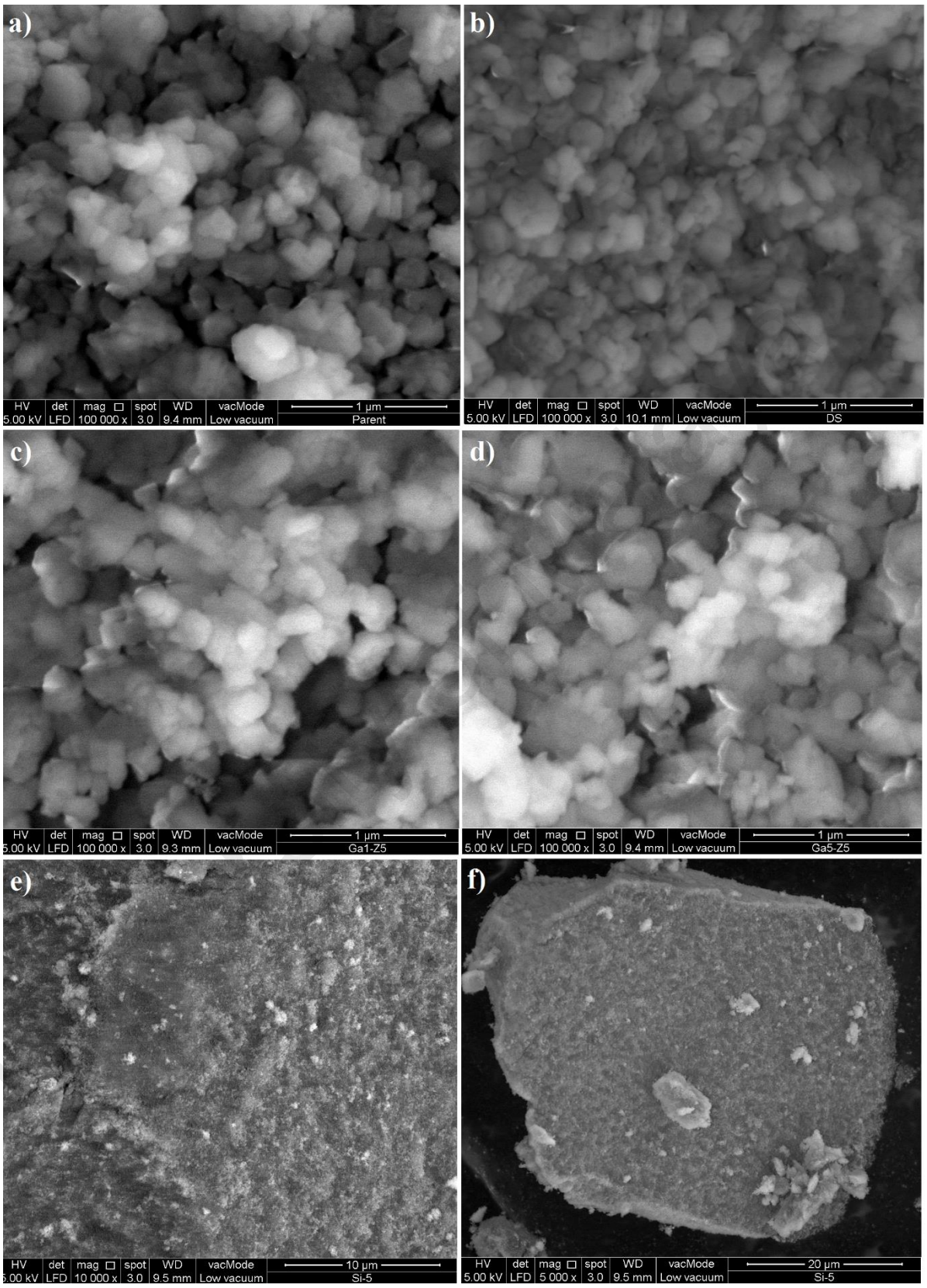

Figure 4.14: SEM photographs of the parent (a), meso- (b), Ga(1)/meso- (c), Ga(5)/meso- (d) HZSM-5 zeolite and Cu(5)/SiO_2 (e,f) catalyst.

4.3.2 Products yield

Among various types of catalysts, model compound investigations showed that zeolite (meso-HZSM-5 and Ga/meso-HZSM-5) and oxide supported metal (Cu/SiO_2) catalysts were very efficient in biomass pyrolysis vapor upgrading reactions comprising; aldol condensation, aromatization, alkylation, deoxygenation and hydrogenation(Asadieraghi et al., 2014; Ausavasukhi et al., 2009; Hoang, Zhu, Lobban, et al., 2010; Sitthisa & Resasco, 2011; Zhu et al., 2010).

The yield of the bio-oil, solid products and gas (wt. %) for the PKS in-situ catalytic pyrolysis process using individual catalysts or different configurations of catalysts (meso-HZSM-5, Ga/meso-HZSM-5 and Cu/SiO_2) in a cascade system are shown in Table 4.12. All measurements were performed in duplicate to ensure reproducibility of the results; the mean of these two tests (with less than ~ 5.0 % difference) was taken to represent each evaluation. These values were compared to the products yield obtained in non-catalytic pyrolysis. The results of products yield were in agreement with the investigations already performed on the biomass pyrolysis and catalytic upgrading (Iliopoulou et al., 2012; H. J. Park et al., 2010a; H. J. Park et al., 2012b).

Table 4.12: The yield of bio-oil, gas and char (wt. % on biomass) for the in-situ catalytic pyrolysis process over different catalyst or a cascade system of catalysts.

PKS (gr)	Meso-H-ZSM-5(gr)[a]	Ga(1)/meso-HZSM-5 (gr)[b]	Ga(5)/meso-HZSM-5 (gr)[b]	$Cu(5)/SiO_2$ (gr)[c]	Bio-oil (wt. %)	Gas [d] (wt. %)	Char (wt. %)	O[e] (wt. %)	Water content[f] (wt.% in the bio-oil)
60	6				32.6	33.1	34.3	58.89	63.3
60		6			35.8	30.0	34.2	66.43	55.1
60			6		39.2	26.7	34.1	71.14	50.8
60				6	42.6	23.0	34.4	66.08	58.7
60	6	6			30.7	35.1	34.2	49.12	66.2
60	6		6		31.8	34.2	34.0	53.87	64.8
60	6		6	6	31.2	34.4	34.4	51.30	65.5
60	6	6		6	29.3	36.5	34.2	47.67	67.3
60 (*)					49.8	16.1	34.1	75.83	49.3

(a) First zone of the catalytic multi-zone reactor.
(b) Second zone of the catalytic multi-zone reactor.
(c) Third zone of the catalytic multi-zone reactor.
(d) Calculated by difference (Gas (wt. %) = 100- (Bio-oil (wt. %) + Char (wt. %)))
(e) Bio-oil oxygen content measured by elemental analysis (O = 100- (C+H+N+S), all in wt. % basis)
(f) Measured using Karl Fischer titration.
(*) Non-Catalytic pyrolysis.

Compared to the non-catalytic upgrading, the bio-oil amount was considerably lower due to the pyrolysis vapors catalytic cracking, whereas there was an increase in the gaseous products yield. The highest liquid bio-oil yield (49.8 wt. %) was observed in non-catalytic runs. Employing the catalysts, the bio-oil water content increased significantly. This was caused by various hydrocarbon conversion reactions including; dehydrogenation, cyclization/aromatization and cracking, which were typically catalyzed by the zeolite Brønsted acid sites (Asadieraghi et al., 2014; Mortensen et al., 2011). Water yield increasing was attributed to the enhanced oxygenated compounds dehydration on the zeolite catalyst acid sites (Iliopoulou et al., 2012). Since the catalysts beds and biomass were not in contact, the existence of the catalysts did not affect the decomposition of the solid biomass feed. Therefore, the char quantity could be considered constant for all experiments and equal to the yield of solid products of the non-catalytic experiments (~ 34.1 wt. % on average).

Among the examined zeolite catalyst, meso-HZSM-5 (bio-oil yield 32.6 wt. %) indicated the highest activity attributed to the synergic effect of strong acidic properties and high porosity, mostly in the deoxygenation of oxygenated compounds (O = 58.89 wt. %) available in the

bio-oil. Although, the meso-HZSM-5 zeolite high acidity conducted to a decrease in the bio-oil quantity.

Gallium incorporation into the meso-HZSM-5 zeolite catalyst could somehow resolve this problem. Particularly, the 1 wt.% Ga/meso-HZSM-5 catalyst enhanced the bio-oil yield (35.8 wt. %) attributed to less cracking of the bio-oil pyrolysis vapor through a decrease in the number of Brønsted acid sites and its strength , as detected in the NH_3 -TPD experiments (Fig.3). Using a cascade system of different catalysts indicated lower bio-oil yield attributed to higher efficiency of hydrocarbon conversion and deoxygenation. A cascade system of three types of catalysts comprising meso-H-ZSM-5, Ga(1)/meso-HZSM-5 and Cu(5)/SiO_2 exhibited lowest bio-oil yield (29.3 wt. %), highest water content (67.3 wt. %) and lowest oxygen content (47.67 wt. %) in the bio-oil. This could be an evidence for efficient catalytic biomass pyrolysis vapor upgrading using aforementioned catalysts in a cascade system.

4.3.3 Bio-oil chemical composition

4.3.3.1 Quantitative analysis using GC-MS

Table 4.13 shows the composition of the bio-oils' organic fraction measured by GC-MS analysis. According to the literature studies various bio-oil's organic compounds have been classified into 13 groups; aromatic hydrocarbons, aliphatic hydrocarbons, phenols, furans, acids, alcohols, esters, ethers, aldehydes, ketones, sugars, polycyclic aromatic hydrocarbons (PAHs) and nitrogen containing compounds. Among these compounds, desirables were aromatic, alcohols and aliphatic hydrocarbons, which were utilized for biofuels production, whereas phenols and furans were regarded as high added value chemicals. Conversely, acids, carbonyls, polycyclic aromatic hydrocarbons (PAHs) and heavier oxygenates were considered as undesirables. Ketones and aldehydes compounds led to the instability of the

bio-oil during transportation, while the high acid contents in the bio-oils created corrosiveness and practically challenging to be used as engines fuels (Iliopoulou et al., 2012; H. J. Park et al., 2010a; S. D. Stefanidis et al., 2011b).

As can be observed in Table 4.13, the produced bio-oil via non-catalytic pyrolysis (without upgrading) had low content of ketones and acids, but was rich in phenolic compounds. Moreover, some components like aliphatic hydrocarbons, aromatic and alcohols were recognized in very low concentrations. High content of phenolic compounds available in the bio-oil could be resulted from high lignin content of PKS biomass (50.7 wt. %). Accordingly, the bio-oil produced through thermal pyrolysis of the biomass was considered as a low quality product.

Table 4.13: The bio-oils (organic phase) composition (wt. %) produced by PKS biomass non-catalytic fast pyrolysis and by catalytic upgrading of pyrolysis vapors through each individual catalyst or a system of cascade catalysts.

Compound	Non-catalytic pyrolysis	HZSM-5	Meso-HZSM-5(A)	Meso-Ga(1)/ H-ZSM-5(B)	Meso-Ga(5)/ H-ZSM-5	$Cu(5)/SiO_2(C)$	A+ B[(1)]	A+B+C[(2)]
Hexanoic acid	3.87	1.56	1.10	1.23	1.58	1.53	1.04	0.94
Furfural	7.15	6.12	5.78	4.49	4.84	0.35	5.73	0.58
2-Butenal, 2-methyl-	4.35	2.41	0.32	2.16	3.67			
Furfuryl alcohol	1.18		1.06	1.16	0.56	6.51	0.98	5.32
2-Propanone, 1-(acetyloxy)	2.28			1.13	1.17	1.07		
m-Xylene		0.71	2.03	4.09	1.83		6.12	6.31
o-Xylene		0.68	1.75	2.67	1.23		3.03	3.08
2-Propenoic acid	4.21	2.51	1.1	2.12	2.48		0.76	
Phenol	61.8	58.12	53.77	46.21	51.96	59.11	44.32	42.92
1,2,3 Trimethyl benzene			0.54	1.63			1.85	2.03
o-Cresol		3.70	4.08	2.32	3.87		2.20	1.97
Acetic acid, phenyl ester		2.31		1.04				
3-Methyl phenol	2.49	4.82	4.03	3.72	4.25			
2- Methyl phenol	3.34		3.80	2.62	2.87	5.79	2.48	2.54
2-Metoxy phenol		0.87						
2,5 dimethyl phenol		2.12	1.23					
Naphthalene		1.14	2.08	3.54	1.18		3.58	3.63
1,2-Benzenediol	4.91	3.4	3.8	2.78	3.94	11.19	2.65	3.12
2-Isopropoxyphenol	1.3		2.28	1.89	2.02	2.64	1.91	0.89
Methyl benzenediol	2.68	2.71	2.14	2.21	3.01	7.02	2.18	2.07

(1)Meso-HZSM(5) + Ga(1)/HZSM-5 in the first and second reaction zones, respectively.
(2)Meso-HZSM(5) + Ga(1)/HZSM-5 + $Cu(5)/SiO_2$ in the first , second and third reaction zones, respectively.

As Table 4.13 illustrates, the catalytic upgrading of the biomass pyrolysis vapor, particularly employing a cascade system of catalysts, was very efficient in the production of high quality bio-oils having appropriate components. Meso-HZSM-5 catalyst conducted to small oxygenates (aldehyde) aldol condensation and the production of diverse kinds of aromatics. An increase of aromatic components and diminution of the phenol concentration in the product were observed with Ga incorporation into the meso-HZSM-5 catalyst. The Ga (1.0 wt. %)/meso-HZSM-5 zeolite increased the aromatics (m-xylene, o-xylene, trimethyl benzene and naphthalene) yield (Cheng, Jae, Shi, Fan, & Huber, 2012) to 11.93 wt. %. In

contrast, the increasing amount of Ga in Ga (5.0 wt. %)/meso-HZSM-5 catalyst reduced it to 7.78 wt. %. This was possibly caused by more reduction of protons (H^+) through incorporation of the excess gallium, conducted to a decrease in the cyclization and oligomerization of light components over acid sites (Figure 4.16). Thus, the selectivity toward desirable compounds, such as aromatic compounds and the catalytic activity for deoxygenation both were dependent on the gallium content and the catalyst's strong acid sites. Probably Ga (1.0 wt. %) /meso-HZSM-5 catalyst provided the optimum Ga amount and Brønsted acid sites. It is worthwhile to mention that providing optimum amount of Brønsted and Lewis acid sites induced by Ga played an important role in the aromatization of light compounds (H. J. Park et al., 2010a).

Compared to the non-catalytic pyrolysis, employment of 5.0% wt. % Cu/SiO_2 catalyst increased the furfuryl alcohol yield from 1.18 wt. % to 6.51 wt. %. It was due to hydrogenation of furfural (a sugar-derived component) carbonyl group (Figure 4.17).

A cascade system of three types of catalysts comprising meso-HZSM-5, Ga (1)/meso-HZSM-5 and Cu (5)/SiO_2 indicated high yield of fuel like components such as aromatics (15.05 wt. %) and furfuryl alcohol (5.32 wt. %) and low yield of non-fuel like chemicals (aldehyde, furfural, carboxylic acids and phenolics) simultaneously. They caused by the conversion of small oxygenates, lignin derived phenolics and sugar-derived components using meso-HZSM-5, Ga (1)/meso-HZSM-5 and Cu (5)/SiO_2 catalysts, respectively.

4.3.3.2 Qualitative analysis using FTIR

Infrared spectroscopy (FTIR) technique was employed to study the chemical structure of the bio-oils components. Figure 4.15 depicts the FTIR spectra of non-catalytic and catalytic pyrolysis bio-oils using meso-HZSM-5 catalyst and a cascade system of three catalysts

(meso-HZSM-5, Ga (1)/ meso-HZSM-5 and Cu (5)/SiO_2). Table 4.14 indicates the FTIR identified chemical bonds and functional groups in the bio-oil.

Table 4.14: Peaks assignment to the chemical functional groups of the bio-oil using FTIR.

Wavenumber(cm^{-1})	Vibration	Functional group	Ref.
3500-3200	O-H Stretch	Phenols, alcohols	(L. Wang et al., 2014)
3000-2800	C-H Stretch	$-CH_2$, $-CH_3$	(L. Wang et al., 2014)
~1700	C=O Stretch	Carboxylic acid, aldehyde, ketones	(Mayer, Apfelbacher, & Hornung, 2012b)
1650-1510	C=C Stretch	Aromatics	(L. Wang et al., 2014)
1440-1400	O-H Bend	Alcohols, carboxylic acids	(Haiping Yang, Yan, Chen, Lee, & Zheng, 2007b)
~1280	C-O Stretch	carboxylic acids	(L. Wang et al., 2014)
1020-700	C-H Bend	Aromatics	(Asadieraghi & Wan Daud, 2014)

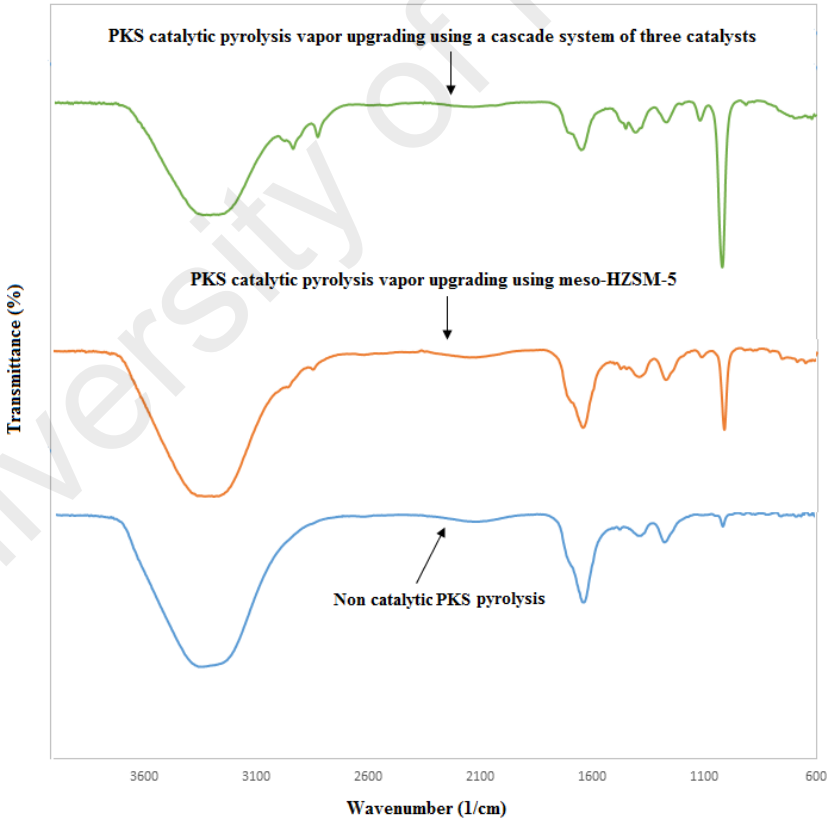

Figure 4.15: FTIR spectra of the bio-oil produced through PKS biomass non-catalytic pyrolysis and its catalytic pyrolysis vapor upgrading using meso-HZSM-5 catalyst and a cascade system of three catalysts (meso-HZSM-5, Ga(1)/meso-HZSM-5 and Cu (5)/SiO_2).

As can be observed in Figure 4.15, the first broad peak between 3500 and 3200 cm^{-1} in the FTIR spectra indicated the O-H stretching vibration of phenolic and alcoholic functional groups. The C-H stretching vibration peak between 3000 and 2800 cm^{-1} was related to the presence of $–CH_3$ and $–CH_2$ functional groups, which was only recognized in the catalytic upgraded bio-oil. This peak illustrated higher intensity once PKS biomass pyrolysis vapor was upgraded using a cascade system of three catalysts. The next spectrum bands around 1700 cm^{-1} was caused by C=O stretching vibration of free carbonyl groups of ketones, carboxylic acids and aldehyde. The lower intensity of this peak in the FTIR spectra was attributed to the upgraded bio-oil, especially in the case of in-situ PKS pyrolysis vapor upgrading in a cascade system of catalysts. The peak around 1650-1510 cm^{-1} indicated C=C stretching vibrations of aromatic components. The spectral region of 1440-1400 cm^{-1} represented different bands in the O-H bending region, which were most likely carboxylic acids and alcohols.

The spectra of C-O stretching characterized at around 1280 cm^{-1} was related to the carboxylic acids. It showed low intensity in the FTIR spectra of upgraded bio-oils. The high intensity of aromatics in-plane C-H bending peaks was detected around 1020 cm^{-1} and 700 cm^{-1}. They evidenced the availability of aromatic hydrocarbons in the upgraded bio-oils. Their high intensity spectra in the upgraded bio-oil confirmed the high contents of aromatics in the generated bio-oil. The qualitative analysis of the bio-oils chemical constituents using FTIR technique compromised with the GC-MS quantitative results.

4.3.4 Mechanism of bio-oil upgrading in a cascade system of catalysts

Small oxygenated components such as aldehydes, acids, ketones and alcohols existed in the PKS biomass pyrolysis vapor could be deoxygenated catalytically through decarbonylation, dehydration and decarboxylation reactions to stable fuel like compounds using parent

HZSM-5 catalyst. Furthermore, by employing the suitable modified catalysts (such as meso-HZSM-5) and utilizing the high reactivity of the oxygen functionalities (hydroxyl carboxylic, ketonic and carbonyl groups) bonds formation reactions (like C–C) through aldol condensation, ketonization, etherification and aromatization could be conducted. It means in place of oxygen functionalities elimination too early, they could be utilized as a potential for production of high carbon fuel like molecules.

The overall proposed reaction pathway comprising condensation followed by cyclization of small aldehyde (2-Butenal-2methyl-) is depicted in Figure 4.16. Direct cyclization could produce aromatics on an acid site in the HZSM-5 zeolite. These first aromatic molecules could then undergo the typical secondary reactions on the catalyst acid sites, such as disproportionation and dealkylation, generating light products and other aromatics (Hoang, Zhu, Sooknoi, et al., 2010).

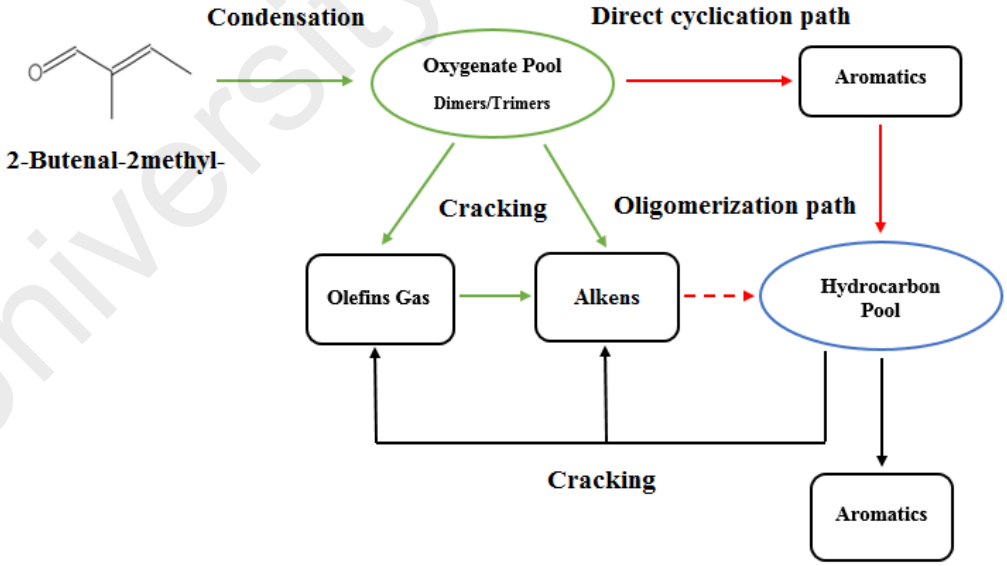

Figure 4.16: Proposed aromatics formation pathway from aldehyde (small oxygenate) over HZSM-5 catalyst. Reproduced with permission from Ref. (Hoang, Zhu, Sooknoi, et al., 2010).

The lignin-derived components in the biomass pyrolysis vapor comprised phenolic molecules ranging from single-ring aromatic oxygenates to multi-ring aromatics. The single-ring components could be successfully alkylated with short alcohols followed by hydrodeoxygenation to generate C_{10}-C_{13} aromatics.

Fig.84.17 indicates reaction pathways for pyrolysis and catalytic pyrolysis vapor upgrading of biomass lignin content over HZSM-5 catalyst. As can be seen in Figure 4.17, lignin pyrolysis primarily produced monomeric phenolic molecules, which had very low reactivity over HZSM-5 catalyst. Phenols acid-dehydration led to large amount of coke generation, whereas phenols cracking created aromatics at times. Another intermediate to aromatics formation may be olefins which produced from alkyl-phenols cracking (Asadieraghi et al., 2015; K. Wang et al., 2014).

As can be observed in Table 4.13, mesoporous HZSM-5 zeolite indicated high activities, in terms of both aromatization and deoxygenation, during the PKS biomass catalytic upgrading of pyrolytic vapors attributed to the synergic effect of its high acidity and porosity. Particularly, mesoporous HZSM-5 zeolite catalyst demonstrated high selectivity toward valuable aromatics, although it decreased the bio-oil yield (Table 4.12). The gallium incorporation into the meso-HZSM-5 zeolite conducted less cracking of the pyrolytic vapors, as well as an increase in the bio-oil. The gallium quantity (wt. %) incorporated into meso-HZSM-5 catalyst exhibited an important effect in the aromatics selectivity. The incorporation of the appropriate gallium amount (1.0 wt. %) enhanced the bifunctional mechanism and the consequent improvement of the aromatics selectivity, while the excess gallium addition to the catalyst (5.0 wt.%) exhibited a negative effect on the aromatics formation due to the loss of protons (H^+) density (H. J. Park et al., 2010a).

Ga-containing zeolites are highly active in reactions involving hydrogen and carbonyl compounds, comprising hydrogenation, decarbonylation, and hydrogenolysis. These types of

catalysts have indicated to exhibit high activity toward reactions involving activation of light alkanes, particularly aromatization (Ausavasukhi et al., 2009).

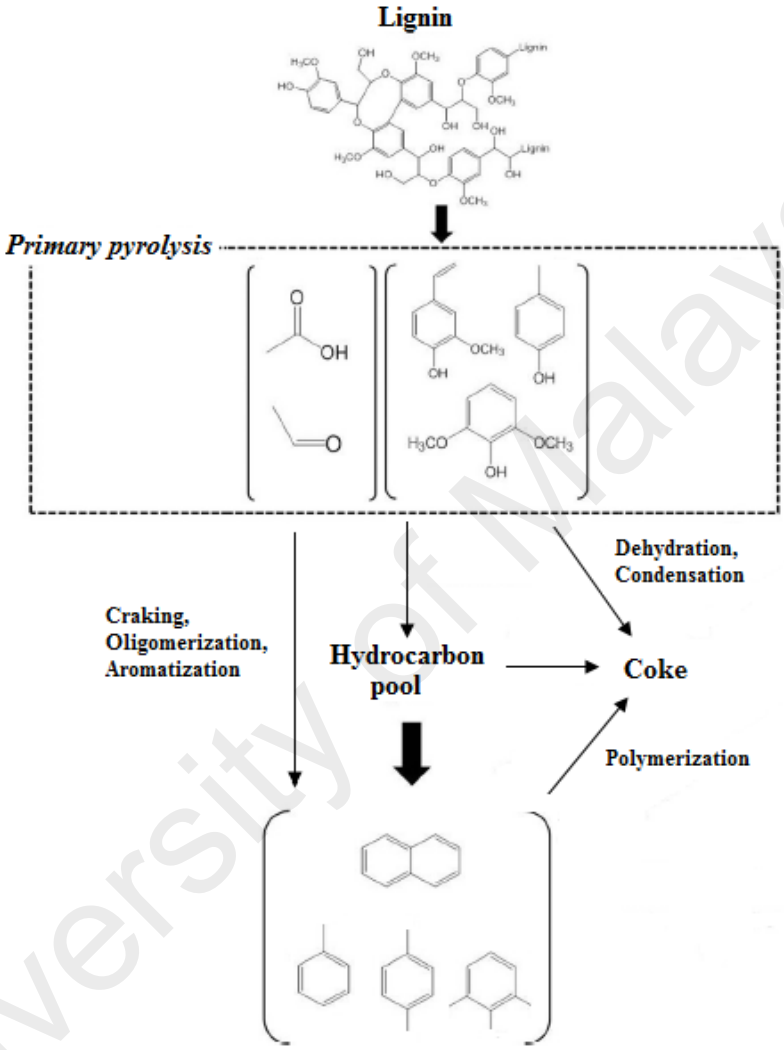

Figure 4.17: Reaction pathways for pyrolysis and catalytic pyrolysis vapor upgrading of lignocellulosic biomass lignin content over HZSM-5 catalyst. Reproduced with permission from Ref.(K. Wang et al., 2014).

Furfural, which is obtained from the fast pyrolysis of lignocellulosic biomass at high heating rate, moderate temperature and short residence time, is one of the known oxygenated compounds usually found in bio-oil. It is generated both during cellulose pyrolysis and the sugars dehydration. Due to the high reactivity of this component, it needs to be catalytically

hydrodeoxygenated to improve bio-oil boiling point range, water solubility and storage stability (Asadieraghi et al., 2014; Sitthisa et al., 2011). Figure 4.18 depicts the possible reaction pathway for furfural conversion to furfuryl alcohol over Cu (5 wt. %) /SiO_2 catalyst. Cu interaction with the ring is so weak and no ring conversion could be observed, although Cu could produce furfuryl alcohol through hydrogenation of the carbonyl group.

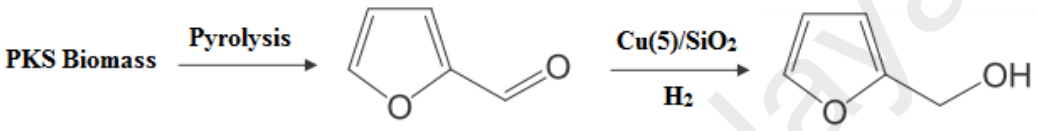

Figure 4.18: Possible reaction pathways for furfural (sugar-derived component) conversion over Cu (5)/SiO_2 catalysts.

Figure 4.19 simply depicts different upgrading reactions (aldol condensation, alkylation, dehydrogenation, hydrogenation and deoxygenation) of major pyrolysis components including small oxygenates, lignin derived phenolics and sugar derived components in different zones of the fixed bed reactor.

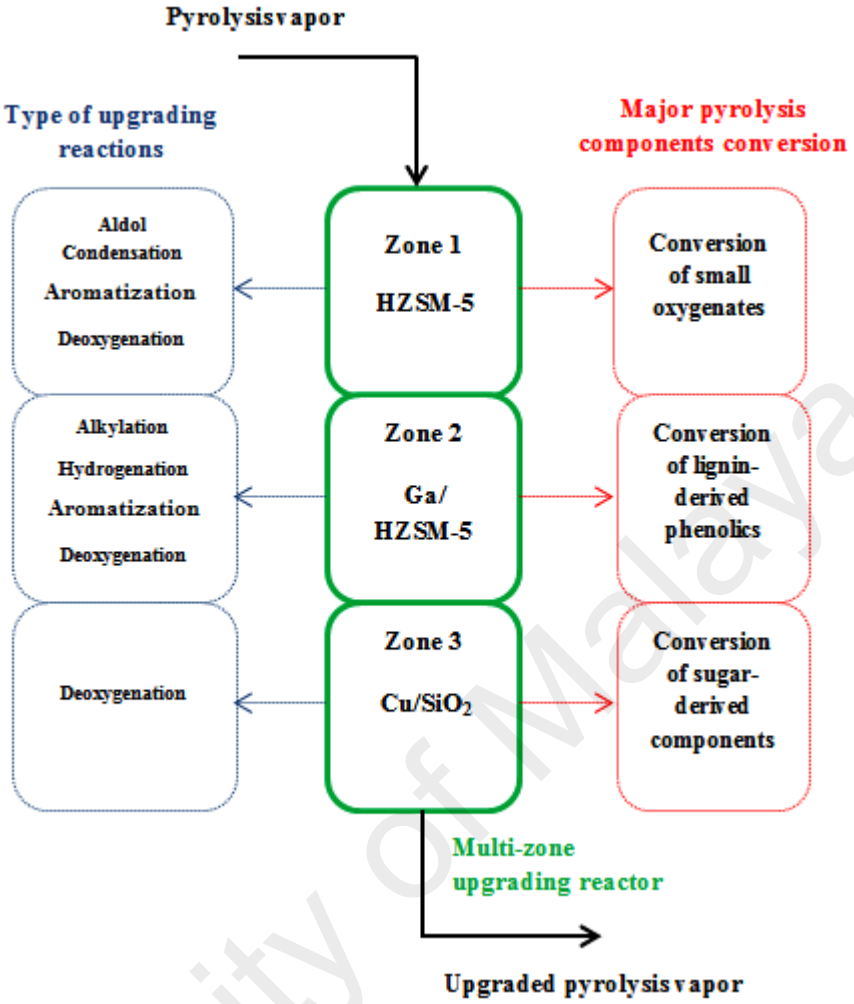

Figure 4.19: A cascade system of various upgrading reactions of the major pyrolysis components in a multi-zone fixed bed reactor.

4.4 Part 4: In-situ catalytic upgrading of biomass pyrolysis vapor: Co-feeding with methanol in a multi-zone fixed bed reactor

4.4.1 Physicochemical characteristics of the zeolite catalyst

The most important physiochemical characteristics of the HZSM-5zeolite catalyst utilized in the catalytic upgrading of PKS pyrolysis vapor (co-feeding with methanol) are shown in Table 4.15.

Table 4.15: Chemical and textural properties of HZSM-5 crystals.

Sample	SiO_2/Al_2O_3 ratio[a]	Crystal length (nm)[b]	Crystal width (nm)[b]	S_{BET} (m^2g^{-1})[c]	S_{meso} (m^2g^{-1})[d]	S_{BET}/S_{meso} (m^2g^{-1})	V_{total} (cm^3g^{-1})[e]	V_{micro} (cm^3g^{-1})[f]	V_{meso} (cm^3g^{-1})[g]	D (nm)[h]
HZSM-5	56.7	326.3	239	325	110	2.95	0.205	0.104	0.101	12.76
HZSM-5 (used-PKS/methanol)*				300	204	1.47	0.196	0.047	0.149	10.34
HZSM-5 (used-PKS)+				275	167	1.64	0.189	0.062	0.127	10.06
HZSM-5 (Regenerated)				319	102	3.13	0.197	0.098	0.099	11.68

[a] Determined by XRF.
[b] Estimated from SEM images.
[c] Surface areas were obtained by the BET method using adsorption data in p/p_0 ranging from 0.05 to 0.25.
[d] Measured by t-plot method.
[e] Total pore volumes were estimated from the adsorbed amount at $p/p_0 = 0.995$.
[f] Measured by t-plot method.
[g] $V_{meso} = V_{ads,p/p0=0.99} - V_{micro}$.
[h] Average pore width was derived from the adsorption branches of the isotherms by the BJH method.
* $C/H_{eff.}$=1.3, TOS=60 min
+ TOS=60 min

HZSM-5 was chosen as a well-known crystalline zeolite catalyst containing a two dimensional channel like pore system with vertically intersection channels of ~0.55 nm in diameter (Stephanidis et al., 2011). The zeolite surface area in the present investigation was 325 m^2/g and it was considerably microporous with few textural and structural defects generated the limited meso/macroporosity. The H^+ form of ZSM-5 zeolite catalyst possessed mostly Brönsted acid sites of high acidic strength. However, during the catalyst's calcination at about 550 °C, for transformation of its NH_4^+-exchanged form into the H^+ -form, few acid sites were generated attributed to positively charged tri-coordinated Si atoms as well as extra-framework octahedrally coordinated aluminum oxyhydroxy species (Iliopoulou et al., 2012).

The acidic properties of HZSM-5 catalyst was evaluated by NH_3-TPD technique and the related profile is indicated in Figure 4.20. As shown in this Figure, two steps of desorption were observed, conducted to the assumption that at least two types of acid sites existed (Carlson et al., 2011a; Jeongnam Kim et al., 2010; Ni et al., 2011). The HZSM-5 virgin catalyst contained two acid sites at ~175 °C (weak acid strength) and ~341°C (strong acid strength).

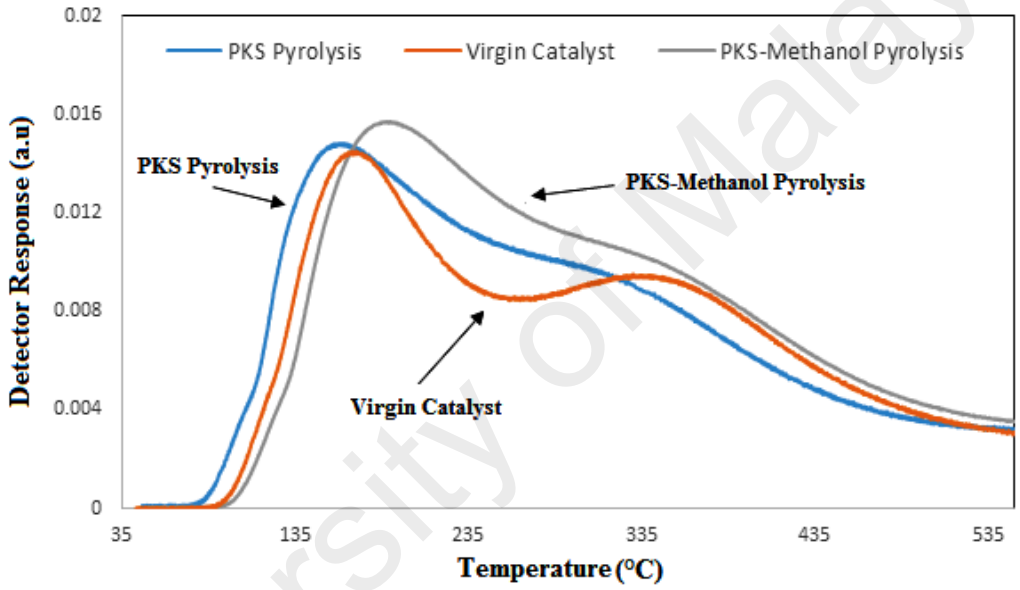

Figure 4.20: NH_3-TPD patterns of HZSM-5 virgin and partially deactivated (TOS=60 min) catalysts.

Zhang et al. (1999) stated that desorption of the NH_3-TPD at temperatures around 250-350 °C for HZSM-5 could be directly attributed to the density of Brönsted acid sites. Moreover, desorption at lower temperatures might be related to both Lewis and Brönsted acid sites. According to the literature, the weak adsorption sites of ammonia at low temperature were almost inactive in oxygenated compound conversion to hydrocarbons (Ni et al., 2011). Therefore, high temperature peak had significant effect on the pyrolysis vapor upgrading. Partially deactivated catalysts showed a decreased high temperature peak position. The shape

of high temperature peaks of partially deactivated catalysts, obtained after PKS and PKS-Methanol pyrolysis vapor upgrading, were similar, but the intensity of the latter was slightly stronger than that of the former. This could evidence that methanol co-feeding during PKS pyrolysis vapor upgrading attenuated catalyst deactivation.

XRD diffractograms of the virgin and regenerated catalysts samples are shown in Figure 4.21. The XRD patterns were coincident with that of the MFI zeolitic structure. As shown, compared to virgin catalyst, the crystalline structure of the HZSM-5 samples was not changed after regeneration.

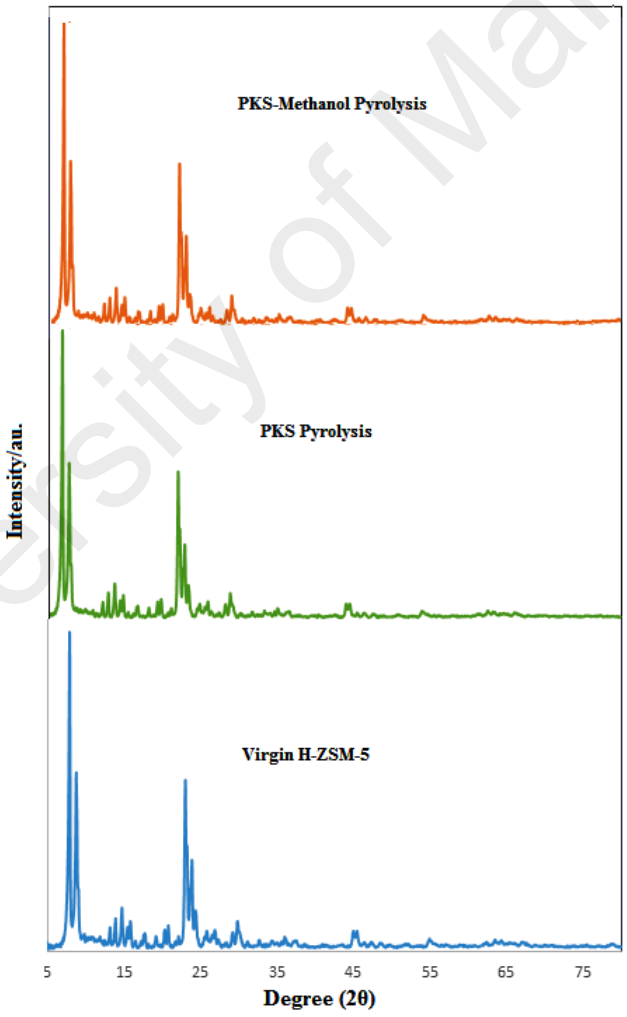

Figure 4.21: X-ray diffraction patterns of the virgin and regenerated partially deactivated (during pyrolysis vapor upgrading of PKS and PKS-Methanol co-feeding) HZSM-5 catalysts.

Figure 4.22 represents SEM photographs of the virgin (a) and regenerated (b) HZSM-5 zeolite catalysts in order to study the effect of regeneration on the catalysts' surface. As can be seen in Figure 4.22, the virgin zeolite was formed by uniform nano-range (100-400 nm) crystals.

The SEM photograph of the regenerated HZSM-5 catalyst ($H/C_{eff.}$ = 1.3) was very similar to that of the fresh one. This could confirm that catalyst recovered its original textural form after the regeneration process.

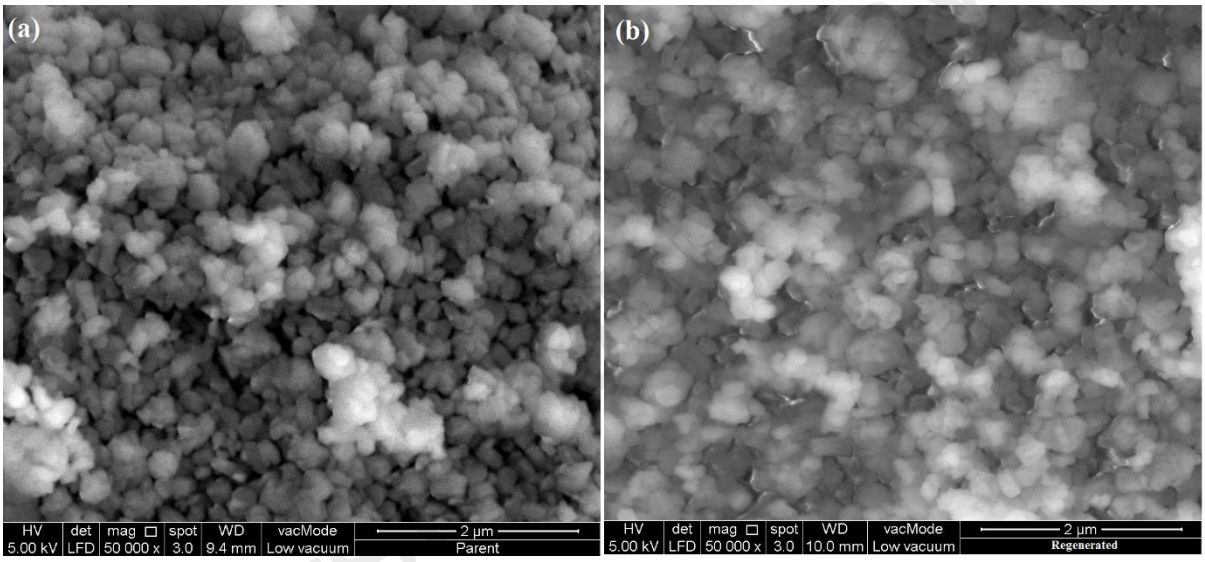

Figure 4.22: SEM photographs of the virgin (a) and regenerated (b) HZSM-5 zeolite catalyst.

4.4.2 Products yield

Among different zeolite catalysts, HZSM-5 has proofed to be very efficient in catalytic pyrolysis of the biomass and also selective towards aromatics formation in the bio-oil (H. J. Park et al., 2010a; S. D. Stefanidis et al., 2011b; Valle et al., 2010; H. Zhang, Y.-T. Cheng, et al., 2011a). The yield of the bio-oil, gas and solid products (wt. %) for the in-situ catalytic pyrolysis process and the co-processing of the biomass pyrolysis vapors and methanol over HZSM-5 catalyst are shown in Table 4.16 (TOS= 60 min). These values were compared to

the products yield obtained in non-catalytic pyrolysis. The results of products yield were in agreement with the investigations already performed on the biomass pyrolysis and catalytic upgrading (Iliopoulou et al., 2012; H. J. Park et al., 2010a; H. J. Park et al., 2012b).

Table 4.16: The yield of bio-oil, gas and char (wt. % on biomass) for the in-situ catalytic pyrolysis process and the co-processing of the biomass pyrolysis vapors and methanol over HZSM-5 zeolite catalyst.

PKS WHSV (h^{-1})	Methanol WHSV (h^{-1})	PKS/Methanol ratio (wt. %)	$H/C_{eff.}$	Bio-oil (wt. %)	Gas (wt. %)	Char (wt. %)	Water content (wt.% in bio-oil)
10	0	100/0	0.004	26.6	39.1	34.3	68
10	6	62.5/37.5	0.631	48	22	30	35.12
10	15.6	39/61	1.09	45.2	41.1	13.7	28.24
10	27	27/73	1.35	42.5	47.8	9.6	20.9
0	18.2	0/100	2	34.9	65.1	0	14.7
Non-Catalytic pyrolysis		100/0	0.004	48.35	17.55	34.1	57

The highest yield of the liquid bio-oil (48.35 wt. %) was achieved in non-catalytic runs. The use of zeolite catalyst decreased the bio-oil yield and increased the gaseous products and water yield. This was caused by different hydrocarbon conversion reactions comprising; cracking, cyclization/aromatization and dehydrogenation, which were mostly catalyzed by the Brönsted acid sites of zeolite (Asadieraghi et al., 2014; Mortensen et al., 2011). Water yield enhancement was attributed to increased dehydration of oxygenated compounds on the zeolite catalyst acid sites (Iliopoulou et al., 2012). Since the catalyst bed and biomass were not in contact, the presence of the catalyst did not affect the decomposition of the solid biomass feed. Hence, the amount of char could be considered constant for all trials and equal to the yield of solid products of the non-catalytic experiments (~ 34.1 wt. % on average). Production of non-condensable gases enhanced in the presence of catalysts as compared to the non-catalytic tests.

The bio-oil yield was slightly decreased from 48 wt. % to 42.6 wt. %, when the methanol WHSV was increased from 6 to 27 h^{-1}. This result might be attributed to alternating of the hydrocarbon pool toward production of more gaseous products like olefins. The bio-oil yields

produced from biomass/methanol catalytic in-situ pyrolysis/upgrading were higher than the yield predicted for each individual methanol and biomass catalytic conversion. The presence of methanol probably promoted the oxygen removal from the biomass pyrolysis/methanol vapors as water. This was already observed by Chantal et al.(1984) and Chen et al.(1986). On the other hand, according to the literature (Horne, Nugranad, & Williams, 1995), the presence of methanol could enhance the production of a large amount of CO. Then, the formed water in the presence of CO could probably contribute to water gas shift reaction to yield H_2 and CO_2. This possibly reduced the amount of water content in the produced bio-oil, as the addition of methanol was increased.

4.4.3 Bio-oil chemical composition

4.4.3.1 Quantitative analysis using GC-MS

The composition of the bio-oils' organic fraction (measured by GC-MS analysis) is shown in Table 4.17. Literature studies showed different bio-oil organic compounds have been classified into 13 groups; aliphatic hydrocarbons, aromatic hydrocarbons, furans, phenols, acids, alcohols, esters, ethers, aldehydes, ketones, sugars, nitrogen containing compounds and polycyclic aromatic hydrocarbons (PAHs). Among the said compounds, desirables were aromatic hydrocarbons, aliphatic hydrocarbons and alcohols, which were used for biofuels production, while furans and phenols were considered as high added value chemicals. On the other hand, carbonyls, acids, polycyclic aromatic hydrocarbons (PAHs) and heavier oxygenates were regarded as undesirables. Aldehydes and ketones components caused instability of the bio-oil during transportation, while the bio-oils with high acid contents were corrosive and practically difficult to be introduced into engines as fuel. On the other hand, esters and ethers were considered as the oxygenate components, which reduced the heating

value of the bio-oil (Iliopoulou et al., 2012; H. J. Park et al., 2010a; S. D. Stefanidis et al., 2011b).

As can be seen in Table 4.17, the bio-oil produced through non-catalytic pyrolysis (without upgrading) was rich in phenolic compounds, but had low content of ketones and acids. Also, some compounds like aromatic, aliphatic hydrocarbons and alcohols were identified in very low concentrations. High phenolic compounds available in the bio-oil could be resulted from high lignin content of PKS biomass (50.7 wt. %). Accordingly, the bio-oil produced through thermal pyrolysis of the biomass was considered as a low quality product.

Table 4.17: Composition (wt. %) of the bio-oils (organic phase) produced by non-catalytic fast pyrolysis of PKS and by catalytic upgrading of the PKS and PKS/methanol pyrolysis vapors.

Compound	Non-catalytic pyrolysis	WHSV(h^{-1})				
		PKS:10 MeOH(*): 0	PKS:10 MeOH:6	PKS:10 MeOH:15.6	PKS:10 MeOH:27	PKS: 0 MeOH:18.2
Hexanoic acid	3.26	1.49				
Furfural	7.08	6.02				
Furfuryl alcohol	1.48					
2-Propanone, 1-(acetyloxy)	2.25					
m-Xylene		0.71	1.89	17.6	25.28	26.36
o-Xylene		0.32	3.05	5.8		19.72
2-Propenoic acid	4.83	2.43	2.27	2.51	2.2	
Phenol	61.4	57.33	50.32	31.22	27.2	
1,2,3 Trimethyl benzene			5.04	5.78	23.48	39.59
o-Cresol		5.45			1.83	
Acetic acid, phenyl ester		2.59				
3-Methyl phenol	2.45	4.69				
2- Methyl phenol	3.18		7.77	1.93		
2-Metoxy phenol		0.99				
1,2,4,5 Tetramethyl benzene					1.26	4.15
2,5 dimethyl phenol		2.03				
Naphtalene		1.04				
1,2-Benzenediol	5.08					
2-Isopropoxyphenol	1					
Methyl benzenediol	2.43					

(*)MeOH=Methanol

As shown in Table 4.17, catalytic upgrading of the biomass pyrolysis vapor, especially in the case of its co-feeding with methanol, was very efficient in producing the bio-oils having desirable components. HZSM-5 catalyst resulted in the production of different kinds of aromatics. A significant increase of aromatics was seen with methanol WHSV increasing. This was possibly due to the cyclization and oligomerization of light components over acid sites of HZSM-5 catalyst. It was in consistent with the data reported in the literature (Iliopoulou et al., 2012; H. Zhang et al., 2012). In contrast, the increasing amount of methanol co-fed to the reactor, caused diminution of the phenol concentration in the product possibly attributed to the hydrocarbon pool alternation. About undesirable components, carboxylic acids and ketones were decreased during catalytic pyrolysis vapor upgrading compared to non-catalytic pyrolysis.

Figure 4.23 indicates the bio-oil organic fraction during catalytic fast pyrolysis of PKS/methanol ($H/C_{eff.}$ = 1.35) as a function of time on stream. As shown in Figure 4.23, aromatics yield, as one of the main bio-oil component (organic fraction), decreased, whereas the phenol yield and coke build up were enhanced during the pyrolysis. This was due to the partial deactivation of zeolite catalyst.

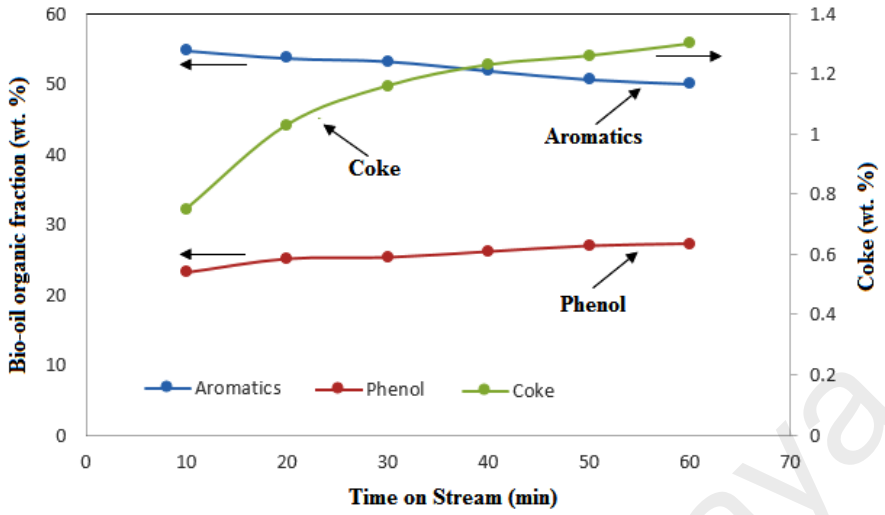

Figure 4.23: The composition of the bio-oil (organic fraction) and formed coke (wt. % on catalyst) during the biomass/methanol (27/73 wt. % or $H/C_{eff.}$ = 1.35) pyrolysis vapors upgrading experiment.

Figure 4.24 shows the effect of hydrogen to carbon effective ratio ($H/C_{eff.}$) on the bio-oil organic fraction. As indicated, the aromatics yield increased with increasing H/C_{eff} ratio, although the phenol yield and coke formation on the catalyst decreased. This was attributed to the synergistic effects of PKS/methanol co-feeding on aromatics formation through oligomerization and aromatization reactions. The reduction of catalytic coke deposition by methanol content increasing is consistent with the literature investigation, when the feed $H/C_{eff.}$ ratio was enhanced during oxygenated compounds cracking (Mentzel & Holm, 2011; Valle et al., 2012).

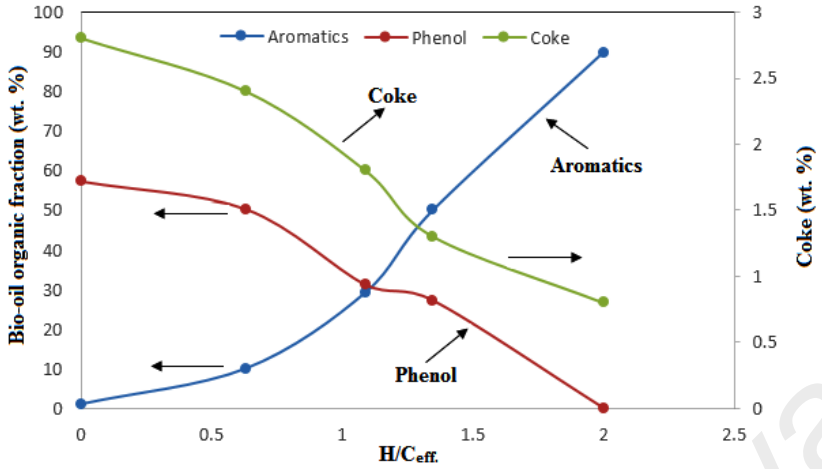

Figure 4.24: The effect of feed (PKS/methanol) effective ($H/C_{eff.}$) ratio on the composition of produced bio-oil (organic fraction) and formed coke (wt. % on catalyst) during the biomass/methanol pyrolysis vapors upgrading experiment.

4.4.3.2 Qualitative analysis using FTIR

The chemical structure of the bio-oil samples components was studied by infrared spectroscopy (FTIR) technique. Figure 4.25 shows the FTIR spectra of the different non-catalytic and catalytic pyrolysis bio-oils. The FTIR identified functional groups and chemical bonds in the bio-oil can be observed in Table (4.14).

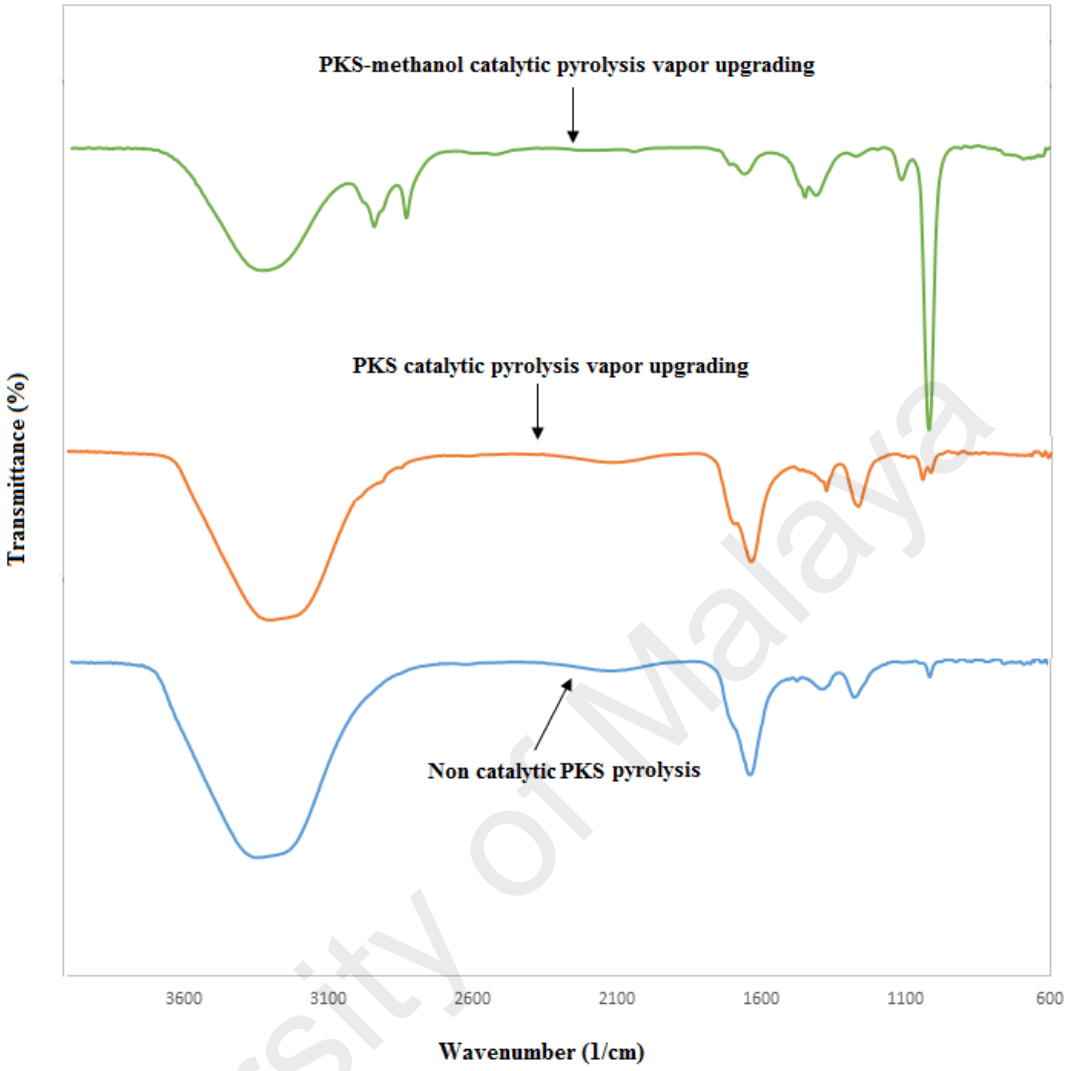

Figure 4.25: FTIR spectra of the bio-oil produced through catalytic (PKS and PKS/methanol) pyrolysis vapor upgrading and non-catalytic (PKS) pyrolysis.

In the FTIR spectra, the first broad peak between 3500 and 3200 cm^{-1} was related to O-H stretching vibration of alcoholic and phenolic functional groups. The peak of C-H stretching vibration between 3000 and 2800 cm^{-1} indicated the presence of $–CH_2$ and $–CH_3$ functional groups, which was only identified in the upgraded bio-oil. This peak had higher intensity once PKS was co-fed with methanol (WHSV (h^{-1}) PKS: 10, methanol: 27 for 60 min). The peak around 1700 cm^{-1} was the result of C=O stretching vibration of free carbonyl groups of aldehyde, ketones and carboxylic acids. This peak showed lower intensity in the FTIR spectra related to catalytic upgrading of the bio-oil, especially in the case of PKS co-feeding with

methanol. The next spectrum bands around 1650-1510 cm^{-1} represented aromatics C=C stretching vibrations. The spectral region of 1440-1400 cm^{-1} contained various bands in the O-H bending region, which were most probably alcohols and carboxylic acids. The spectra around 1280 cm^{-1} indicated C-O stretching related to carboxylic acids, which was detected with low intensity in the catalytic bio-oil upgrading of PKS and methanol co-feeding. The peaks around 1020 cm^{-1} (aromatic in-plane C-H bending) and 700 cm^{-1} evidenced the high amount of aromatic hydrocarbons in the upgraded bio-oils. High intensity spectra related to the bio-oil upgrading through PKS-methanol co-feeding confirmed high contents of aromatics in the produced bio-oil. The FTIR qualitative studies of the bio-oil chemical constituents were in agreement with the quantitative results of GC-MS.

4.4.4 Deposited coke on the catalysts

4.4.4.1 Coke analysis

The total amount of oxidable hydrocarbons on the used HZSM-5 zeolite catalysts was assigned using TGA. The BET surface area and micropore volume of the catalysts are listed in Table 4.15. For the moderately deactivated catalysts, a reduction in BET surface area was observed. This reduction, in both micropore volume and surface area, might reasonably be attributed to the fairly high quantity of oxidable materials available on the catalyst, as determined by TGA. The contents of different soluble coke components, determined by GC-MS, is shown in Table 4.18. The aromatics were the compounds with approximately 1-3 rings. The oxo-aromatics with various structures were representative of the components participated in thermal coke build up.

Table 4.18: Main components of the soluble coke, extracted from the spent catalysts ($H/C_{eff.}$ =1.35).

Residence time	Peak Area	Name	Formula
4.444	12.15	Cyclopropane, 2-methylene-1-pentyl	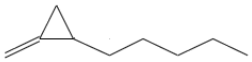
7.294	9.55	2-Propenoic acid, butyl ester	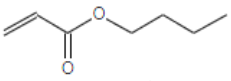
9.333	8.92	Anthracene, 9-ethyl-9,10-dihydro	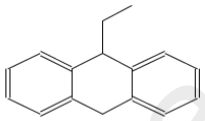
12.506	3.72	2,2-Bis(4-hydroxyphenyl)propane	
13.585	13.65	Benzoic acid, 4-(4-ethylcyclohexyl)-, 4-butoxy ester	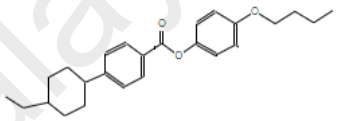
15.951	4.46	Acetophenone	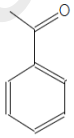
19.599	1.83	Cyclohexene, 3-butyl-3,5,5-trimethyl	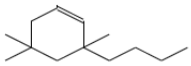

Figure 4.26 indicates the proposed kinetic for the biomass/methanol conversion into hydrocarbons and coke (catalytic and thermal) over the HZSM-S catalyst. The amount and composition of the deposited coke on the HZSM-5 catalyst indicated the significance of catalyst acidity for the formation of catalytic and thermal coke fractions. The most fraction of the produced coke was possibly attributed to the polymerization of the products derived from the biomass components pyrolysis (mostly lignin). In fact, two fractions of coke were formed on the catalyst. The fraction of coke which was burned at low temperature was formed by condensation- degradation of lignin based oxygenated compounds. This type of coke was deposited on macro- and mesoporous structure of the zeolite catalyst matrix (Valle et al., 2012). The other one, which was burned at higher temperature and being deposited on catalyst's micropores, was formed by condensation reactions activated by the acid sites.

Formation of this type of coke was prominent in pure methanol catalytic conversion. The addition of methanol to the pyrolysis vapor decreased the coke formation (Figure 4.24) due to the attenuation of the phenolic compounds (lignin originated) polymerization and their deposition on the catalyst. According to the literature, pure methanol catalytic conversion on the HZSM-5 catalyst formed non- oxygenated aromatics and aliphatic hydrocarbons as major components (Valle et al., 2012).

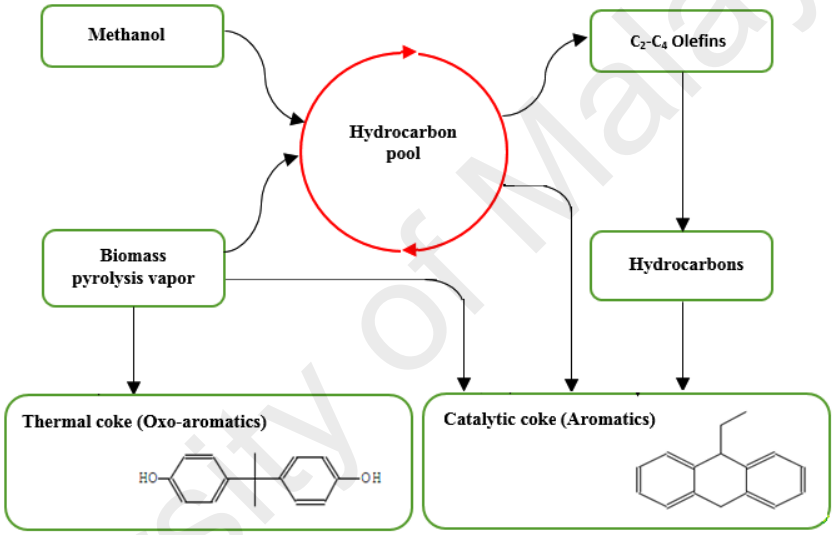

Figure 4.26: Proposed kinetic for the conversion of biomass (PKS)/methanol mixture into hydrocarbon and coke (thermal and catalytic) over HZSM-5 catalyst.

4.4.4.2 Internal and external coke

During PKS-methanol pyrolysis vapor upgrading (having WHSV (h^{-1}) PKS: 10, methanol: 27 for 60 min), coke was deposited over HZSM-5 catalyst. To determine whether the produced coke was deposited within the catalyst pore and/or on the outer surface of HZSM-5 zeolite, adsorption of nitrogen on the catalyst before and after reaction was studied. Figure 4.27 indicates the adsorption isotherm of the virgin and coked catalysts. Table 4.15 summarizes the calculated pore volumes from isotherms. It could be observed that, compared

to virgin catalyst, the quantity of the adsorbed nitrogen (micropore volume) reduced from 0.104 to 0.047 cm^3/g as the coke level enhanced from zero to 1.3 wt. % (Figure 4.23). The total deposited coke on the catalyst could be subdivided into external and internal coke, based on the combined information from gas adsorption measurements and thermogravimetric analysis. The internal amount of coke (~ 0.07 wt. %) was determined by decrease in micropore volume of the deactivated fractions respect to the related virgin sample, as assigned by t-plot method (using adsorption isotherm). The external coke was calculated from difference of the two (1.23 wt. %).

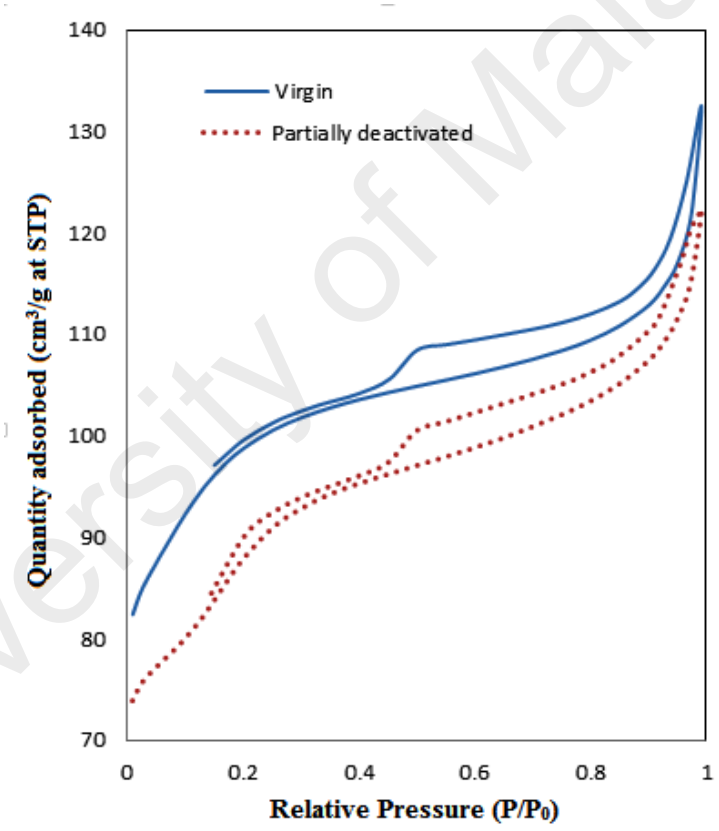

Figure 4.27: Adsorption isotherms of the virgin and partially deactivated HZSM-5 zeolite catalyst.

Figure 4.28 depicts the catalyst coking rate and the bio-oil's yield as a function of time on stream (TOS). As indicated, at the initial time of the reaction, which the catalyst acid sites were active enough, a higher coking rate and the lower bio-oil yield could be observed. Then,

the coking rate decreased sharply from 0.075 to 0.013 wt. %/ min at the early stage of the reaction, whereas the bio-oil yield was increased. At the next stage, lower coking rate and the higher bio-oil's yield were observed. Coke formation is attributed to the production of the hydrocarbons, oxo-aromatics and aromatics on the outer surface of the HZSM-5 catalyst and also inside the catalyst cavities. The later could not diffuse out of the cavities and caused coke build up. The similar results was observed by Zhang et al. (2014). The bio-oil's yield enhancement was probably attributed to the partly deactivation of the catalyst and consequently, reducing the degree of bio-oil's upgrading (gaseous products yield diminution).

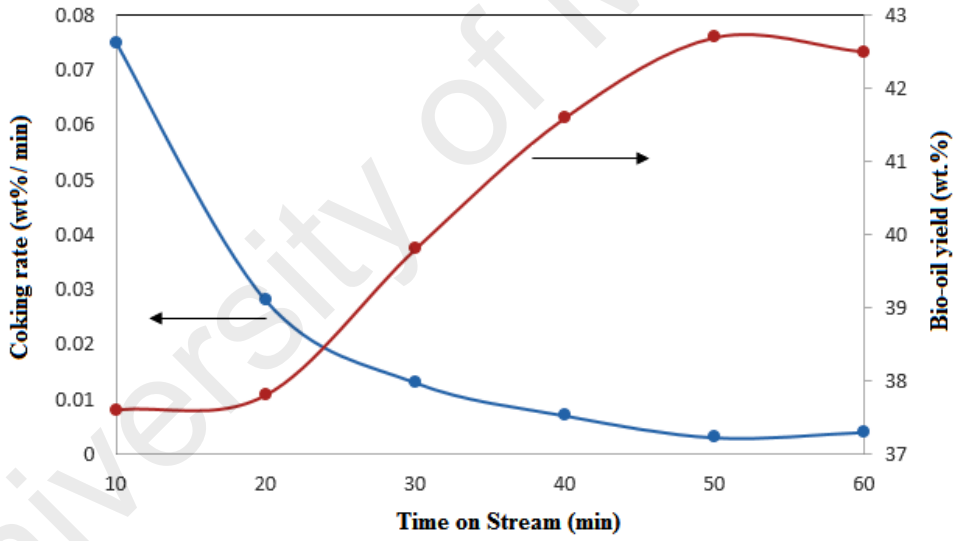

Figure 4.28: Coking rate and the bio-oil yield as a function of time on stream (WHSV (h^{-1}) PKS: 10, MeOH: 27 for 60 min).

CHAPTER 5: CONCLUSIONS AND RECOMMENDATIONS FOR FUTURE STUDIES

5.1 Conclusion

5.1.1 Part1: Heterogeneous catalysts for advanced bio-fuel production through catalytic biomass pyrolysis vapor upgrading: A review

Catalytic biomass pyrolysis vapor upgrading process to enhance the bio-oil quality indicates immense potential to convert renewable biomass to bio-fuel. Fast pyrolysis, which is known as a promising process to convert pretreated biomass to bio-oil, is affected by the biomass types and reaction conditions. Catalytic vapor phase upgrading is aiming to treat the fast pyrolysis vapor before condensation. It recently has attracted the attentions of bio-fuel researchers due to the prominent techno-economical characteristics of this type of upgrading in comparison with conventional hydro-deoxygenation (HDO) process. Despite HDO process which consumes high hydrogen quantity and requires complicated equipment working at high pressure, this upgrading approach is carried out at atmospheric condition without hydrogen feeding. The produced bio-oils yields and qualities are strongly dependant on catalysts types and properties (e.g. structure, acidity and pore size), reaction conditions and feed type.

Three most important classes of catalysts including zeolites, mesoporous catalysts, and metal based catalysts are used for vapor phase bio-oil upgrading. Among zeolite catalysts, HZSM-5 (which possesses a three dimensional pore structure, high acidity and shape selectivity) indicates the superior performance in deoxygenation, aromatic compounds production and resistance to coke formation. However, to keep the catalyst activity and selectivity for long time, deactivation through dealumination as well as coke deposition need to be minimized. The product distribution and coke formation amount over catalyst are strong function of catalyst shape selectivity and acidity. Shape selectivity of the zeolite catalyst are mostly influenced by pore size and shape as well as crystallite size. Mesoporous catalysts having

pore diameter larger than 2 nm can resolve large molecules mass transfer limitation, associated with microporous zeolites. Contrary to mesoporous MCM-41 based catalysts, which have lower thermal stability and acidity compared to zeolite based catalysts, mesoporous MFI catalysts simultaneously possess high acidity as well as large pore diameter to overcome mass transfer limitation (which is micro-zeolites drawback). On the other hand, metal based catalysts, exhibit high acidity and outstanding resistance to coke deposition; therefore they can be reputable catalysts for bio-oil upgrading.

Efforts to transform lignocellulosic biomass to intermediate and base chemicals for the biofuels production have been fruitful to a considerable extent in recent years. In the next decades, it will be expected to find more techno-economical processes which can employ advanced catalytic processes to convert biomasses from various resources into fine chemicals, base chemicals and fuels. We will be approaching to more sustainable and renewable economy, although further efforts will be required. Biofuel upgrading technologies still need development to create cost-competitive products with acceptable productivity and selectivity. Promising improvement on heterogeneously catalyzed transformation of lignocellulosic biomasses to fuel like and value added chemicals with low coke formation over catalysts has attracted intensive attention in the past few years and breakthroughs have been attained up to some extent. It might be proper to mention that conversion of biomasses to desired chemicals with low coke formation, high selectivity and yield remains in its infancy until there are considerable developments in heterogeneous catalysts. Biomasses catalytic pyrolysis vapor upgrading through a cascade system of different catalysts (micropore zeolites, mesopore and metal based catalysts), that includes several consecutive steps for various bio-oil fractions upgrading, seems to be a promising thermochemical conversion/upgrading technology. Each individual mentioned catalysts or their employment in a cascade system indicated high potential for industrialization, although bio-oil

upgrading through a cascade systems of catalysts most probably in the near future would attract the researchers' attentions.

5.1.2 Part 2: Model compound approach to design process and select catalysts for in-situ bio-oil upgrading

This study is targeting to analyze the results of model compound approach researches to present the knowledge needed to develop catalysts and processes to upgrade pyrolysis bio-oil. In this investigation, special attentions are drawn on (a) maximizing carbon retention in the upgraded products, (b) minimizing hydrogen consumption in the upgrading processes, and (c) optimizing product fuel properties. Model compounds approach has been utilized to identify the reaction conditions and catalysts that are active and selective for several classes of reactions. Condensation, ketonization and etherization reactions have been investigated to build longer (fuel molecule) carbon chains from small oxygenates (aldehydes, ketones, acids) by using metal oxides and zeolites catalysts. Zeolites and supported metal catalysts could be employed for deoxygenation of furfurals (as models of sugar-derived compounds in bio-oil) and phenolics (lignin derived compound). Alkylation and transalkylation by zeolite and zeolite supported metals improve carbon retention. Based on this profound investigation a set of catalysts have been proposed to be used in a catalytic upgrading cascade process which comprises several consecutive steps for different bio-oil components upgrading. They were selected from four catalyst's classes of zeolites, zeolites supported metals, oxide supported metals and metal oxides. An integrated fast pyrolysis process followed by catalytic bio oil vapor upgrading reactions has been dedicated to produce high quality and stabilized bio-fuel. The proposed catalytic upgrading process is enough flexible for different reactors configurations. In the future action, authors will intend to comprehensively investigate on in-situ biomass to bio-oil upgrading based on suggested catalysts and process.

5.1.3 Part 3: In-depth investigation on thermochemical characteristics of palm oil biomasses as potential biofuel sources

The thermochemical properties of the different palm oil biomasses (PKS, EFB and PMF) were investigated to evaluate their potential to be used as renewable energy feedstock for the bio-fuel production through pyrolysis process. Pyrolysis of biomasses was divided into three stages: moisture evolution, slow depolymerization and thermal degredation.

Differential scanning calorimetry (DSC) was employed to compute the required energy for the biomass samples pyrolysis in different stages. The biomasses thermal behavior and evolved gases (H_2, CO_2 and CO) produced during pyrolysis were investigated by TGA-MS and TGA-FTIR. Most of these gaseous products were generated at pyrolysis temperature between 250-400 °C (stage 3) where cellulose and hemicelluloses reached their highest weight loss rate. The kinetics model satisfactorily predicted the biomasses pyrolysis behavior.

Proximate analysis indicated that all the biomasses samples have high volatile and low ash and moisture content. Ultimate analysis showed all the biomass samples have a similar carbon, hydrogen and oxygen contents with very low level of nitrogen and sulphur. So, they are advantageous to gasification, combustion and pyrolysis processes for clean energy generation.

The bio-oil produced from EFB pyrolysis indicated the highest yield (58.2 wt. %) attributed to its high fraction of volatile components (79.2 wt. %). PKS bio-oil showed high quantity of phenolic compounds (67.63 wt. %) caused by relatively high lignin content of the biomass (50.7 wt. %), whereas EFB and PMF exhibited high quantity of furan based components (27.61 wt. % and 23.15 wt. %, respectively) attributed to their hollocellulose content of 77.9 and 74.3 wt. %, respectively.

The outcome of this thermochemical analysis investigation proved that the palm oil biomasses are promising materials to conduct pyrolysis for the purpose of bio-fuel production.

5.1.4 Part 4: Characterization of lignocellulosic biomass thermal degradation and physiochemical structure: Effects of demineralization by diverse acid solutions

The different palm oil biomass samples (PKS, EFB and PMF) were demineralized by diverse diluted acid solutions (H_2SO_4, $HClO_4$, HF, HNO_3, HCl). HF pretreatment showed interesting results on significant minerals removal from EFB and PMF, whereas HCl indicated considerable inorganic constituent removal from PKS. The pretreated biomasses, which exhibited the highest efficiency of minerals removal, were deeply investigated. Their physiochemical structure studies showed that acid pretreatment introduced some impacts on the structure of the biomass samples. The virgin and demineralized biomasses thermal behavior and evolved gases (H_2, CO_2 and CO) produced during pyrolysis were investigated by TGA-MS and TGA-FTIR. Most of these gaseous products were generated at pyrolysis temperature between 250-400 °C, while at high temperature (> 600 °C) the dominant released gas was hydrogen. The kinetics model satisfactorily predicted the biomasses pyrolysis behavior. The shift of pyrolysis to higher temperature, diminishing of the released gas and activation energy enhancement after demineralization could suggest the catalytic effects of the biomasses inorganics.

The outcome of the present analysis investigation provides valuable information can be employed for the efficient thermochemical conversion of the palm oil biomasses.

5.1.5 Part 5: In-situ catalytic upgrading of biomass pyrolysis vapor: Using a cascade system of various catalysts in a multi-zone fixed bed reactor

A cascade system of different catalysts including meso-HZSM-5, Ga(1)/meso-HZSM-5 and Cu(5)/ SiO_2 exhibited the best performance to produce high quality bio-oil, in terms of both aromatics and deoxygenated compounds contents, during the in-situ catalytic pyrolysis vapors upgrading of the PKS biomass. From operational point of view, catalytic pyrolysis vapor upgrading of different bio-oil fractions including small oxygenates, lignin derived phenolics and sugar derived components in a cascade process comprised various consecutive upgrading steps of aldol condensation, alkylation, hydrogenation, aromatization, and deoxygenation. A cascade catalytic process exhibited a very good performance toward aromatics formation (15.05 wt. %), although it decreased bio-oil yield (29.3 wt. %). The gallium incorporation into the mesoporous HZSM-5 zeolite caused less cracking of the biomass pyrolysis vapor, even though it increased the produced bio-oil yield. The gallium amount added into the meso-HZSM-5 zeolite played an important role in the aromatics formation. The incorporation of the gallium appropriate amount (1.0 wt. %) led to the enhancement of the aromatics yield (11.93 wt. %) attributed to the synergic effect of catalyst moderate acidity and high porosity, whereas the excess amount of gallium (5.0 wt. %) indicated a negative effect on the aromatics formation (4.24 wt. %) due to the high loss of catalyst's protons.

5.1.6 Part 6: In-situ catalytic upgrading of biomass pyrolysis vapor: Co-feeding with methanol in a multi-zone fixed bed reactor

In this contribution, in-situ catalytic fast pyrolysis of PKS, methanol and their mixture were conducted over HZSM-5 zeolite catalyst in a multi-zone fixed bed reactor. PKS and methanol mixtures, co-fed to the reactor with different ratios, were tested at 500 °C. The results indicated that the aromatics yield enhanced with increasing H/C_{eff} ratio of the feed and more

aromatics could be produced from PKS biomass, when methanol was added to the pyrolysis process. Also, the coke yield was decreased with methanol WHSV increasing. The maximum aromatics yielded (50.02 wt. %), when PKS to methanol ratio (wt.%) was 27/73 (H/C_{eff} =1.35). The methanol presence during the pyrolysis vapor upgrading appeared to reduce the phenol formation.

The catalyst deactivation in the catalytic step was attributed to the coke deposition. The deposited coke on the catalyst had a considerable content of aromatics, oxygenates and oxo-aromatics. Moreover, it comprised two fractions corresponding to internal and external coke in the zeolite crystals. The coke formed on the partially deactivated zeolites could be removed by regeneration of the zeolites and the initial surface area could be recovered. This investigation provides insights into how the biomass resources can be utilized more efficiently to produce renewable fuels and chemicals.

5.2 Recommendations for future studies

The present investigation was trying to dedicate the fundamental understanding of the palm biomasses thermal behavior during pyrolysis and in-situ catalytic upgrading of pyrolysis vapors to yield stabilized deoxygenated bio-oils. Methanol co-feeding (increasing $H/C_{eff.}$ ratio of the feed) to the reactor, during biomass pyrolysis vapor upgrading, caused the aromatics yield enhancement. Also, the coke yield was decreased with methanol WHSV increasing. In addition, cascade system of various catalysts in a multi-zone pyrolysis/ upgrading reactor indicated very good results on the conversion of small oxygenates, lignin phenolics and sugar-derived components of the biomasses pyrolysis vapors. Upon these efforts, further investigations can now build. Various catalysts can be utilized individually or in a cascade system in a multi-zone reactor to yield higher quality bio-oil. However, the main drawback of such a system is the low yield of bio-oil, which is caused by the high yield of water and coke formed on the catalysts. This problem can be likely mitigated applying modified operating conditions. Apart from the process development, catalyst system modification should be addressed. Considering HZSM-5, as one of the key catalysts for the biomass pyrolysis vapors upgrading, the hydrophilic character and diffusion characteristics control need to be investigated in detail. More aluminum incorporation into ZSM-5 structure, which can be conducted to an increase in hydrophilicity inside the zeolite, plays a considerable role on achieving high yield of aromatics. In addition, any enhancements in the diffusion properties in ZSM-5 catalyst can have a positive effect on catalytic activity. ZSM-5 catalyst diffusion properties improvements by decreasing the particle size of ZSM-5 catalyst can have a positive effect on catalytic activity and enhance the aromatic yield. In addition, to mitigate the undesired coke generation, exterior surface sites of the mesoporous ZSM-5 catalyst should be better tuned. Catalysts regenerability is a

considerable aspect to take into account in any catalytic investigation. It was indicated that catalysts have lost part of theirs activity towards bio-oil deoxygenation after regeneration. For the purpose of catalysts regenerability improvement and therefore their applicability, identifying the mechanism of catalysts deactivation is necessary.

Incorporation of various metals (such as Ni, Fe and etc.) into ZSM-5 catalyst need to be studied in detail. Replacement of some protons in HZSM-5 catalyst by metals caused reduction of Brønsted acid sites. These metals incorporation can possibly increase the aromatics production through enhancement of light alkane aromatization and decarbonylation. So, more mechanistic studies will offer a better insight into the exact role of metals species on bio-oils deoxygenation.

REFERENCES

A.Agblevor, F. (2009). 2009/0165378 A1. U. S. patent.

A.Agblevor, F. (2010). 2010/0212215 A1. U. S. patent.

Adam, Judit, Blazsó, Marianne, Mészáros, Erika, Stöcker, Michael, Nilsen, Merete H., Bouzga, Aud, . . . Øye, Gisle. (2005). Pyrolysis of biomass in the presence of Al-MCM-41 type catalysts. *Fuel, 84*(12–13), 1494-1502. doi: http://dx.doi.org/10.1016/j.fuel.2005.02.006

Adjaye, J. D., & Bakhshi, N. N. (1995a). Production of hydrocarbons by catalytic upgrading of a fast pyrolysis bio-oil. Part I: Conversion over various catalysts. *Fuel Processing Technology, 45*(3), 161-183. doi: http://dx.doi.org/10.1016/0378-3820(95)00034-5

Adjaye, J. D., & Bakhshi, N. N. (1995b). Production of hydrocarbons by catalytic upgrading of a fast pyrolysis bio-oil. Part II: Comparative catalyst performance and reaction pathways. *Fuel Processing Technology, 45*(3), 185-202. doi: http://dx.doi.org/10.1016/0378-3820(95)00040-E

Adjaye, John D., Katikaneni, Sai P. R., & Bakhshi, Narendra N. (1996). Catalytic conversion of a biofuel to hydrocarbons: effect of mixtures of HZSM-5 and silica-alumina catalysts on product distribution. *Fuel Processing Technology, 48*(2), 115-143. doi: http://dx.doi.org/10.1016/S0378-3820(96)01031-4

Agostini, Giovanni, Lamberti, Carlo, Palin, Luca, Milanesio, Marco, Danilina, Nadiya, Xu, Bin, . . . van Bokhoven, Jeroen A. (2009). In Situ XAS and XRPD Parametric Rietveld Refinement To Understand Dealumination of Y Zeolite Catalyst. *Journal of the American Chemical Society, 132*(2), 667-678. doi: 10.1021/ja907696h

Aho, A., Kumar, N., Eränen, K., Salmi, T., Hupa, M., & Murzin, D. Y. (2007). Catalytic Pyrolysis of Biomass in a Fluidized Bed Reactor: Influence of the Acidity of H-Beta Zeolite. *Process Safety and Environmental Protection, 85*(5), 473-480. doi: http://dx.doi.org/10.1205/psep07012

Aho, A., Kumar, N., Eränen, K., Salmi, T., Hupa, M., & Murzin, D. Yu. (2008). Catalytic pyrolysis of woody biomass in a fluidized bed reactor: Influence of the zeolite structure. *Fuel, 87*(12), 2493-2501. doi: 10.1016/j.fuel.2008.02.015

Aho, A., Kumar, N., Lashkul, A. V., Eränen, K., Ziolek, M., Decyk, P., . . . Murzin, D. Yu. (2010). Catalytic upgrading of woody biomass derived pyrolysis vapours over iron modified zeolites in a dual-fluidized bed reactor. *Fuel, 89*(8), 1992 .2000-doi: http://dx.doi.org/10.1016/j.fuel.2010.02.009

Álvarez, P., Santamaría, R., Blanco, C., & Granda, M. (2005). Thermal degradation of lignocellulosic materials treated with several acids. *Journal of Analytical and Applied Pyrolysis, 74*(1-2), 337-3 .43doi: 10.1016/j.jaap.2004.11.030

Amutio, M., Lopez, G., Artetxe, M., Elordi, G., Olazar, M., & Bilbao, J. (2012). Influence of temperature on biomass pyrolysis in a conical spouted bed reactor. *Resources, Conservation and Recycling, 59*(0), 23-31. doi : http://dx.doi.org/10.1016/j.resconrec.2011.04.002

Antonakou, Eleni, Lappas, Angelos, Nilsen, Merete H., Bouzga, Aud, & Stöcker, Michael. (2006). Evaluation of various types of Al-MCM-41 materials as catalysts in biomass pyrolysis for the production of bio-fuels and chemicals. *Fuel, 85*(14–15), 2202-2212. doi: http://dx.doi.org/10.1016/j.fuel.2006.03.021

Asadieraghi, Masoud, Ashri Wan Daud, Wan Mohd, & Abbas, Hazzim F. (2015). Heterogeneous catalysts for advanced bio-fuel production through catalytic biomass pyrolysis vapor upgrading: a review. *RSC Advances, 5*(28), 22234-22255. doi: 10.1039/C5RA00762C

Asadieraghi, Masoud, & Wan Daud, Wan Mohd Ashri. (2014). Characterization of lignocellulosic biomass thermal degradation and physiochemical structure: Effects of demineralization by diverse acid solutions. *Energy Conversion and Management, 82*, 71-82. doi: 10.1016/j.enconman.2014.03.007

Asadieraghi, Masoud, & Wan Daud, Wan Mohd Ashri. (2015). In-situ catalytic upgrading of biomass pyrolysis vapor: Co-feeding with methanol in a multi-zone fixed bed reactor. *Energy Conversion and Management, 92*, 448-458. doi: 10.1016/j.enconman.2014.12.082

Asadieraghi, Masoud, Wan Daud, Wan Mohd Ashri, & Abbas, Hazzim F. (2014). Model compound approach to design process and select catalysts for in-situ bio-oil upgrading. *Renewable and Sustainable Energy Reviews, 36*, 286-303. doi: 10.1016/j.rser.2014.04.050

Asadullah, M., Anisur Rahman, M., Mohsin Ali, M., Abdul Motin, M., Borhanus Sultan, M., Robiul Alam, M., & Sahedur Rahman, M .(2008) .Jute stick pyrolysis for bio-oil production in fluidized bed reactor. *Bioresour Technol, 99*(1), 44-50. doi: 10.1016/j.biortech.2006.12.002

Ausavasukhi, Artit, Sooknoi, Tawan, & Resasco, Daniel E. (2009). Catalytic deoxygenation of benzaldehyde over gallium-modified ZSM-5 zeolite. *Journal of Catalysis, 268*(1), 68-78. doi: 10.1016/j.jcat.2009.09.002

Ball, R., McIntosh, A. C., & Brindley, J. (2004). Feedback processes in cellulose thermal decomposition: implications for fire-retarding strategies and treatments. *Combustion Theory and Modelling, 8*(2), 281-291. doi: 10.1088/1364-7830/8/2/005

Basta, A. H., Fierro, V., Saied, H., & Celzard, A. (2011). Effect of deashing rice straws on their derived activated carbons produced by phosphoric acid activation .*Biomass and Bioenergy, 35*(5), 1954-1959. doi: 10.1016/j.biombioe.2011.01.043

Béguin, Pierre, & Aubert, Jean-Paul. (1994). The biological degradation of cellulose. *FEMS Microbiology Reviews, 13*(1), 25-58. doi: http://dx.doi.org/10.1016/0168-6445(94)90099-X

Bejblová, Martina, Zámostný, Petr, Červený, Libor, & Čejka, Jiří. (2005). Hydrodeoxygenation of benzophenone on Pd catalysts. *Applied Catalysis A: General, 296*(2), 169-175. doi: http://dx.doi.org/10.1016/j.apcata.2005.07.061

Ben, Haoxi, & Ragauskas, Arthur J. (2012). One step thermal conversion of lignin to the gasoline range liquid products by using zeolites as additives. *RSC Advances, 2*(33), 12892. doi: 10.1039/c2ra22616b

Bertero, Melisa, de la Puente, Gabriela, & Sedran, Ulises. (2012). Fuels from bio-oils: Bio-oil production from different residual sources, characterization and thermal conditioning. *Fuel, 95*, 263-271. doi: 10.1016/j.fuel.2011.08.041

Bibby, David M., Howe, Russell F., & McLellan, Gavin D. (1992). Coke formation in high-silica zeolites. *Applied Catalysis A: General, 93*(1), 1-34. doi: http://dx.doi.org/10.1016/0926-860X(92)80291-J

Bjorgen, M., Svelle, S., Joensen, F., Nerlov, J., Kolboe, S., Bonino, F., . . . Olsbye, U. (2007). Conversion of methanol to hydrocarbons over zeolite H-ZSM ;5-On the origin of the olefinic species. *Journal of Catalysis, 249*(2), 195-207. doi: 10.1016/j.jcat.2007.04.006

Bleken, Francesca Lønstad, Barbera, Katia, Bonino, Francesca, Olsbye, Unni, Lillerud, Karl Petter, Bordiga, Silvia, . . . Svelle, Stian. (201 .(3Catalyst deactivation by coke formation in microporous and desilicated zeolite H-ZSM-5 during the conversion of methanol to hydrocarbons. *Journal of Catalysis, 307*(0), 62-73. doi: http://dx.doi.org/10.1016/j.jcat.2013.07.004

Bridgwater, A., Czernik, S ,.Diebold, J., Meier, D., Oasmaa, A., Peacocke, C., . . . Radlein, D. (2008). *The Fast Pyrolysis of Biomass: A Handbook*. Newbury: CPL Press.

Brown, R.C., & Stevens, C. (2011). *Thermochemical Processing of Biomass: Conversion into Fuels, Chemicals and Power*: Wiley.

Carlson, Torren R., Cheng, Yu-Ting, Jae, Jungho, & Huber, George W. (2011a). Production of green aromatics and olefins by catalytic fast pyrolysis of wood sawdust. *Energy & Environmental Science, 4*(1), 145. doi: 10.1039/c0ee00341g

Carlson, Torren R., Cheng, Yu-Ting, Jae, Jungho, & Huber, George W. (2011b). Production of green aromatics and olefins by catalytic fast pyrolysis of wood sawdust. *Energy & Environmental Science, 4*(1), 145-161 .

Carrier, Marion, Neomagus, Hein Wjp, Görgens, Johann & ,Knoetze, Johannes H. (2012). Influence of Chemical Pretreatment on the Internal Structure and Reactivity of Pyrolysis Chars Produced from Sugar Cane Bagasse. *Energy & Fuels, 26*(7), 4497-4506. doi: 10.1021/ef300500k

Çepelioğullar, Özge, & Pütün, Ayşe E. (2 .(013Thermal and kinetic behaviors of biomass and plastic wastes in co-pyrolysis. *Energy Conversion and Management, 75*, 263-270. doi: 10.1016/j.enconman.2013.06.036

Chal, R., Gerardin, C., Bulut, M., & van Donk, S. (2011). Overview and industrial assessment of synthesis strategies towards zeolites with mesopores. *ChemCatChem, 3*(1), 67-81. doi: 10.1002/cctc.201000158

Chang, Chau-Shang, & Lee, Min-Dar. (1995). Effects of hydrogen pretreatment on the acidic and catalytic properties of gallium-supported H-ZSM-5 in n-hexane aromatization. *Applied Catalysis A: General, 123*(1), 7-21. doi: http://dx.doi.org/10.1016/0926-860X(94)00230-4

Chang, Clarence D., & Silvestri, Anthony J. (1977). The conversion of methanol and other O-compounds to hydrocarbons over zeolite catalysts. *Journal of Catalysis, 47*(2), 249-259. doi: http://dx.doi.org/10.1016/0021-9517(77)90172-5

Channiwala, S. A., & Parikh, P. P. (2002). A unified correlation for estimating HHV of solid, liquid and gaseous fuels. *Fuel, 81*(8), 1051-1063. doi: http://dx.doi.org/10.1016/S0016-2361(01)00131-4

Chantal, P., Kaliaguine, S., Grandmaison, J. L., & Mahay, A. (1984). Production of hydrocarbons from aspen poplar pyrolytic oils over H-ZSM5. *Applied Catalysis, 10*(3), 317-332. doi: http://dx.doi.org/10.1016/01-80127(84)9834-66X

Chen, D., Zheng, Y., & Zhu, X. (2013). In-depth investigation on the pyrolysis kinetics of raw biomass. Part I: Kinetic analysis for the drying and devolatilization stages. *Bioresource Technology, 131*, 40-46. doi: 10.1016/j.biortech.2012.12.136

Chen, N.Y., Jr., T.F. Degnan, & Koenig, L.R. (1986). Liquid Fuels from Carbohydrates. *Chemtech, 16*, 506–511 .

Chen, NY, Degnan, TF, & Koenig, LR. (1986). Liquid fuel from carbohydrates. *Chemtech, 16*(8), 506-511 .

Cheng, Y. T., Jae, J., Shi, J., Fan, W., & Huber, G. W. (2012). Production of renewable aromatic compounds by catalytic fast pyrolysis of lignocellulosic biomass with bifunctional Ga/ZSM-5 catalysts. *Angew Chem Int Ed Engl, 51*(6), 1387-1390. doi: 10.1002/anie.201107390

Chiaramonti, David ,Oasmaa, Anja, & Solantausta, Yrjö. (2007). Power generation using fast pyrolysis liquids from biomass. *Renewable and Sustainable Energy Reviews, 11*(6), 1056-1086. doi: http://dx.doi.org/10.1016/j.rser.2005.07.008

Choi, Suek Joo, Park, Sung Hoon, Jeon, Jong-Ki, Lee, In Gu, Ryu, Changkook, Suh, Dong Jin, & Park, Young-Kwon. (2013). Catalytic conversion of particle board over microporous catalysts. *Renewable Energy, 54*, 105-110. doi: 10.1016/j.renene.2012.08.050

Coats, A. W., & Redfern, J. P. (1964). Kinetic Parameters from Thermogravimetric Data. *Nature, 201*(4914 .(

Csicsery, S.M. (1986). Catalysis by shape selective zeolites - science and technology. *Pure & Applied Chemistry 58*, 841-856 .

Czernik, S., & Bridgwater, A. V. (2004). Overview of applications of biomass fast pyrolysis oil. *Energy Fuels, 18*(2), 590–598 .

Damartzis, T., Vamvuka, D., Sfakiotakis, S., & Zabaniotou, A. (2011). Thermal degradation studies and kinetic modeling of cardoon (Cynara cardunculus) pyrolysis using thermogravimetric analysis) TGA). *Bioresource Technology, 102*(10), 6230-6238. doi: 10.1016/j.biortech.2011.02.060

Das, Piyali, Ganesh, Anuradda, & Wangikar, Pramod. (2004). Influence of pretreatment for deashing of sugarcane bagasse on pyrolysis products. *Biomass and Bioenergy, 27* ,(5) .457-445doi: 10.1016/j.biombioe.2004.04.002

Deng, Li, Fu, Yao, & Guo, Qing-Xiang. (2009). Upgraded Acidic Components of Bio-oil through Catalytic Ketonic Condensation. *Energy Fuels, 23*(1), 564–568 .

Do, Phuong T. M., Crossley, Steven, Santikunaporn ,Malee, & Resasco, Daniel E. (2007). Catalytic strategies for improving specific fuel properties *Catalysis: Volume 20* (Vol. 20, pp. 33-64): The Royal Society of Chemistry.

Dong, Chang-qing, Zhang, Zhi-fei, Lu, Qiang, & Yang, Yong-ping. (2012). Characteristics and mechanism study of analytical fast pyrolysis of poplar wood. *Energy Conversion and Management, 57*, 49-59. doi: 10.1016/j.enconman.2011.12.012

Dooley, Kerry M., Bhat, Arvind K., Plaisance, Craig P., & Roy, Amitava D. (2007). Ketones from acid condensation using supported CeO2 catalysts: Effect of additives. *Applied Catalysis A: General, 320*(0), 122-133. doi: http://dx.doi.org/10.1016/j.apcata.2007.01.021

Dutta, Saikat. (2012). Catalytic materials that improve selectivity of biomass conversions. *RSC Advances, 2*(33), 12575. doi: 10.1039/c2ra20922e

Edreis, Elbager M. A., Luo, Guangqian, Li, Aijun, Chao, Chen, Hu, Hongyun, Zhang, Sen, . . . Yao, Hong. (2013). CO2 Co-gasification of lower Sulphur Petroleum coke and Sugar Cane Bagasse via TG-FTIR Analysis Technique. *Bioresource Technology*. doi: 10.1016/j.biortech.2013.02.112

Elliott, D. C., Beckman, D., Bridgwater, A. V., Diebold, J. P., Gevert, S. B., & Solantausta, Y. (1991). Developments in direct thermochemical liquefaction of biomass: 1983-1990. *Energy Fuels, 5*(3), 399–410 .

Elliott, Douglas C. (2007). Historical Developments in Hydroprocessing Bio-oils. *Energy & Fuels, 21*(3), 1792-1815. doi: 10.1021/ef070044u

Eom, I. Y., Kim, J. Y., Kim, T. S., Lee, S. M., Choi, D., Choi, I. G., & Choi, J. W. (201 .(2 Effect of essential inorganic metals on primary thermal degradation of lignocellulosic biomass. *Bioresource Technology, 104*, 687-694. doi: 10.1016/j.biortech.2011.10.035

Eom, I. Y., Kim, J. Y., Lee, S. M., Cho, T. S., Yeo, H., & Choi, J. W. (2013). Comparison of pyrolytic products produced from inorganic-rich and demineralized rice straw (Oryza

sativa L.) by fluidized bed pyrolyzer for future biorefinery approach. *Bioresource Technology, 128*, 664-672. doi: 10.1016/j.biortech.2012.09.082

Eom, I. Y., Kim, K. H., Kim, J. Y., Lee, S. M., Yeo, H. M., Choi, I. G., & Choi, J. W. (2011). Characterization of primary thermal degradation features of lignocellulosic biomass after removal of inorganic metals by diverse solvents. *Bioresource Technology, 102*(3), 343 .3444-7doi: 10.1016/j.biortech.2010.10.056

Eom, In-Yong, Kim, Jae-Young, Lee, Soo-Min, Cho, Tae-Su, Choi, In-Gyu, & Choi, Joon-Weon. (2012). Study on the thermal decomposition features and kinetics of demineralized and inorganic metal-impregnated lignocellulosic biomass. *Journal of Industrial and Engineering Chemistry, 18*(6), 2069-2075. doi: 10.1016/j.jiec.2012.06.001

Escola, J. M., Aguado, J., Serrano, D. P., García, A., Peral, A., Briones, L., . . . Fernandez, E. (2011). Catalytic hydroreforming of the polyethylene thermal cracking oil over Ni supported hierarchical zeolites and mesostructured aluminosilicates. *Applied Catalysis B: Environmental, 106*(3-4), 405-415. doi: 10.1016/j.apcatb.2011.05.048

Fahmi, R., Bridgwater, A. V., Darvell, L. I., Jones, J .M., Yates, N., Thain, S., & Donnison, I. S. (2007). The effect of alkali metals on combustion and pyrolysis of Lolium and Festuca grasses, switchgrass and willow. *Fuel, 86*(10-11), 1560-1569. doi: 10.1016/j.fuel.2006.11.030

Fahmi, R., Bridgwater, A. V ,.Donnison, I., Yates, N., & Jones, J. M. (2008). The effect of lignin and inorganic species in biomass on pyrolysis oil yields, quality and stability. *Fuel, 87*(7), 1230-1240. doi: 10.1016/j.fuel.2007.07.026

Faix, O., Jakab, E., Till, F., & Székely, T. (198 .(8Study on low mass thermal degradation products of milled wood lignins by thermogravimetry-mass-spectrometry. *Wood Science and Technology, 22*(4), 323-334. doi: 10.1007/bf00353322

Fasina, Oladiran, & Littlefield, Brad. (2012). TG-FTIR analysis of pecan shells thermal decomposition. *Fuel Processing Technology, 102*, 61-66. doi: 10.1016/j.fuproc.2012.04.015

Fernandes, Eveline Ribas Kasper, Marangoni, Cintia, Souza, Ozair, & Sellin, Noeli. (2013). Thermochemical characterization of banana leaves as a potential energy source. *Energy Conversion and Management, 75*, 603-608. doi: 10.1016/j.enconman.2013.08.008

Fierro, V., Torne-Fernandez, V., Celzard, A., & Montane, D. (2007). Influence of the demineralisation on the chemical activation of Kraft lignin with orthophosphoric acid. *Journal of hazardous materials, 149*(1), 126-133. doi: 10.1016/j.jhazmat.2007.03.056

Fogassy, Gabriella, Thegarid, Nicolas, Schuurman, Yves, & Mirodatos, Claude. (2011). From biomass to bio-gasoline by FCC co-processing: effect of feed composition and catalyst structure on product quality. *Energy & Environmental Science, 4*(12), 5068-5076 .

Foster, Andrew J., Jae, Jungho, Cheng, Yu-Ting, Huber, George W., & Lobo, Raul F. (2012). Optimizing the aromatic yield and distribution from catalytic fast pyrolysis of biomass over ZSM-5. *Applied Catalysis A: General, 423–424*(0), 154-161. doi: http://dx.doi.org/10.1016/j.apcata.2012.02.030

French, Richard, & Czernik, Stefan. (2010). Catalytic pyrolysis of biomass for biofuels production. *Fuel Processing Technology, 91*(1), 25-32. doi: http://dx.doi.org/10.1016/j.fuproc.2009.08.011

Fu, P., Yi, W., Bai, X., Li, Z., Hu, S., & Xiang, J. (2011). Effect of temperature on gas composition and char structural features of pyrolyzed agricultural residues. *Bioresource Technology, 102*(17), 8211-8219. doi: 10.1016/j.biortech.2011.05.083

Fu, Peng, Hu, Song, Xiang, Jun, Li, Peisheng, Huang, Dan, Jiang, Long, . . . Zhang, Junying. (2010). FTIR study of pyrolysis products evolving from typical agricultural residues. *Journal of Analytical and Applied Pyrolysis, 88*(2), 117-123. doi: 10.1016/j.jaap.2010.03.004

Furimsky, Edward. (2000). Catalytic hydrodeoxygenation. *Applied Catalysis A: General, 199*(2), 147-190. doi: http://dx.doi.org/10.1016/S0926-860X(99)00555-4

G. Ertl ,H. Knözinger, Schüth, F., & Weitkamp, J. (2008). *Handbook of Heterogeneous Catalysis* (2nd ed.): Wiley-VCH.

Gaertner, Christian A., Serrano-Ruiz, Juan Carlos, Braden, Drew J., & Dumesic, James A. (2009). Catalytic coupling of carboxylic acids by ketonization as a processing step in biomass conversion. *Journal of Catalysis, 266*(1), 71-78. doi: http://dx.doi.org/10.1016/j.jcat.2009.05.015

Gaertner, Christian A., Serrano-Ruiz, Juan Carlos, Braden, Drew J., & Dumesic, James A. (2010). Ketonization Reactions of Carboxylic Acids and Esters over Ceria−Zirconia as Biomass-Upgrading Processes. *Industrial & Engineering Chemistry Research, 49*(13), 6027-6033. doi: 10.1021/ie1004338

Gangadharan, Anirudhan, Shen, Min, Sooknoi, Tawan, Resasco, Daniel E., & Mallinson, Richard G. (2010). Condensation reactions of propanal over CexZr1−xO2 mixed oxide catalysts. *Applied Catalysis A: General, 385*(1-2), 80-91. doi: 10.1016/j.apcata.2010.06.048

Gärtner, Christian A, Serrano-Ruiz, Juan Carlos, Braden, Drew J, & Dumesic, James A . .(2009)Catalytic Upgrading of Bio-Oils by Ketonization. *ChemSusChem, 2*(12), 1121-1124. doi: 10.1002/cssc.200900178

Gayubo, A. G., Valle, B., Aguayo, A. T., Olazar, M., & Bilbao, J. (2010). Pyrolytic lignin removal for the valorization of biomass pyrolysis crude bio-oil by catalytic transformation. *Journal of Chemical Technology & Biotechnology, 85*(1), 132-144. doi: 10.1002/jctb.2289

Gayubo, Ana G., Aguayo, Andrés T., Atutxa, Alaitz, Aguado, Roberto, & Bilbao, Javier. (2004). Transformation of Oxygenate Components of Biomass Pyrolysis Oil on a

HZSM-5 Zeolite. I. Alcohols and Phenols. *Industrial & Engineering Chemistry Research, 43*(11), 2610-2618. doi: 10.1021/ie030791o

Gayubo, Ana G., Aguayo, Andrés T., Atutxa, Alaitz, Aguado, Roberto, Olazar, Martin & , Bilbao, Javier. (2004). Transformation of Oxygenate Components of Biomass Pyrolysis Oil on a HZSM-5 Zeolite. II. Aldehydes, Ketones, and Acids. *Industrial & Engineering Chemistry Research, 43*(11), 2619-2626. doi: 10.1021/ie030792g

Gayubo, Ana G., Aguayo ,Andrés T., Atutxa, Alaitz, Prieto, Rubén, & Bilbao, Javier. (2004). Deactivation of a HZSM-5 Zeolite Catalyst in the Transformation of the Aqueous Fraction of Biomass Pyrolysis Oil into Hydrocarbons. *Energy & Fuels, 18*(6), 1640-1647. doi: 10.1021/ef040027u

Gayubo, Ana G., Aguayo, Andrés T., Atutxa, Alaitz, Valle, Beatriz, & Bilbao, Javier. (2005). Undesired components in the transformation of biomass pyrolysis oil into hydrocarbons on an HZSM-5 zeolite catalyst. *Journal of Chemical Technology & Biotechnology, 80*(11), 1244-1251. doi: 10.1002/jctb.1316

Gayubo, Ana G., Valle, Beatriz, Aguayo, Andrés T., Olazar, Martín, & Bilbao, Javier. (2009). Attenuation of Catalyst Deactivation by Cofeeding Methanol for Enhancing the Valorisation of Crude Bio-oil. *Energy & Fuels, 23*(8), 4129-4136. doi: 10.1021/ef900301y

Gliński, M., Szymański, W., & Łomot, D. (2005). Catalytic ketonization over oxide catalysts: X. Transformations of various alkyl heptanoates. *Applied Catalysis A: General, 281*(1–2), 107-113. doi: http://dx.doi.org/10.1016/j.apcata.2004.11.018

González-Borja, Miguel Ángel, & Resasco, Daniel E. (2011). Anisole and Guaiacol Hydrodeoxygenation over Monolithic Pt–Sn Catalysts. *Energy & Fuels, 25*(9), 4155-4162. doi: 10.1021/ef200728r

González, María Dolores ,Cesteros, Yolanda, & Salagre, Pilar. (2011). Comparison of dealumination of zeolites beta, mordenite and ZSM-5 by treatment with acid under microwave irradiation. *Microporous and Mesoporous Materials, 144*(1-3), 162-170. doi: 10.1016/j.micromeso.2011.04.009

Graça, I., Comparot, J. D., Laforge, S., Magnoux, P., Lopes, J. M., Ribeiro, M. F., & Ribeiro, F. Ramôa. (2009). Effect of phenol addition on the performances of H–Y zeolite during methylcyclohexane transformation. *Applied Catalysis A: General, 353*(1 ,(.129-123doi: http://dx.doi.org/10.1016/j.apcata.2008.10.032

Graça, I., Lopes, J. M., Ribeiro, M. F., Badawi, M., Laforge, S., Magnoux, P., & Ramôa Ribeiro, F. (2012a). n-Heptane cracking over mixtures of HY and HZSM-5 zeolites: Influence of the presence of phenol. *Fuel, 94*(0), 571-577. doi: http://dx.doi.org/10.1016/j.fuel.2011.11.033

Graça, I., Lopes, J. M., Ribeiro, M. F., Badawi, M., Laforge, S., Magnoux, P., & Ramôa Ribeiro, F. (2012b). n-Heptane cracking over mixtures of HY and HZSM-5 zeolites: Influence of the presence of phenol. *Fuel, 94*, 571-577. doi: 10.1016/j.fuel.2011.11.033

Graça, Inês, Comparot, Jean-Dominique, Laforge, Sébastien, Magnoux, Patrick, Lopes, José Manuel, Ribeiro, Maria Filipa, & Ramôa Ribeiro, Fernando. (2009). Influence of Phenol Addition on the H-ZSM-5 Zeolite Catalytic Properties during Methylcyclohexane Transformation. *Energy & Fuels, 23*(9), 4224-4230. doi: 10.1021/ef9003472

Groen, Johan C., Jansen, Jacobus C., Moulijn, Jacob A., & Pérez-Ramírez, Javier. (2004). Optimal Aluminum-Assisted Mesoporosity Development in MFI Zeolites by Desilication. *The Journal of Physical Chemistry B, 108*(35), 13062-13065. doi: 10.1021/jp047194f

GW, Huber, S, Iborra, & A, Corma. (2006). Synthesis of transportation fuels from biomass: chemistry, catalysts, and Engineering. *Chem Rev. , 106*(9 .(

Habbache, N., Alane, N., Djerad, S., & Tifouti, L. (2009). Leaching of copper oxide with different acid solutions. *Chemical Engineering Journal, 152*(2-3), 503-508. doi: 10.1016/j.cej.2009.05.020

Haykiri-Acma, H., Yaman, S., & Kucukbayrak, S. (2011). Burning characteristics of chemically isolated biomass ingredients. *Energy Conversion and Management, 52*(1), 746-751. doi: 10.1016/j.enconman.2010.07.054

He, Fang, Yi, Weiming, & Bai, Xueyuan. (2006). Investigation on caloric requirement of biomass pyrolysis using TG–DSC analyzer. *Energy Conversion and Management, 47*(15-16), 2461-2469. doi: 10.1016/j.enconman.2005.11.011

Hendren, Travis S., & Dooley, Kerry M. (2003). Kinetics of catalyzed acid/acid and acid/aldehyde condensation reactions to non-symmetric ketones. *Catalysis Today, 85*(2–4), 333-351. doi: http://dx.doi.org/10.1016/S0920-5861(03)00399-7

Heo, H. S., Kim, S. G., Jeong, K. E., Jeon, J. K., Park, S. H., Kim, J. M., . . . Park, Y. K. (2011). Catalytic upgrading of oil fractions separated from food waste leachate. *Bioresource Technology, 102*(4), 3952-3957. doi: 10.1016/j.biortech.2010.11.099

Hicks, Jason C. (2011a). Advances in C-O Bond Transformations in Lignin- Derived Compounds for Biofuels Production. *J. Phys. Chem. Lett., 2*(18), 2280–2287. doi: 10.1021/jz2007885

Hicks, Jason C. (2011b). Advances in C–O Bond Transformations in Lignin-Derived Compounds for Biofuels Production. *The Journal of Physical Chemistry Letters*, 2280-2287. doi: 10.1021/jz2007885

Hoang, Trung Q., Zhu, Xinli, Lobban, Lance L., Resasco, Daniel E., & Mallinson, Richard G. (2010). Effects of HZSM-5 crystallite size on stability and alkyl-aromatics product distribution from conversion of propanal. *Catalysis Communications, 11*-977 ,(11) .981doi: 10.1016/j.catcom.2010.04.014

Hoang, Trung Q., Zhu, Xinli, Sooknoi, Tawan, Resasco, Daniel E., & Mallinson, Richard G. (2010). A comparison of the reactivities of propanal and propylene on HZSM-5. *Journal of Catalysis, 271*(2), 201-208. doi: 10.1016/j.jcat.2010.01.017

Horne, Patrick A., Nugranad, Nittaya, & Williams, Paul T. (1995). Catalytic coprocessing of biomass-derived pyrolysis vapours and methanol. *Journal of Analytical and Applied Pyrolysis, 34*(1), 87-108. doi: http://dx.doi.org/14-00877(94)2370-0165/0.1016

Horne, Patrick A., & Williams, Paul T. (1995). The effect of zeolite ZSM-5 catalyst deactivation during the upgrading of biomass-derived pyrolysis vapours. *Journal of Analytical and Applied Pyrolysis, 34*(1), 65-85. doi: http//:dx.doi.org/10.1016/0165-2370(94)00875-2

Hua, Z. L., Zhou, J., & Shi, J. L. (2011). Recent advances in hierarchically structured zeolites: synthesis and material performances. *Chem Commun (Camb), 47*(38), 10536-10547. doi: 10.1039/c1cc10261c

Huang, Y. F., Chiueh, P. T., Kuan, W. H., & Lo, S. L. (2013). Pyrolysis kinetics of biomass from product information. *Applied Energy, 110*, 1-8. doi: 10.1016/j.apenergy.2013.04.034

Huang, Y. F., Kuan, W. H., Chiueh, P. T., & Lo, S. L. (2011a). Pyrolysis of biomass by thermal analysis-mass spectrometry (TA-MS). *Bioresource Technology, 102*(3), 3527-3534. doi: 10.1016/j.biortech.2010.11.049

Huang, Y. F., Kuan, W. H., Chiueh, P. T., & Lo, S. L. (2011b). A sequential method to analyze the kinetics of biomass pyrolysis. *Bioresource Technology, 102*(19), 9241-9246. doi: 10.1016/j.biortech.2011.07.015

Huang, Yao-Bing, Yang, Zhen, Dai, Jian-Jun, Guo, Qing-Xiang, & Fu, Yao. (2012). Production of high quality fuels from lignocellulose-derived chemicals: a convenient C–C bond formation of furfural, 5-methylfurfural and aromatic aldehyde. *RSC Advances, 2*(30), 11211. doi: 10.1039/c2ra22008c

Huber, G.W., Cheng, Y.-t., T. Carlson, T.Vispute, & J. Jae, G. Tompsett. (2009). 2009/0227823 A1. U. S. patent.

Huber, George W., Iborra, Sara, & Corma, Avelino. (2006). Synthesis of Transportation Fuels from Biomass: Chemistry, Catalysts, and Engineering. *Chemical Reviews, 106*(9), 4044-4098. doi: 10.1021/cr068360d

Ibáñez, María, Valle, Beatriz, Bilbao, Javier, Gayubo, Ana G., & Castaño, Pedro. (20 .(12 Effect of operating conditions on the coke nature and HZSM-5 catalysts deactivation in the transformation of crude bio-oil into hydrocarbons. *Catalysis Today, 195*(1), 106-113. doi: http://dx.doi.org/10.1016/j.cattod.2012.04.030

Idris, S. S., Abd Rahman, N., Ismail, K., Alias, A. B., Abd Rashid, Z., & Aris, M. J. (2010). Investigation on thermochemical behaviour of low rank Malaysian coal, oil palm biomass and their blends during pyrolysis via thermogravimetric analysis (TGA). *Bioresource Technology* .4592-4584 ,(12)101 ,doi: 10.1016/j.biortech.2010.01.059

Ilias, Samia, & Bhan, Aditya. (2012). Tuning the selectivity of methanol-to-hydrocarbons conversion on H-ZSM-5 by co-processing olefin or aromatic compounds. *Journal of Catalysis, 290*, 186-192. doi/10.1016 :j.jcat.2012.03.016

Iliopoulou, E. F., Stefanidis, S. D., Kalogiannis, K. G., Delimitis, A., Lappas, A. A., & Triantafyllidis, K. S. (2012). Catalytic upgrading of biomass pyrolysis vapors using transition metal-modified ZSM-5 zeolite. *Applied Catalysis B: Environmental, 127*, 281-290. doi: 10.1016/j.apcatb.2012.08.030

Imran, Ali, Bramer, Eddy A., Seshan, Kulathuiyer, & Brem, Gerrit. (2014). High quality bio-oil from catalytic flash pyrolysis of lignocellulosic biomass over alumina-supported sodium carbonate. *Fuel Processing Technology, 127*, 72-79. doi: 10.1016/j.fuproc.2014.06.011

Ingram, Leonard, Mohan, Dinesh, Bricka, Mark, Steele, Philip, Strobel, David, Crocker, David, . . . Charles U. Pittman , Jr. (2008). Pyrolysis of wood and bark in an auger reactor: Physical properties and chemical analysis of the produced bio-oils. *Energy Fuels, 22*(1), 614–625. doi: 10.1021/ef700335k

Isahak, Wan Nor Roslam Wan, Hisham, Mohamed W. M., Yarmo, Mohd Ambar, & Yun Hin, Taufiq-yap. (2012). A review on bio-oil production from biomass by using pyrolysis method. *Renewable and Sustainable Energy Reviews, 16*(8), 5910-5923. doi: 10.1016/j.rser.2012.05.039

Jae, Jungho, Tompsett, Geoffrey A., Foster, Andrew J., Hammond, Karl D., Auerbach, Scott M., Lobo, Raul F., & Huber, George W. (2011). Investigation into the shape selectivity of zeolite catalysts for biomass conversion. *Journal of Catalysis, 279*(2), 257-268. doi: 10.1016/j.jcat.2011.01.019

Jae, Jungho, Tompsett, Geoffrey A., Lin, Yu-Chuan, Carlson, Torren R., Shen ,Jiacheng, Zhang, Taiying, . . . Huber, George W. (2010). Depolymerization of lignocellulosic biomass to fuel precursors: maximizing carbon efficiency by combining hydrolysis with pyrolysis. *Energy & Environmental Science, 3*(3), 358-365. doi: 10.1039/b924621p

Jiang, L., Hu, S., Sun, L. S., Su, S., Xu, K., He, L. M., & Xiang, J. (2013). Influence of different demineralization treatments on physicochemical structure and thermal degradation of biomass. *Bioresource Technology, 146*, 254-260. doi: 10.1016/j.biortech.2013.07.063

Jørgensen, Henning, Kristensen, Jan Bach, & Felby, Claus. (2007). Enzymatic conversion of lignocellulose into fermentable sugars: challenges and opportunities. *Biofuels, Bioproducts and Biorefining, 1*(2), 119-134. doi: 10.1002/bbb.4

Junming, Xu, Jianchun, Jiang, Yunjuan, Sun, & Yanju, Lu. (2008). Bio-oil upgrading by means of ethyl ester production in reactive distillation to remove water and to improve storage and fuel characteristics. *Biomass and Bioenergy, 32*(11), 1056-1061. doi: http//:dx.doi.org/10.1016/j.biombioe.2008.02.002

Kazansky, V. B., Subbotina, I. R., van Santen, R. A., & Hensen, E. J. M. (2004). DRIFTS study of the chemical state of modifying gallium ions in reduced Ga/ZSM-5 prepared by impregnationI. Observation of gallium hydrides and application of CO adsorption as a molecular probe for reduced gallium ions. *Journal of Catalysis, 227*(2), 263-269. doi: 10.1016/j.jcat.2004.07.021

Kim, J. (2015). Production, separation and applications of phenolic-rich bio-oil - A review. *Bioresour Technol, 178C*, 90-98. doi: 10.1016/j.biortech.2014.08.121

Kim, Jeongnam, Choi, Minkee, & Ryoo, Ryong. (2010). Effect of mesoporosity against the deactivation of MFI zeolite catalyst during the methanol-to-hydrocarbon conversion process. *Journal of Catalysis, 269*(1), 219-228. doi: 10.1016/j.jcat.2009.11.009

Kim, Tae-Seung, Kim, Jae-Young, Kim, Kwang-Ho, Lee, Soomin, Choi, Donha, Choi, In-Gyu, & Choi, Joon Weon. (2012). The effect of storage duration on bio-oil properties. *Journal of Analytical and Applied Pyrolysis, 95*, 118-125. doi: 10.1016/j.jaap.2012.01.015

Kim, Tae-Seung, Oh, Shinyoung, Kim, Jae-Young, Choi, In-Gyu, & Choi, Joon Weon. (2014). Study on the hydrodeoxygenative upgrading of crude bio-oil produced from woody biomass by fast pyrolysis. *Energy, 68*, 437-443. doi: 10.1016/j.energy.2014.03.004

Klimkiewicz, Roman, Fabisz, Ernest, Morawski, Ireneusz, Grabowska, Hanna, & Syper, Ludwik. (2001). Ketonization of long chain esters from transesterification of technical waste fats. *Journal of Chemical Technology & Biotechnology, 76*(1), 35-38. doi: 10.1002/1097-4660(200101)76:1<35::aid-jctb328>3.0.co;2-t

Kuhad, RameshChander, Singh, Ajay, & Eriksson, Karl-ErikL. (1997). Microorganisms and enzymes involved in the degradation of plant fiber cell walls. In K. E. L. Eriksson, W. Babel, H. W. Blanch, C. L. Cooney, S. O. Enfors, A. Fiechter, A. M. Klibanov, B. Mattiasson, S. B. Primrose, H. J. Rehm, P. L. Rogers, H. Sahm, K. Schügerl, G. T. Tsao, K. Venkat, J. Villadsen, U. Stockar & C. Wandrey (Eds .(*Biotechnology in the Pulp and Paper Industry* (Vol. 57, pp. 45-125): Springer Berlin Heidelberg.

Kumar, Parveen, Barrett, Diane M., Delwiche, Michael J., & Stroeve, Pieter. (2009). Methods for Pretreatment of Lignocellulosic Biomass for Efficient Hydrolysis and Biofuel Production. *Industrial & Engineering Chemistry Research, 48*(8), 3713-3729. doi: 10.1021/ie801542g

Kwak, B. S., Sachtler, W. M. H., & Haag, W. O. (1994). Catalytic Conversion of Propane to Aromatics: Effects of Adding Ga and/or Pt to HZSM-5 .*Journal of Catalysis, 149*(2), 465-473. doi: http://dx.doi.org/10.1006/jcat.1994.1313

Lappas, A. A., Bezergianni, S., & Vasalos, I. A. (2009). Production of biofuels via co-processing in conventional refining processes. *Catalysis Today, 145*(1–2), 55-62. doi: http://dx.doi.org/10.1016/j.cattod.2008.07.001

Lee Hw Fau - Jeon, Jong-Ki, Jeon Jk Fau - Park, Sung Hoon, Park Sh Fau - Jeong, Kwang-Eun, Jeong Ke Fau - Chae, Ho-Jeong, Chae Hj Fau - Park, Young-Kwon, & YK, Park. (2011). - Catalytic pyrolysis of Laminaria japonica over nanoporous catalysts using Py-GC/MS. *Nanoscale Res Lett, 6*(1), 6-500 .

Li, Yuning, Liu, Shenglin, Zhang, Zekai, Xie, Sujuan, Zhu, Xiangxue, & Xu, Longya. (2008). Aromatization and isomerization of 1-hexene over alkali-treated HZSM-5 zeolites:

Improved reaction stability. *Applied Catalysis A: General, 338*(1-2), 100-113. doi: 10.1016/j.apcata.2007.12.026

Lim, W. S., Kim, J. Y., Kim, H. Y., Choi, J. W., Choi, I. G., & Lee, J. W. (2013). Structural properties of pretreated biomass from different acid pretreatments and their effects on simultaneous saccharification and ethanol fermentation. *Bioresource Technology, 139*, 214-219. doi: 10.1016/j.biortech.2013.04.009

Lim, Xiao Y., & Andrésen, John M. (2011). Pyro-catalytic deoxgenated bio-oil from palm oil empty fruit bunch and fronds with boric oxide in a fixed-bed reactor. *Fuel Processing Technology, 92*(9), 1796-1804. doi: http://dx.doi.org/10.1016/j.fuproc.2011.04.033

Lin, Yuyu, Zhang, Chu, Zhang, Mingchuan, & Zhang, Jian. (2010). Deoxygenation of Bio-oil during Pyrolysis of Biomass in the Presence of CaO in a Fluidized-Bed Reactor. *Energy & Fuels, 24*(10), 5686-5695. doi: 10.1021/ef1009605

Lissianski, V.V., & R.G. Rizeq, S.P. Singh. (2012). 2012/ 0029252 A1. U. S. patent.

Liu, Wenwu, Hu, Changwei, Yang, Yu, Tong, Dongmei, Li, Guiying, & Zhu, Liangfang. (2010). Influence of ZSM-5 zeolite on the pyrolytic intermediates from the co-pyrolysis of pubescens and LDPE. *Energy Conversion and Management, 51*(5), 1025-1032. doi: http://dx.doi.org/10.1016/j.enconman.2009.12.005

Liu, Wu-Jun, Zhang, Xue-Song, Qv, Yan-Chao, Jiang, Hong, & Yu, Han-Qing. (2012). Bio-oil upgrading at ambient pressure and temperature using zero valent metals. *Green Chemistry, 14*(8), 2226-2233 .

Liu, Xinliang, & Bi, Xiaotao T. (2 .(011Removal of inorganic constituents from pine barks and switchgrass. *Fuel Processing Technology, 92*(7), 1273-1279. doi: 10.1016/j.fuproc.2011.01.016

Lu, Ke-Miao, Lee, Wen-Jhy, Chen, Wei-Hsin, & Lin, Ta-Chang. (2013). Thermogravimetric analysis and kinetics of co-pyrolysis of raw/torrefied wood and coal blends. *Applied Energy, 105*, 57-65. doi: 10.1016/j.apenergy.2012.12.050

Lu, Qiang, Li, Wen-Zhi, & Zhu, Xi-Feng. (2009). Overview of fuel properties of biomass fast pyrolysis oils. *Energy Conversion and Management, 50*(5), 1376-1383. doi: http://dx.doi.org/10.1016/j.enconman.2009.01.001

Lu, Qiang, Tang, Zhe, Zhang, Ying, & Zhu, Xi-feng. (2010). Catalytic Upgrading of Biomass Fast Pyrolysis Vapors with Pd/SBA-15 Catalysts. *Industrial & Engineering Chemistry Research, 49*(6), 2573-2580. doi: 10.1021/ie901198s

Lu, Qiang, Zhang, Ying, Tang, Zhe, Li, Wen-zhi, & Zhu, Xi-feng. (2010). Catalytic upgrading of biomass fast pyrolysis vapors with titania and zirconia/titania based catalysts. *Fuel, 89*(8), 2096-2103. doi: http://dx.doi.org/10.1016/j.fuel.2010.02.030

Magdziarz, Aneta, & Wilk, Małgorzata. (2013). Thermogravimetric study of biomass, sewage sludge and coal combustion. *Energy Conversion and Management, 75*, 425-430. doi: 10.1016/j.enconman.2013.06.016

Mante ,OfeiDaku, & Agblevor, FosterA. (2011). Catalytic conversion of biomass to bio-syncrude oil. *Biomass Conversion and Biorefinery, 1*(4), 203-215. doi: 10.1007/s13399-011-0020-4

Mayer, Zsuzsa A., Apfelbacher, Andreas, & Hornung, Andreas. (2012a). Effect of sample preparation on the thermal degradation of metal-added biomass. *Journal of Analytical and Applied Pyrolysis, 94*, 170-176. doi: 10.1016/j.jaap.2011.12.008

Mayer, Zsuzsa A., Apfelbacher, Andreas, & Hornung, Andreas. (2012b). Effect of sample preparation on the thermal degradation of metal-added biomass. *Journal of Analytical and Applied Pyrolysis, 94*(0), 170-176. doi: http://dx.doi.org/10.1016/j.jaap.2011.12.008

Melligan, F., Hayes, M. H. B., Kwapinski, W., & Leahy, J. J. (2012). Hydro-Pyrolysis of Biomass and Online Catalytic Vapor Upgrading with Ni-ZSM-5 and Ni-MCM-41. *Energy & Fuels, 26*(10), 6080-6090. doi: 10.1021/ef301244h

Melligan, F., Hayes, M. H. B., Kwapinski, W., & Leahy, J. J. (2013). A study of hydrogen pressure during hydropyrolysis of Miscanthus x giganteus and online catalytic vapour upgrading with Ni on ZSM-5. *Journal of Analytical and Applied Pyrolysis, 103*, 369-377. doi: 10.1016/j.jaap.2013.01.005

Meng, Xianghai, Xu, Chunming, & Gao, Jinsen. (2007). Coking behavior and catalyst deactivation for catalytic pyrolysis of heavy oil. *Fuel, 86*(12-13), 1720-1726. doi: 10.1016/j.fuel.2006.12.023

Mentzel, Uffe V., & Holm, Martin S. (2011). Utilization of biomass: Conversion of model compounds to hydrocarbons over zeolite H-ZSM-5. *Applied Catalysis A: General, 396*(1-2), 59-67. doi: 10.1016/j.apcata.2011.01.040

Mercader, F. de Miguel, Groeneveld, M. J., Kersten, S. R. A., Venderbosch, R. H., & Hogendoorn, J. A. (2010). Pyrolysis oil upgrading by high pressure thermal treatment. *Fuel, 89*(10), 2829 .2837-doi: http://dx.doi.org/10.1016/j.fuel.2010.01.026

Mihalcik, David J., Boateng, Akwasi A., Mullen, Charles A., & Goldberg, Neil M. (2011). Packed-Bed Catalytic Cracking of Oak-Derived Pyrolytic Vapors. *Industrial & Engineering Chemistry Research, 50* .13312-13304 ,(23)doi: 10.1021/ie201831e

Mihalcik, David J., Mullen, Charles A., & Boateng, Akwasi A. (2011). Screening acidic zeolites for catalytic fast pyrolysis of biomass and its components. *Journal of Analytical and Applied Pyrolysis, 92*(1), 224-232 .doi: http://dx.doi.org/10.1016/j.jaap.2011.06.001

Mohammed, M. A. A., Salmiaton, A., Wan Azlina, W. A. K. G., Mohammad Amran, M. S., Fakhru'l-Razi, A., & Taufiq-Yap, Y. H. (2011). Hydrogen rich gas from oil palm

biomass as a potential source of renewable energy in Malaysia. *Renewable and Sustainable Energy Reviews, 15*(2), 1258-1270. doi: 10.1016/j.rser.2010.10.003

Mohan, Dinesh, Charles U. Pittman, Jr., & Steele, Philip H. (2006

.(Pyrolysis of Wood/Biomass for Bio-oil: A Critical Review. *Energy Fuels*–848 ,(3)20 , .889doi: 10.1021/ef0502397

Mohan, Dinesh, Pittman, Charles U., & Steele, Philip H. (2006). Pyrolysis of Wood/Biomass for Bio-oil: A Critical Review. *Energy & Fuels, 20*(3), 848-889. doi: 10.1021/ef0502397

Moller, K., & Bein, T. (2013). Mesoporosity--a new dimension for zeolites. *Chem Soc Rev, 42*(9), 3689-3707. doi: 10.1039/c3cs35488a

Mortensen, P. M., Grunwaldt, J. D., Jensen, P. A., Knudsen, K. G., & Jensen, A. D. (2011). A review of catalytic upgrading of bio-oil to engine fuels. *Applied Catalysis A: General, 407*(1–2), 1-19. doi: http://dx.doi.org/10.1016/j.apcata.2011.08.046

Mosier, N., Wyman, C., Dale, B., Elander, R., Lee, Y. Y., Holtzapple, M., & Ladisch, M. (2005). Features of promising technologies for pretreatment of lignocellulosic biomass. *Bioresource Technology, 96*(6), 673-686. doi: 10.1016/j.biortech.2004.06.025

Mullen, Charles A., & Boateng, Akwasi A. (2008). Chemical Composition of Bio-oils Produced by Fast Pyrolysis of Two Energy Crops†. *Energy & Fuels, 22*(3), 2104-2109. doi/10.1021 :ef700776w

Mullen, Charles A., & Boateng, Akwasi A. (2010). Catalytic pyrolysis-GC/MS of lignin from several sources. *Fuel Processing Technology, 91*(11), 1446-1458. doi: http://dx.doi.org/10.1016/j.fuproc.2010.05.022

Mullen, Charles A., Boateng, Akwasi A., Hicks, Kevin B., Goldberg, Neil M., & Moreau, Robert A. (2009). Analysis and Comparison of Bio-Oil Produced by Fast Pyrolysis from Three Barley Biomass/Byproduct Streams. *Energy & Fuels, 24*(1), 699-706. doi: 10.1021/ef900912s

Mullen, Charles A ,.Boateng, Akwasi A., Mihalcik, David J., & Goldberg, Neil M. (2011). Catalytic Fast Pyrolysis of White Oak Wood in a Bubbling Fluidized Bed. *Energy & Fuels, 25*(11), 5444-5451. doi: 10.1021/ef201286z

Müller-Hagedorn, M., Bockhorn, H., Krebs, L., & Müller ,U. (2003). A comparative kinetic study on the pyrolysis of three different wood species. *Journal of Analytical and Applied Pyrolysis, 68-69*, 231-249. doi: 10.1016/s0165-2370(03)00065-2

Na, Kyungsu, Choi, Minkee, & Ryoo, Ryong. (2013). Recent advances in the synthesis of hierarchically nanoporous zeolites. *Microporous and Mesoporous Materials, 166*, 3-19. doi: 10.1016/j.micromeso.2012.03.054

NABC, Catalytic Fast Pyrolysis: Pyrolysis Vapors Upgrading. (2011). from http://www.nabcprojects.org/pdfs/pyrolysis_vapors_upgrading.pdf.

Nguyen, T. S., Zabeti, M., Lefferts, L., Brem, G., & Seshan, K. (2013a). Catalytic upgrading of biomass pyrolysis vapours using faujasite zeolite catalysts. *Biomass and Bioenergy, 48*, 100-110. doi: 10.1016/j.biombioe.2012.10.024

Nguyen, T. S., Zabeti, M., Lefferts, L., Brem, G., & Seshan, K. (2013b). Conversion of lignocellulosic biomass to green fuel oil over sodium based catalysts. *Bioresour Technol, 142*, 353-360. doi: 10.1016/j.biortech.2013.05.023

Ni, Youming, Sun, Aiming, Wu, Xiaoling, Hai, Guoliang, Hu, Jianglin, Li, Tao, & Li, Guangxing. (2011). The preparation of nano-sized H[Zn, Al]ZSM-5 zeolite and its application in the aromatization of methanol. *Microporous and Mesoporous Materials, 143*(2-3), 435-442. doi: 10.1016/j.micromeso.2011.03.029

Nowakowski, D., Jones, J., Brydson, R., & Ross, A. (2007). Potassium catalysis in the pyrolysis behaviour of short rotation willow coppice. *Fuel, 86*(15), 2389-2402. doi: 10.1016/j.fuel.2007.01.026

Oasmaa, Anja, Elliott, Douglas C., & Korhonen, Jaana. (2010). Acidity of Biomass Fast Pyrolysis Bio-oils. *Energy & Fuels, 24*(12), 6548-6554. doi: 10.1021/ef100935r

Ogura, Masaru, Shinomiya, Shin-ya, Tateno, Junko, Nara, Yasuto, Nomura, Mikihiro, Kikuchi, Eiichi, & Matsukata, Masahiko. (2001). Alkali-treatment technique — new method for modification of structural and acid-catalytic properties of ZSM-5 zeolites. *Applied Catalysis A: General, 219*(1–2), 33-43. doi: http://dx.doi.org/10.1016/S0926-860X(01)00645-7

Önal, Eylem P., Uzun, Başak Burcu, & Pütün, Ayşe Eren. (2011). Steam pyrolysis of an industrial waste for bio-oil production. *Fuel Processing Technology, 92*(5), 879-885. doi: http://dx.doi.org/10.1016/j.fuproc.2010.12.006

Otero, M., Sanchez, M. E., & Gomez, X. (2011). Co-firing of coal and manure biomass: a TG-MS approach. *Bioresource Technology, 102*(17), 8304-8309. doi: 10.1016/j.biortech.2011.06.040

Park, H. J., Dong, J. I., Jeon, J. K., Yoo, K. S., Yim, J. S., Sohn, J. M., & Park, Y. K. (2007). Conversion of the Pyrolytic Vapor of Radiata Pine over Zeolites. *Journal of Industrial and Engineering Chemistry, 13*(2), 182-189 .

Park, Hyun Ju, Dong, Jong-In, Jeon, Jong-Ki, Yoo, Kyung-Seun, Yim, Jin-Heong, Sohn, Jung Min, & Park, Young-Kwon. (2007). Conversion of the Pyrolytic Vapor of Radiata Pine over Zeolites. *Journal of Industrial and Engineering Chemistry, 13*(2), 182-189 .

Park, Hyun Ju, Heo, Hyeon Su, Jeon, Jong-Ki, Kim, Jeongnam, Ryoo, Ryong, Jeong, Kwang-Eun, & Park, Young-Kwon. (2010a). Highly valuable chemicals production from catalytic upgrading of radiata pine sawdust-derived pyrolytic vapors over

mesoporous MFI zeolites. *Applied Catalysis B: Environmental, 95*(3-4), 365-373. doi: 10.1016/j.apcatb.2010.01.015

Park, Hyun Ju, Heo, Hyeon Su, Jeon, Jong-Ki, Kim, Jeongnam, Ryoo, Ryong, Jeong, Kwang-Eun, & Park, Young-Kwon. (2010b). Highly valuable chemicals production from catalytic upgrading of radiata pine sawdust-derived pyrolytic vapors over mesoporous MFI zeolites. *Applied Catalysis B: Environmental, 95*(3–4), 365-373. doi: http://dx.doi.org/10.1016/j.apcatb.2010.01.015

Park, Hyun Ju, Park, Kyu-Hong, Jeon, Jong-Ki, Kim, Jeongnam, Ryoo, Ryong, Jeong, Kwang-Eun, . . . Park, Young-Kwon. (2012a). Production of phenolics and aromatics by pyrolysis of miscanthus. *Fuel, 97*(0), 379-384. doi: http://dx.doi.org/10.1016/j.fuel.2012.01.075

Park, Hyun Ju, Park, Kyu-Hong, Jeon, Jong-Ki, Kim, Jeongnam, Ryoo, Ryong, Jeong, Kwang-Eun, . . . Park, Young-Kwon. (2012b). Production of phenolics and aromatics by pyrolysis of miscanthus. *Fuel, 97*, 379-384. doi: 10.1016/j.fuel.2012.01.075

Park, HyunJu, Jeon, Jong-Ki, Suh, DongJin, Suh, Young-Woong, Heo, HyeonSu, & Park, Young-Kwon. (2011). Catalytic Vapor Cracking for Improvement of Bio-Oil Quality. *Catalysis Surveys from Asia, 15*(3), 161-180. doi: 10.1007/s107-9119-011-563

Parshetti, G. K., Kent Hoekman, S., & Balasubramanian, R. (2013). Chemical, structural and combustion characteristics of carbonaceous products obtained by hydrothermal carbonization of palm empty fruit bunches. *Bioresource Technology, 135* .689-683 , doi: 10.1016/j.biortech.2012.09.042

Payormhorm, J., Kangvansaichol, K., Reubroycharoen, P., Kuchonthara, P., & Hinchiranan, N. (2013). Pt/Al(2)O(3)-catalytic deoxygenation for upgrading of Leucaena leucocephala-pyrolysis oil. *Bioresour Technol, 1* .135-128 ,39doi: 10.1016/j.biortech.2013.04.023

Peralta, Maria A., Sooknoi, Tawan, Danuthai, Tanate, & Resasco, Daniel E. (2009). Deoxygenation of benzaldehyde over CsNaX zeolites. *Journal of Molecular Catalysis A: Chemical, 312*(1-2), 78-86. doi: 10.1016/j.molcata.2009.07.008

Perego, Carlo, & Ingallina, Patrizia. (2002). Recent advances in the industrial alkylation of aromatics: new catalysts and new processes. *Catalysis Today, 73*(1–2), 3-22. doi: http://dx.doi.org/10.1016/S0920-5861(01)00511-9

Pérez, J ,.Muñoz-Dorado, J., de la Rubia, T., & Martínez, J. (2002). Biodegradation and biological treatments of cellulose, hemicellulose and lignin: an overview. *International microbiology : the official journal of the Spanish Society for Microbiology, 5*(2), 53-6 .3

Pham, Trung T., Crossley, Steven P., Sooknoi, Tawan, Lobban, Lance L., Resasco, Daniel E., & Mallinson, Richard G. (2010). Etherification of aldehydes, alcohols and their mixtures on Pd/SiO2 catalysts. *Applied Catalysis A: General, 379*(1-2), 135-140 .doi: 10.1016/j.apcata.2010.03.014

Pham, Trung T., Lobban, Lance L., Resasco, Daniel E., & Mallinson, Richard G. (2009). Hydrogenation and Hydrodeoxygenation of 2-methyl-2-pentenal on supported metal catalysts. *Journal of Catalysis, 266*(1), 9-14. doi: 10.1/016j.jcat.2009.05.009

Pham, Tu Nguyet, Shi, Dachuan, & Resasco, Daniel E. (2014). Evaluating strategies for catalytic upgrading of pyrolysis oil in liquid phase. *Applied Catalysis B: Environmental, 145*, 10-23. doi: 10.1016/j.apcatb.2013.01.002

Popov, Andrey, Kondratieva, Elena, Goupil, Jean Michel, Mariey, Laurence, Bazin, Philippe, Gilson, Jean-Pierre, . . . Maugé, Francoise. (2010). Bio-oils Hydrodeoxygenation: Adsorption of Phenolic Molecules on Oxidic Catalyst Supports. *The Journal of Physical Chemistry C, 114*(37), 15661-15670. doi: 10.1021/jp101949j

Possato, Luiz Gustavo, Diniz, Rosiane N., Garetto, Teresita, Pulcinelli, Sandra H., Santilli, Celso V., & Martins, Leandro. (2013). A comparative study of glycerol dehydration catalyzed by micro/mesoporous MFI zeolites. *Journal of Catalysis, 300*, 102-112. doi: 10.1016/j.jcat.2013.01.003

Prasomsri, Teerawit, To, Anh T., Crossley, Steven, Alvarez, Walter E., & Resasco, Daniel E. (2011). Catalytic conversion of anisole over HY and HZSM-5 zeolites in the presence of different hydrocarbon mixtures. *Applied Catalysis B: Environmental, 106*(1–2), 204-211. doi: http://dx.doi.org/10.1016/j.apcatb.2011.05.026

Pütün, Ersan. (2010). Catalytic pyrolysis of biomass: Effects of pyrolysis temperature, sweeping gas flow rate and MgO catalyst. *Energy, 35*(7), 2761-2766. doi: http://dx.doi.org/10.1016/j.energy.2010.02.024

Pütün, Ersan, Ateş, Funda, & Pütün, Ayşe Eren. (2008). Catalytic pyrolysis of biomass in inert and steam atmospheres. *Fuel, 87*(6), 815-824. doi: http://dx.doi.org/10.1016/j.fuel.2007.05.042

Resasco, Daniel E. (2011a). What Should We Demand from the Catalysts Responsible for Upgrading Biomass Pyrolysis Oil? *The Journal of Physical Chemistry Letters, 2*(18), 2294-2295. doi: 10.1021/jz201135x

Resasco, Daniel E2011) .b). What Should We Demand from the Catalysts Responsible for Upgrading Biomass Pyrolysis Oil? *The Journal of Physical Chemistry Letters, 2*, 2294–2295 .

Rinaldi, Roberto, & Schüth, Ferdi. (2009). Design of solid catalysts for the conversion of biomass. *Energy & Environmental Science, 2*, 610-626 .

Rioche, Cyrille, Kulkarni, Shrikant, Meunier, Frederic C., Breen, John P., & Burch, Robbie. (2005). Steam reforming of model compounds and fast pyrolysis bio-oil on supported noble metal catalysts. *Applied Catalysis B: Environmental, 61*(1–2), 130-139. doi: http://dx.doi.org/10.1016/j.apcatb.2005.04.015

Roberts, Virginia M., Stein, Valentin, Reiner, Thomas, Lemonidou , Angeliki, Li, Xuebing, & Lercher, Johannes A. (2011). Towards Quantitative Catalytic Lignin

Depolymerization. *Chemistry – A European Journal, 17*(21), 5939-5948. doi: 10.1002/chem.201002438

Ruan, R., Yang, C., Zhang, B., Lin, X., Chen, L., & Wan, Y. (2010). Improved process for preparing bio-oils from biomass: Google Patents.

Sanchez-Silva, L ,.Lopez-Gonzalez, D., Villasenor, J., Sanchez, P., & Valverde, J. L. (2012). Thermogravimetric-mass spectrometric analysis of lignocellulosic and marine biomass pyrolysis. *Bioresource Technology, 109*, 163-172. doi: 10.1016/j.biortech.2012.01.001

Sanna, A & ,.Andresen, J. M. (2012). Bio-oil deoxygenation by catalytic pyrolysis: new catalysts for the conversion of biomass into densified and deoxygenated bio-oil. *ChemSusChem, 5*(10), 1944-1957. doi: 10.1002/cssc.201200245

Sanna, A., Li, S., Linforth, R., Smart ,K. A., & Andresen, J. M. (2011). Bio-oil and bio-char from low temperature pyrolysis of spent grains using activated alumina. *Bioresour Technol, 102*(22), 10695-10703. doi: 10.1016/j.biortech.2011.08.092

Schmidt, Franz, Lohe, Martin R., Büchner, Bernd, Giordanino, Filippo, Bonino, Francesca, & Kaskel, Stefan. (2013). Improved catalytic performance of hierarchical ZSM-5 synthesized by desilication with surfactants. *Microporous and Mesoporous Materials, 165*, 148-157. doi: 10.1016/j.micromeso.2012.07.045

Scott, Donald S., Majerski, Piotr, Piskorz, Jan, & Radlein, Desmond. (1999). A second look at fast pyrolysis of biomass—the RTI process. *Journal of Analytical and Applied Pyrolysis, 51*(1–2), 23-37. doi: http://dx.doi.org/10.1016/S0165-2370(99)00006-6

Serrano-Ruiz, Juan Carlos, & Dumesic, James A. (2011). Catalytic routes for the conversion of biomass into liquid hydrocarbon transportation fuels. *Energy & Environmental Science, 4*, 83-99. doi: 10.1039/C0EE00436G

Sharma, Ramesh K., & Bakhshi, Narendra N. (1993 .(Catalytic upgrading of pyrolysis oil. *Energy & Fuels, 7*(2), 306-314. doi: 10.1021/ef00038a022

Shen, Dekui, Xiao, Rui, Gu, Sai, & Luo, Kaihong. (2011). The pyrolytic behavior of cellulose in lignocellulosic biomass: a review. *RSC Advances, 1*(9), 1641. doi: 10.1039/c1ra00534k

Shetti, V., Kim, J., Srivastava, R., Choi, M., & Ryoo, R. (2008). Assessment of the mesopore wall catalytic activities of MFI zeolite with mesoporous/microporous hierarchical structures. *Journal of Catalysis, 254*(2), 296-303. doi: 1/0.1016j.jcat.2008.01.006

Shi, Lei, Yang, Rui-qin, Tao, Kai, Yoneyama, Yoshiharu, Tan, Yi-sheng, & Tsubaki, Noritatsu. (2012). Surface impregnation combustion method to prepare nanostructured metallic catalysts without further reduction: As-burnt Cu–ZnO/SiO2 catalyst for low-temperature methanol synthesis. *Catalysis Today, 185*(1), 54-60. doi: 10.1016/j.cattod.2011.10.015

Silaghi, Marius-Christian, Chizallet, Céline, & Raybaud, Pascal. (2014). Challenges on molecular aspects of dealumination and desilication of zeolites. *Microporous and Mesoporous Materials, 191*, 82-96. doi: 10.1016/j.micromeso.2014.02.040

Sitthisa, Surapas, Pham, Trung, Prasomsri, Teerawit, Sooknoi, Tawan, Mallinson, Richard G., & Resasco, Daniel E. (2011). Conversion of furfural and 2-methylpentanal on Pd/SiO2 and Pd–Cu/SiO2 catalysts. *Journal of Catalysis, 280*(1), 17-27. doi: 10.1016/j.jcat.2011.02.006

Sitthisa, Surapas, & Resasco, Daniel E. (2011). Hydrodeoxygenation of Furfural Over Supported Metal Catalysts: A Comparative Study of Cu ,Pd and Ni. *Catalysis Letters, 141*(6), 784-791. doi: 10.1007/s10562-011-0581-7

Smidt, E., & Schwanninger, M. (2005). Characterization of Waste Materials Using FTIR Spectroscopy: Process Monitoring and Quality Assessment. *Spectroscopy Letters, 38*(3), 247 .270-doi: 10.1081/sl-200042310

Srivastava, R. D., & Guha, A. K. (1985). Kinetics and mechanism of deactivation of Pd□Al2O3 catalyst in the gaseous phase decarbonylation of furfural. *Journal of Catalysis, 91*(2), 254-262. doi: http://dx.doi.org/10.1016/00212-90339(85)9517-

Srivastava, Rajendra, Choi, Minkee, & Ryoo, Ryong. (2006). Mesoporous materials with zeolite framework: remarkable effect of the hierarchical structure for retardation of catalyst deactivation. *Chemical Communications*(43), 4489-4491. doi : /10.1039b612116k

Stefanidis, S. D., Kalogiannis, K. G., Iliopoulou, E. F., Lappas, A. A., & Pilavachi, P. A. (2011a). In-situ upgrading of biomass pyrolysis vapors: catalyst screening on a fixed bed reactor. *Bioresour Technol., 102*(17), 8261-8267 .

Stefanidis, S. D., Kalogiannis, K. G., Iliopoulou, E. F., Lappas, A. A., & Pilavachi, P. A. (2011b). In-situ upgrading of biomass pyrolysis vapors: catalyst screening on a fixed bed reactor. *Bioresource Technology, 102*(17), 8261-8267. doi: 10.1016/j.biortech.2011.06.032

Stefanidis, S., Kalogiannis, K., Iliopoulou, E. F., Lappas, A. A., Triguero, J. Martínez, Navarro, M. T., . . . Rey, F. (2013). Mesopore-modified mordenites as catalysts for catalytic pyrolysis of biomass and cracking of vacuum gasoil processes .*Green Chemistry, 15*(6), 1647. doi: 10.1039/c3gc40161h

Stephanidis, S., Nitsos, C., Kalogiannis, K., Iliopoulou, E. F., Lappas, A. A., & Triantafyllidis, K. S. (2011). Catalytic upgrading of lignocellulosic biomass pyrolysis vapours: Effect of hydrothermal pre-treatment of biomass. *Catalysis Today, 167*(1), 37-45. doi: 10.1016/j.cattod.2010.12.049

Sulaiman, F., & Abdullah, N. (2011). Optimum conditions for maximising pyrolysis liquids of oil palm empty fruit bunches. *Energy, 36*(5), 2352-2359. doi: http//:dx.doi.org/10.1016/j.energy.2010.12.067

Sun, Ye, & Cheng, Jiayang. (2002). Hydrolysis of lignocellulosic materials for ethanol production: a review. *Bioresource Technology, 83*(1), 1-11. doi: http://dx.doi.org/10.1016/S0960-8524(01)00212-7

Taarning, Esben ,Osmundsen, Christian M., Yang, Xiaobo, Voss, Bodil, Andersen, Simon I., & Christensen, Claus H. (2011). Zeolite-catalyzed biomass conversion to fuels and chemicals. *Energy & Environmental Science, 4*(3), 793-804 .

Talmadge, Michael S., Baldwin, Robert M ,.Biddy, Mary J., McCormick, Robert L., Beckham, Gregg T., Ferguson, Glen A., . . . Nimlos, Mark R. (2014). A perspective on oxygenated species in the refinery integration of pyrolysis oil. *Green Chemistry, 16*(2), 407-453. doi: 10.1039/C3GC41951G

Tang, Yang, Yu, Wanjin, Mo, Liuye, Lou, Hui, & Zheng, Xiaoming. (2008). One-Step Hydrogenation−Esterification of Aldehyde and Acid to Ester over Bifunctional Pt Catalysts: A Model Reaction as Novel Route for Catalytic Upgrading of Fast Pyrolysis Bio-Oil. *Energy & Fuels, 22*(5), 3484-3488. doi: 10.1021/ef800148q

Thangalazhy-Gopakumar, Suchithra, Adhikari, Sushil, Gupta, Ram B., Tu, Maobing, & Taylor, Steven. (2011). Production of hydrocarbon fuels from biomass using catalytic pyrolysis under helium and hydrogen environments. *Bioresource Technology, 102*(12), 6742-6749. doi: http://dx.doi.org/10.1016/j.biortech.2011.03.104

To, Anh T., & Resasco, Daniel E. (2014). Role of a phenolic pool in the conversion of m-cresol to aromatics over HY and HZSM-5 zeolites. *Applied Catalysis A: General, 487*, 62-71. doi: 10.1016/j.apcata.2014.09.006

Torri, Cristian, Reinikainen, Matti, Lindfors, Christian, Fabbri, Daniele, Oasmaa, Anja, & Kuoppala, Eva. (2010). Investigation on catalytic pyrolysis of pine sawdust: Catalyst screening by Py-GC-MIP-AED. *Journal of Analytical and Applied Pyrolysis, 88*(1), 7-13. doi: http://dx.doi.org/10.1016/j.jaap.2010.02.005

Triantafyllidis, Kostas S., Iliopoulou, Eleni F., Antonakou, Eleni V., Lappas, Angelos A., Wang, Hui, & Pinnavaia, Thomas J. (2007 .(Hydrothermally stable mesoporous aluminosilicates (MSU-S) assembled from zeolite seeds as catalysts for biomass pyrolysis. *Microporous and Mesoporous Materials, 99*(1–2), 132-139. doi: http://dx.doi.org/10.1016/j.micromeso.2006.09.019

Valle, Beatriz, Castaño, Pedro, Olazar, Martin, Bilbao, Javier, & Gayubo, Ana G. (2012). Deactivating species in the transformation of crude bio-oil with methanol into hydrocarbons on a HZSM-5 catalyst. *Journal of Catalysis, 285*(1), 304-314. doi: 10.1016/j.jcat.2011.10.004

Valle, Beatriz, Gayubo, Ana G., Aguayo, Andrés T., Olazar, Martin, & Bilbao, Javier. (2010). Selective Production of Aromatics by Crude Bio-oil Valorization with a Nickel-Modified HZSM-5 Zeolite Catalyst. *Energy & Fuels, 24*(3), 2060-2070. doi: 10.1021/ef901231j

Vamvuka, D., Kakaras, E., Kastanaki, E., & Grammelis, P. (2003). Pyrolysis characteristics and kinetics of biomass residuals mixtures with lignite☆. *Fuel, 82*(15-17), 1949-1960. doi: 10.1016/s0016-2361(03)00153-4

Van de Velden, Manon, Baeyens, Jan ,Brems, Anke, Janssens, Bart, & Dewil, Raf. (2010). Fundamentals, kinetics and endothermicity of the biomass pyrolysis reaction. *Renewable Energy, 35*(1), 232-242. doi: http://dx.doi.org/10.1016/j.renene.2009.04.019

Vassilev, Stanislav V., Baxter, David, Andersen, Lars K., Vassileva, Christina G., & Morgan, Trevor J. (2012). An overview of the organic and inorganic phase composition of biomass. *Fuel, 94*, 1-33. doi: 10.1016/j.fuel.2011.09.030

Venderbosch, R. H., & Prins, W. (2010). Fast pyrolysis technology development. *Biofuels, Bioproducts and Biorefining, 4*(2), 178-208. doi: 10.1002/bbb.205

Vichaphund, Supawan, Aht-ong, Duangdao, Sricharoenchaikul, Viboon, & Atong, Duangduen. (2014). Catalytic upgrading pyrolysis vapors of Jatropha waste using metal promoted ZSM-5 catalysts: An analytical PY-GC/MS. *Renewable Energy, 65*, 70-77. doi: 10.1016/j.renene.2013.07.016

Vispute, T. P., Zhang, H., Sanna, A., Xiao, R., & Huber, G. W. (2010). Renewable chemical commodity feedstocks from integrated catalytic processing of pyrolysis oils. *Science, 330*(6008), 1222-1227. doi: 10.1126/science.1194218

Vitolo, S., Bresci, B., Seggiani, M., & Gallo, M. G. (2001). Catalytic upgrading of pyrolytic oils over HZSM-5 zeolite: behaviour of the catalyst when used in repeated upgrading–regenerating cycles. *Fuel, 80*(1), 17-26. doi: http://dx.doi.org/10.1016/S0016-2361(00)00063-6

Wang, Denghui, Xiao, Rui, Zhang, Huiyan, & He, Guangying. (2010). Comparison of catalytic pyrolysis of biomass with MCM-41 and CaO catalysts by using TGA–FTIR analysis. *Journal of Analytical and Applied Pyrolysis, 89*(2), 171-177. doi: http://dx.doi.org/10.1016/j.jaap.2010.07.008

Wang, Kaige, Kim, Kwang Ho, & Brown, Robert C. (2014). Catalytic pyrolysis of individual components of lignocellulosic biomass. *Green Chemistry, 16*(2), 727. doi: 10.1039/c3gc41288a

Wang, Lu, Lei, Hanwu, Bu, Quan, Ren, Shoujie, Wei, Yi, Zhu, Lei, . . . Tang, Juming. (2014). Aromatic hydrocarbons production from ex situ catalysis of pyrolysis vapor over Zinc modified ZSM-5 in a packed-bed catalysis coupled with microwave pyrolysis reactor. *Fuel, 129*(0), 78-85. doi: http://dx.doi.org/10.1016/j.fuel.2014.03.052

Wang, Yuxin, He, Tao, Liu, Kaituo, Wu, Jinhu, & Fang, Yunming. (2012). From biomass to advanced bio-fuel by catalytic pyrolysis/hydro-processing: Hydrodeoxygenation of bio-oil derived from biomass catalytic pyrolysis. *Bioresource Technology, 108*(0), 280-284. doi: http://dx.doi.org/10.1016/j.biortech.2011.12.132

White, John E., Catallo, W. James, & Legendre, Benjamin L. (2011). Biomass pyrolysis kinetics: A comparative critical review with relevant agricultural residue case studies. *Journal of Analytical and Applied Pyrolysis, 91*(1), 1-33. doi: 10.1016/j.jaap.2011.01.004

Widyawati, Meilina, Church, Tamara L., Florin, Nicholas H & ,.Harris, Andrew T. (2011). Hydrogen synthesis from biomass pyrolysis with in situ carbon dioxide capture using calcium oxide. *International Journal of Hydrogen Energy, 36*(8), 4800-4813. doi: 10.1016/j.ijhydene.2010.11.103

Wildschut, Jelle, Iqbal, Muhammad ,Mahfud, Farchad H., Cabrera, Ignacio Melian, Venderbosch, Robbie H., & Heeres, Hero J. (2010). Insights in the hydrotreatment of fast pyrolysis oil using a ruthenium on carbon catalyst. *Energy & Environmental Science, 3*(7), 962-970 .

Wildschut, Jelle, Mahfud, Farchad H., Venderbosch, Robbie H., & Heeres, Hero J. (2009). Hydrotreatment of Fast Pyrolysis Oil Using Heterogeneous Noble-Metal Catalysts. *Industrial & Engineering Chemistry Research, 48*(23), 10324-10334. doi: 10.1021/ie9006003

Wilson, Lugano, Yang, Weihong, Blasiak, Wlodzimierz, John, Geoffrey R., & Mhilu, Cuthbert F. (2011). Thermal characterization of tropical biomass feedstocks. *Energy Conversion and Management, 52*(1), 191-198. doi: 10.1016/j.enconman.2010.06.058

Yamada, Yasuhiro, Segawa, Masaki, Sato, Fumiya, Kojima, Takashi, & Sato, Satoshi. (2011a). Catalytic performance of rare earth oxides in ketonization of acetic acid. *Journal of Molecular Catalysis A: Chemical, 346*(1-2), 79-86. doi: 10.1016/j.molcata.2011.06.011

Yamada, Yasuhiro, Segawa, Masaki, Sato, Fumiya, Kojima, Takashi, & Sato, Satoshi. (2011b). Catalytic performance of rare earth oxides in ketonization of acetic acid. *Journal of Molecular Catalysis A: Chemical, 346*(1–2), 79-86. doi: http://dx.doi.org/10.1016/j.molcata.2011.06.011

Yan, Junwei, Jiang, Xiumin, Han, Xiangxin, & Liu, Jianguo. (2013). A TG–FTIR investigation to the catalytic effect of mineral matrix in oil shale on the pyrolysis and combustion of kerogen. *Fuel, 104*, 307-317. doi: 10.1016/j.fuel.2012.10.024

Yang, H ,.Yan, R., Chen, H., Zheng, C., Lee, D., & Liang, D. (2006). Influence of mineral matter on pyrolysis of palm oil wastes. *Combustion and Flame, 146*(4), 605-611. doi: 10.1016/j.combustflame.2006.07.006

Yang, Haiping, Yan, Rong, Chen, Hanping, Lee, Dong Ho & ,Zheng, Chuguang. (2007a). Characteristics of hemicellulose, cellulose and lignin pyrolysis. *Fuel, 86*(12-13), 1781-1788. doi: 10.1016/j.fuel.2006.12.013

Yang, Haiping, Yan, Rong, Chen, Hanping, Lee, Dong Ho, & Zheng, Chuguang. (2007b). Characteristics of hemicellulose, cellulose and lignin pyrolysis. *Fuel, 86*(12–13), 1781-1788. doi: http://dx.doi.org/10.1016/j.fuel.2006.12.013

Yu, C. T., Chen, W. H., Men, L. C., & Hwang, W. S. (2009). Microscopic structure features changes of rice straw treated by boiled acid solution. *Industrial Crops and Products, 29*(2-3), 308-315. doi: 10.1016/j.indcrop.2008.06.005

Yu, Wanjin, Tang, Yang, Mo, Liuye, Chen, Ping, Lou, Hui, & Zheng, Xiaoming. (2011a). Bifunctional Pd/Al-SBA-15 catalyzed one-step hydrogenation–esterification of furfural and acetic acid: A model reaction for catalytic upgrading of bio-oil. *Catalysis Communications, 13*(1), 35-39. doi: 10.1016/j.catcom.2011.06.004

Yu, Wanjin, Tang, Yang, Mo, Liuye, Chen, Ping, Lou, Hui, & Zheng, Xiaoming. (2011b). One-step hydrogenation–esterification of furfural and acetic acid over bifunctional Pd catalysts for bio-oil upgrading. *Bioresource Technology, 102*(17), 8241-8246. doi: http://dx.doi.org/10.1016/j.biortech.2011.06.015

Zakzeski, Joseph, Bruijnincx, Pieter C. A., Jongerius, Anna L., & Weckhuysen, Bert M. (2010). The Catalytic Valorization of Lignin for the Production of Renewable Chemicals. *Chemical Reviews, 110*(6), 3552-3599. doi: 10.1021/cr900354u

Zhang, Bin, Zhu, Yulei, Ding, Guoqiang, Zheng, Hongyan, & Li, Yongwang. (2012). Modification of the supported Cu/SiO2 catalyst by alkaline earth metals in the selective conversion of 1,4-butanediol to γ-butyrolactone. *Applied Catalysis A: General, 443-444*, 191-201. doi: 10.1016/j.apcata.2012.07.042

Zhang, Huiyan, Carlson ,Torren R., Xiao, Rui, & Huber, George W. (2012). Catalytic fast pyrolysis of wood and alcohol mixtures in a fluidized bed reactor. *Green Chemistry, 14*(1), 98. doi: 10.1039/c1gc15619e

Zhang, Huiyan, Cheng, Yu-Ting, Vispute, Tushar P., Xiao, Rui, & Huber, George W. (2011a). Catalytic conversion of biomass-derived feedstocks into olefins and aromatics with ZSM-5: the hydrogen to carbon effective ratio. *Energy & Environmental Science, 4*(6), 2297. doi: 10.1039/c1ee01230d

Zhang, Huiyan, Cheng, Yu-Ting, Vispute ,Tushar P., Xiao, Rui, & Huber, George W. (2011b). Catalytic conversion of biomass-derived feedstocks into olefins and aromatics with ZSM-5: the hydrogen to carbon effective ratio. *Energy & Environmental Science, 4*(6), 2297-2307 .

Zhang, Huiyan, Shao, Shanshan, Xiao, Rui, Shen, Dekui, & Zeng, Jimin. (2014). Characterization of Coke Deposition in the Catalytic Fast Pyrolysis of Biomass Derivates. *Energy & Fuels*, *28*(1), 52-57. doi: 10.1021/ef401458y

Zhang, Huiyan, Xiao, Rui, Wang, Denghui, He, Guangying, Shao, Shanshan, Zhang, Jubing, & Zhong, Zhaoping. (2011). Biomass fast pyrolysis in a fluidized bed reactor under N2, CO2, CO, CH4 and H2 atmospheres. *Bioresource Technology, 102*(5), 4258-4264. doi: http://dx.doi.org/10.1016/j.biortech.2010.12.075

Zhang, Qi ,Chang, Jie, Wang, Tiejun, & Xu, Ying. (2007). Review of biomass pyrolysis oil properties and upgrading research. *Energy Conversion and Management, 48*(1), 87-92. doi: 10.1016/j.enconman.2006.05.010

Zhang, Wenmin, Burckle, Eric C., & Smirniotis, Panagiotis G. (1999). Characterization of the acidity of ultrastable Y, mordenite, and ZSM-12 via NH3-stepwise temperature programmed desorption and Fourier transform infrared spectroscopy. *Microporous and Mesoporous Materials, 33*(1–3), 173-185. doi: http://dx.doi.org/10.1016/S1387-1811(99)00136-5

Zhang, Zhijun, Wang, Qingwen, Tripathi, Prabhat, & Jr, Charles U. Pittman. (2011). Catalytic upgrading of bio-oil using 1-octene and 1-butanol over sulfonic acid resin catalysts. *Green Chemistry, 13*, 940-949 .

Zhao, Chen ,He, Jiayue, Lemonidou, Angeliki A., Li, Xuebing, & Lercher, Johannes A. (2011). Aqueous-phase hydrodeoxygenation of bio-derived phenols to cycloalkanes. *Journal of Catalysis*, *280*(1), 8-16. doi: 10.1016/j.jcat.2011.02.001

Zheng, Hong-Yan, Zhu, Yu-Lei, Teng, Bo-Tao, Bai, Zong-Qing, Zhang, Cheng-Hua, Xiang, Hong-Wei, & Li, Yong-Wang. (2006). Towards understanding the reaction pathway in vapour phase hydrogenation of furfural to 2-methylfuran. *Journal of Molecular Catalysis A: Chemical, 246*(1–2), 18-23. doi : http://dx.doi.org/10.1016/j.molcata.2005.10.003

Zheng, Ji-Lu, & Wei, Qin. (2011). Improving the quality of fast pyrolysis bio-oil by reduced pressure distillation. *Biomass and Bioenergy, 35*(5), 1804-1810. doi: http://dx.doi.org/10.1016/j.biombioe.2011.01.006

Zhu, Xinli, Lobban, Lance L., Mallinson, Richard G., & Resasco, Daniel E. (2011). Bifunctional transalkylation and hydrodeoxygenation of anisole over a Pt/HBeta catalyst. *Journal of Catalysis*, *281*(1), 21-29. doi: 10.1016/j.jcat.2011.03.030

Zhu, Xinli, Mallinson, Richard G., & Resasco, Daniel E. (2010). Role of transalkylation reactions in the conversion of anisole over HZSM-5. *Applied Catalysis A: General, 379*(1-2), 172-181. doi: 10.1016/j.apcata.2010.03.018

LIST OF PUBLICATIONS

Academic Journals

- **Asadieraghi, Masoud**, Ashri Wan Daud, Wan Mohd, & Abbas, Hazzim F. (2015). Heterogeneous catalysts for advanced bio-fuel production through catalytic biomass pyrolysis vapor upgrading: a review. *RSC Advances*, *5*(28), 22234-22255.
- **Asadieraghi, Masoud**, & Wan Daud, Wan Mohd Ashri. (2014). Characterization of lignocellulosic biomass thermal degradation and physiochemical structure: Effects of demineralization by diverse acid solutions. *Energy Conversion and Management, 82*, 71-82.
- **Asadieraghi, Masoud**, & Wan Daud, Wan Mohd Ashri. (2015). In-situ catalytic upgrading of biomass pyrolysis vapor: Co-feeding with methanol in a multi-zone fixed bed reactor. *Energy Conversion and Management, 92*, 448-458.
- **Asadieraghi, Masoud**, Wan Daud, Wan Mohd Ashri, & Abbas, Hazzim F. (2014). Model compound approach to design process and select catalysts for in-situ bio-oil upgrading. *Renewable and Sustainable Energy Reviews, 36*, 286-303.
- **Asadieraghi, Masoud**, & Wan Daud, Wan Mohd Ashri. (2015). In-depth investigation on thermochemical characteristics of palm oil biomasses as potential biofuel sources. *Journal of Analytical and Applied Pyrolysis*. doi: http://dx.doi.org/10.1016/j.jaap.2015.08.017
- **Asadieraghi, Masoud**, & Wan Daud, Wan Mohd Ashri. (2015). In-situ catalytic upgrading of biomass pyrolysis vapor: Using a cascade system of various catalysts in a multi-zone fixed bed reactor. *Energy Conversion and Management, 101*, 151-163.